Fluoro-Substituted Cationic and Neutral Antibiotic NHC* Silver Derivatives of SBC3: Continuous Flow versus Conventional Synthesis

By

Zoe Beato
16201470

School of Chemistry

This thesis is submitted to University College Dublin in fulfilment of the requirements for the degree Master of Science

Head of School

Associate Prof. Michael Casey

Supervisors

Associate Prof. Matthias Tacke

Assistant Prof. Marcus Baumann

Table of contents

Table of contents ii
Acknowledgements iv
Abstract v
Declaration vi
Chapter 1 Introduction 1
1.1 A Brief History of Antibiotics 2
1.2 Antibiotic Resistance 4
1.3 Silver in Medicine, its Antibacterial Mechanisms, and Resistance 6
1.4 Carbenes 9
1.5 *N*-Heterocyclic Carbenes 10
1.6 *N*-Heterocyclic Carbene Complexes with Transition Metals 11
1.7 Silver Complexes of *N*-Heterocyclic Carbenes 13
1.8 The Role of Fluorination in Medicinal Chemistry 17
1.9 Continuous Flow Chemistry 17
1.10 References 20
Chapter 2 Results and Discussion 28
2.1 Synthesis of Imidazolium Bromide Salts 29
2.2 Synthesis of Fluorinated NHC Silver (I) Acetate Complexes 31
2.3 Synthesis of Imidazole-2-ylidene Silver (I) (*p*-trifluoromethyl) Benzoate Complexes 33
2.3.1 Synthesis via generation of a free carbene intermediate 33
2.3.2 Synthesis from an imidazolium salt and a silver base 37
2.3.2.1 Synthesis of imidazolium (p-trifluoromethyl) benzoate salts 37
2.3.2.2 Formation of imidazol-2-ylidene silver (I) (p-trifluoromethyl) benzoate complexes by reaction with silver (I) oxide 39
2.4 Synthesis of Cationic *Bis*-imidazol-2-ylidene Silver (I) Complexes with Non-coordinating Anions 41
2.4.1 Synthesis of anion-exchanged imidazolium salts 41
2.4.2 Synthesis of *bis*-carbene silver complexes 42
2.5 Synthesis of Cationic *Bis*-imidazol-2-ylidene Silver (I) Complexes with Coordinating Anions 48
2.5.1 Synthesis of cationic *bis*-imidazol-2-ylidene silver (I) gluconate complexes 49
2.5.2 Synthesis of cationic *bis*-imidazol-2-ylidene silver (I) chloride complexes 52
2.5.3 Synthesis of a *bis*-imidazol-2-ylidene silver (I) acetate complex 55
2.6 Biological Testing 58
2.7 Conclusion 61

2.8 References 62
Chapter 3 Experimental Details 65
3.1 General Considerations 66
3.2 Synthetic Procedures 67
3.3 Biological Testing 85
3.4 Crystallography Data 86
3.4.1 Crystal Structure and Refinement Data 86
3.4.2 Selected Bond Lengths and Angles 89
3.5 References 94
Appendix 1: Spectral Data 95

Acknowledgements

I would like to thank my supervisors Assoc. Prof. Matthias Tacke and Assist. Prof. Marcus Baumann for their support and wisdom throughout the project. Their encouragement and guidance was always warmly welcome. I would also like to thank Dr. Cillian O'Beirne for the huge role he played in helping me find my feet in the lab, and for always being reachable when I had questions.

I extend my appreciation to Cian, Danielle, and especially Shane for always being friendly and keeping me company in the lab.

A special thanks to my mom who, though far away, has always been my biggest supporter. Her belief in me carried me when I wasn't so sure of myself. And to my late grandfather Louis, an inspiration to pursue chemistry, but more importantly for reminding me to always continue learning new things.

Finally, I would like to thank all the technical staff for their assistance, and especially Dr. Helge Müller-Bunz, who was always accommodating and quick to measure my crystals.

Abstract

The emergence of antibiotic resistance is an impending crisis which requires that new antibiotics possessing novel mechanisms of action are introduced into the clinical regime. Silver, which is biologically active as the Ag^+ cation, has seen a resurgence in popularity as an antimicrobial agent due to its multiple antibiotic mechanisms, its relatively few reported instances of resistance, and its low human toxicity. For silver to be useful as a systemic antibiotic it must exist in a complex which is stable enough to reach the biological target before release of the silver ion. *N*-heterocyclic carbenes (NHCs) have become a popular choice of stabilising ligand due to their excellent σ-donating abilities and the ease with which they can be functionalised.

Herein, we describe the synthesis and characterisation of neutral and cationic NHC complexes of silver with ligands based on the 1,3-dibenzyl-4,5-diphenyl imidazole scaffold used in the lead compound **SBC3** of the Tacke group. Eleven new imidazolium salt precursors were synthesised in moderate to excellent yields (56 - 97%). NHC silver acetate and NHC silver (trifluoromethyl)benzoate complexes were synthesised as fluorinated derivatives of the lead compound **SBC3** and were achieved in moderate to good yields (53 - 68%). Fluorination was incorporated on the ligands to increase the lipophilicity of the complexes and improve cellular uptake *in vivo*. Cationic *bis*-NHC silver complexes were synthesised to improve overall stability by introduction of a second NHC ligand. The *bis*-NHC silver complexes with non-coordinating anions (PF_6^- and BF_4^-) were synthesised directly from their imidazolium salts in good to excellent yields (77 - 94%). We also describe a continuous flow method using anion exchange resins in a packed bed reactor to achieve *bis*-NHC silver complexes with non-traditional, coordinating gluconate (66 - 97% yield) and acetate (90% yield) which would not be achievable by direct synthesis in batch mode. An attempt to synthesise *bis*-NHC complexes with a chloride anion was unsuccessful. Instead, the complexes which have the empirical formula [(NHC)AgX], were obtained in low to moderate yield (27 - 63%).

Evaluation of all novel complexes for their biological activity was carried out *in vitro* by Kirby-Bauer disk diffusion method. This preliminary testing method indicates that all silver complexes synthesised herein show antibacterial activity comparable to that of the lead compound **SBC3**.

Declaration

I hereby declare that all the work presented in this thesis, unless stated below or clearly indicated by citation, is my own and was completed while registered as a candidate for the degree of Master of Science at University College Dublin.

Signed

_____

Zoe Beato

Abbreviations

δ	chemical shift in ppm (NMR)
µ	micro
Å	Angstrom
Ag_2O	silver oxide
AgCl	silver chloride
ATP	adenosine triphosphate
br	broad (NMR)
$CDCl_3$	chloroform-*d*
Cy	cyclohexyl
d	doublet (NMR)
dd	doublet of doublets (NMR)
DCM	dichloromethane
DMSO	dimethyl sulfoxide
DMSO-d_6	dimethyl sulfoxide-d_6
E. coli	*Escherichia coli*
eq	equivalent
HMBC	heteronuclear multiple bond correlation spectroscopy
HRMS	high-resolution mass spectrometry
IR	infrared spectroscopy
J	coupling constant
K_2CO_3	potassium carbonate
KO^tBu	potassium *tert*-butoxide
KPF_6	potassium hexafluorophosphate
MeCN	acetonitrile
MeOH	methanol
MIC	minimum inhibitory concentration
mM	millimolar
MRSA	methicillin-resistant *Staphylococcus aureus*
$NaBF_4$	sodium tetrafluoroborate
NHC	*N*-heterocyclic carbene
NMR	nuclear magnetic resonance
OAc	acetate/acetyl
Ph	phenyl
ppm	parts per million
q	quartet (NMR)
ROS	reactive oxygen species
rt	room temperature
s	singlet (NMR)
S. aureus	*Staphylococcus aureus*
SBC3	1,3-dibenzyl-4,5-diphenylimidazol-2-ylidene silver (I) acetate
t	triplet (NMR)
THF	tetrahydrofuran

Chapter 1 Introduction

1.1 A Brief History of Antibiotics

It was not until the late nineteenth century, largely due to the work of Robert Koch, that it was understood that infectious diseases were caused by microorganisms.[1] Following on from this discovery, scientists began identifying and isolating disease-causing bacteria. While working on staining bacteria, Paul Ehrlich noted that different dyes had affinities for different bacteria, leading him to theorise that a chemical could be created to specifically target and kill pathogens, leaving the host unharmed.[2] Along with his colleagues Alfred Bertheim and Sahachiro Hata, Ehrlich worked on the systematic development and screening of hundreds of compounds in search of an antibiotic 'magic bullet'.[3] This led to the discovery of the first antimicrobial drug, Salvarsan, an aniline-derived organoarsenic compound effective at treating syphilis and trypanosomiasis. The interest in the ability of dye molecules to act as drugs continued with the work of Gerhard Domagk and his chemists, Joseph Klarer and Fritz Mietzsch; together producing Prontosil, the first of the sulfonamides, in 1932.[4] Prontosil was a prodrug of sulfanilamide, an already well-known dye component (*Fig. 1.1*). Its broad-spectrum activity made it a popular treatment, and its ease of modification saw many sulfanilamide derivatives become available relatively quickly, some of which are still in use today.[2, 5, 6]

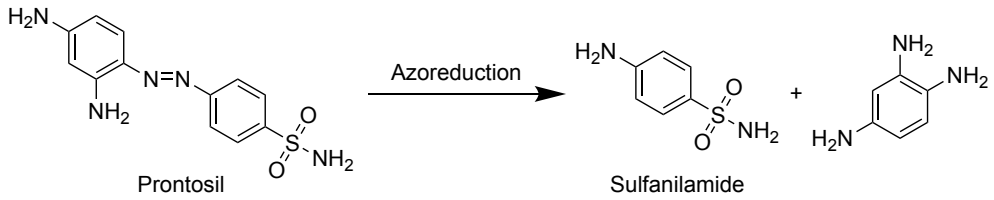

Figure 1.1: In vivo reduction of the sulfonamide prodrug Prontosil releases the active sulfanilamide moiety and 1,2,4-triaminobenzene[7]

The popularity and use of synthetic antibiotics waned only with the introduction of penicillin. The bactericidal effect of *Penicillium* moulds was first reported by Alexander Fleming in 1929.[8] However, it was not until the isolation and clinical testing of penicillin by Florey and Chain in 1940 that the compound was able to be developed for use in patients.[9] The discovery of another new antibacterial, an aminoglycoside named streptomycin isolated

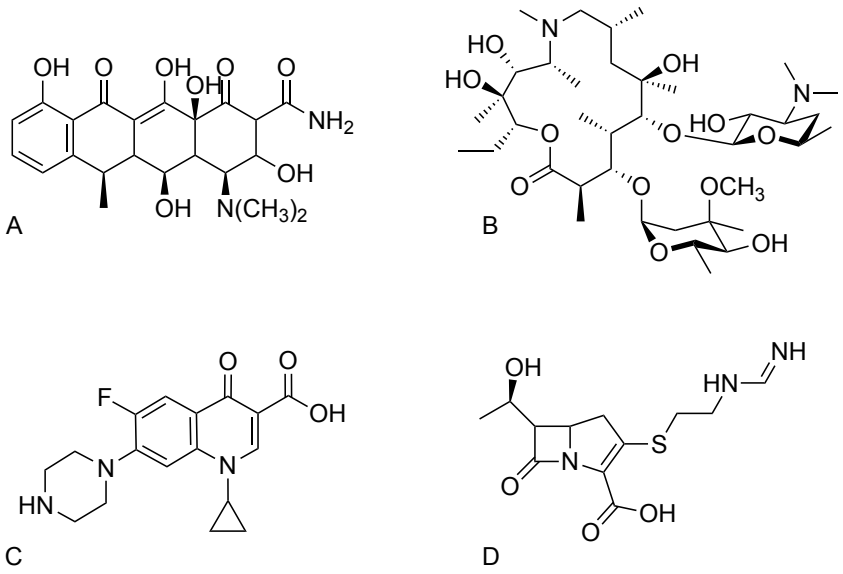

Figure 1.1: Doxycycline (A), a tetracycline; Azithromycin (B), a macrolide; Ciprofloxacin (C), a quinolone; Imipenem (D), a carbapenem.

from the soil bacteria *Streptomyces griseus,* marked somewhat of turning point in the quest for antibiotics as scientists began to focus on naturally-derived antibiotics rather than synthetic compounds.[10]

These new drugs, developed largely during the 1950s and 1960s, included β-lactams (penicillins, cephalosporins, and carbapenems), glycopeptides, macrolides, chloramphenicol, and tetracyclines (*Fig. 1.2*).[4, 11] With the exception of chloramphenicol, the previously listed antibiotics represent classes consisting of multiple drugs which share a central active structure (e.g., the fused ring backbone of the tetracyclines). Modifications around the central structures of each class created subsequent generations of drugs with higher activity and a broader spectrum of susceptible microbes.[11, 12] Two new classes of synthetic antibiotics were also introduced during the same booming period of antimicrobial discovery: the quinolones derived from nalidixic acid and the oxazolidinones.[10] Though the number of available antibiotic drugs seemed to be growing exponentially in the middle of the twentieth century, the development of new drugs and new drug classes quickly began to taper off. Only one new class of antibiotics, lipopeptides like daptomycin, have been discovered in the last 50 years.[13] Even the introduction of new drugs of the existing classes has seen a steady decline over past decades.[14] Despite the number of available antibiotics, the fight against infectious diseases is far from over.

1.2 Antibiotic Resistance

Although the arsenal of antibiotics expanded rapidly during the twentieth century, the almost-concurrent emergence and spread antimicrobial resistance threatens the viability of antibiotic therapies. Resistance against sulfonamides was noted as early as 1942, and β-lactamase enzymes were discovered to naturally occur in some bacteria even before exposure to penicillin.[12, 15] Many common antibiotics have seen resistance develop in at least one species of bacteria within 15 years of the drugs being introduced.[16] The widespread use (and often misuse) of antibiotics in healthcare and agriculture has also led to the evolution of bacteria which are resistant to multiple drugs. The emergence of these 'superbugs' has created a crisis in healthcare settings, leading to reduced treatment options and increased mortality and morbidity associated with infections (*Table 1*).[17] Though it is a natural phenomenon, humans have helped to expediate the spread of antibiotic resistance. Antibiotics are often misused or overused, especially when a specific pathogen is not identified before treatment or where antibiotics are available without prescription.[18]

Bacteria	Diseases caused	Has shown resistance to
Salmonella enterica	Gastroenteritis, enteric fever	Ampicillin, chloramphenicol, streptomycin, tetracycline, fluoroquinolones
Escherichia coli	Bloodstream infections, urinary tract infections	Penicillins, cephalosporins, fluoroquinolones
Klebsiella pneumoniae	Pneumonia, urinary tract infections, bloodstream infections	Penicillins, cephalosporins, carbapenems, cotrimoxazole, fluoroquinolones
Staphylococcus aureus	Wound infections, bloodstream infections	All beta-lactam drugs, vancomycin

Table 1.1: Examples of some common pathogenic bacteria and drugs to which they show resistance[19]

Resistance develops naturally in microorganisms due to random genetic mutations; however, mutations which confer resistance offer a distinct survival advantage, thus they persist and are shared within populations of bacteria.[18] Genes can be shared via uptake of free DNA of closely related bacteria (transformation), or by the dissemination of mobile genetic elements such as bacteriophages (transduction) or plasmids (conjugation).[20] This phenomenon, called horizontal gene transfer, allows the sharing of genetic elements between a diverse range of different species of bacteria. The sharing of mobile genetic elements and horizontal gene transfer allow the resistance-developing mutations to spread

rapidly, helping to explain the pace at which resistance appears to develop once a drug becomes widely used.[21]

Many resistance mechanisms developed by bacteria are specific to individual drugs, however there are a few general types of mechanisms (*Fig. 1.3*). Bacteria may limit the cellular concentration of a drug either by decreasing its uptake, or by developing efflux pumps to actively transport the drug from the cell. If the drug can't accumulate within the cell, it will not be present in a high enough concentration to be effective.[22] Decreasing drug uptake can manifest as a downregulation in the number of non-specific porin proteins on the outer cell membrane to limit diffusion into the cell, as has been seen in *Pseudomonas* and *Acinetobacter* species.[23] Efflux pumps are considered innate resistance mechanisms as they are already present in bacterial cells, but may become upregulated when exposed to antibiotics.[22]

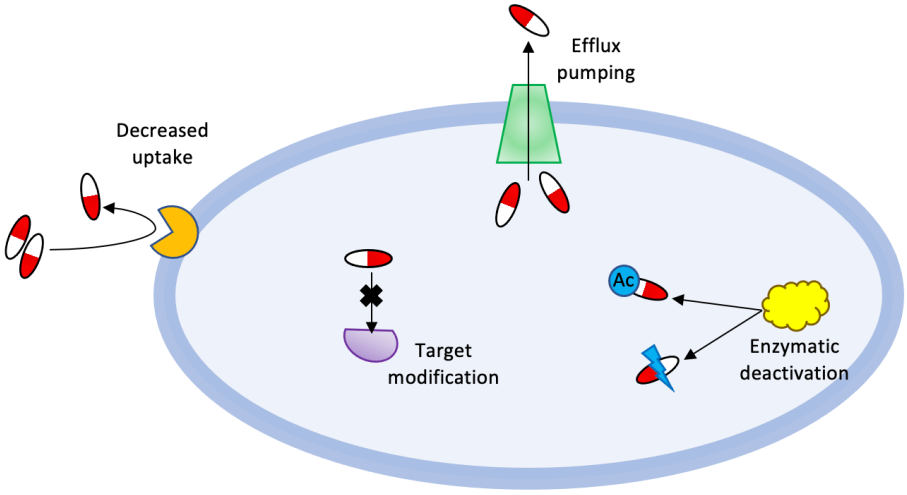

Figure 1.3: Some mechanisms by which bacteria may develop resistance to antimicrobial drugs

Even if the drug is able to enter the bacterial cell and accumulate, there are other mechanisms which can give the organism resistance to the drug. Drug molecules may be modified by enzymes within the bacterial cell which leads to inactivation of the drug. One well known example of this is the hydrolysis of the four-membered β-lactam ring by serine or metallo-β-lactamase enzymes.[24] Once the ring structure is opened the drugs are no longer active. In non-hydrolysable drugs, inactivation may occur by derivatisation of an active functional group on the molecule. Aminoglycoside resistance occurs this way—through *N*-acetylation, *O*-phosphorylation or *O*-adenylation— which impedes RNA binding ability.[22]

Modification of the drug target by mutation of the target gene or by enzymatic modification of the target (like methylation) may decrease a drug's binding affinity or the

drug's ability to reach its target.[23, 24] For example, a mutation which inserts an extra aspartic acid residue into the penicillin binding proteins of *Neisseria gonorrhoea* has greatly lowered the affinity of the enzyme for drug molecules, and has led to a greatly decreased susceptibility of the pathogen to β-lactam antibiotics including penicillins and cephalosporins.[25]

Efforts to overcome antibiotic resistance have had limited success outside of the introduction of new drugs, and even those have mostly been modified versions of existing drugs. One of few examples is the discovery of clavulanic acid, a β-lactamase inhibitor, which allowed the reintroduction of amoxicillin to treat infections that had previously been resistant.[17] However, resistance to clavulanic acid and similar β-lactamase inhibitors has also been seen.[26, 27] Other strategies have been focused on minimising infection risk and better stewardship of antibiotics, but it has become widely accepted that resistance is an inevitable consequence of the use of antibiotics.[18, 19] In order to be able to continue to treat infectious diseases, new antibiotics with novel mechanisms of action must continue to be developed.

1.3 Silver in Medicine, its Antibacterial Mechanisms, and Resistance

Historically, the medicinal value of silver has been well-documented. Beginning in ancient times it was used to purify and preserve water, and eventually became a ubiquitous treatment to prevent wound infection, ophthalmia, and even sepsis.[28] In the twentieth century, silver was added to the already-in-use drugs salvarsan and sulfadiazine to improve their activity against syphilis and wound infections, respectively.[29, 30] The latter, silver sulfadiazine, is still commonly used as a burn cream to this day. Overall, the popularity of silver-based treatments waned with the introduction of oral antibiotics, but interest in the metal has seen a recent renaissance in the face of the antibiotic resistance crisis. Currently, clinical use of silver is focused in medical devices including catheters, endotracheal tubes, and wound dressings to thwart the infections associated with their use.[31]

Despite the continued presence of silver in clinical settings over the last few decades, reports of resistance to the metal have been relatively few.[32] This could be in part due to silver having multiple mechanisms of action against bacteria, which makes a resistance-conferring mutation far less likely.[32, 33] Silver exhibits its biological activity as the Ag^+ ion,

and has been seen to interact with many parts of the bacterial cell including the cell wall, DNA, and respiratory enzymes.[34]

Silver begins its action against bacterial cells at the cell membrane. Treatment of *E. coli* and *S. aureus* with Ag^+ ions led to visible shrinking of the cytoplasm and detachment from the cell wall.[35] Ag^+ ions also bind to transport proteins and negatively charged residues on the membrane surface.[36] This disrupts surface proteins, damages the membrane and can lead to increased cell permeability, impairing the overall integrity of the membrane.[36, 37] In *Vibrio cholerae*, Ag^+ ions were shown to cause proton leakage from membranes; collapsing the proton motive force and deenergising the membrane.[38] Treatment of *E. coli* and *S. aureus* with Ag^+ ions led to visible detachment of the cytoplasm from the cell wall.

Within cells, silver ions begin to accumulate and interact with proteins and enzymes in the cell. Many of these interactions are mediated by silver's properties as a soft acid, which give it a high affinity for sulfur.[37] In fact, the thiol groups were shown to be the most important substrate for silver binding: addition of equimolar amounts of cysteine was shown to completely negate the antibacterial activity of silver while the same was not seen with addition of equimolar amounts of DNA, potassium phosphate, or other non-thiol containing amino acids.[39] Ag^+ ions attack oxidative enzymes such as cytochromes a_1 and *b* in *E. coli or* succinate dehydrogenase in *Staphylococcus epidermidis*.[39, 40] It also targets enzymes involved in the mediation of redox processes such as thioredoxin reductase.[41] Deactivation of oxidative enzymes interferes with metabolism of substrates like glucose and succinate, and disruption of redox enzymes may inhibit bacteria from controlling the formation of reactive oxygen species (ROS).

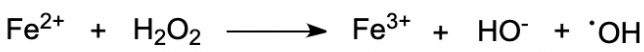

Figure 1.3: The Fenton reaction leads to the production of hydroxyl radicals when free iron is present in the cell

ROS like $O_2^{\cdot -}$ or H_2O_2 are by-products of normal cell metabolism; however, when they are not enzymatically neutralised, ROS can damage internal cell components like proteins, and iron-sulfur clusters.[42] When silver enters the cells and damages enzymes like superoxide dismutase, where the Ag^+ ion displaces the native Cu^+, ROS accumulate within the cell.[37] The damage of iron-sulfur clusters releases free iron into the cell which then undergoes the

Fenton reaction, leading to the formation of the hydroxyl radical, which is altogether more damaging to the cell than the previously mentioned ROS (*Fig. 1.4*).[42]

Silver has some lesser modes of action including damage to DNA which may occur either through direct DNA binding, by the formation of a condensed form of DNA, or through ROS-mediated damage.[35, 43, 44] Silver ions have been shown to bind specifically to N7 of guanine bases, and to a lesser extent, to adenine.[44] However, it has been shown that silver will preferentially bind to thiol groups in the presence of DNA, so a high intracellular concentration of silver may be required before direct binding to DNA occurs.[39] Silver may also bind to surface transport proteins, blocking channels for the transport of essential ions like phosphate into cells, which in turn interferes with ATP synthesis.[34] The high affinity of silver ions for protein-integrated thiol groups means Ag^+ has a plethora of targets within bacterial cells, causing cell death through multiple routes, and making the development of resistance considerably more difficult compared to single-target drugs.[32, 33]

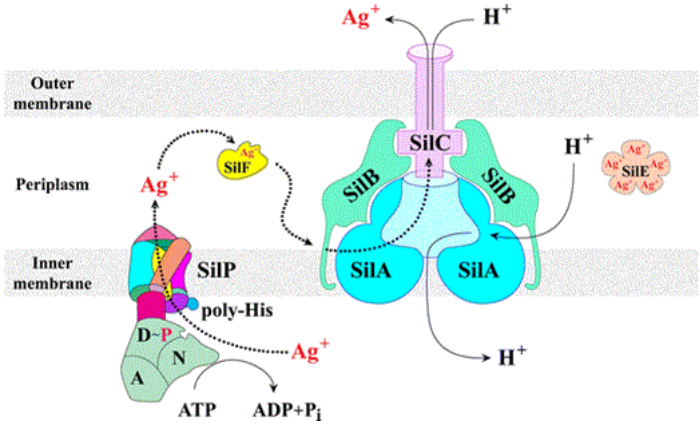

Figure 1.5: The silver efflux pumping system encoded by multiple Sil genes. The ATP-ase SilP pump transports silver ions from the cytoplasm to the periplasm and the SilCBA cation-proton antiporter transports silver ions out of the cell. SilF and SilE are silver binding proteins. Taken from [45]

Instances of silver-resistant bacteria have been limited (fewer than 20 reports between 1975 and 2007), but have emerged nonetheless.[32] Initially, clinical resistance was seen in *Salmonella enterica* in a hospital burn unit where silver sulfadiazine was used as a wound treatment.[43] Similar instances of silver resistance after exposure to silver sulfadiazine were seen in Enterobacteriaceae including *Klebsiella pneumoniae* and *E. coli*, and in *Pseudomonas aeruginosa* in clinical settings. [46, 47] Silver resistance appears to be controlled by a set of genes called *Sil* genes (*Fig. 1.5*). They encode two types of efflux pump: a p-type ATPase pump encoded by the *Sil*P gene, and a three-component cation/proton antiporter efflux pump encoded by the *Sil*CBA genes.[48] The ATPase pump transports silver ions from the cytoplasm

to the periplasm, and the cation/proton antiporter pump transports the ions from the periplasm out of the cell.[43] In addition to the efflux pumps there is also a gene, *Sil*E, which encodes an Ag^+ binding protein. Interestingly, the binding site for silver contains histidine residues instead of cysteine which is commonly seen in other heavy metal transporters.[49] Another Ag^+ binding protein, *Sil*F is presumed to carry silver ions to the *Sil*CBA pump since it is homologous to a similar protein seen in copper efflux systems.[45]

The *Sil* genes appear to mainly be encoded on bacterial plasmids, which can be shared through conjugation. There has, however, been evidence of silver resistance developing in *E.coli* which did not contain plasmids.[50] A study of silver resistance in MRSA found the *Sil*E gene to be present in some bacterial strains isolated from the environment; however, this gene alone was not enough to confer significant resistance, meaning the presence of all *Sil* genes may be necessary for silver resistance to be observed.[51]

1.4 Carbenes

Carbenes are neutral six-electron carbon species with two single bonds and two non-bonding electrons. The spins of the non-bonding electrons may either be paired (singlet state) or unpaired (triplet state) (*Fig. 1.6*). Triplet carbenes are generally regarded as diradicals and thus are unstable, transient species.[52] They may take on either linear or bent geometries, with the carbene carbon being sp or sp^2 hybridised, respectively. In the linear geometry, the non-bonding electrons are contained one each in a pair of degenerate P orbitals. In the case of bent triplet carbenes, one electron resides in a p orbital (termed the P_π orbital), and the other in a lower energy sp^2 orbital (termed the σ orbital).[53] Though the two orbitals in a bent triplet carbene are not degenerate, their energy difference is not as great as the cost of pairing the electrons. Ground-state singlet carbenes exist only in the bent geometry with the two non-bonding electrons paired in the σ orbital, while the P_π orbital remains empty. The difference between bent triplet and bent singlet carbenes can be visualised in the R-C:-R' bond angle. The angle is smaller in singlet carbenes (100-110°) than in triplet carbenes (130-150°).[54] This is because singlets have an extra electron in the sp^2 plane, causing greater repulsion of the two bonding pairs of electrons versus triplet carbenes where the electron in the P_π orbital does not interact with the bonding pairs.

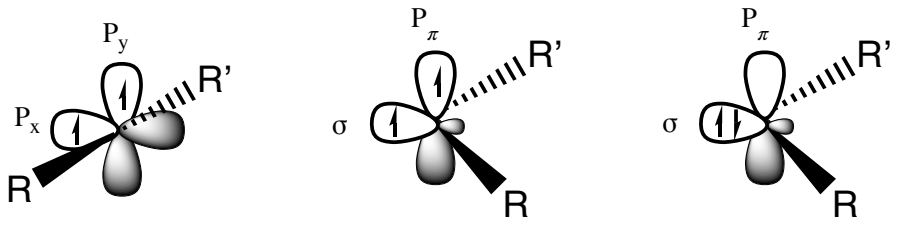

Figure 1.6: Ground state electron distribution in a linear triplet (left), a bent triplet (centre), and a bent singlet carbene (right)

Where non-bonding orbitals are not degenerate, the inductive and mesomeric effects of the α-substituents influence the energy gap between the σ and P_π orbitals. Thus, the electronic effects of the substituents determine the ground state spin multiplicity of the carbene.[55] Inductively electron withdrawing substituents lower the energy of the σ orbital, which widens the σ- P_π energy gap and favours the singlet state. Inductively donating α-substituents have the opposite effect: they raise the energy of the σ orbital, bringing it closer in energy to the P_π orbital and favouring the triplet state.[52] Mesomeric effects play a larger role in influencing the ground state multiplicity. Substituents which are π-acceptors lower the energy of the P_π orbital, leading to a triplet ground state. Conversely, π-donating substituents add electron density to the P_π orbital of the carbene, raising its energy relative to the σ orbital, and creating a larger energy gap.[53]

1.5 *N*-Heterocyclic Carbenes

The additive effect of inductively withdrawing, π-donating α-substituents leads to a singlet carbene which is especially stable in the ground state. Diaminocarbenes, especially *N*-heterocyclic carbenes (NHCs), are widely exploited examples of this. The electronegative nitrogen atoms draw electron density away from the carbene σ orbital while simultaneously donating π-electron density from their lone pairs into the carbene P_π orbital.

Wanzlick was the first to propose these stable species, postulating that the free carbenes were in an equilibrium with enetetraamine dimers.[56] He later showed the nucleophilic carbene species could act as ligands with transition metals, however his inability to isolate the carbenes themselves meant the work did not initially gain significant interest.[57] It was not until much later in 1991 that the first stable diaminocarbene, derived from 1,3-di-1-adamantylimidazolium chloride, was isolated and characterised by Arduengo.[58] Initially, it was thought that a combination of the bulky adamantyl substituents and the unsaturation of the imidazole ring were both crucial to the stabilisation

of the free carbene over the dimeric species Wanzlick had observed. However, subsequent isolation of other free carbenes including an *N*-methyl substituted imidazol-2-ylidene and a saturated imidazolin-2-ylidene proved this to not necessarily be true.[59, 60] It is unclear, however, how much of a role the large *N*-mesityl substituents of the saturated carbene played in the stabilisation of the free carbene species. While unsaturated NHCs don't necessarily experience true aromatic delocalisation between the C=C double bond and the N lone pairs, they are still stabilised by roughly 20 kcal mol^{-1} more than their saturated analogues.[61]

1.6 *N*-Heterocyclic Carbene Complexes with Transition Metals

Undoubtedly, the most common application of NHCs in recent years has been as ligands in metal complexes, but metal-carbene complexes are not a new concept. Fischer was the first to synthesise such complexes from metal carbonyls in the 1960s; making a singlet carbene that was a good σ-donor but relied heavily on π-back donation from a low oxidation state metal for stability.[62] Schrock pioneered an alternate type of carbene complexes which differ in that they are triplet carbenes, and require a high oxidation state early transition metal to minimise repulsion between the electron in the carbene P_π orbital and electrons in metal d orbitals.[63] Both Fischer and Schrock carbenes are considered to have double bonds to the metal centre since they interact in the σ and π planes (*Fig.* 1.7). Although NHCs bear more similarity to Fischer carbenes in structure— they are ground state singlets and good σ-donors with at least one π-donating α-substituent on the carbene centre— they differ in that NHCs experience far less π-back donation from the metal to the carbene P_π orbital leaving the metal-NHC bond to be considered only a single bond.[64] Because of the differences in stability and extent of occupation of the carbene P_π orbital, NHCs behave as nucleophiles while Fischer carbenes are considered electrophilic.[52]

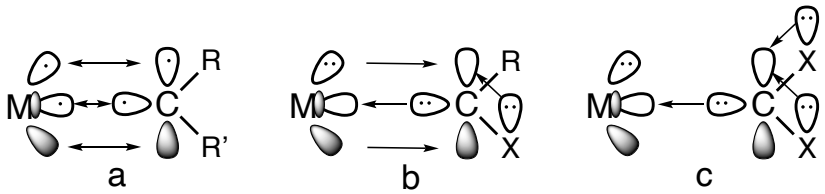

Figure 1.7: Metal-carbene bonding in (a) Schrock-type carbenes, (b) Fischer-type carbenes, and (c) NHCs. X=electron donating substituent

Strong σ-donation from the carbene lone pair into the metal dz^2 orbital is the major bonding interaction between metals and NHCs.[65] Back donation from the metal d_{xz} or d_{yz}

orbitals into the carbene P_π orbital exists but is generally not considered significant due to the carbene orbital already being stabilised by the nitrogen lone pairs. This becomes apparent in the existence of NHC adducts of metals like magnesium and beryllium which lack π valence electrons altogether.[53] However, computational studies have shown the possibility of appreciable π interactions in complexes with the electron-rich group 11 metals.[66, 67]

Much initial interest in NHCs as ligands arises from their consideration as phosphine analogues since both are neutral, two-electron donors. In fact, NHCs appear to be better donor ligands than phosphines, showing higher bond dissociation energies in ruthenium complexes in all cases except for extremely sterically demanding *N*-substituents on the carbenes.[52] NHCs are also favourable to phosphines since their steric properties can be varied with little effect on electronics. This is a result of the substituent groups in NHCs being two or more bonds away from the donor atom, whereas substituents are directly bonded to the P donor atom in phosphines.[68] Changes to electronic effects in NHCs may be achievable by variation of the type of azole ring, with saturated imidazoline derivatives showing greater donor abilities than imidazole derived NHCs.[69]

These attractive properties of NHCs have seen them replace phosphines in the case of some transition metal catalysts—notably Grubbs' olefin metathesis catalyst (*Fig. 1.8*). Substitution of tri-cyclohexyl phosphine for a saturated 1,3-dimesitylimidazolin-2-ylidene ligand improved the ability of the catalyst to bind the olefin substrate and increased the catalyst's thermal stability.[70] There have also been examples of the incorporation of NHC ligands into palladium catalysts for C-C and C-N cross coupling reactions.[71]

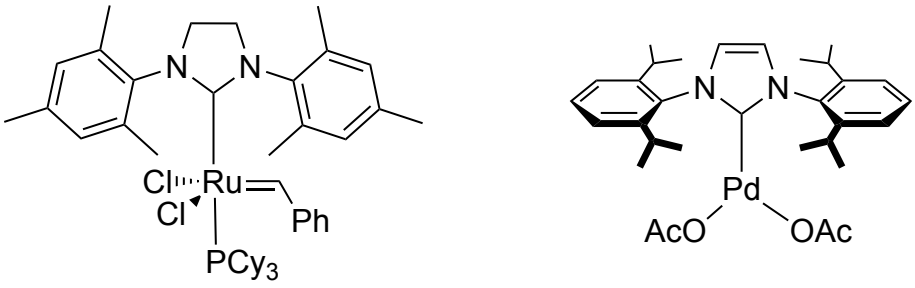

Figure 1.8: Incorporation of NHC ligands into Grubbs' olefin metathesis catalyst (left),[70] and a palladium pre-catalyst for Suzuki-Miyaura couplings (right) [72]

Steric effects can play a significant role in the strength of NHC-metal bonding. The buried volume ($\%V_{bur}$) of the NHC ligand refers to the extent which an NHC ligand occupies a sphere which is centred on the metal.[73] The buried volume changes based on the identity of the

N-substituents on the ligand. Bulkier substituents show a negative correlation with the dissociation energy of the metal carbene bond.[69] This is likely a result of sterically demanding substituents interfering with orbital overlap between the carbene and metal.

1.7 Silver Complexes of *N*-Heterocyclic Carbenes

While NHCs are seen as ligands with a wide range of metals and main group elements, silver has become an exceptionally popular choice of metal for carbene complexes. One reason for this is that silver NHC complexes are easily achievable by a wide range of relatively mild reaction conditions. Silver complexes can be synthesised directly from the reaction of a free carbene species with a silver salt.[74] The anion of the salt can vary broadly from halides to non-coordinating anions like tetrafluoroborate, and to carboxylate species. The major drawbacks of this synthetic route are the sensitivity of the free carbenes to air and moisture, and the formation of side products due to the reactivity of the carbene.[75]

A milder approach employs a silver base in the presence of an azolium salt. The silver base deprotonates the salt *in situ,* forming the carbene while simultaneously metalating it. The concerted nature of this reaction bypasses the generation of the free carbene and thus can be easily carried out in atmospheric conditions.[64] In fact, reactions of this type have even been carried out successfully with water as the solvent.[76] Multiple silver bases have been used, the most popular being silver (I) oxide. Silver carbonate can also be used but generally requires longer reaction times.[77] Silver acetate may also be used in reactions where the desired product is an NHC-Ag-acetate complex.[78] Other synthetic routes exist which use an azolium salt and a silver salt (such as AgCl or AgBr) in the presence of a weak base (e.g., potassium carbonate) as well as a phase transfer catalyst.[79] However, the outcome of this is the same as if silver (I) oxide were used as the base, so it does not hold a necessary advantage.

In both the free-carbene synthesis and the silver base synthesis, the identity of the anion (of the silver salt or the azolium salt, respectively) plays a crucial role in the structure of the product complex. Where the anion is non-coordinating, the result is a cationic *bis*-carbene silver complex, the main exception being chelating ligands with more than one carbene centre which may form polymeric species.[64] For coordinating anions such as halogens or carboxylates, the product generally has the empirical formula [(NHC)Ag]X. However, where X

is a halogen, there exist a multitude of structural motifs in the solid state (*Fig*. 1.9).[64, 80] The solid-state structures are dependent on multiple factors including the steric demands and functionality of the N-substituents, the type of azole ring, and the identity of the halide, making it difficult to predict the solid-state structure of the complexes.[64, 80]

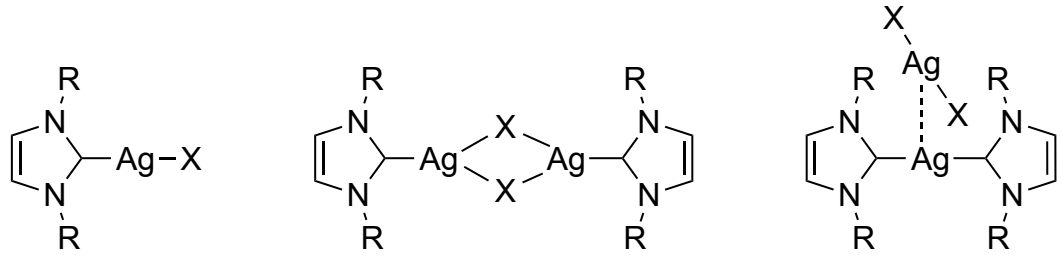

Figure 1.9: Examples of structural motifs in [(NHC)Ag]X complexes. X=Cl, Br, or I

Because of their facile synthesis and the relative lability of the Ag-carbene bond, Ag(I)-NHC complexes have found popular use as carbene transfer reagents for metals such as Au^{I}, Pd^{II}, Pt^{II}, Ru^{III}, and Rh^{I}.[75] Generally, NHC-Ag-X complexes are chosen as the transmetallating agents because the precipitation of an insoluble silver halide salt drives the reaction.[81]

NHC-silver complexes have also gained exceptional popularity as possible antibiotic drug candidates. Because of the strong σ-donating ability of the NHC ligand, silver is stabilised, and even in the presence of chloride ions, decomposes much more slowly than a silver salt (whose precipitation of AgCl would be almost immediate).[64] NHCs are also easily functionalised which is another very attractive feature in drug design. A number of diverse NHC-silver complexes have been synthesised and tested against common pathogenic bacteria and fungi (*Fig. 1.10*).[82]

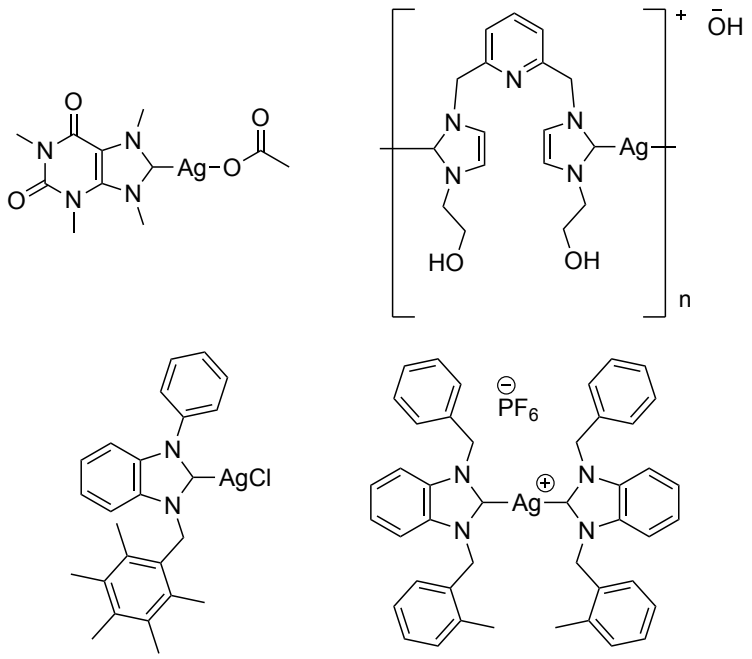

Figure 1.10: Silver NHC complexes developed by the Youngs group[83] (top), the Gok group[84] (bottom left), and the Haque group[85] (bottom right)

Some of the first examples of complexes synthesised for the investigation of their antibacterial properties were introduced by the Youngs group. They reported complexes of pyridine-linked pincer ligands which formed polymeric *bis*-NHC silver complexes in the solid state.[86] The Youngs group also reported an NHC precursor from methylated caffeine that was used to form both an NHC-Ag-acetate complex as well as cationic *bis*-NHC silver complexes.[87] All the reported complexes showed superior stability compared to silver nitrate, as well as improved minimum inhibitory concentrations (MICs) against *E. coli*, *S. aureus*, and *Pseudomonas aeruginosa*. The caffeine-derived silver acetate complex showed MIC values of between 1 and 10 μg mL^{-1} against a range of bacteria including *E. coli*, *S. aureus,* and *Burkholderia cepacia,* as well as the fungus *Candida albicans*.[83] The Youngs group also reported an 'electronically tuned' NHC ligand from a 4,5-dichloro-1,3-dimethyl imidazole whose silver acetate complex showed exceptional stability in deuterated water (only 34% had decomposed after 17 weeks).[78] The complex also displayed good antimicrobial activity, with MIC value of 1-4 μg mL^{-1} against a range of clinically relevant pathogenic bacteria.

The work of Gok *et al.* focused on the synthesis of *N*-phenyl substituted benzimidazole derived NHCs and their silver chloride complexes. They reported MIC values of 25-100 μg mL^{-1} against bacteria including *E. coli, Klebsiella pneumoniae, S. aureus,* and *Bacillus subtilis*. The silver complexes were outperformed by the in-use antibiotic tetracycline in most all cases.[84] The Haque group also reported benzimidazole-derived NHC complexes of silver. They

synthesised both mono- and bidentate ligands, leading to mono- and dinuclear silver complexes, respectively. In disc-diffusion tests, the silver complexes showed activity which was comparable to or slightly below that of the antibiotic drug ampicillin.[85] Importantly, both Gok and Haque saw a trend of increasing antimicrobial activity with the increasing lipophilicity of their compounds, which was accredited to the improved ability of the complexes to cross the cell membrane.[84, 85, 88]

Further work in the area of NHC-silver antimicrobials has been carried out by our group.[89-94] The NHC ligands were derived from *N*-alkylated or N-arylated 4,5-diphenyl imidazole and were initially used to form the corresponding silver acetate. The lead compound identified by our group, SBC3, was formed from 1,3-dibenzyl-4,5-diphenyl imidazolium bromide and silver acetate (*Fig. 1.11*).

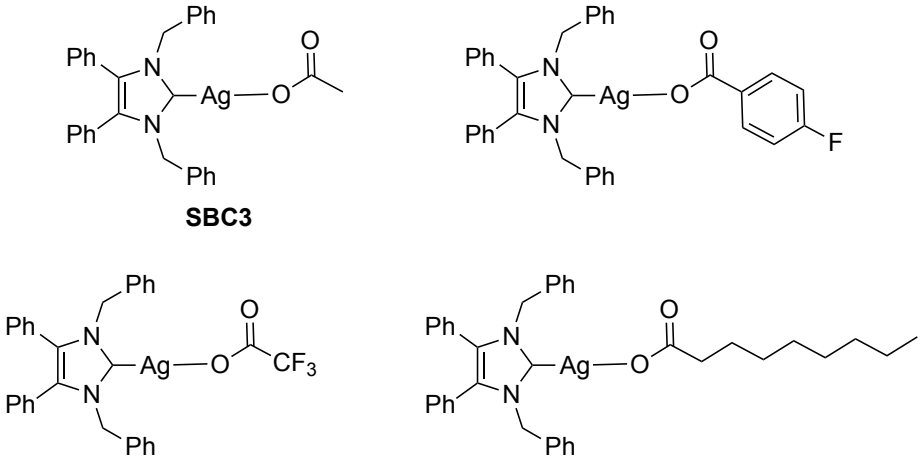

Figure 1.11: The Tacke group lead compound SBC3 and other complexes synthesised by the group which utilise the 1,3-dibenzyl-4,5-diphenyl imidazol-2-ylidene ligand

Of the complexes synthesised by the Tacke group, SBC3 has continuously shown good antimicrobial activity with MIC values between 3 and 12.5 μg mL^{-1} against bacteria such as *P. aeruginosa, E. coli,* and MRSA.[95] An insect model of SBC3 in *Galleria mellonella* larvae showed increased survival in larvae infected with either *S. aureus* or *C. albicans* which were subsequently administered SBC3.[96] More recent work in the group has utilised the same NHC ligand used in SBC3, but has looked at variation of the carboxylate ligand to target specific virulence factors such as biofilm formation.[93] Similar to previous results, the complexes show activity which is overall comparable to that of SBC3, but none have significantly outperformed the lead compound.

1.8 The Role of Fluorination in Medicinal Chemistry

Despite the presence of fluorine in natural products being a relatively rare phenomenon,[97] fluorination has become a popular motif in the design of drug molecules (*Fig. 1.12*). Among its purported advantages are increased metabolic stability, increased lipophilicity, and increased enzyme binding affinities.[98] Fluorination can also have a very pronounced effect on molecular conformations and on pK_a of nearby functional groups.[99] The small size of the fluorine atom makes it bioisosteric to hydrogen, meaning it does not significantly affect the steric properties of a molecule so as to alter biological recognition.[100] This makes fluorine substitution a convenient method of modulating physical properties of molecules without changing the steric profile.

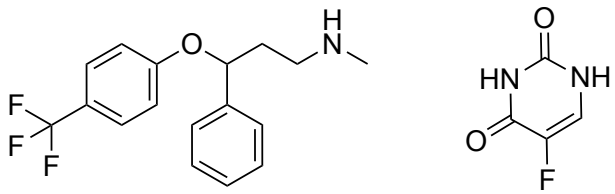

Fluoxetine 5-Fluorouracil

Figure 1.12: Examples of fluorinated drugs fluoxetine, an antidepressant, and 5-fluorouracil, an antineoplastic [98]

Incorporation of fluorine or trifluoromethyl groups is an efficient strategy for improving drug lipophilicity. In fact, the substitution of a trifluoromethyl group onto benzene increase the partition coefficient (log P) by 0.88.[101] Increased lipophilicity in drugs can improve their uptake by facilitating diffusion across lipid bilayers in cells.[102]

The strength of the C-F bond can also play an important role in metabolism of drugs. Fluorination of aromatic rings can block oxidation by cytochrome enzymes at specific sites, and incorporation of trifluoromethyl groups may completely inhibit oxidation. Where drugs show short half lives *in vivo* fluorination becomes an attractive tool to increase bioavailability.[100, 102] Fluorination represents an attractive route to tuning physicochemical and pharmacokinetic properties in drug design.

1.9 Continuous Flow Chemistry

Flow chemistry utilises the continuous pumping of liquid or dissolved reagents through a reactor. Types of common reactors include coiled reactors, chip reactors and packed bed reactors.[103] Continuous flow reactors can be combined in-line to incorporate multiple facets such as heating, pressurisation, microwave technology, electrochemistry,

heterogeneous catalysis, and solid-supported reagents to facilitate multiple transformations in a single process (*Fig. 1.13*).[104] Beyond reactors, there are also multiple separation techniques that can be employed in flow processes such as liquid-liquid extractions and solid-supported scavengers. Among the benefits of flow synthesis are higher yields, shortened reaction times, ease of scalability, and the ability to safely carry out reactions that would otherwise be dangerous (e.g., formation of unstable intermediates or high-pressure reactions). Furthermore, continuous flow reactors can be utilised to carry out reactions which would not be possible at all in batch synthesis, such as high temperature reactions in low boiling solvents, or electrochemical reactions which become limited by diffusion in larger-volume reactors.[103, 105] Much of the benefit of continuous flow chemistry results from the increased surface area at reagent interfaces caused by the small internal volume of the tubing.[106] Greater surface area leads to more interaction of reagents, increasing reaction rates and conversion of reagents to products.[103] Small volumes in reactors and tubing also allow for excellent heat transfer, expediting heating and cooling processes and negating temperature variation which might occur in a bulk solution.[107]

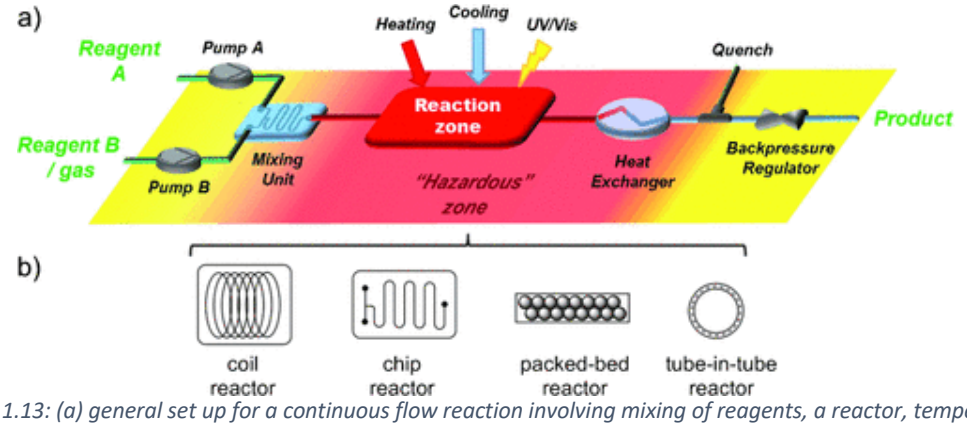

Figure 1.13: (a) general set up for a continuous flow reaction involving mixing of reagents, a reactor, temperature regulation, quenching, and pressure regulation. (b) examples of some commonly used reactors. Taken from [104]

The application of flow chemistry to industry has led to the production of active pharmaceutical ingredients from chemical intermediates, through the reaction, work up, purification, and formulation steps in a continuous manner.[108] In-line monitoring and precise control of parameters such as flow rate and temperature lead to consistent results without the need for rigorous post-production testing. Continuous flow chemistry poses an opportunity in industry for lowering costs and increasing efficiency, especially when looking at factors like energy input. Even in a research setting flow chemistry has many advantages

over traditional batch experiments, especially improved yields, ease of running reactions in small quantities, and ability to more safely handle hazardous reagents and intermediates. Despite the wealth of advantages presented by continuous flow chemistry, it is not always advantageous or even feasibly to carry out reactions in flow. For example, reactions which are already reliable and high yielding in batch mode present no need to be transferred into flow. Additionally reactions which rely on the formation of precipitates as a driving force are impractical to run in flow as precipitates will cause blockages in the reactors and tubing.[103]

1.10 References

[1] A.S. Evans, Causation and Disease - Henle-Koch Postulates Revisited, *Yale J. Biol. and Med.* 49(2) (1976) 175-195.

[2] R.I. Aminov, A Brief History of the Antibiotic Era: Lessons Learned and Challenges for the Future, *Frontiers in Microbiol.* 1 (2010).

[3] S. Riethmiller, From Atoxyl to Salvarsan: Searching for the Magic Bullet, *Chemotherapy* 51(5) (2005) 234-242.

[4] L. Zaffiri, J. Gardner, L.H. Toledo-Pereyra, History of Antibiotics. From Salvarsan to Cephalosporins, *J. Invest. Surg.* 25(2) (2012) 67-77.

[5] G. Domagk, Further Progress in Chemotherapy of Bacterial Infections, Nobel Lectures, Physiology or Medicine 1922-1941, Elsevier, Amsterdam, 1965.

[6] D. Greenwood, Sulfonamides, in: R.G. Finch, D. Greenwood, S.R. Norrby, R.J. Whitley (Eds.), *Antibiot. and Chemother.*, Elsevier2011, pp. 337-343.

[7] L. Jourova, P. Anzenbacher, E. Anzenbacherova, Human gut microbiota plays a role in the metabolism of drugs, *Biomed. Pap. Olomouc* 160(3) (2016) 317-326.

[8] A. Fleming, On the Antibacterial Action of Cultures of a *Penicillium*, with Special Reference to their Use in the Isolation of *B. influenzae*, *Brit. J. Exp. Pathol.* 10((3)) (1929) 226-236.

[9] E. Chain, H.W. Florey, A.D. Gardner, N.G. Heatley, et al., Penicillin as a Chemotherapeutic Agent, *Lancet* 239(6104) (1940) 226-228.

[10] K. Gould, Antibiotics: From Prehistory to the Present Day, *J. Antimicrob. Chemother.* 71(3) (2016) 572-575.

[11] T. Saga, K. Yamaguchi, History of Antimicrobial Agents and Resistant Bacteria, *Jap. Med. Assoc. J.* 52(2) (2009) 103-108.

[12] S. Malmir, M. Bahreinian, S.Z. Yeganeh, R. Mirnejad, M.M. Moghaddam, F. Saberi, Molecular Mechanisms of Resistance to Conventional Antibiotics in Bacteria, *Int. J. Med. Rev.* 5(3) (2018) 118-129.

[13] K. Lewis, Recover the lost art of drug discovery, *Nature* 485(7399) (2012) 439-440.

[14] B. Spellberg, J.H. Powers, E.P. Brass, L.G. Miller, J.E. Edwards, Trends in Antimicrobial Drug Development: Implications for the Future, *Clin. Infect. Dis.* 38(9) (2004) 1279-1286.

[15] W.M.M. Kirby, L.A. Rantz, Quantitative Studies of Sulfonamide Resistance, *J. Exper. Med.* 77(1) (1943) 11.

[16] C.L. Ventola, The Antibiotic Resistance Crisis Part 1: Causes and Threats, *Pharm. and Therap.* 40(4) (2015) 277-283.

[17] J. Davies, D. Davies, Origins and Evolution of Antibiotic Resistance, *Microbiol. and Mol. Biol. Rev.* 74(3) (2010) 417-433.

[18] C.A. Michael, D. Dominey-Howes, M. Labbate, The antimicrobial resistance crisis: causes, consequences, and management, *Frontiers in Pub. Health* 2 (2014) 145-145.

[19] WorldHealthOrganisation, Antimicrobial Resistance Global Report on Surveillance, World Health Organisation, Geneva, Switzerland, 2014.

[20] L.S. Frost, R. Leplae, A.O. Summers, A. Toussaint, Mobile Genetic Elements: The Agents of Open Source Evolution, *Nat. Rev. Microbiol.* 3(9) (2005) 722-732.

[21] D. Sun, K. Jeannot, Y. Xiao, C.W. Knapp, Editorial: Horizontal Gene Transfer Mediated Bacterial Antibiotic Resistance, *Frontiers in Microbiol.* 10 (2019).

[22] C. Walsh, Molecular Mechanisms that Confer Antibacterial Drug Resistance, *Nature* 406(6797) (2000) 775-781.

[23] J.M.A. Blair, M.A. Webber, A.J. Baylay, D.O. Ogbolu, L.J.V. Piddock, Molecular Mechanisms of Antibiotic Resistance, *Nat. Rev. Microbiol.* 13(1) (2015) 42-51.

[24] G.D. Wright, Molecular Mechanisms of Antibiotic Resistance, *Chem. Comm.* 47(14) (2011) 4055-4061.

[25] J.A. Brannigan, I.A. Tirodimos, Q.Y. Zhang, C.G. Dowson, B.G. Spratt, Insertion of and Extra Amino Acid is the Main Cause of the Low Affinity of Penicillin-Binding Protein-2 in Penicillin-Resistant Strains of *Neisseria-Gonorrhoeae*, *Mol. Microbiol.* 4(6) (1990) 913-919.

[26] C.J. Thomson, S.G.B. Amyes, TRC-1 - Emergence of a Clavulanic Acid-Resistant TEM Beta-Lactamase in a Clinical Strain, *Fems Microbiol. Lett.* 91(2) (1992) 113-117.

[27] N. London, C.J. Thomson, S.G.B. Amyes, E. Stobberingh, A Piperacillin-Tazobactam Resistant *Escherichia coli* Strain Isolated from a Fecal Sample of a Healthy Volunteer, *Fems Immunol. and Med. Microbiol.* 11(2) (1995) 107-111.

[28] J.W. Alexander, History of the Medical Use of Silver, *Surg. Infect.* 10(3) (2009) 289-292.

[29] V.G. Vecki, M.R. Ottinger, Treatment of Syphilis with Silver Salvarsan, *California State J. Med.* 19(11) (1921) 438-438.

[30] C.L. Fox, S.M. Modak, Mechanism of Silver Sulfadiazine Action on Burn Wound Infections, *Antimicrob. Agents and Chemother.* 5(6) (1974) 582-588.

[31] A.D. Politano, K.T. Campbell, L.H. Rosenberger, R.G. Sawyer, Use of Silver in the Prevention and Treatment of Infections: Silver Review, *Surg. Infect.* 14(1) (2013) 8-20.

[32] I. Chopra, The Increasing Use of Silver-Based Products as Antimicrobial Agents: A Useful Development or a Cause for Concern?, *J. Antimicrob. Chemother.* 59(4) (2007) 587-590.

[33] H. Brötz-Oesterhelt, N.A. Brunner, How Many Modes of Action Should an Antibiotic Have?, *Curr. Opin. Pharm.* 8(5) (2008) 564-573.

[34] S. Medici, M. Peana, V.M. Nurchi, M.A. Zoroddu, Medical Uses of Silver: History, Myths, and Scientific Evidence, *J. Med. Chem.* 62(13) (2019) 5923-5943.

[35] Q.L. Feng, J. Wu, G.Q. Chen, F.Z. Cui, T.N. Kim, J.O. Kim, A Mechanistic Study of the Sntibacterial Effect of Silver Ions on *Escherichia coli* and *Staphylococcus aureus*, *J. Biomed. Mater. Res.* 52(4) (2000) 662-668.

[36] S.A. Anuj, H.P. Gajera, D.G. Hirpara, B.A. Golakiya, Interruption in Membrane Permeability of Drug-Resistant Staphylococcus aureus with Cationic Particles of Nano-Silver, *Eur. J. Pharm. Sci.* 127 (2019) 208-216.

[37] J.A. Lemire, J.J. Harrison, R.J. Turner, Antimicrobial activity of metals: mechanisms, molecular targets and applications, *Nat. Rev. Microbiol.* 11(6) (2013) 371-384.

[38] P. Dibrov, J. Dzioba, K.K. Gosink, C.C. Hase, Chemiosmotic Mechanism of Antimicrobial Activity of Ag+ in *Vibrio cholerae*, *Antimicrob. Agents and Chemother.* 46(8) (2002) 2668-2670.

[39] O. Gordon, T.V. Slenters, P.S. Brunetto, A.E. Villaruz, D.E. Sturdevant, M. Otto, R. Landmann, K.M. Fromm, Silver Coordination Polymers for Prevention of Implant Infection: Thiol Interaction, Impact on Respiratory Chain Enzymes, and Hydroxyl Radical Induction, *Antimicrob. Agents and Chemother.* 54(10) (2010) 4208-4218.

[40] P.D. Bragg, D.J. Rainnie, Effect of Silver Ions on the Respiratory-Chain of *Escherichia coli*, *Can. J. Microbiol.* 20(6) (1974) 883-889.

[41] J. O'Loughlin, S. Napolitano, F. Alkhathami, C. O'Beirne, D. Marhofer, M. O'Shaughnessy, O. Howe, M. Tacke, M. Rubini, The Antibacterial Drug Candidate SBC3 is a Potent Inhibitor of Bacterial Thioredoxin Reductase, *Chembiochem* 22(6) (2021) 1093-1098.

[42] J.A. Imlay, Pathways of oxidative damage, *Ann. Rev. Microbiol.* 57 (2003) 395-418.

[43] K. Mijnendonckx, N. Leys, J. Mahillon, S. Silver, R. Van Houdt, Antimicrobial silver: uses, toxicity and potential for resistance, *Biometals* 26(4) (2013) 609-621.

[44] H. Arakawa, J.F. Neault, H.A. Tajmir-Riahi, Silver(I) Complexes with DNA and RNA Studied by Fourier Transform Infrared Spectroscopy and Capillary Electrophoresis, *Biophys. J.* 81(3) (2001) 1580-1587.

[45] S. Silver, L.T. Phung, G. Silver, Silver as Biocides in Burn and Wound Dressings and Bacterial Resistance to Silver Compounds, *J. Ind. Microbiol. & Biotech.* 33(7) (2006) 627-634.

[46] A.T. Hendry, I.O. Stewart, Silver-Resistant Enterobacteriacae from Hospital Patients, *Can. J. Microbiol.* 25(8) (1979) 915-921.

[47] S.M. Modak, C.L. Fox, Sulfadiazine Silver-Resistant *Pseudomonas* in Burns - New Topical Agents, *Archives Surg.* 116(7) (1981) 854-857.

[48] S. Silver, Bacterial Silver Resistance: Molecular Biology and Uses and Misuses of Silver Compounds, *Fems Microbiol. Rev.* 27(2-3) (2003) 341-353.

[49] A. Gupta, K. Matsui, J.F. Lo, S. Silver, Molecular Basis for Resistance to Silver Cations in *Salmonella*, *Nat. Med.* 5(2) (1999) 183-188.

[50] D.E. Marx, D.J. Barillo, Silver in medicine: the basic science, *Burns : J. Int. Soc. Burn Inj.* 40 Suppl 1 (2014) S9-S18.

[51] J.V. Loh, S.L. Percival, E.J. Woods, N.J. Williams, C.A. Cochrane, Silver resistance in MRSA isolated from wound and nasal sources in humans and animals, *Int. Wound J.* 6(1) (2009) 32-38.

[52] P. de Fremont, N. Marion, S.P. Nolan, Carbenes: Synthesis, Properties, and Organometallic Chemistry, *Coord. Chem. Rev.* 253(7-8) (2009) 862-892.

[53] D. Bourissou, O. Guerret, F.P. Gabbai, G. Bertrand, Stable Carbenes, *Chem. Rev.* 100(1) (2000) 39-91.

[54] J. Clayden, N. Greeves, S. Warren, Organic Chemistry, Second ed., Oxford University Press, New York, 2001.

[55] F.E. Hahn, M.C. Jahnke, Heterocyclic carbenes: Synthesis and coordination chemistry, *Angewandte Chemie Int. Ed.* 47(17) (2008) 3122-3172.

[56] V.P.W. Bohm, W.A. Herrmann, The "Wanzlick Equilibrium", *Angewandte Chemie Int. Ed.* 39(22) (2000) 4036-4038.

[57] H.W. Wanzlick, Schonher.Hj, Direct Synthesis of a Mercury Salt Carbene Complex, *Angewandte Chemie Int. Ed.* 7(2) (1968) 141-&.

[58] A.J. Arduengo, R.L. Harlow, M. Kline, A Stable Crystalline Carbene, *J. Am. Chem. Soc.* 113(1) (1991) 361-363.

[59] A.J. Arduengo, J.R. Goerlich, W.J. Marshall, A Stable Diaminocarbene, *J. Am. Chem. Soc.* 117(44) (1995) 11027-11028.

[60] A.J. Arduengo, H.V.R. Dias, R.L. Harlow, M. Kline, Electronic Stabilization of Nucleophilic Carbenes, *J. Am. Chem. Soc.* 114(14) (1992) 5530-5534.

[61] C. Heinemann, T. Muller, Y. Apeloig, H. Schwarz, On the question of stability, conjugation, and ''aromaticity'' in imidazol-2-ylidenes and their silicon analogs, *J. Am. Chem. Soc.* 118(8) (1996) 2023-2038.

[62] G. Frenking, M. Sola, S.F. Vyboishchikov, Chemical Bonding in Transition Metal Carbene Complexes, *J. Organomet. Chem.* 690(24-25) (2005) 6178-6204.

[63] J. Santamaria, E. Aguilar, Beyond Fischer and Schrock Carbenes: Non-Heteroatom-Stabilized Group 6 Metal Carbene Complexes - A General Overview, *Org. Chem. Frontiers* 3(11) (2016) 1561-1588.

[64] J.C. Garrison, W.J. Youngs, Ag(I) N-Heterocyclic Carbene Complexes: Synthesis, Structure, and Application, *Chem. Rev.* 105(11) (2005) 3978-4008.

[65] H. Jacobsen, A. Correa, A. Poater, C. Costabile, L. Cavallo, Understanding the M-(NHC) (NHC = N-heterocyclic carbene) bond, *Coord. Chem. Rev.* 253(5-6) (2009) 687-703.

[66] D. Nemcsok, K. Wichmann, G. Frenking, The Significance of Pi Interactions in Group 11 Complexes with N-heterocyclic Carbenes, *Organometallics* 23(15) (2004) 3640-3646.

[67] X.L. Hu, Y.J. Tang, P. Gantzel, K. Meyer, Silver complexes of a novel tripodal N-heterocyclic carbene ligand: Evidence for significant metal-carbene pi-interaction, Organometallics 22(4) (2003) 612-614.

[68] R.H. Crabtree, NHC Ligands versus Cyclopentadienyls and Phosphines as Spectator Ligands in Organometallic Catalysis, *J. Organomet. Chem.* 690(24-25) (2005) 5451-5457.

[69] A.C. Hillier, W.J. Sommer, B.S. Yong, J.L. Petersen, L. Cavallo, S.P. Nolan, A combined experimental and theoretical study examining the binding of N-heterocyclic carbenes (NHC) to the Cp*RuCl (Cp* = eta(5)-C5Me5) moiety: Insight into stereoelectronic differences between unsaturated and saturated NHC ligands, *Organometallics* 22(21) (2003) 4322-4326.

[70] M. Scholl, T.M. Trnka, J.P. Morgan, R.H. Grubbs, Increased Ring Closing Metathesis Activity of Ruthenium-Based Olefin Metathesis Catalysts Coordinated with Imidazolin-2-ylidene Ligands, *Tetrahedron Lett.* 40(12) (1999) 2247-2250.

[71] E.A.B. Kantchev, C.J. O'Brien, M.G. Organ, Palladium complexes of N-heterocyclic carbenes as catalysts for cross-coupling reactions - A synthetic chemist's perspective, *Angewandte Chemie Int. Ed.* 46(16) (2007) 2768-2813.

[72] R. Singh, M.S. Viciu, N. Kramareva, O. Navarro, S.P. Nolan, Simple (imidazol-2-ylidene)-Pd-Acetate Complexes as Effective Precatalysts for Sterically Hindered Suzuki-Miyaura Couplings, *Org. Lett.* 7(9) (2005) 1829-1832.

[73] M.N. Hopkinson, C. Richter, M. Schedler, F. Glorius, An overview of N-heterocyclic carbenes, *Nature* 510(7506) (2014) 485-496.

[74] A.J. Arduengo, H.V.R. Dias, J.C. Calabrese, F. Davidson, Homoleptic Carbene Silver (I) and Carbene Copper (I) Complexes, *Organometallics* 12(9) (1993) 3405-3409.

[75] I.J.B. Lin, C.S. Vasam, Silver(I) N-heterocyclic carbenes, *Comments on Inorg. Chem.* 25(3-4) (2004) 75-129.

[76] J.C. Garrison, R.S. Simons, C.A. Tessier, W.J. Youngs, Synthesis and Structural Characterization of a Ag-4 (4+) Cluster Stabilized by a Mixed-Donor N-Heterocyclic Carbene Linked Cyclophane and the First Reported Synthesis of a N-Heterocyclic Carbene Complex in Water, *J. Organomet. Chem.* 673(1-2) (2003) 1-4.

[77] A.A.D. Tulloch, A.A. Danopoulos, S. Winston, S. Kleinhenz, G. Eastham, N-Functionalised heterocyclic carbene complexes of silver, *J. Chem. Soc. Dalton Trans.* (24) (2000) 4499-4506.

[78] K.M. Hindi, T.J. Siciliano, S. Durmus, M.J. Panzner, D.A. Medvetz, D.V. Reddy, L.A. Hogue, C.E. Hovis, J.K. Hilliard, R.J. Mallet, C.A. Tessier, C.L. Cannon, W.J. Youngs, Synthesis, stability, and antimicrobial studies of electronically tuned silver acetate N-heterocyclic carbenes, *J. Med. Chem.* 51(6) (2008) 1577-1583.

[79] H.M.J. Wang, I.J.B. Lin, Facile Synthesis of Silver(I)-Carbene complexes. Useful Carbene Transfer Agents, *Organometallics* 17(5) (1998) 972-975.

[80] I.J.B. Lin, C.S. Vasam, Preparation and application of N-heterocyclic carbene complexes of Ag(I), *Coord. Chem. Rev.* 251(5-6) (2007) 642-670.

[81] H.V. Huynh, Group 11 Metal-NHC Complexes, The Organometallic Chemistry of N-heterocyclic Carbenes, Wiley2017, pp. 183-194.

[82] N.A. Johnson, M.R. Southerland, W.J. Youngs, Recent Developments in the Medicinal Applications of Silver-NHC Complexes and Imidazolium Salts, *Molecules* 22(8) (2017).

[83] A. Kascatan-Nebioglu, M.J. Panzner, C.A. Tessier, C.L. Cannon, W.J. Youngs, N-Heterocyclic carbene-silver complexes: A new class of antibiotics, *Coord. Chem. Rev.* 251(5-6) (2007) 884-895.

[84] Y. Gok, S. Akkoc, S. Albayrak, M. Akkurt, M.N. Tahir, N- Phenyl- substituted carbene precursors and their silver complexes: synthesis, characterization and antimicrobial activities, *App. Organomet Chem.* 28(4) (2014) 244-251.

[85] R.A. Haque, S.Y. Choo, S. Budagumpi, M.A. Iqbal, A.A.-A. Abdullah, Silver(I) complexes of mono- and bidentate N-heterocyclic carbene ligands: Synthesis, crystal structures, and in vitro antibacterial and anticancer studies, *Eur. J. Med. Chem.* 90 (2015) 82-92.

[86] A. Melaiye, R.S. Simons, A. Milsted, F. Pingitore, C. Wesdemiotis, C.A. Tessier, W.J. Youngs, Formation of water-soluble pincer silver(I)-carbene complexes: A novel antimicrobial agent, *J. Med. Chem.* 47(4) (2004) 973-977.

[87] A. Kascatan-Nebioglu, A. Melaiye, K. Hindi, S. Durmus, M.J. Panzner, L.A. Hogue, R.J. Mallett, C.E. Hovis, M. Coughenour, S.D. Crosby, A. Milsted, D.L. Ely, C.A. Tessier, C.L. Cannon, W.J. Youngs, Synthesis from caffeine of a mixed N-heterocyclic carbene-silver acetate complex active against resistant respiratory pathogens, *J. Med. Chem.* 49(23) (2006) 6811-6818.

[88] C.M. Che, R.W.Y. Sun, Therapeutic Applications of Gold Complexes: Lipophilic Gold(III) Cations and Gold(I) Complexes for Anti-Cancer Treatment, *Chem. Comm.* 47(34) (2011) 9554-9560.

[89] S. Patil, A. Deally, B. Gleeson, H. Mueller-Bunz, F. Paradisi, M. Tacke, Novel benzyl-substituted N-heterocyclic carbene-silver acetate complexes: synthesis, cytotoxicity and antibacterial studies, *Metallomics* 3(1) (2011) 74-88.

[90] C. O'Beirne, H.T. Althani, O. Dada, J. Cassidy, K. Kavanagh, H. Muller-Bunz, Y. Ortin, X. Zhu, M. Tacke, Novel Derivatives of the Antibiotic NHC-Ag(I) Drug Candidate SBC3: Synthesis, Biological Evaluation and Ag-109 NMR Studies, *Polyhedron* 149 (2018) 95-103.

[91] C. O'Beirne, N.F. Alhamad, Q.X. Ma, H. Muller-Bunz, K. Kavanagh, G. Butler, X.M. Zhu, M. Tacke, Synthesis, Structures and Antimicrobial Activity of Novel NHC*- and Ph3P-Ag (I)-Benzoate Derivatives, *Inorg. Chimica Acta* 486 (2019) 294-303.

[92] W. Streciwilk, J. Cassidy, F. Hackenberg, H. Muller-Bunz, F. Paradisi, M. Tacke, Synthesis, cytotoxic and antibacterial studies of p-benzyl-substituted NHC-silver(I) acetate compounds derived from 4,5-di-p-diisopropylphenyl- or 4,5-di-p-chlorophenyl-1H-imidazole, *J. Organomet. Chem.* 749 (2014) 88-99.

[93] C. O'Beirne, M.E. Piatek, J. Fossen, H. Muller-Bunz, D.R. Andes, K. Kavanagh, S.A. Patil, M. Baumann, M. Tacke, Continuous Flow Synthesis and Antimicrobial Evaluation of NHC* Silver Carboxylate Derivatives of SBC3 *in vitro* and *in vivo*, *Metallomics* 13(2) (2021).

[94] F. Hackenberg, G. Lally, H. Muller-Bunz, F. Paradisi, D. Quaglia, W. Streciwilk, M. Tacke, Novel symmetrically p-benzyl-substituted 4,5-diaryl-imidazole N-heterocyclic carbene-silver(I) acetate complexes - Synthesis and biological evaluation, *J. Organomet. Chem.* 717 (2012) 123-134.

[95] M. Sharkey, J. O'Gara, S. Gordon, F. Hackenberg, C. Healy, F. Paradisi, S. Patil, B. Schaible, M. Tacke, Investigations into the Antibacterial Activity of the Silver-Based Antibiotic Drug Candidate SBC3, *Antibiotics* 1 (2012) 25-28.

[96] N. Browne, F. Hackenberg, W. Streciwilk, M. Tacke, K. Kavanagh, Assessment of *in vivo* Antimicrobial Activity of the Carbene Silver(I) Acetate Derivative SBC3 using *Galleria mellonella* Larvae, *Biometals* 27(4) (2014) 745-752.

[97] D.B. Harper, D. Ohagan, The Fluorinated Natural-Products, *Nat. Prod. Rep.* 11(2) (1994) 123-133.

[98] S. Purser, P.R. Moore, S. Swallow, V. Gouverneur, Fluorine in Medicinal Chemistry, *Chem. Soc. Rev.* 37(2) (2008) 320-330.

[99] E.P. Gillis, K.J. Eastman, M.D. Hill, D.J. Donnelly, N.A. Meanwell, Applications of Fluorine in Medicinal Chemistry, *J. Med. Chem.* 58(21) (2015) 8315-8359.

[100] N.A. Meanwell, Fluorine and Fluorinated Motifs in the Design and Application of Bioisosteres for Drug Design, *J. Med. Chem.* 61(14) (2018) 5822-5880.

[101] W.R. Dolbier, Fluorine NMR for Organic Chemists, Second Edition ed., Jon Wiley & Sons, Inc., Hoboken, New Jersey, 2016.

[102] B.K. Park, N.R. Kitteringham, P.M. O'Neill, Metabolism of Fluorine-Containing Drugs, *Ann. Rev. Pharmacol. and Toxicol.* 41 (2001) 443-470.

[103] M.B. Plutschack, B. Pieber, K. Gilmore, P.H. Seeberger, The Hitchhiker's Guide to Flow Chemistry(II), *Chem. Rev.* 117(18) (2017) 11796-11893.

[104] J. Wegner, S. Ceylan, A. Kirschning, Flow Chemistry - A Key Enabling Technology for (Multistep) Organic Synthesis, *Adv. Synth. & Cat.* 354(1) (2012) 17-57.

[105] M.R. Chapman, Y.M. Shafi, N. Kapur, B.N. Nguyen, C.E. Willans, Electrochemical Flow-Reactor for Expedient Synthesis of Copper-N-Heterocyclic Carbene Complexes, *Chem. Comm.* 51(7) (2015) 1282-1284.

[106] B. Gutmann, D. Cantillo, C.O. Kappe, Continuous-Flow Technology—A Tool for the Safe Manufacturing of Active Pharmaceutical Ingredients, *Angewandte Chemie Int. Ed.* 54(23) (2015) 6688-6728.

[107] R. Porta, M. Benaglia, A. Puglisi, Flow Chemistry: Recent Developments in the Synthesis of Pharmaceutical Products, *Org. Process Res. & Dev.* 20(1) (2016) 2-25.

[108] S. Mascia, P.L. Heider, H.T. Zhang, R. Lakerveld, B. Benyahia, P.I. Barton, R.D. Braatz, C.L. Cooney, J.M.B. Evans, T.F. Jamison, K.F. Jensen, A.S. Myerson, B.L. Trout, End-to-End Continuous Manufacturing of Pharmaceuticals: Integrated Synthesis, Purification, and Final Dosage Formation, *Angewandte Chemie Int. Ed.* 52(47) (2013) 12359-12363.

Chapter 2 Results and Discussion

2.1 Synthesis of Imidazolium Bromide Salts

Imidazolium salts are convenient precursors to *N*-heterocyclic carbene ligands. The carbene can be directly achieved by deprotonating the salt with a base. Nucleophilic substitution at the N atoms of an imidazole ring leads to the formation of the salt from the neutral imidazole and allows simultaneous and facile addition of functionality (*Scheme 2.1)*.

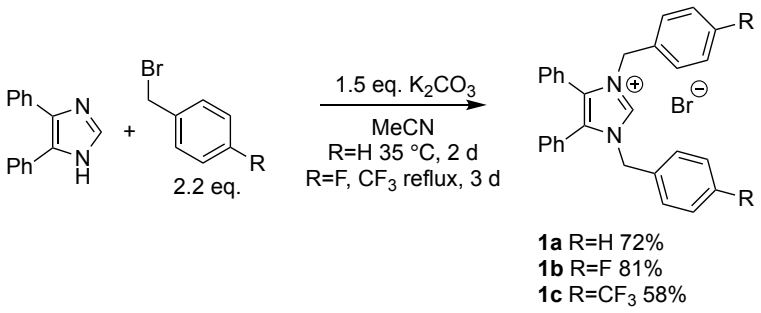

Scheme 2.1: Reaction scheme for the synthesis of 1,3-disubsituted imidazolium bromide salts

Beginning from 4,5-diphenyl imidazole, benzyl (or *p*-substituted benzyl) groups were added to the 1- and 3- positions of the imidazole ring to give a symmetrically *N*-substituted imidazolium bromide (*Scheme 2.1*). First the 4,5-diphenyl imidazole was stirred with potassium carbonate in acetonitrile to deprotonate the N-H bond, causing the suspension to become a light blue colour. The benzyl bromide acts as a substrate for an S_n2 reaction with the deprotonated nitrogen behaving as the nucleophile (*Fig. 2.1*). The second equivalent of the benzyl bromide then reacts with the lone pair of the other nitrogen of the ring in the same fashion to yield the symmetrically substituted product.

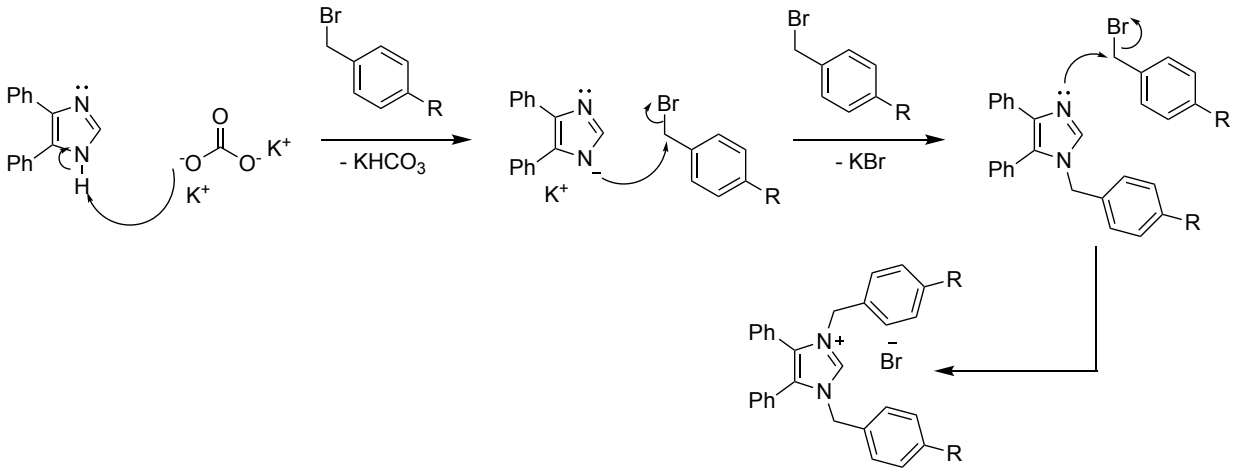

Figure 2.1: Proposed reaction mechanism for the substitution of benzyl groups onto 4,5-diphenyl imidazole to form an N,N-disubstituted imidazolium bromide salt

The procedure for the synthesis of **1a** was taken from literature,[1] and the conditions for **1b** and **1c** were adapted from that of **1a**. Yields for the benzyl (**1a**) and *p*-fluoro benzyl (**1b**) substituted salts were very good; however, the yield for the *p*-trifluoromethyl benzyl substituted salt (**1c**) was significantly lower. Optimisation of the reaction conditions for the synthesis of **1c** was carried out (*Table 2.1*), yet the best yield achieved was 58%. Initial conditions tested were stirring for one week at room temperature, stirring for three days at reflux, and reaction for three days at 120 °C in a sealed container. The initial yields for each set of conditions are detailed below:

*Table 2.1: Reaction conditions and yields for the optimisation of the synthesis of **1c***

Reaction Conditions	Yield
Rt, 7 d	32%
Reflux, 3 d	30%
120 °C, 3 d	25%

Yields in all three instances were similar, with the 120 °C reaction giving a slightly lower yield compared to the others. This is likely due the amount of solvent being limited to 5 mL in the container used leaving some 4,5-diphenyl imidazole undissolved, and the inability to initially deprotonate the imidazole before addition of *p*-trifluoromethyl benzyl bromide. The three-day reaction at reflux gave the best balance between reaction time and yield. Further improvement to the yield of **1c** was achieved by increasing the amount of time that 4,5-diphenyl imidazole was stirred with potassium carbonate from 15 min to 30 min. This allowed more time for the imidazole to be deprotonated before the addition of the *p*-trifluoromethyl benzyl bromide and raised the yield from 30% to 58%. Initial stirring time was increased for **1a** and **1b** as well but only led to nominal improvements in yield.

Formation of the salts was confirmed by ^{1}H NMR spectroscopy. The spectra show signals in the region of 5.51-5.66 ppm corresponding to the benzyl CH_2 peaks, and signals further downfield between 11.19 and 11.60 ppm which correspond to the proton at C2 of the imidazole ring. The general trend for the chemical shifts of the C2 proton is **1a** < **1b** < **1c**, coinciding with the increasing electron-withdrawing ability of the *p*-benzyl substituents (H < F < CF_3).

The presence of fluorine in compounds **1b** and **1c** is reflected by ^{19}F NMR, where signals are seen at -112 ppm and -63 ppm respectively. Both signals are in the expected region for

their respective functional groups.[2] Fluorination also leads to splitting in the ^{13}C spectra of **1b** and **1c** due to coupling between the ^{19}F and ^{13}C nuclei. The substitution of a single fluorine atom to the benzyl groups in **1b** leads to the signals for the carbon atoms of the benzyl ring appearing as doublets. The addition of the trifluoromethyl group to **1c** leads to signals of the CF_3 carbon as well as *para* and *meta* C atoms appearing as quartets. In both cases coupling constants are initially very large and decrease as the distance from the fluorine atoms increases.

2.2 Synthesis of Fluorinated NHC Silver (I) Acetate Complexes

Using imidazolium salts **1b** and **1c**, two fluorinated derivatives of **SBC3**[1] were synthesised. The imidazolium salts were stirred with two equivalents of silver (I) acetate at 40 °C for 24 h in the absence of light (*Scheme* 2.2). One equivalent of silver (I) acetate is used to deprotonate the imidazolium salt, forming acetic acid and silver bromide, and the carbene complexes with the second equivalent of silver (I) acetate. Considering the pK_a of the C2 proton is expected to be between 21 and 23,[3] it is rather surprising that it is readily removed by such a weak base as acetate. After reaction, the silver bromide precipitate was filtered out and the mixture was concentrated. Addition of diethyl ether and cooling of the solution to -18 °C for 24 h afforded the pure product in the form of clear crystals in the case of **2a** and as a white powder in the case of **2b**.

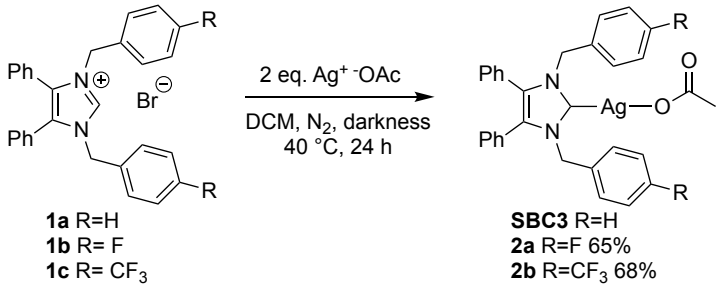

*Scheme 2.2: Synthesis of fluorinated NHC silver (I) acetate complexes **2a** and **2b** from imidazolium salts **1b** and **1c***

The structures of **2a** and **2b** were confirmed with ^1H NMR and compared to that of **SBC3**. The proton spectra of the products show the expected upfield shift of the signal for the benzyl CH_2 groups versus the same signal for their corresponding imidazolium salts, **1b** and **1c**. They also show the appearance of a singlet at 2.08 and 2.09 ppm for **2a** and **2b**, respectively, corresponding to the acetate CH_3 group. No signals are observed downfield of

the aromatic region, signifying the deprotonation of the C2 position of the imidazole ring to form the carbene species.

The crystal structure of **2a**[1] (*Fig*. 2.2) shows the expected linear carbon-silver-oxygen bond in the case of a two-coordinate silver complex. Bond lengths and angles are in good agreeance with those previously seen for similar complexes.[1, 4] Though there is a close Ag-O2 distance of 2.810 Å which is within the range silver-oxygen close contact,[5] there is no significant distortion of the C-Ag-O bond angle away from 180°. In general, where non-covalent silver-oxygen interactions have been reported for NHC-silver-carboxylate species the observed C-Ag-O bond angle is close to 165°.[6, 7]

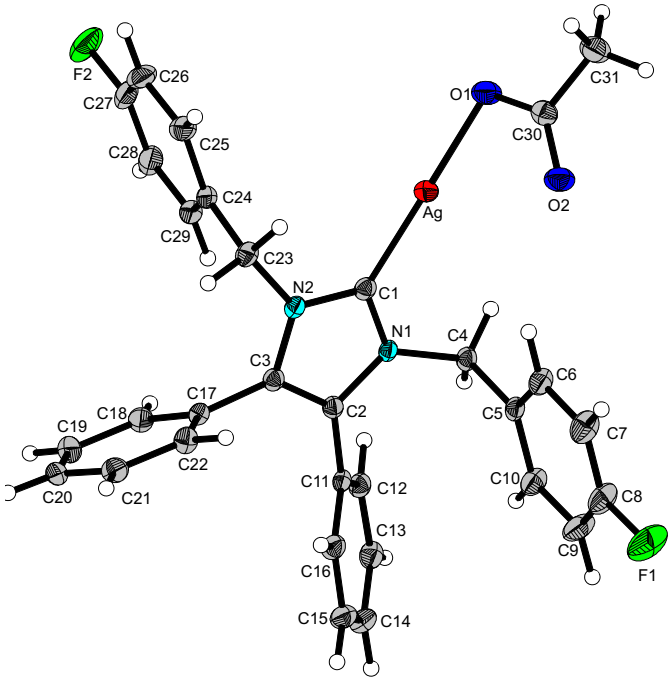

*Figure 2.2: X-ray crystal structure of complex **2a**. Thermal ellipsoids are drawn at the 50% level*

*Table 2.2: Selected bond lengths and angles of **2a***

Bond Lengths (Å)	
C1-Ag	2.0616(15)
O1-Ag	2.1157(12)
Bond Angles (°)	
C1-Ag-O1	174.38(5)
O1-C30-O2	123.98 (15)

[1] All crystallographic measurements, data collection and structure refinements, including X-ray crystal structures and data tables in this chapter and the next, were carried out by Dr Helge Müller-Bunz.

High resolution mass spectrometry of compounds **2a** and **2b** did not show signals corresponding to the molecular ions. Instead, the most abundant peak for each corresponded to the *bis*-carbene silver complex and two protons ($(NHC)_2Ag^+ + 2H^+$). This suggests that ligand exchange occurs in the gas phase during the electrospray ionisation process.

The effect of the *p*-benzyl trifluoromethyl groups on the solubility of **2b** was clearly demonstrated by the complex's solubility in diethyl ether. Both **SBC3** and **2a** remained dissolved in diethyl ether at room temperature and crystallised slowly from solution at -18 °C. **2b**, while soluble at room temperature, crashed out of solution at -18 °C too quickly to be able to crystallise.

Both complexes **2a** and **2b** showed similar stability toward moisture and light exposure compared to **SBC3**. When made into solutions in wet DMSO and left exposed to ambient light, solutions of all three complexes began to develop a purple colour after 30 min owing to the precipitation of elemental silver.

2.3 Synthesis of Imidazole-2-ylidene Silver (I) (*p*-trifluoromethyl) Benzoate Complexes

2.3.1 Synthesis via generation of a free carbene intermediate

Stable, free *N*-heterocyclic carbene species can be easily achieved by the deprotonation of an imidazolium salt.[8] Addition of the free carbene to a silver salt results in the formation of a silver complex.[9] This route is especially convenient for the formation of NHC silver (I) carboxylate species.

Compounds **3** and **4a-c** were prepared by a modified literature method.[10] Silver carboxylate salt **3** was prepared from silver (I) oxide and *p*-trifluoromethyl benzoic acid (*Scheme 2.3a*). The reagents were stirred at room temperature in acetonitrile for 24 h. The mixture was filtered, and the solid product was washed with hot acetonitrile followed by diethyl ether. The product was then dried *in vacuo* for 2 h.

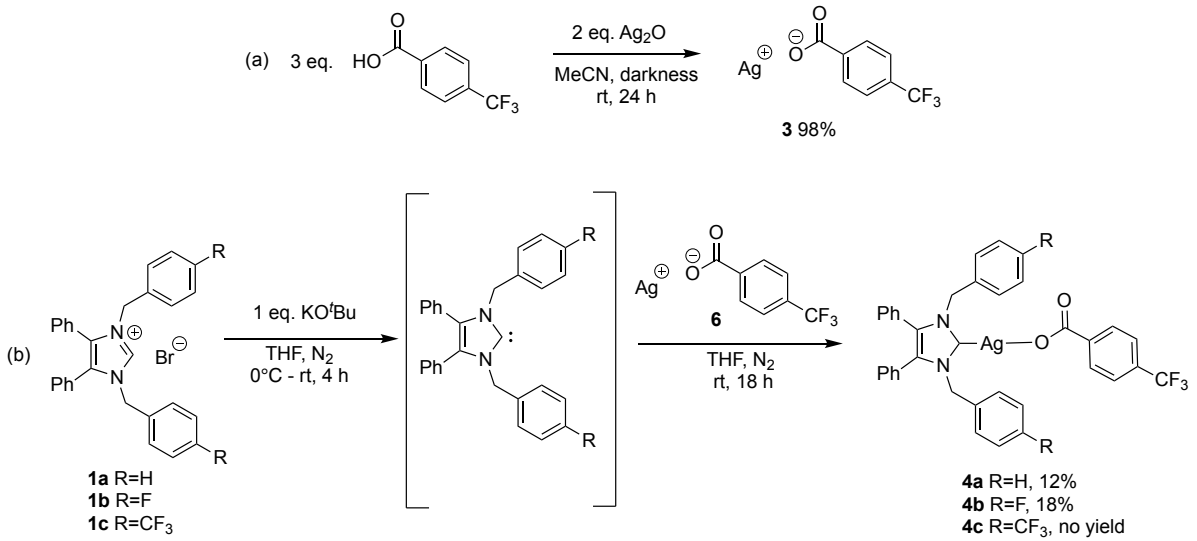

*Scheme 2.3: Reaction schemes for (a) the formation of silver benzoate salt **6** and (b) formation of silver complexes **7a-c** via generation of a free carbene*

Equimolar amounts of an imidazolium salt **1a-c** and **3** were placed in separate flasks and dried under vacuum for one hour prior to addition of THF which had been distilled over benzophenone and sodium wire. Glassware was flame dried beforehand to exclude moisture and the reaction was carried out under nitrogen. The mixture of **1a-c** in THF was cooled to 0°C followed by the addition of equimolar potassium *tert*-butoxide (1 M in THF) and stirring for 4 h. The potassium *tert*-butoxide acted as a base to deprotonate the imidazolium salts to form the corresponding free carbene species (*Scheme 2.3b*). Generation of the carbene could be monitored by colour change from white suspension to dark red solution in the case of **1a**. A precipitate of potassium bromide formed during the reaction which was allowed to settle to the bottom of the flask. Several attempts to generate the corresponding free carbenes of **1b** and **1c** were unsuccessful as evidenced by an orange-brown colour and a precipitate that remained suspended after 1 h. Successful generation of the carbenes from **1b** and **1c** still did not yield the expected dark red colour seen with **1a**. This may indicate incomplete conversion of the imidazolium salts to the carbenes, possibly due to the presence of moisture.

The solution containing the carbene was transferred from the flask via syringe and injected into the suspension of **3** in THF. On addition of the carbene, the mixture became a dark brown to black colour. The product mixture was filtered through a bed of celite to remove precipitated silver species followed by gravity filtration. The resulting yellow-brown solution was concentrated under reduced pressure. The resulting waxy substance was redissolved in chloroform and allowed to sit for 15 min to allow the precipitation of any insoluble species before filtration through a grade 4 sinter funnel followed by gravity

filtration. The solution was again concentrated under reduced pressure, followed by the addition of pentane to precipitate the product. **4a** was obtained as a brown solid, while **4b** and **7c** were obtained as orange wax-like substances.

From this synthetic method, only **4a** was able to be obtained as a product with only minor impurities in the ^{1}H NMR spectrum. The largest issue with the spectrum of **4a** was that the doublets which represent the aromatic protons of the *p*-trifluoromethyl benzoate ligand integrated for an extra proton relative to the benzyl CH_2 signal. The reason for this was reflected in an x-ray crystal structure obtained of the complex (*Fig. 2.3*).

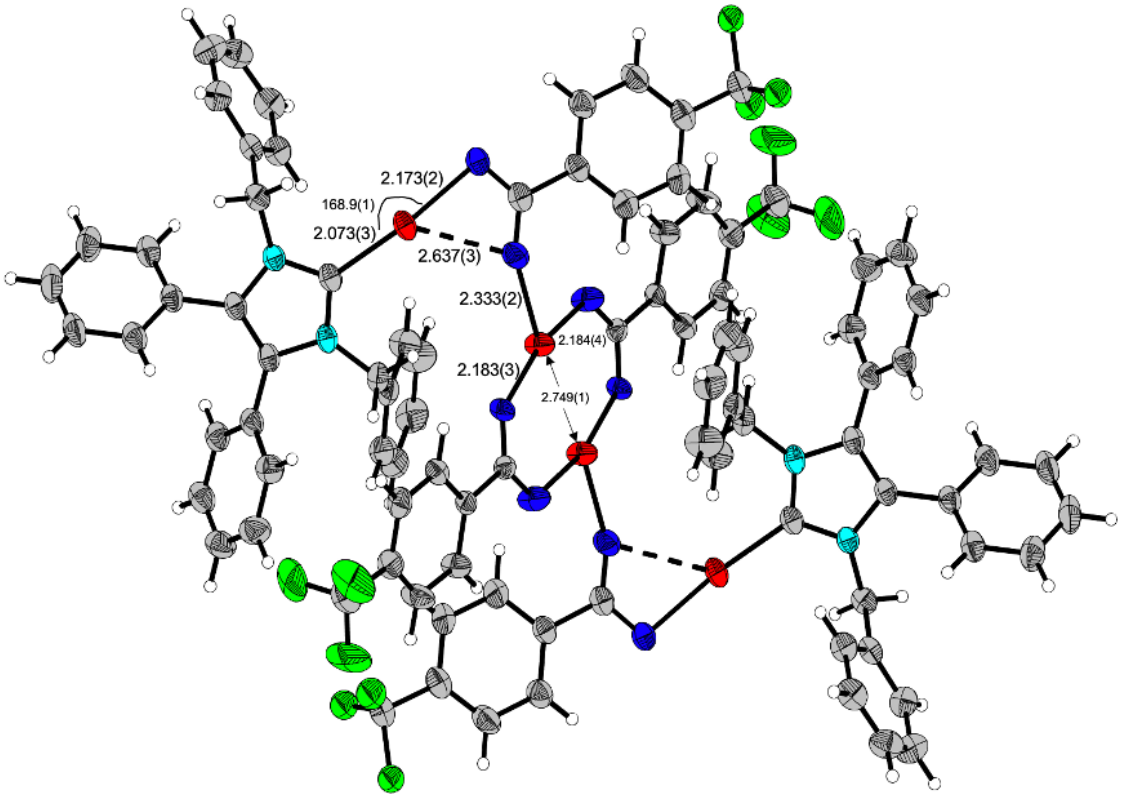

*Figure 2.3: X-ray crystal structure of **4a** shows two molecules with a bridging silver (p-trifluoromethyl) benzoate dimer. Selected bond lengths and angles are quoted on the image (grey = C, blue = O, cyan = N, red = Ag, green = F)*

The Ag-C bond length quoted on the image is in general agreeance with values from similar complexes.[6, 10] However, the Ag-O bond length in the complex does appear longer than expected, more comparable to the Ag-O lengths of the ionic silver carboxylate cluster than to other covalently bonded NHC-silver-carboxylates. This could be consequential of the electron withdrawing trifluoromethyl group which significantly lowers the basicity of the carboxylate, making it a poor donor ligand.[11]

The structure shown in figure 2.6 was not the only species present in the crystal; it also contained some monomeric species with either a single equivalent of silver *p*-

trifluoromethylbenzoate or a molecule of solvent. The existence of multiple species within the crystal draws into question whether the association of the extra molecule of silver *p*-trifluoromethyl benzoate with the complex led to the presence of the impurity or whether its presence was simply a consequence of crystallising an impure substance.

Both **4b** and **4c** contained significant impurities in their respective spectra. The ^{1}H NMR spectrum of **4b** shows the expected pattern of signals as the major product, but the impurities are also very significant with the benzoate proton peaks integrating for more than twice the expected value.

Purification of **4b** was attempted by passing a solution of the product in dichloromethane over a 'pencil column' fashioned from a Pasteur pipet and approximately 1 cm of silica. This led to minimal removal of impurities, but a pronounced increase in the relative amount of the benzoate present (*Fig.* 2.4), which may reflect the instability of the complex in solution.

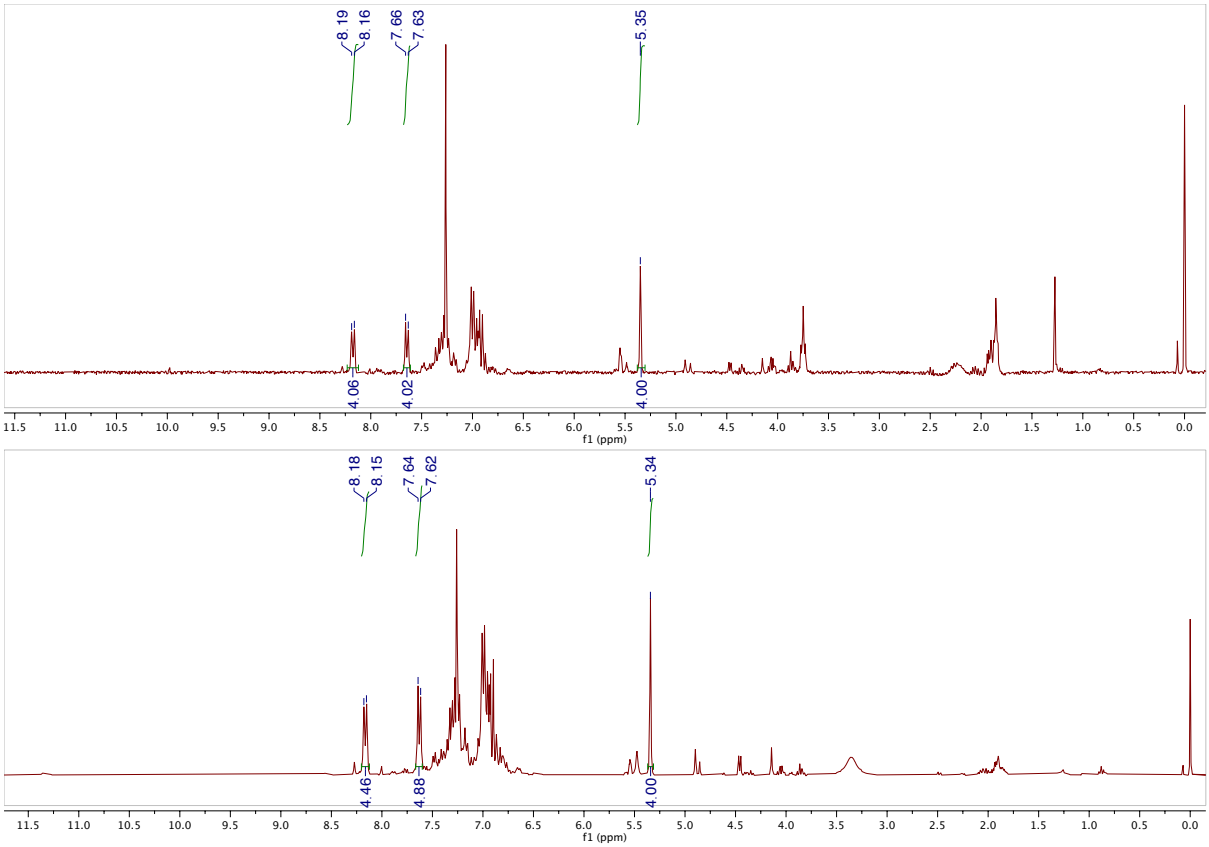

*Figure 2.4: Product mixture of complex **4b** before (top) and after (bottom) purification by pencil column shows an increase in the relative amount of benzoate present, suggesting decomposition of the product.*

The ^{1}H NMR spectrum of **4c** showed the desired complex as the minor product (*Fig.* 2.5). The signal which represents the benzyl CH_2 protons of the product at 5.45 ppm integrates

for only one proton (instead of four) when set relative to the benzoate signals. Two singlets of equal integration (two protons each) appear in the same region as the benzyl CH_2 signal. Neither signal represents a re-protonated imidazolium salt as there are no downfield singlets for an imidazole C2 proton. The aromatic proton signals (not including benzoate signals) integrate for more than expected for even a 1:1 mixture of carbene to benzoate. This signifies that the unidentified side product(s) contain aromatic rings. The ^{19}F spectrum shows three major signals in the chemical shift region for trifluoromethyl groups,[2] representing the NHC ligand, the *p*-trifluoromethylbenzoate ligand, and some unknown species which can be expected to represent an aryl CF_3 group.

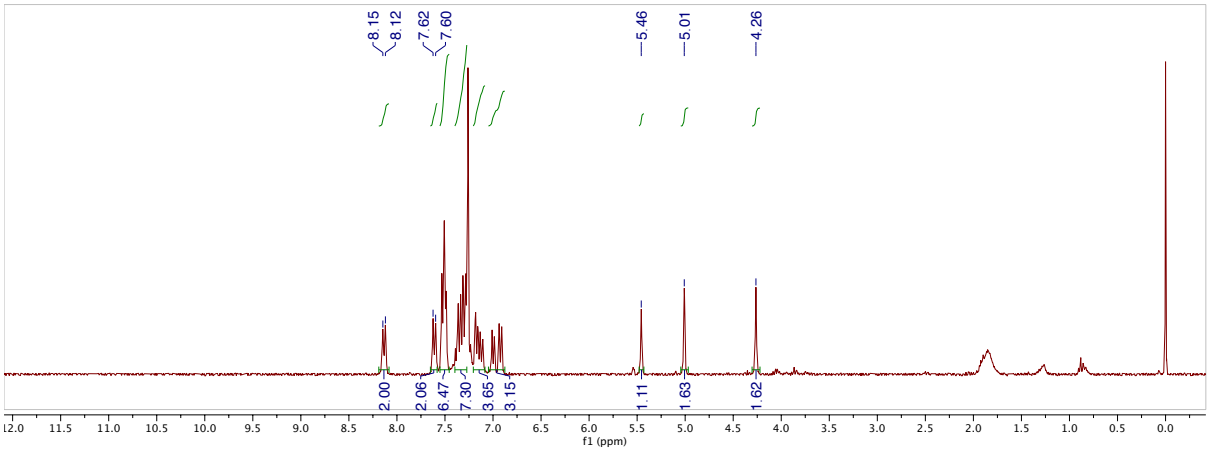

*Figure 2.5: Proton NMR of the product mixture obtained for complex **4c**, showing two unidentified signals at 5.01 and 4.26 ppm, and over-integration in the aromatic region*

From the results obtained in the synthesis of complexes **4a-c** it becomes obvious that complex formation from a free carbene intermediate has multiple issues. Not only does the reaction have to take place in the absence of moisture and air, but even so, yields are very low and significant impurities are present in the isolated products. Thus, the free carbene synthesis appears to be a poor choice of synthetic route if the complexes are to be obtained in good yield and purity.

2.3.2 Synthesis from an imidazolium salt and a silver base

2.3.2.1 Synthesis of imidazolium (p-trifluoromethyl) benzoate salts

The bromide anion of imidazolium salts **1a-c** was exchanged for *p*-trifluoromethyl benzoate by stirring with a previously prepared potassium *p*-trifluoromethyl benzoate, **5**, in a mixture of methanol and acetonitrile (*Scheme 2.4*).

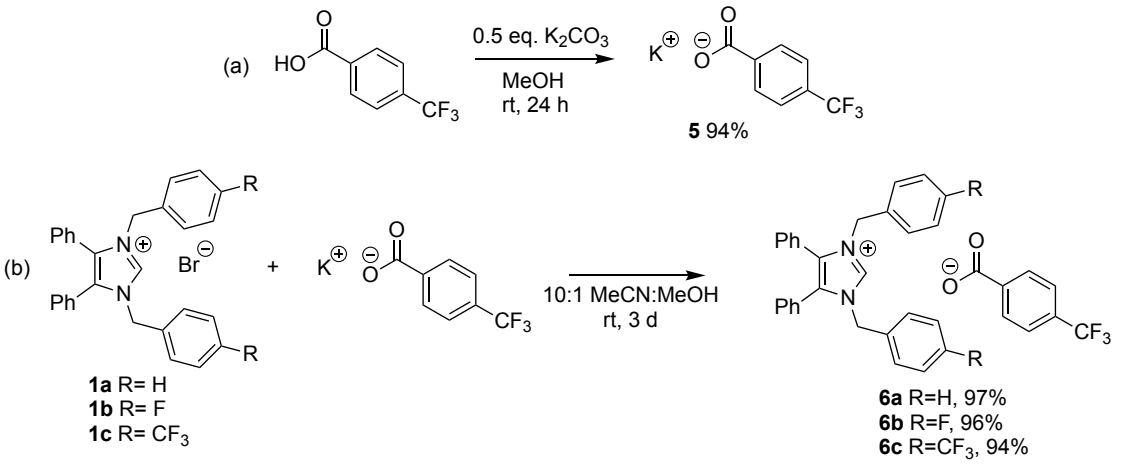

*Scheme 2.4: Reaction schemes for the synthesis of (a) potassium p-trifluoromethyl benzoate **5**, and (b) imidazolium p-trifluoromethyl benzoate salts **6a-c***

Potassium salt **5** was synthesised by the deprotonation of *p*-trifluoromethyl benzoic acid with potassium carbonate (*Scheme 2.4a*). The reaction was carried out in an open flask to allow the evolution of carbon dioxide as a side product. Successful synthesis of **5** was confirmed by infrared spectroscopy and elemental analysis. The IR spectrum was compared to that of the *p*-trifluoromethyl benzoic acid starting material. The notable changes are the disappearance of a broad signal from 3000 cm^{-1} to 2500 cm^{-1} which corresponds to O-H stretching and hydrogen bonding in the acid species, and the disappearance of the signal for the carbonyl C=O stretch at 1687 cm^{-1}. The loss of the carbonyl stretch signifies the delocalisation of the negative charge across both C-O bonds in the salt. Elemental analysis was in good agreement with calculated values.

The synthesis of compounds **6a-c** was carried out by stirring **1a-c** with **5** in a mixture of 10:1 acetonitrile and methanol for 3 d (*Scheme 2.4b*) Potassium bromide precipitated from solution and was removed by filtration before the product was concentrated under reduced pressure. Poor solubility of **5** was a prohibitive factor in the preparation of **6a-c**. Methanol was the only solvent in which **5** showed good solubility, however potassium bromide is also soluble in methanol and would not precipitate from solution in pure methanol. The solvent system of 10:1 acetonitrile and methanol was chosen in order to minimise the volume of methanol necessary to fully dissolve all reagents. Additionally, acetonitrile has a higher boiling point than methanol, allowing the removal of methanol by rotary evaporator and causing any potassium bromide which was dissolved in the methanol to precipitate.

The ^1H NMR spectra of **6a-c** showed upfield shifts of the imidazolium C2 protons compared to their bromide salt precursors to 10.03 ppm for **6a**, 9.93 ppm for **6b**, and to 10.20

ppm for **6c**. Most notable is the appearance of two doublets around 7.65 ppm and 8.04 ppm which correspond to the aromatic protons of the *p*-trifluoromethyl benzoate anion.

Despite the apparent purity of the NMR spectra, elemental analysis for **6a-c** was in very poor agreeance with the calculated values. In all three salts, the found values for C, H, N, and F are lower than the calculated values, suggesting the presence of an inorganic impurity—most likely potassium bromide. Large amounts of KBr present in the product suggest the salt metathesis reaction was not successful. However, the significant shift in the signal for the imidazolium C2 proton does suggest a different anion than Br^- associated with the cations.

2.3.2.2 Formation of imidazol-2-ylidene silver (I) (p-trifluoromethyl) benzoate complexes by reaction with silver (I) oxide

Imidazolium carboxylate salts can be reacted with silver (I) oxide under mild conditions to form the corresponding NHC-silver-carboxylate complex. Though the salts **6a-c** were not obtained in good purity, upon reaction with an equimolar amount of silver oxide the desired products were obtained in moderate yields (*Scheme 2.5*).

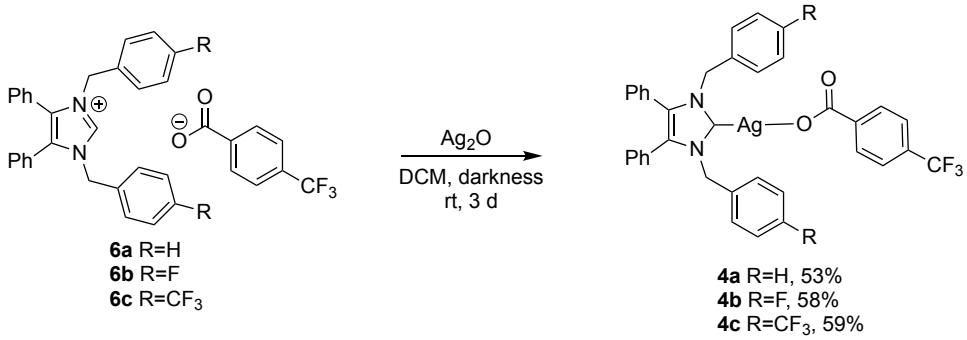

6a R=H
6b R=F
6c R=CF_3

4a R=H, 53%
4b R=F, 58%
4c R=CF_3, 59%

*Scheme 2.5: Formation of NHC-Ag-carboxylate species **4a-c** from the reaction of imidazolium salts **6a-c** with silver oxide*

Two filtration steps, first using celite then a sinter funnel (after concentration and re-dissolution of the product in chloroform), were employed in the work-up to remove any remaining silver oxide or other impurities. The complexes were concentrated to approx. 3 mL under reduced pressure and finally precipitated from solution by the addition of pentane.

The reactions were also tested in both acetonitrile and methanol in an attempt to improve yields but neither solvent led to any noticeable improvement in the products obtained. Thus, dichloromethane was kept as the solvent as its lower boiling point makes it easier to remove by rotary evaporation. Powdered 4 Å molecular sieves were also added to

the reaction mixture in an attempt to improve yield as reported in literature. However, this method also showed no marked increase in the yield of the products.[12]

^{1}H NMR spectroscopy of the products showed the expected signals for the compounds, with the only impurities being residual solvent and small amounts of the imidazolium salt starting material. Integration of the doublet signals which arise from the protons of the benzoate ligand was correct relative to the carbene benzyl CH_2 protons to confirm a 1:1 ratio of carbene to benzoate. Elemental analysis of the products shows relatively good agreeance with calculated values.

High resolution mass spectrometry (ESI^+, TOF) of the complexes was of little diagnostic use, as the molecular ion peak appears for the $[(NHC)_2Ag]^+$ species rather than the NHC-Ag-carboxylate complex. This phenomenon has been seen previously in complexes **2a-b** and in literature,[13] and suggests ligand exchange in the gas phase during ionisation.

Despite the apparent impurity of the intermediate salts, the complexes were still able to be formed. However, improved purity of the intermediate salts would likely lead to better conversion to the desired products and higher yields.

The stability of complexes **4a-c** is quite low in solution, especially when exposed to light. Solutions of the products in $CDCl_3$ began to form a black precipitate, likely elemental silver, at the bottom of the NMR tube after roughly 15 min of being exposed to light. As solids, the complexes began to decompose after approximately one week at room temperature, even in the absence of light. Poor stability means that the complexes are unlikely to be good candidates for drug molecules as the complexes would decompose rapidly in biological media, and the active silver ion would form insoluble silver chloride.

2.4 Synthesis of Cationic *Bis*-imidazol-2-ylidene Silver (I) Complexes with Non-coordinating Anions

2.4.1 Synthesis of anion-exchanged imidazolium salts

The identity of the counter ion in NHC-silver complexes has a large influence on the structure of the product, especially in the solid state. The presence of non-coordinating counterions reliably leads to the formation of cationic *bis*-carbene complexes when the precursor is a simple substituted imidazolium salt.[14]

The bromide counter ion of compounds **1a-c** was exchanged for the non-coordinating ions hexafluorophosphate (**2a-c**) and tetrafluoroborate (**3a-c**). The procedure for the synthesis of **2a-c** was taken from literature,[4] and adapted for **3a-c** by using a sodium tetrafluoroborate salt. For the synthesis of **2a-c**, bromide salts **1a-c** were stirred with potassium hexafluorophosphate in a 4:1 mixture of methanol and water. Similarly, to form the tetrafluoroborate salts, **1a-c** were stirred with sodium tetrafluoroborate in the same solvent mixture (*Scheme 2.6*). The resulting solutions were poured into deionised water, causing the imidazolium salts with their corresponding counter ions to precipitate, while the potassium or sodium bromide by-product remained in solution.

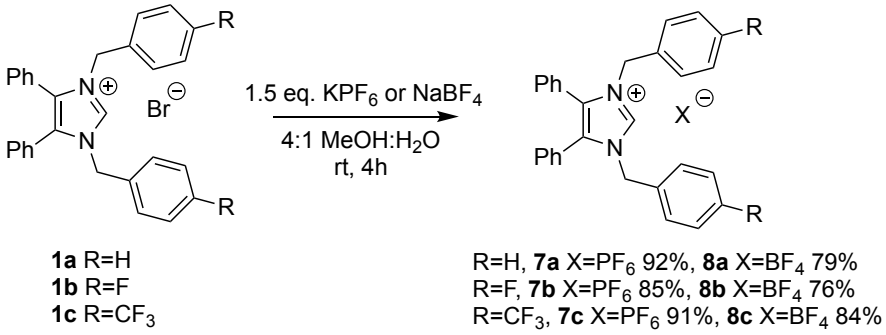

*Scheme 2.6: Reaction scheme for the synthesis of substituted imidazolium hexafluorophosphate (**7a-c**) and tetrafluoroborate (**8a-c**) salts from **1a-c***

Formation of the ion-exchanged salts is evidenced in both ^{1}H and ^{19}F NMR. In the proton spectra, the signal for the C2 proton is shifted considerably upfield compared to **1a-c** (*Fig. 2.6*) as neither hexafluorophosphate nor tetrafluoroborate hydrogen bond with the C2 proton while the bromide anion does.[15] A similar upfield shift is seen in the signals for the benzyl groups, however it is not as pronounced. ^{19}F NMR shows signals for the anions. Hexafluorophosphate appears as a doublet with a very large coupling constant of roughly 711 Hz due to coupling between the ^{31}P and ^{19}F nuclei which both have a spin of ½. The tetrafluoroborate anion produces two signals within one ppm of each other which correspond

to coupling of ^{19}F to ^{10}B (spin 3) and ^{11}B (spin 3/2) nuclei with the ^{10}B signal being slightly downfield of ^{11}B.[16] Coupling to ^{10}B would be expected to produce a septet and coupling to ^{11}B would be expected to produce a quartet; however, the signals were often not well enough resolved to observe the expected splitting patterns.

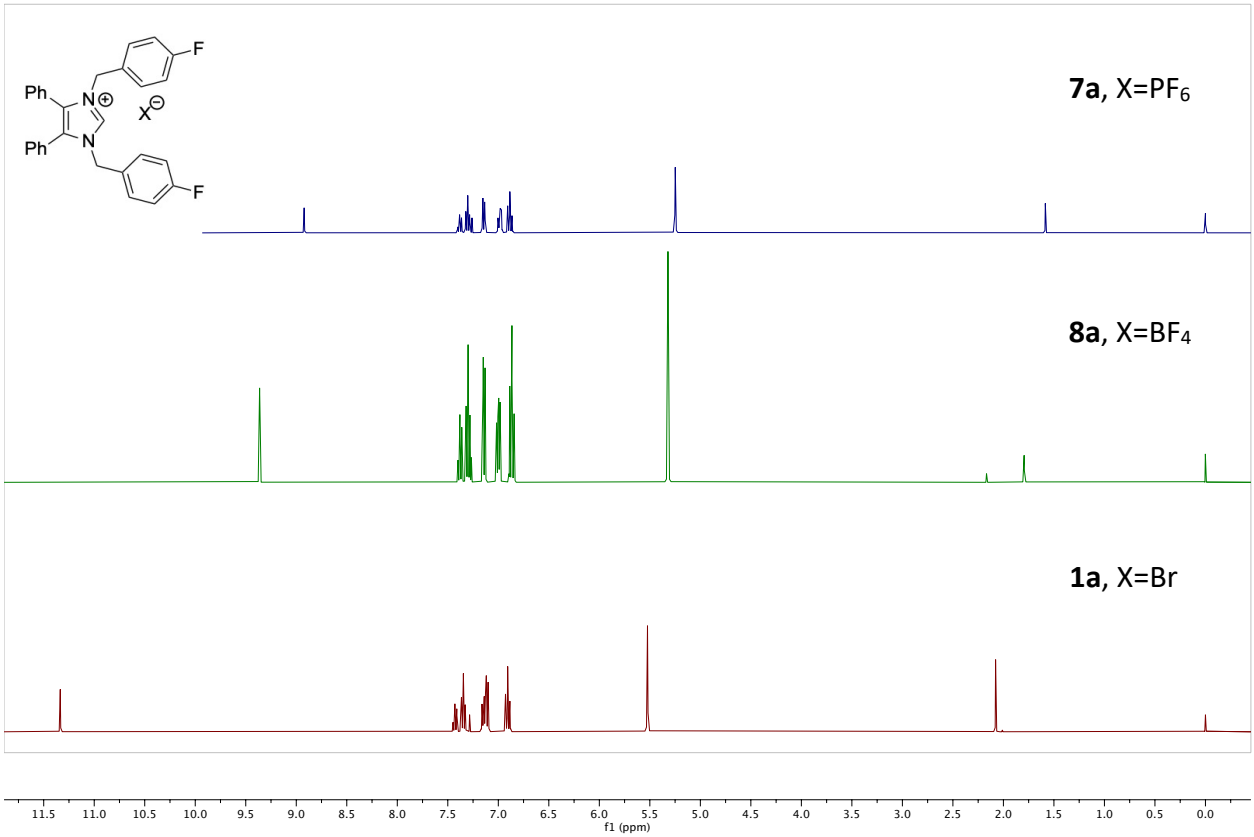

Figure 2.6: A comparison of ^1H NMR spectra (400 MHz, $CDCl_3$) of p-fluorobenzyl substituted imidazolium salts with hexafluorophosphate (top), tetrafluoroborate (middle), and bromide (bottom) anions

The ion exchange reactions were also confirmed by infrared spectroscopy and elemental analysis. Both hexafluorophosphate and tetrafluoroborate ions show strong infrared signals corresponding to P-F and B-F stretching, respectively. The hexafluorophosphate signal is strong and broad, at roughly 840 cm^{-1} while the tetrafluoroborate signal appears as a strong, broad peak centred around 1065 cm^{-1}. Elemental analysis for all six ion exchanged salts were in good agreeance with the calculated values. It should be noted that fluorine composition analysis is not accurate for the tetrafluoroborate salts as the presence of boron interferes with fluorine analysis.[17]

2.4.2 2.4.2 Synthesis of *bis*-carbene silver complexes

Reaction conditions were modified from those found in literature.[4] Imidazolium salts **7a-c** and **8a-c** were reacted with equimolar amounts of silver (I) oxide in acetonitrile to

form the corresponding cationic *bis*-imidazol-2-ylidene silver (I) complexes (*Scheme 2.7*). Reaction vessels were wrapped in aluminium foil to exclude light. Silver oxide acts as a base which deprotonates the imidazolium salts to form the *N*-heterocyclic carbene which coordinates to the silver centre. The formation of water as a by-product of the reaction does not appear to interfere with the reaction as evidenced by the high yields, suggesting that deprotonation to form the carbene and coordination to silver happen in a concerted fashion without the generation of a free carbene intermediate.

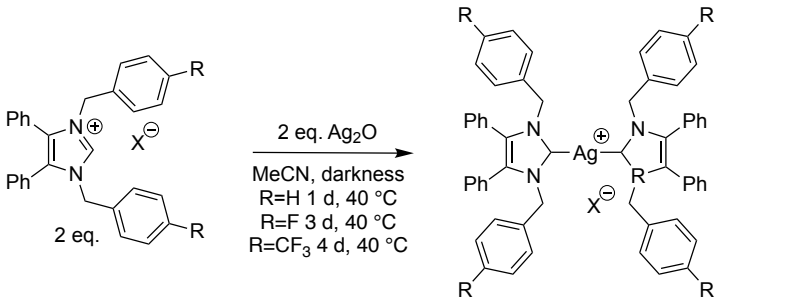

*Scheme 2.7: Reaction scheme for the formation of substituted bis-imidazol-2-ylidene silver (I) complexes with either hexafluorophosphate or tetrafluoroborate anions beginning from salts **2a-c** and **3a-c**, respectively*

Initially all reactions were carried out for 1 d; for complexes **9b-c** and **10b-c** this led to yields below 50%. Reactions for the fluoro- and trifluoromethyl substituted complexes were then run for 2 and 3 d, with 3 d showing a significant improvement in the yields of complexes **9b** and **10b**. The trifluoromethyl substituted complexes **9c** and **10c** still returned yields in the 50-60% range. The reactions for **9c** and **10c** were then run for 3, 4, 5, and 6 d, with the best yield being obtained after 4 d.

The product mixture was filtered through a celite bed to remove excess silver oxide, concentrated under reduced pressure, and initially, the product was precipitated using diethyl ether according to a procedure from Patil and co-workers.[4] However, yields greater than 100% were obtained and elemental analysis of the products showed significant impurities despite none being visible in the ^{1}H NMR spectra. This is most likely due to the formation of silver salts of hexafluorophosphate and tetrafluoroborate as side products in the respective reactions. This was affirmed in the ^{19}F NMR spectra of the complexes: signals corresponding to the anions integrated for more ^{19}F nuclei than expected in reference to the signals for *p*-fluoro- and *p*-trifluoromethyl groups of the NHC ligands. The $AgPF_6$ and $AgBF_4$ salts are insoluble in diethyl ether and precipitated with the products. To eliminate this issue,

2-propanol was added to the concentrated product mixture instead of diethyl ether, and it was left at -18°C for 24 h to precipitate the pure products.

Complexation of the ligands to silver could be determined by ^{1}H NMR. The singlet peak which appears near 9 ppm in the spectra for the imidazolium salts is not present in the spectra of the complexes, confirming that there was no longer a proton at the C2 position. The signals for the benzyl CH_2 groups see an upfield shift upon coordination to silver, a common trend in N-benzylated imidazole-2-ylidene complexes.[1, 4]

The ^{13}C spectra of complexes **9a-c** showed signals at 180.8 ppm for **9a** and **9b** and at 181.3 ppm for **9c** which correspond to the carbene carbon (*Fig*. *2.7*). The signals are doublets of doublets (in the case of **9a** the signals were not well enough resolved and appear only as a doublet) with large coupling constants of 161 Hz. The carbene C couples to both ^{107}Ag and ^{109}Ag nuclei, both with spin 1/2. The splitting of the signal and the low sensitivity of silver nuclei make the signals difficult to observe.[18] The same carbene C signals were not observed in the ^{13}C spectra of **10a-c**. However, signals were visible in the 2-D proton-carbon HMBC spectra near 181 ppm showing the through-bond correlation of the carbene C with the benzyl CH_2 protons.

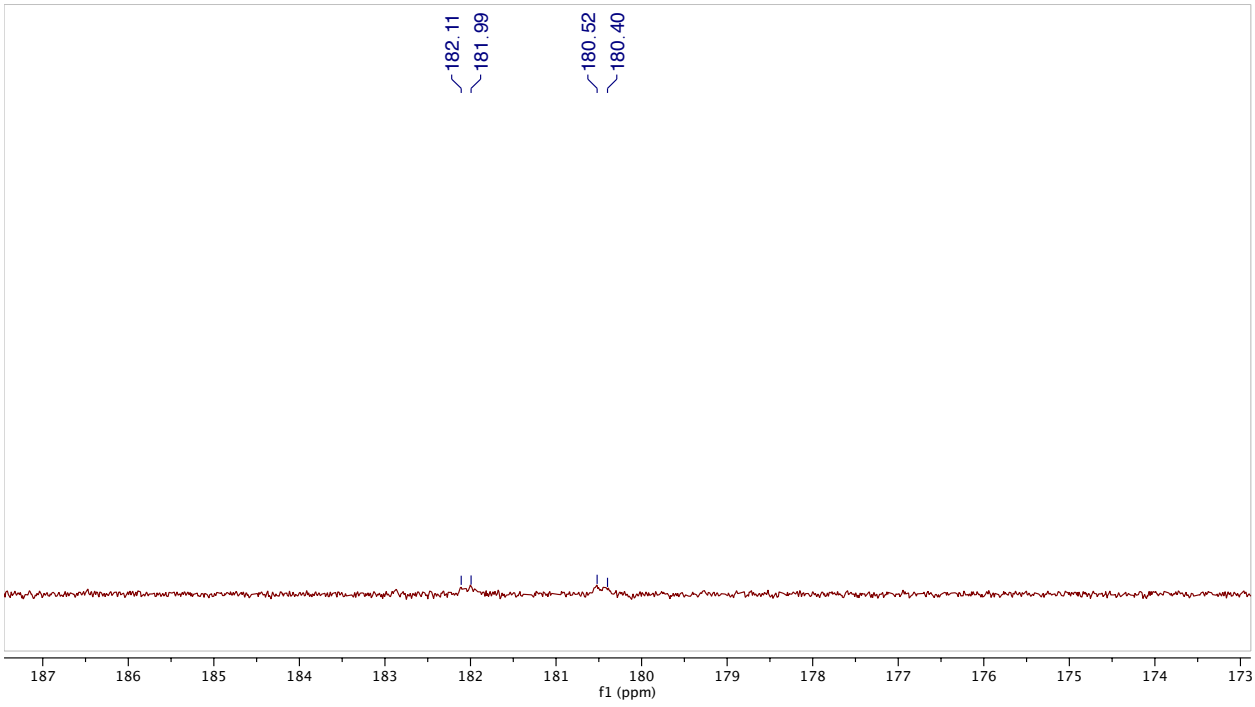

*Figure 2.7: ^{13}C NMR signal of the carbene C in complex **9c** can be observed as a doublet of doublets due to coupling to ^{107}Ag and ^{109}Ag nuclei*

Formation of selected complexes was also confirmed by single crystal x-ray diffraction. Single crystals of complexes **9a**, **9c** and **10b** were grown from a saturated solution in dichloromethane by slow infusion of pentane at -18°C.

The structure of complex **9a** shows a silver atom linearly bonded to two NHC ligands (*Fig. 2.8)*. The planes of the two imidazole rings of the NHCs are nearly perpendicular to each other, offset by an angle of 88.01°. The distance from the silver centre to the nearest fluorine atom of the PF_6^- anion is 3.382 Å, which is too far to be considered a contact. This along with the linear C-Ag-C angle confirm that hexafluorophosphate behaves as a non-coordinating anion.

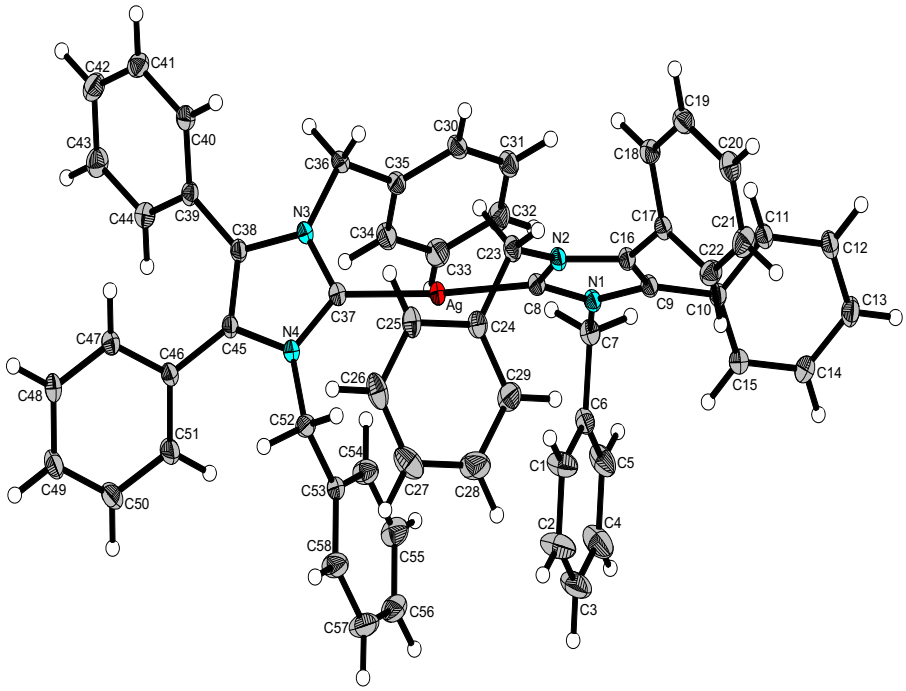

*Figure 2.8: X-ray structure of complex **9a**. PF_6^- anion is omitted. Thermal ellipsoids are drawn at the 50% level*

*Table 2.3: Selected bond lengths and angles in the crystal structure of **9a***

Bond Lengths (Å)	
C8-Ag	2.0832(13)
C37-Ag	2.0834(13)
Bond Angles (°)	
C8-Ag-C37	175.86(5)

Similar to **9a,** the structure of **9c** shows a linearly coordinated silver atom with two NHC ligands (*Fig*. 2.9). However, the imidazole rings in this case are close to being co-planar, offset by an angle of only 20.76°. The benzyl groups all face the same direction, causing the trifluoromethyl groups to sit on the same side of the NHC-Ag-NHC plane. Though the fluorine atoms on the molecule appear to aggregate, the distances between them are greater than the sum of two fluorine Van der Waals radii, ruling out intramolecular F-F interactions.[19] However, in the crystal packing, the -CF_3 groups of two molecules of the complex face each other. This leads to a fluorine-fluorine distance of 2.760 Å which is well within the range to consider a fluorine-fluorine interaction. In **9c** the hexafluorophosphate anion sits significantly further away from the silver atom than in **9a**, at an average distance of 4.153 Å.

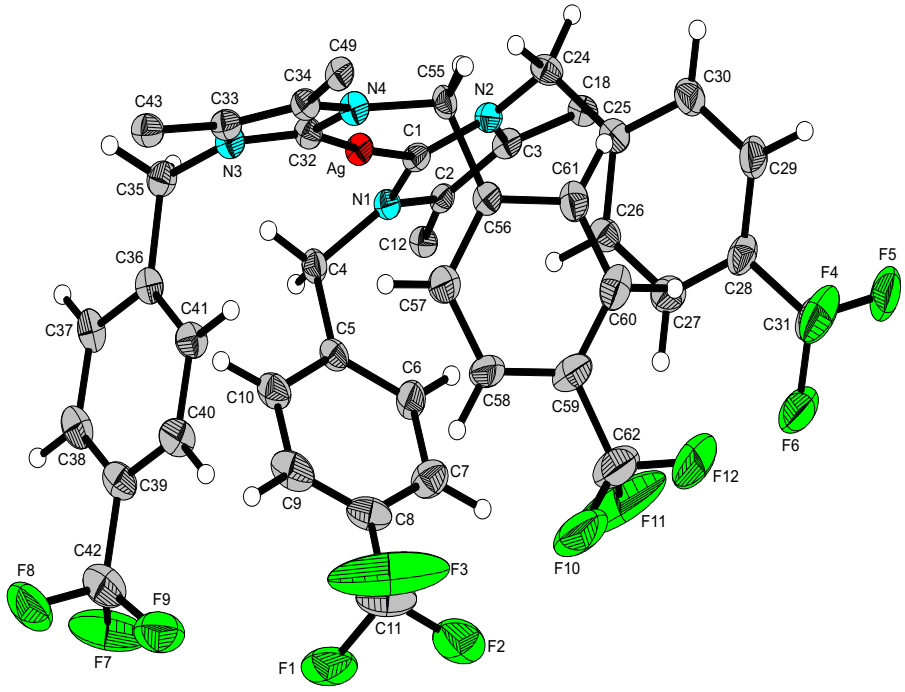

*Figure 2.9: X-ray structure of **9c**. PF_6^- anion is omitted. Thermal ellipsoids are drawn at the 50% level. Phenyl groups are represented by their ipso- carbons*

*Table 2.4: Selected bond lengths and angles in the crystal structure of **9c***

Bond lengths (Å)	
C1-Ag	2.093(4)
C32-Ag	2.095(5)
Bond Angles (°)	
C1-Ag-C32	175.71

Complex **10b** shows a similar conformation to **9c** in the solid state (*Fig*. 2.10) with a smaller torsional angle between the two imidazole rings of 15.87°. Again, the benzyl groups all face in the same direction. In the unit cell, the tetrafluoroborate anion resides near the fluorine substituents of the benzyl groups, but a rather far distance of 4.932 Å from the silver atom.

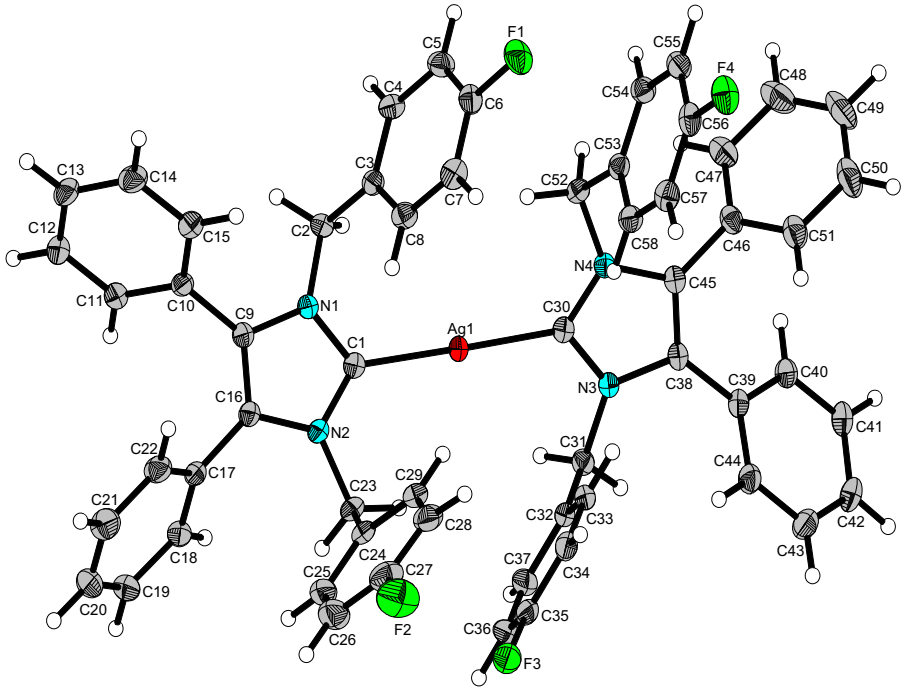

*Figure 2.10: X-ray structure of complex **10b**. BF_4^- counterion is omitted. Thermal ellipsoids are drawn on the 50% level*

*Table 2.5: Selected bond lengths and angles for complex **10b***

Bond lengths (Å)	
C1-Ag1	2.0883(15)
C30-Ag1	2.0881(14)
Bond Angles (°)	
C1-Ag1-C30	177.15

Despite the apparent light sensitivity of silver compounds,[20] the *bis*-NHC silver (I) complexes appear quite stable to light, even in solution. The stability of complex **9a** was monitored by ^{1}H NMR in DMSO-d_6 over four weeks. The sample was kept in solution in wet solvent and exposed to light. Since decomposition of the complex in this case is expected to result in protonation of the NHC ligands by water molecules present in the DMSO, the extent of decomposition of the complex was measured by the change in relative integration of the

benzyl CH_2 peak corresponding to the imidazolium salt (slightly downfield of the same signal for the complex) compared to that of the complex. Over the measurement period, there was no observed change in the integration for the peak corresponding to the imidazolium salt. When compared to an NHC silver(I) acetate complex which, in solution in DMSO-d_6 and exposed to light, begins to turn purple within 30 min, introduction of a second NHC ligand appears to contribute significantly to the stability of the complex.

Both the hexafluorophosphate and tetrafluoroborate complexes showed poor solubility. The complexes were readily soluble in acetonitrile, dichloromethane and DMSO, but insoluble in diethyl ether and chloroform. The tetrafluoroborate complexes were soluble in methanol and partially soluble in ethanol, while the hexafluorophosphate complexes were not readily soluble in either. This difference can be attributed to their anions, as that is the only apparent difference between the sets of complexes.

Both sets of complexes were overall very hydrophobic and aggregated when added to deionised water. An attempt at formulation of complex **10a** (theoretically the most water-soluble of the set) at 1 mg mL^{-1} in a 5% (v/v) solution of DMSO in water was attempted by first dissolving 20 mg of **10a** in 1 mL of DMSO. The solution was added dropwise to 19 mL of stirring deionised water. Upon addition of the solution of **10a**, the solution became slightly cloudy, and when stirring was stopped a precipitate accumulated at the bottom of the vial.

The extremely poor solubility of the complexes in aqueous media poses a potential issue for the application of the complexes as systemic drugs, as they would be likely to see poor absorption profiles *in vivo*.

2.5 Synthesis of Cationic *Bis*-imidazol-2-ylidene Silver (I) Complexes with Coordinating Anions

The direct synthesis of imidazole-2-ylidene complexes from imidazolium salts with coordinating anions almost invariably leads to the formation of species with the empirical formula [(NHC)(Ag)(X)] where X is the anion.[21, 22] In order to achieve a *bis*-NHC complex with the empirical formula of $[(NHC)_2Ag]^+ X^-$ where X (a carboxylate or halide) would normally coordinate to silver, complexes were formed first with non-coordinating tetrafluoroborate anions (**10a-c**), then a solution of the complex was passed through a column packed with an ion exchange resin which was previously loaded with the desired anion.

2.5.1 Synthesis of cationic *bis*-imidazol-2-ylidene silver (I) gluconate complexes

The incorporation of the gluconate anion into the silver complexes not only adds better biological compatibility over tetrafluoroborate and hexafluorophosphate anions[23] but could also help to increase the solubility of the complexes in aqueous media.

An ion exchange resin **11** was prepared from sodium gluconate and Amberlite IRA-402 Cl^- type resin from a modified literature method.[6] Sodium gluconate was dissolved in deionised water and passed through a column packed with the resin at a flow rate of 0.5 mL min^{-1}. The resin was then washed with deionised water, followed by methanol, then dried under vacuum.

Chloride content of the resin both before and after the ion exchange was determined by elemental analysis. Initial percent by mass of Cl in the resin was 8.77%, corresponding to 87.7 mg chloride per gram of resin or 2.47 mmol chloride per gram of resin. After the ion exchange, the percent by mass of chloride was 1.14%, corresponding to 0.322 mmol of chloride still present, or a loading of 2.15 mmol gluconate per gram of resin. Thus an 87% conversion of the resin **11** was achieved.

The gluconate resin, **11**, was then used in an ion exchange reaction with complexes **10a-c** (*Scheme 2.8*). The tetrafluoroborate complexes were chosen as the starting material because they showed better solubility in polar solvents. The complexes were dissolved in acetonitrile, then deionised water was added to make up a 2:1 acetonitrile to water mixture. The solution was passed through the column containing the resin at a flow rate of 0.133 mL min^{-1} to obtain a residence time of 15 min. The resulting solution was concentrated by rotary evaporation to remove acetonitrile. For complexes **12a** and **12b** a white precipitate formed after acetonitrile was removed from the solution. The precipitate was dried *in vacuo* to yield the pure products. In the case of **12c**, removal of acetonitrile resulted in a viscous, hygroscopic gel-like material. The gel was dried in a 60° C oven for 3 d to remove excess water. The product obtained for **12c** was not elementally pure. Initially the issue was presumed to be the hygroscopic nature of the product, however, all analyses (C, H, N, and F) were below the theoretical values. If water was the main impurity, the found H composition would be expected to be greater than the theoretical value.

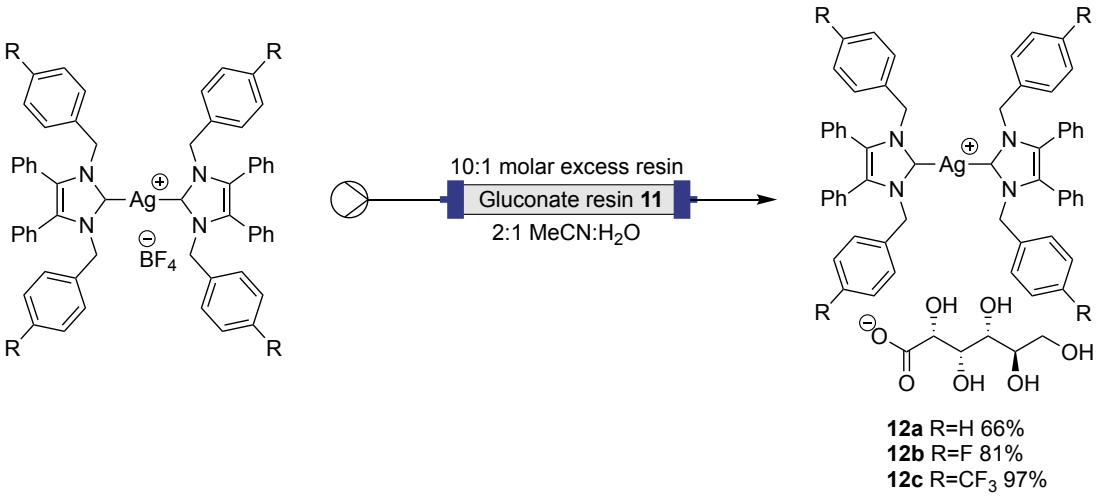

*Scheme 2.8: Reaction scheme for the formation of complexes **12a-c** by anion exchange from complexes **10a-c***

The ^{1}H NMR spectra of all three complexes were clean of impurities and showed the appearance of multiplet peaks in the range of 3.2-3.8 ppm corresponding the CH and CH_2 protons of the gluconate anions.[24] There are also broad peaks in each spectrum between 4 and 5 ppm which represent OH groups of the gluconate. The ^{13}C NMR spectra also show the appearance of a signal near 175 ppm for the carbonyl C atoms, four signals between 71 and 73 ppm which belong to the C(H)OH carbon atoms, and one signal at 63.7 ppm belonging to the CH_2 of the gluconate.[24] The appearance of these signals in the NMR spectra confirm the presence of the gluconate anion. The ^{19}F NMR spectra of **12a-c** no longer show the two distinct signals at -149 ppm that were present in the spectra of **10a-c** which represent the tetrafluoroborate anion.

Infrared spectroscopy of the products **12a-c** shows broad signals centred around 3300 cm^{-1}, signifying O-H stretching and hydrogen bonding from the gluconate anions. Broad peaks at 1100 cm^{-1} from B-F stretching in the starting material (**10a-c**) were no longer present in the spectra.

A single crystal of complex **12c** was grown in a saturated solution of dichloromethane by slow infusion of pentane at room temperature (*Fig. 2.11*). The resulting crystal began to decompose rapidly when taken from the vial which led to a disordered structure. Thus, the data has a high error margin and exact quotations of bond lengths and angles cannot be given. However, the SCXRD data can be used to confirm the overall structure of the complex and the general range of measurements.

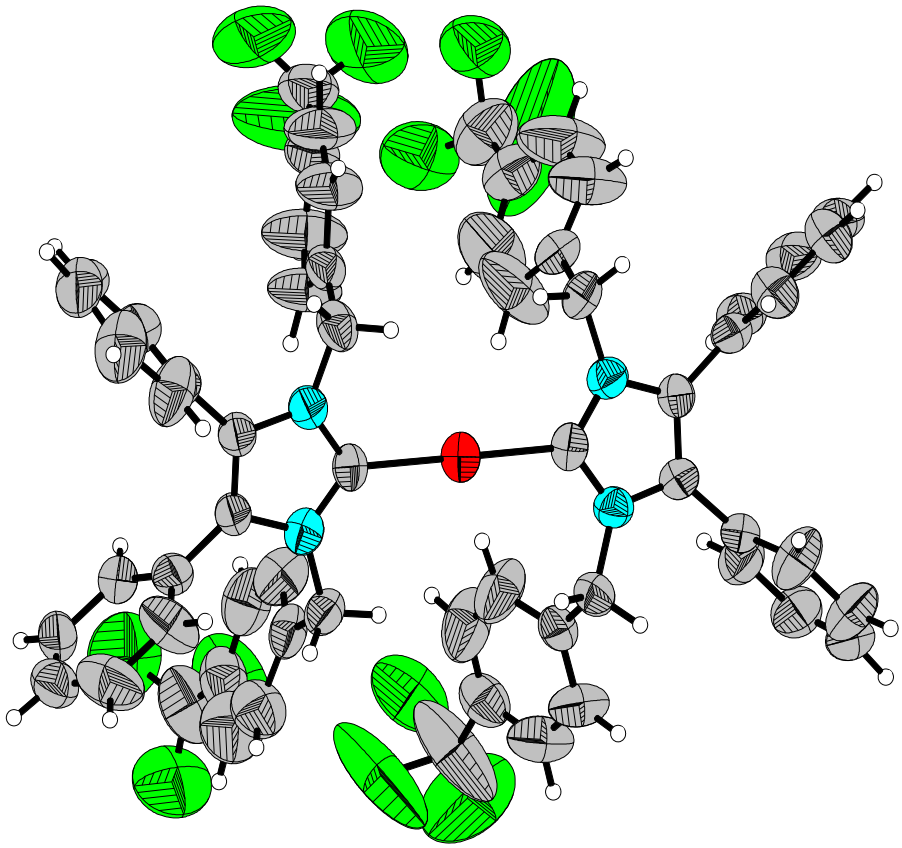

*Figure 2.11: X-ray crystal structure of complex **12c**. Thermal ellipsoids are drawn at the 50% level. Gluconate anion is omitted. (Red = Ag, grey = C, green = F, cyan = N).*

The average carbon silver bond length is roughly 2.08 Å and the C-Ag-C bond angle is 173°, which are consistent with the general range seen in other *bis*-carbene complexes herein and in literature.[14] Similar to crystal structure of complex **9c**, the trifluoromethyl groups all face the same direction, and the two imidazole rings are approximately co-planar. The gluconate anion sits on the opposite side of the imidazole-Ag-imidazole plane to the trifluoromethyl groups. In the crystal packing, this creates a layer of two gluconate anions with a silver complex above and below.

The water solubility of complex **12a** was measured by quantitative NMR to indicate whether the incorporation of the gluconate anion imparted significant water solubility on the complex. The measurement was carried out in deuterated water with maleic acid as the internal standard. The following equation was used to calculate the concentration of **12a** present:

$$\frac{I_a}{I_{std}} \times \frac{N_{std}}{N_a} \times mol_{std} = mol_a, \quad C_a = \frac{mol_a}{volume}$$

I is the integration of the peak, N is the number of protons represented by the peak. C is concentration. Subscript a denotes analyte (**12a**) and subscript std denotes internal standard (maleic acid). The signal for the vinyl protons on maleic acid was compared to the signal for the benzyl protons of **12a**. The resulting spectrum shows a very small amount of **12a** present, and calculations based on the above equation determine the solubility of **12a** to be 51.6 µmol L^{-1}. Despite the incorporation of a very hydrophilic anion, the solubility of the complex in water is still almost negligible.

2.5.2 Synthesis of cationic *bis*-imidazol-2-ylidene silver (I) chloride complexes

When NHC silver complexes are synthesised directly from an azolium salt, the presence of halide anions generally leads to the formation of complexes with the empirical formula [(NHC)(Ag)(X)]. By instead using an anion exchange from a NHC complex with a non-coordinating tetrafluoroborate anion (**10a-c**) the formation of a complex with the formula $[(NHC)_2(Ag)]X$ (X=Cl) was attempted in order to maintain the stability of the *bis*-NHC complexes while including a small, biologically compatible anion (*Scheme 2.9*).

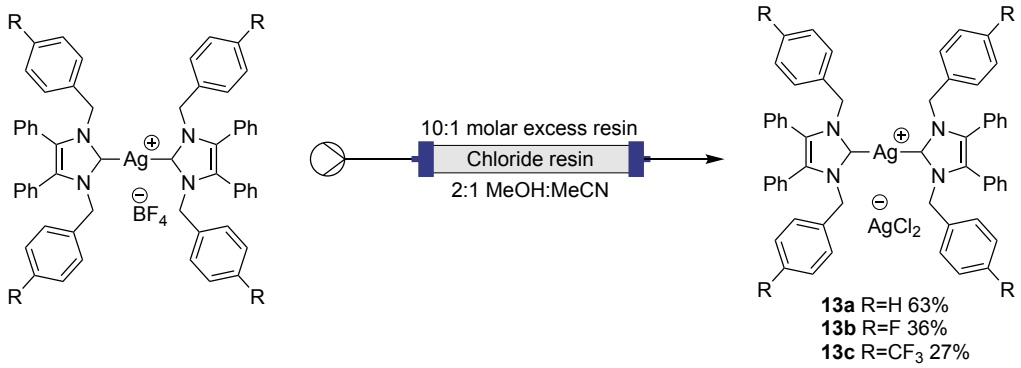

*Scheme 2.9: Reaction scheme for the formation of complexes **13a-c** by anion exchange from complexes **10a-c***

The complexes were synthesised starting from complexes **10a-c**, first dissolving them in 2:1 methanol to acetonitrile. Initially only acetonitrile was used as it is the solvent that best dissolves **10a-c**, however there was still a very significant amount of tetrafluoroborate remaining after the reaction. The solutions of **10a-c** passed through a column containing an excess of Amberlite IRA402 Cl^- type resin. Eluent was collected then concentrated under reduced pressure. As the solvent was removed, solutions became a yellow colour. Proton NMR of the crude products revealed a large amount of imidazolium salt (protonated carbene) present in the products. Complexes were crystallised from solution by slow evaporation of ethanol, followed by washing with cold ethanol to yield the products **13a-c**.

Proton NMR of the crystalline product showed no impurities but could give no information about the identity of the anion. ^{19}F NMR showed no remaining tetrafluoroborate in the complexes. A single crystal of **13a** was obtained by slow evaporation of ethanol at 4 °C. The single crystal x-ray diffraction structure of the complex showed two *bis*-NHC complexes with a bridging $[Ag_2Cl_4]^{2-}$ anion (*Fig. 2.12*).

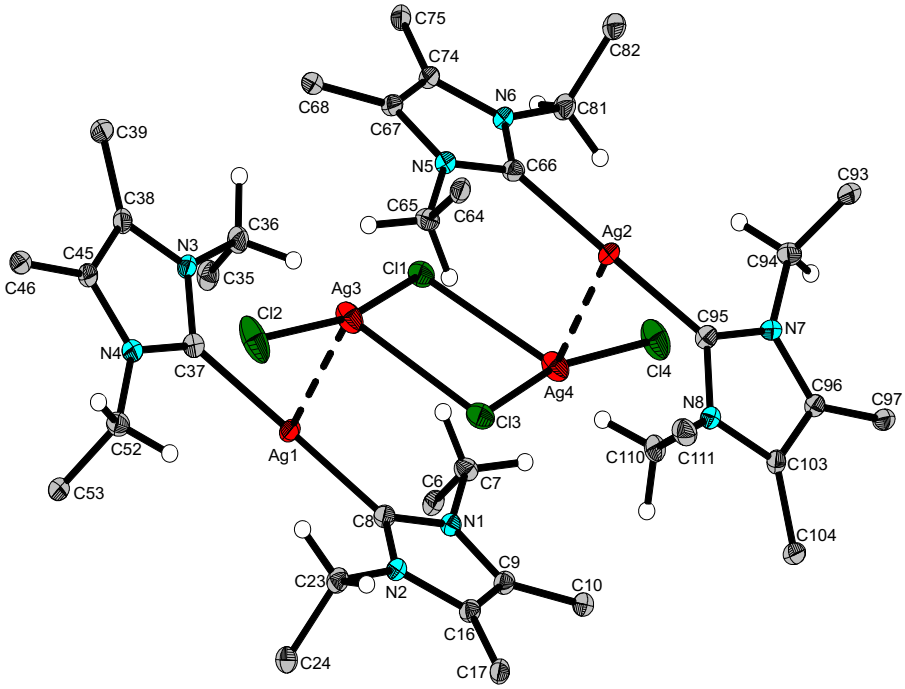

*Figure 2.12: Single crystal X-ray diffraction structure of **13a**. Thermal ellipsoids are drawn at the 50% probability level. Phenyl groups are represented by their ipso carbons only*

*Table2.6: Selected bond lengths and angles in complex **13a***

Bond lengths (Å)	
C8-Ag1	2.0794(16)
C37-Ag1	2.0840(17)
C66-Ag2	2.0794(16)
C95-Ag2	2.0821(17)
Bond Angles (°)	
C8-Ag1-C37	171.49(7)
C66-Ag1-C95	171.34(7)

The silver-carbene bonds are in the expected range for the two complexes present based on what has been seen previously with similar complexes. The bond angles deviate from linearity slightly, which is likely due to the interaction between the silver atoms of the

complexes with the silver atoms of the $[Ag_2Cl_4]^{2-}$ anion. The Ag-Ag distances are 2.962 Å for Ag1-Ag3 and 3.024 Å for Ag2-Ag4. These distances are well within the accepted range for Ag-Ag interactions and are comparable to similar examples in literature.[22, 25] The presence of the $[Ag_2Cl_4]^{2-}$ clusters in the crystal structure when the starting material was a *bis*-carbene complex insinuates that ligand exchange occurred *in situ* during the reaction wherein carbene ligands were exchanged for chloride ligands. This would also help to explain the large amount of imidazolium salt present in the crude product when none was present in the starting material. The silver-carbene bond is known to be quite labile compared to other metal carbene bonds.[26] It is likely that in solution the structure is in equilibrium between the ionic $[(NHC)_2Ag]_2$ $[Ag_2Cl_4]$ species and two neutral [(NHC)AgCl] species.[25, 27] The tendency for ligand exchange of these types of complexes has been shown by John *et al.* using low-temperature ^{13}C NMR which showed two different signals and different C-Ag coupling constants for the carbene carbons corresponding to the mono- and *bis*-NHC complexes.[18]

Based on the solid-state structure of complex **13a**, it was assumed that both **13b** and **13c** display the same pattern of ligand exchange. Elemental analysis of the latter two complexes was consistent with this assumption. Elemental analysis of **13a** was not within the range to establish purity, but ^1H NMR of the product showed visible significant impurities. The low yields of the complexes, especially **13b** and **13c,** may be due to the loss of silver as insoluble AgCl during the exchange process.

The stability of complex **13a** in solution in wet DMSO-d_6 and exposed to light was monitored by ^1H NMR. Decomposition was determined by the change in relative integration of a peak which corresponds to the benzyl groups of the protonated NHC ligand (an imidazolium salt). The study found that the complex decomposed quite slowly over the four-week period and did so in a linear fashion (*Fig*. 2.22). This is a contrast to complex **9a** (section

2.4.2) which showed no decomposition under similar conditions. This may be a consequence of the ligand exchange which occurs due to the presence of the coordinating chloride ion.

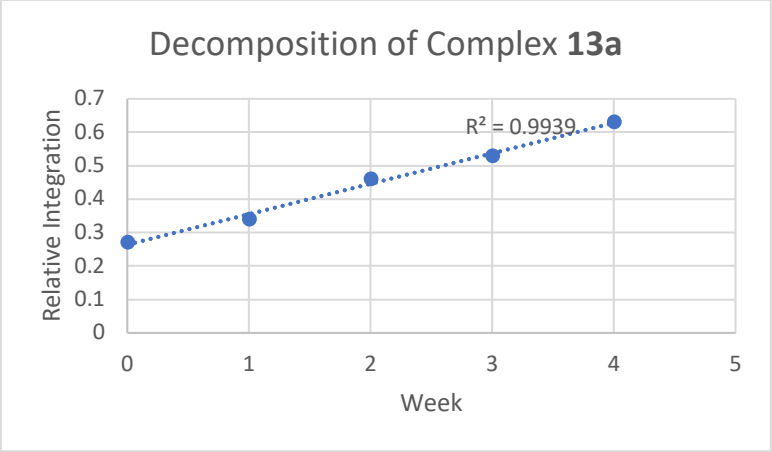

*Figure 2.13: Plotting of the change in integration of a signal corresponding to the decomposition product of **13a** shows slow, linear decomposition over a four week period*

2.5.3 Synthesis of a *bis*-imidazol-2-ylidene silver (I) acetate complex

The acetate ligand has been commonly utilised in the synthesis of NHC silver complexes; however, it is as a coordinating ligand and is usually seen covalently bonded to silver.[1, 28-31] In order to obtain a *bis*-carbene complex with an acetate anion, the tetrafluoroborate complex **10a** was passed over an ion exchange resin, **14** (*Scheme 2.10*). The resin was prepared as described in literature from an aqueous solution of sodium acetate and Amberlite 402 chloride-type resin.[6] The resin (initially 10.69% Cl by mass, 3.1 mmol Cl g^{-1}) was only 0.6% chloride by mass after the exchange, corresponding to 0.17 mmol Cl per gram of resin, or a loading of 2.93 mmol of acetate per gram of resin. This represents a 95% conversion of the resin.

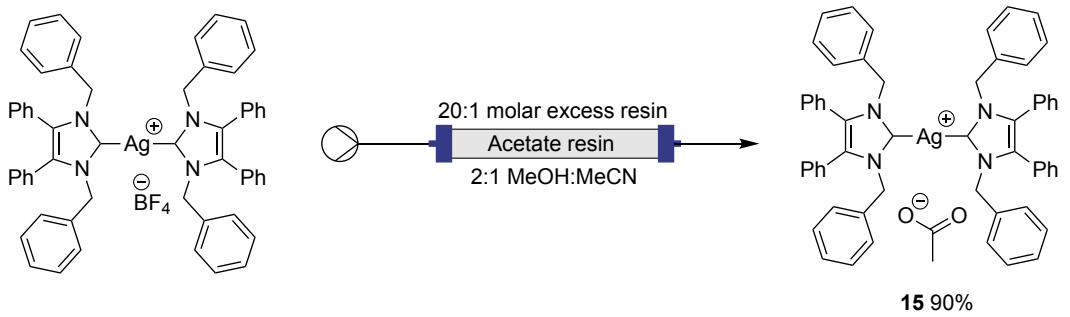

*Scheme 2.10: Synthesis of complex **15** by anion exchange from **10a** using previously prepared exchange resin **14***

The reaction was high yielding and gave a product which was pure by elemental analysis. The proton NMR spectrum showed the appearance of a singlet at 1.54 ppm which

corresponds to the methyl group of the acetate ion. Comparison of the ^{1}H NMR spectrum of **15** to that of **SBC3** showed that both the benzyl CH_2 signals and the acetate CH_3 signals were shifted upfield in **15** (*Fig*. 2.14).

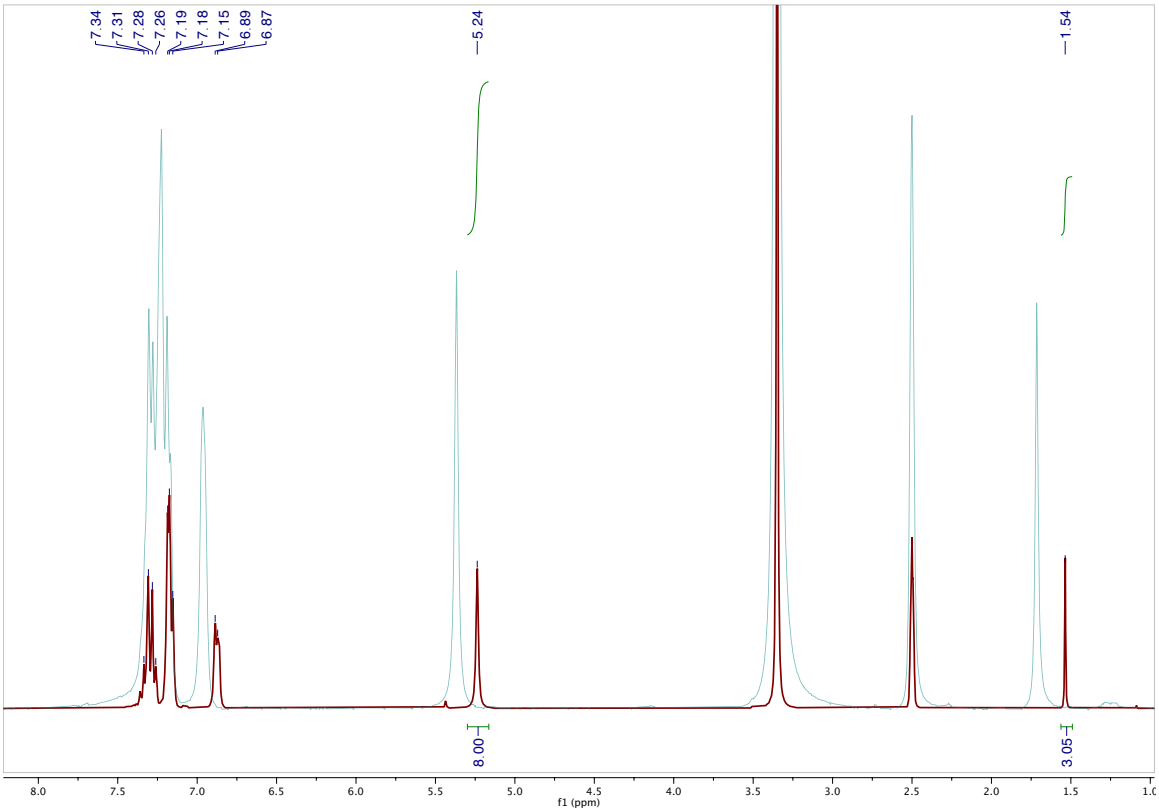

*Figure 2.14: Comparison of the proton NMR spectra of **15** (red) and **SBC3** (blue) in DMSO-d_6*

Comparison of infrared spectra of the two complexes show a similar pattern, but the spectrum of complex **15** a broad signal at 3380 cm^{-1} corresponding to O-H stretching from the hydrogen bonding of the acetate ligand with water present in the sample. This suggests the acetate ligand is not coordinated as in **SBC3**.

A single crystal of **15** was grown from diethyl ether at -18°C. Single crystal X-ray diffraction confirmed the structure of **15** and showed that the complex crystallises with one equivalent of water (*Fig*. 2.15). The crystal structure shows a linear, two coordinate silver centre and two carbene ligands. The carbon-silver bond lengths and C-Ag-C bond angle are consistent with what has been observed in similar complexes herein.

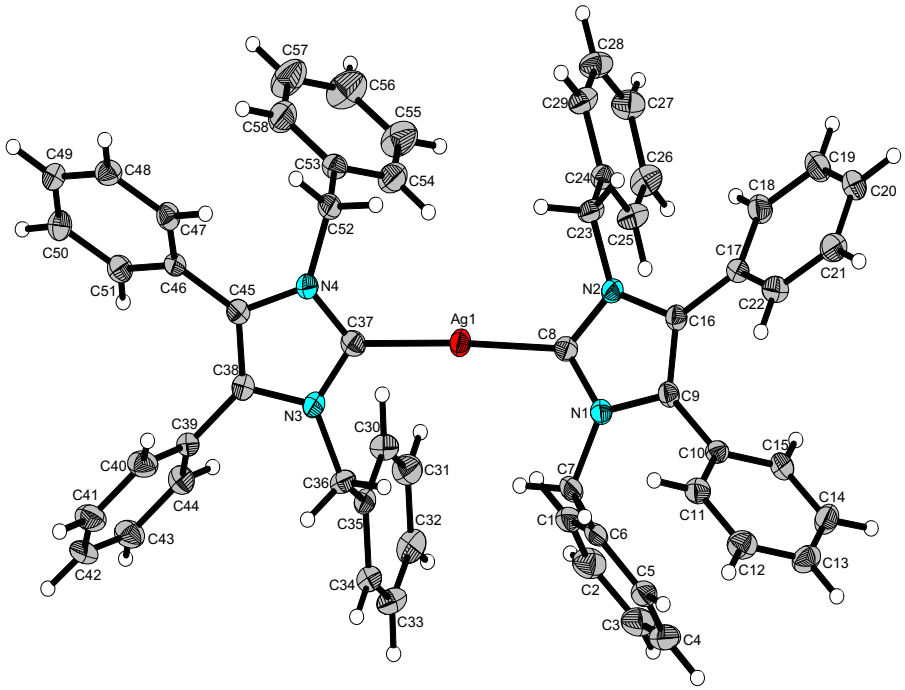

*Figure 2.15: Single crystal X-ray structure of complex **15**. Acetate anion is omitted. Thermal ellipsoids are drawn on the 50% probability level*

*Table 2.7: Selected bond lengths and angles in complex **15***

Bond lengths (Å)	
C8-Ag1	2.079(3)
C37-Ag1	2.089(3)
Bond Angles (°)	
C8-Ag1-C37	176.52(12)

The carbene ligands are approximately co-planar in this structure and the benzyl groups all sit on the same side of the carbene-silver-carbene plane. This contrasts with the structure of **9a** in which the imidazole rings were perpendicular to each other; however, a similar conformation is seen in the structure of **13a**. Since the anions of **13a** and **15** sit near to the silver atom (the Ag to acetate O distance in **15** is approximately 3.2 Å), the benzyl groups sit on the opposite side of the carbene-silver-carbene plane to avoid steric clash. The anion of **9a** sits much further from the silver atom, allowing the carbene ligands to take on the staggered conformation.

2.6 Biological Testing

All silver complexes synthesised in the previous sections were tested for their antibacterial properties using the Kirby-Bauer disk diffusion method. Complexes were tested against *Escherichia coli* and methicillin-resistant *Staphylococcus aureus* (MRSA) to represent gram-negative and gram-positive pathogenic bacteria, respectively. Complexes were compared against the clinical antibiotic tetracycline and **SBC3**.

Bacteria were first cultured on agar plates, then single colonies were taken and incubated in lysogeny broth at 37 °C for 24 h. Growth of bacteria was indicated by turbidity of the broth solution after incubation. The solution of bacteria was pipetted onto agar plates and spread over the agar. The plates were divided into quadrants and a 5.5 mm circle of filter paper was placed in the centre of each quadrant. Solutions of tetracycline, **SBC3**, and the complexes **2a-b**, **4a-c**, **9a-c**, **10a-c**, **12a-c**, **13a-c**, and **15** were made to a concentration of 1 mg mL^{-1} in DMSO and pipetted onto the filter paper circles at volumes of 5 µL and 10 µL. Plates were incubated for 37 °C for 24 h before measurement. The standards tetracycline and **SBC3** were tested once at each loading volume. All novel complexes were tested in triplicate at each volume. Pure DMSO was also tested once at each volume to establish that it had not antimicrobial effect.

Results are reported as the zone of inhibition (in mm): the diameter of a circle centred on the filter paper which showed no bacterial growth (*Fig.* 2.26). For the novel complexes the results are reported as the average of three trials. Because the complexes were tested in two cohorts, they are reported in separate tables (*Table 2.8 and Table 2.*9) because results can only be compared within and not between experiments.

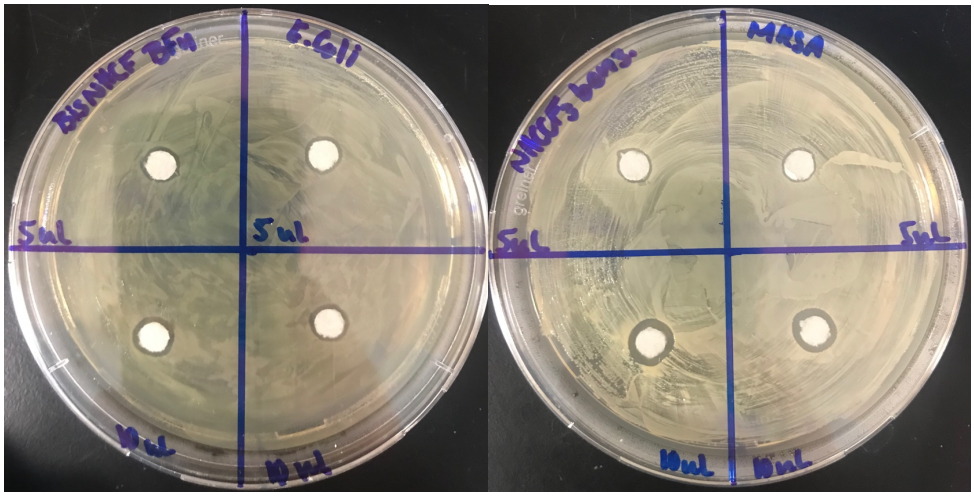

*Figure 2.16: examples of results from the Kirby-Bauer testing of **10b** against E. coli (left) and **4c** against MRSA (right). In both images the top two quadrants represent 5 µL loading and the bottom two represent 10 µL loading*

*Table 2.8: Kirby-Bauer test results for complexes **4a-c**, **9a-c**, and **10a-c**. Results are reported as the zone of clearance in mm*

Compound	**MRSA**		***E. coli***	
	5 µL	**10 µL**	**5 µL**	**10 µL**
DMSO	0	0	0	0
Tetracycline	23	25	23	25
SBC3	6	8	7	12
4a	7	10	7	9
4b	6	8	7	11
4c	7	10	7	9
9a	7	9	6	9
9b	6	9	6	8
9c	7	9	6	7
10a	6	8	7	9
10b	7	9	8	9
10c	7	9	7	8

*Table 2.9: Kirby-Bauer test results for complexes **2a-b**, **12a-c**, **13a-c**, and **15**. Results reported as zone of clearance in mm*

Compound	**MRSA**		***E. coli***	
	5 µL	**10 µL**	**5 µL**	**10 µL**
DMSO	0	0	0	0
Tetracycline	24	26	19	24
SBC3	15	18	8	10
2a	15	18	8	10
2b	11	17	8	10
12a	11	16	9	10
12b	12	16	8	11
12c	10	13	8	9
13a	10	16	10	11
13b	10	14	10	12
13c	11	13	10	11
15	10	12	8	11

For each cohort of experiments, the activity of the novel complexes is similar to that of SBC3, but in all cases is significantly below the activity of tetracycline. Because the Kirby-Bauer test is by nature a qualitative test, these are only indicative results which establish that the complexes display antibacterial properties.[32] The observed zone of clearance of a compound is not only a function of its activity as a drug, but also of the ability of the compound to diffuse across the agar.[33] Because the novel complexes are inherently lipophilic, they likely do not diffuse significantly past the initial area of application, while water-soluble tetracycline can diffuse much more readily across the gel. The high molecular weight of the novel complexes, especially the *bis*-carbene complexes, may also be an inhibitory factor in their ability to diffuse across the agar medium. To obtain quantitative results about the activity of the novel complexes and to accurately make comparisons between them and the standards, further testing must be carried out. Minimum inhibitory concentration testing or toxicity assays would give a better indication of the differences in activity between the complexes. These tests would also better evaluate the stability and behaviour of the complexes in biological media because they require the dissolution of the complexes within the growth medium containing the bacterium.[32]

For more complete results, imidazolium salt precursors should be evaluated by the same method to discern whether the ligand shows any inherent antibacterial activity, or if activity is attributable solely to the silver ion.

2.7 Conclusion

Eleven novel imidazolium salts and 18 novel NHC silver complexes were successfully synthesised and characterised. Synthesis of NHC silver complexes from an imidazolium salt and a silver base is a reliable and convenient method to achieve a diverse range of complexes. From the synthesis of trifluoromethylbenzoate complexes **4a-c** we see that the use of a silver base is a superior method to the free carbene synthesis to achieve products in higher yield and good purity. The former method tolerates an impure intermediate salt to yield the desired product and does not require the strict exclusion of air or moisture.

The addition of a second carbene ligand to NHC silver complexes greatly increases the stability of the *bis*-NHC complexes versus *mono*-NHC complexes both as solids and in solution. Formation of cationic *bis*-carbene complexes can be done simply using the silver base method to obtain complexes with non-coordinating anions in high yields. In order to incorporate anions which would normally coordinate to silver, or which may not be stable to base, we have devised an efficient method of anion exchange from pre-formed *bis*-carbene complexes using ion exchange resins in continuous flow. The identity of the anions of the *bis*-carbene complexes showed some influence on physical properties of the complexes, namely solubility, but the effects were not as pronounced as was hoped. It was observed that at high concentrations, chloride will not behave as a free anion in the presence of even stable *bis*-carbene complexes and prefers coordination to silver either in an NHC silver complex or in an anionic $[AgCl_2]_x^{-x}$ cluster.

Biological testing has shown that all novel complexes display antibacterial activity which is on par with that of the lead compound **SBC3**. The silver complexes display activity which is well below that of tetracycline in the disk diffusion test. This may be a function of overall drug potency, ability to diffuse across agar, or both. Further testing must be carried out to gain a more accurate understanding of the antibiotic activity of the novel complexes. The effects of fluorination of the complexes on their uptake cannot be evaluated from the data obtained and would require further biological experiments.

2.8 References

[1] S. Patil, A. Deally, B. Gleeson, H. Mueller-Bunz, F. Paradisi, M. Tacke, Novel benzyl-substituted N-heterocyclic carbene-silver acetate complexes: synthesis, cytotoxicity and antibacterial studies, *Metallomics* 3(1) (2011) 74-88.

[2] W.R. Dolbier, Fluorine NMR for Organic Chemists, Second Edition ed., Jon Wiley & Sons, Inc., Hoboken, New Jersey, 2016.

[3] T.L. Amyes, S.T. Diver, J.P. Richard, F.M. Rivas, K. Toth, Formation and Stability of N-Heterocyclic Carbenes in Water: The Carbon Acid pK(a) of Imidazollum Cations in Aqueous Solution, *J. Am. Chem. Soc.* 126(13) (2004) 4366-4374.

[4] C.R. Shahini, G. Achar, S. Budagumpi, M. Tacke, S.A. Patil, Non-Symmetrically *p*-Nitrobenzyl-Substituted N-Heterocyclic Carbene-Silver(I) Complexes as Metallopharmaceutical Agents, *App. Organomet. Chem.* 31(12) (2017).

[5] S. Alvarez, A Cartography of the van der Waals Territories, *Dalton Trans.* 42(24) (2013) 8617-8636.

[6] C. O'Beirne, M.E. Piatek, J. Fossen, H. Muller-Bunz, D.R. Andes, K. Kavanagh, S.A. Patil, M. Baumann, M. Tacke, Continuous Flow Synthesis and Antimicrobial Evaluation of NHC* Silver Carboxylate Derivatives of SBC3 *in vitro* and *in vivo*, *Metallomics* 13(2) (2021).

[7] C. O'Beirne, H.T. Althani, O. Dada, J. Cassidy, K. Kavanagh, H. Muller-Bunz, Y. Ortin, X. Zhu, M. Tacke, Novel Derivatives of the Antibiotic NHC-Ag(I) Drug Candidate SBC3: Synthesis, Biological Evaluation and Ag-109 NMR Studies, *Polyhedron* 149 (2018) 95-103.

[8] A.J. Arduengo, R.L. Harlow, M. Kline, A Stable Crystalline Carbene, *J. Am. Chem. Soc.* 113(1) (1991) 361-363.

[9] M. Chung, Synthesis and Molecular Structure of (1,3-dimethyl-4,5-dimethylimidazol-2-ylidene)ag(I)(benzoate), *Bulletin Korean Chem. Soc.* 23(8) (2002) 1160-1162.

[10] C. O'Beirne, N.F. Alhamad, Q.X. Ma, H. Muller-Bunz, K. Kavanagh, G. Butler, X.M. Zhu, M. Tacke, Synthesis, Structures and Antimicrobial Activity of Novel NHC*- and Ph3P-Ag (I)-Benzoate Derivatives, *Inorg. Chimica Acta* 486 (2019) 294-303.

[11] D.H. McDaniel, H.C. Brown, An Extended Table of Hammett Substituents Constants Based on the Ionization of Substituted Benzoic Acids, *J. Org. Chem.* 23(3) (1958) 420-427.

[12] P.L. Arnold, Organometallic chemistry of silver and copper N-heterocyclic carbene complexes, *Heteroatom Chem.* 13(6) (2002) 534-539.

[13] A.A.D. Tulloch, A.A. Danopoulos, S. Winston, S. Kleinhenz, G. Eastham, N-Functionalised heterocyclic carbene complexes of silver, *J. Chem. Soc. Dalton Trans.* (24) (2000) 4499-4506.

[14] J.C. Garrison, W.J. Youngs, Ag(I) N-Heterocyclic Carbene Complexes: Synthesis, Structure, and Application, *Chem. Rev.* 105(11) (2005) 3978-4008.

[15] A.G. Avent, P.A. Chaloner, M.P. Day, K.R. Seddon, T. Welton, Evidence for Hydrogen-Bonding in Solutions of 1-Ethyl-3-Methylimidazolium Halides, and its Implications for Room-Temperature Halogenoaluminate (III) Ionic Liquids, *J. Chem. Soc. Dalton Trans.* (23) (1994) 3405-3413.

[16] R.J. Gillespie, J.S. Hartman, M. Parekh, Solvent Effects on the Boron-Fluorine Coupling Constant and on Fluorine Exchange in the Tetrafluoroborate Anion, *Can. J. Chem.* 46(10) (1968) 1601-1610.

[17] T.S. Light, R.F. Mannion, Microdetermination of Fluorine in Organic Compounds by Potentiometric Titration Using a Fluorine Electrode, *Anal. Chem.* 41(1) (1969) 107-&.

[18] S. Weske, Y.J. Li, S. Wiegmann, M. John, H(C)Ag: a Triple Resonance NMR Experiment for Ag-109 Detection in Labile Silver-Carbene Complexes, *Magn. Reson. Chem.* 53(4) (2015) 291-294.

[19] N. Ramasubbu, R. Parthasarathy, P. Murray-rust, Angular Preferences of Intermolecular Forces Around Halogen Centres - Preferred Directions of Approach of Electrophiles and Nucleophiles Around the Carbon Halogen Bond, *J. Am. Chem. Soc.* 108(15) (1986) 4308-4314.

[20] M. Long, W. Cai, Advanced nanoarchitectures of silver/silver compound composites for photochemical reactions, *Nanoscale* 6(14) (2014) 7730-7742.

[21] I.J.B. Lin, C.S. Vasam, Preparation and application of N-heterocyclic carbene complexes of Ag(I), *Coord. Chem. Rev.* 251(5-6) (2007) 642-670.

[22] K.M. Lee, H.M.J. Wang, I.J.B. Lin, Structural diversity of N-heterocyclic carbene complexes of silver(I), *J. Chem. Soc. Dalton Trans.* (14) (2002) 2852-2856.

[23] A. Costa, A. Forte, K. Zalewska, G. Tiago, Z. Petrovski, L.C. Branco, Novel Biocompatible Ionic Liquids Based on Gluconate Anion, *Green Chem. Lett. and Rev.* 8(1) (2015) 8-12.

[24] A. Pallagi, P. Sebok, P. Forgo, T. Jakusch, I. Palinko, P. Sipos, Multinuclear NMR and molecular modelling investigations on the structure and equilibria of complexes that form in aqueous solutions of Ca2+ and gluconate, *Carbohydr. Res.* 345(13) (2010) 1856-1864.

[25] J. Ramirez, R. Corberan, M. Sanau, E. Peris, E. Fernandez, Unprecedented Use of Silver(I) N-Heterocyclic Carbene Complexes for the Catalytic Preparation of 1,2-Bis(boronate) Esters, *Chem. Comm.* (24) (2005) 3056-3058.

[26] H.V. Huynh, Group 11 Metal-NHC Complexes, The Organometallic Chemistry of N-heterocyclic Carbenes, Wiley2017, pp. 183-194.

[27] I.J.B. Lin, C.S. Vasam, Silver(I) N-heterocyclic carbenes, *Comments on Inorg. Chem.* 25(3-4) (2004) 75-129.

[28] K.M. Hindi, T.J. Siciliano, S. Durmus, M.J. Panzner, D.A. Medvetz, D.V. Reddy, L.A. Hogue, C.E. Hovis, J.K. Hilliard, R.J. Mallet, C.A. Tessier, C.L. Cannon, W.J. Youngs, Synthesis,

stability, and antimicrobial studies of electronically tuned silver acetate N-heterocyclic carbenes, *J. Med. Chem.* 51(6) (2008) 1577-1583.

[29] W. Streciwilk, J. Cassidy, F. Hackenberg, H. Muller-Bunz, F. Paradisi, M. Tacke, Synthesis, cytotoxic and antibacterial studies of p-benzyl-substituted NHC-silver(I) acetate compounds derived from 4,5-di-p-diisopropylphenyl- or 4,5-di-p-chlorophenyl-1H-imidazole, *J. Organomet. Chem.* 749 (2014) 88-99.

[30] A. Kascatan-Nebioglu, A. Melaiye, K. Hindi, S. Durmus, M.J. Panzner, L.A. Hogue, R.J. Mallett, C.E. Hovis, M. Coughenour, S.D. Crosby, A. Milsted, D.L. Ely, C.A. Tessier, C.L. Cannon, W.J. Youngs, Synthesis from caffeine of a mixed N-heterocyclic carbene-silver acetate complex active against resistant respiratory pathogens, *J. Med. Chem.* 49(23) (2006) 6811-6818.

[31] F. Hackenberg, G. Lally, H. Muller-Bunz, F. Paradisi, D. Quaglia, W. Streciwilk, M. Tacke, Novel symmetrically p-benzyl-substituted 4,5-diaryl-imidazole N-heterocyclic carbene-silver(I) acetate complexes - Synthesis and biological evaluation, *J. Organomet. Chem.* 717 (2012) 123-134.

[32] J.H. Jorgensen, M.J. Ferraro, Antimicrobial Susceptibility Testing: A Review of General Principles and Contemporary Practices, *Clin. Infect. Dis.* 49(11) (2009) 1749-1755.

[33] A.W. Bauer, W.M.M. Kirby, J.C. Sherris, M. Turck, Antibiotic Susceptibility Testing by a Standardized Single Disk Method, *Am. J. Clin. Pathol.* 45(4) (1966) 493-496.

Chapter 3 Experimental Details

3.1 General Considerations

All chemicals and reagents were used as supplied from commercial suppliers unless otherwise stated. ^{1}H, ^{13}C, and ^{19}F NMR spectra were obtained on a Varian spectrometer at 400 0r 500 MHz, 101 or 126 MHz, or 376 or 470 MHz, respectively. All spectra were obtained at room temperature. ^{1}H spectra obtained in $CDCl_3$ with 0.03% (v/v) TMS were referenced to TMS. ^{1}H spectra obtained in DMSO-d_6 were referenced to DMSO. All ^{13}C and ^{19}F spectra were referenced to the respective ^{1}H spectrum. Chemical shifts are described as chemical shift (δ) in parts per million (ppm). Coupling constants (*J*) are reported in Hz. Infrared spectroscopy was performed on a Bruker ALPHA Platinum ATR spectrometer. Melting points were assessed using a Stuart SMP10 melting point apparatus, 230 Volt AC input, and were uncorrected. Total elemental analysis was carried out on an Exeter Analytical CE-440 elemental analyser. High resolution mass spectrometry was performed on an Agilent 6546 Q-ToF system equipped with an Agilent 1260 Infinity Prime II LC. All samples were acquired in ESI+ mode and results processed using Agilent MassHunter software. Single crystal X-ray diffraction data was collected on a Rigaku Oxford Diffraction (former Agilent Technologies, former Oxford Diffraction) SuperNova A diffractometer. Complexes **2a** and **9a** were measured using Mo-Kα (λ=0.71073 Å). All other measurements were made using Cu-Kα (λ=1.54184 Å). A complete dataset was collected with the Friedel pairs assumed not equivalent. An analytical absorption correction was performed based on the shape of the crystal[1]. The structures were solved by direct methods using SHELXS and refined by full matrix least- squares on F2 for all data using SHELXL.[2] Hydrogen atoms were added at calculated positions and refined using a riding model. Their isotropic temperature factors were fixed to 1.2 times the equivalent isotropic displacement parameters of the parent atom. Anisotropic thermal displacement parameters were used for all non-disordered non-hydrogen atoms.

3.2 Synthetic Procedures

(1) General procedure for imidazolium bromides

4,5-Diphenyl imidazole (1.00 mmol, 0.220 g), potassium carbonate (1.50 mmol, 0.207 g) and the corresponding benzyl bromide (2.20 mmol) were stirred in acetonitrile (25 mL). The resulting mixture was filtered *in vacuo* to remove the potassium bromide precipitate and any excess potassium carbonate. Solvent was removed under reduced pressure to approximately 5 mL. The product was precipitated from addition of diethyl ether (30 mL), filtered *in vacuo,* and dried for two hours.

1,3-Dibenzyl-4,5-diphenyl imidazolium bromide, 1a:

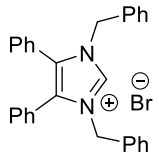

Chemical Formula: $C_{29}H_{25}N_2Br$
Exact Mass: 480.1201

Imidazolium bromide **1a** was prepared from 4,5-diphenyl imidazole (2.20 g, 10.0 mmol), potassium carbonate (2.07 g, 15.0 mmol) and benzyl bromide (2.61 mL, 22.0 mmol). The reagents were stirred in acetonitrile (80 mL) at 35 °C for 2d. The product was isolated according to the general procedure yielding a white solid in 67% yield (3.20 g, 6.68 mmol).

^{1}H NMR (300 MHz, $CDCl_3$): δ ppm 11.19 (s, 1H, NCHN), 7.42 (t, *J* = 7.4 Hz, 2H), 7.33 (t, *J* = 7.3 Hz, 4H), 7.27 (dd, *J* = 5.0, 1.9 Hz, 6H) 7.15- 7.06 (m, 8 H), 5.51 (s, 4H, CH_2).

Spectral data matched with previous reports.[3]

1,3-Di(*p*-fluoro)benzyl-4,5-diphenyl imidazolium bromide, 1b:

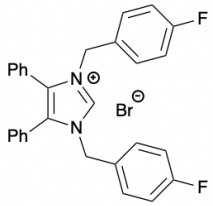

Chemical Formula: $C_{29}H_{23}N_2F_2Br$
Exact Mass: 516.1013

Imidazolium bromide **1b** was prepared from 4,5-diphenyl imidazole (1.10 g, 5.00 mmol), potassium carbonate (1.04 g, 7.50 mmol) and (4-fluoro)benzyl bromide (1.40 mL, 11.0 mmol). The reaction mixture was stirred in acetonitrile (80 mL) at 70 °C for 3d. The product was isolated according to the general procedure to produce a white solid in a yield of 81% (2.10 g, 4.05 mmol).

^{1}H NMR (400 MHz, $CDCl_3$): δ ppm 11.34 (s, 1H, NCHN), 7.43 (t, *J* = 7.5 Hz, 2H), 7.35 (t, *J* = 7.4 Hz, 4H), 7.18 – 7.09 (m, 8H), 6.91 (t, *J* = 8.6 Hz, 4H), 5.52 (s, 4H, CH_2).

^{13}C NMR (101 MHz, $CDCl_3$): δ ppm 162.9 (d, $^1J_{CF}$ = 249.0 Hz), 137.6 (s, NCN), 132.1 (phenyl C), 130.8 (d, $^3J_{CF}$ = 8.4 Hz), 130.8 (phenyl CH), 130.6 (phenyl CH), 129.2 (phenyl CH), 129.1 (d, $^4J_{CF}$ = 3.1 Hz), 124.7 (NC=C), 116.1 (d, $^2J_{CF}$ = 21.8 Hz), 50.8 (CH_2).

^{19}F NMR (376 MHz, $CDCl_3$): δ ppm -112.0 (m, CF).

ATR-IR (neat, cm^{-1}): 3116 (w), 2957 (m), 1604 (m), 1558 (m), 1510 (s), 1451 (m), 1219 (s), 1156 (m), 1025 (w), 814 (s), 761 (s), 699 (s), 589 (m), 497 (m).

Elemental analysis: Calculated: C 67.32 H 4.48 N 5.41 F 7.34 %; Found: C 66.93 H 4.34 N 5.34 F 7.15 %.

HRMS (TOF, ESI+): calculated for $C_{29}H_{23}N_2F_2$ 437.1829, found 437.1826 (M^+)

Melting point: 231-233 °C.

4,5-diphenyl-1,3-di(*p*-trifluoromethyl) benzyl imidazolium bromide, 1c:

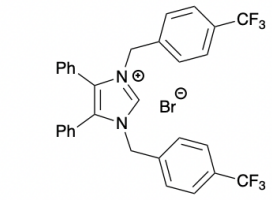

Chemical Formula: $C_{31}H_{23}N_2F_6Br$
Exact Mass: 616.0949

Imidazolium bromide **1c** was prepared from 4,5-diphenyl imidazole (1.10 g, 5.00 mmol), potassium carbonate (1.04 g, 7.50 mmol) and (4-trifluoromethyl) benzyl bromide (1.70 mL, 11.0 mmol). The reagents were stirred in acetonitrile (80 mL) at 70 °C for 3d. The product was isolated according to the general procedure to produce a white solid in a yield of 56% (1.72 g, 2.78 mmol).

^{1}H NMR (400 MHz, $CDCl_3$): δ ppm 11.60 (s, 1H, NCHN), 7.48 (d, *J* = 7.9 Hz, 4H), 7.45-7.40 (m, 2H), 7.35-7.27 (m, 8H), 7.11-7.05 (m, 4H), 5.66 (s, 4H, benzyl CH_2).

^{13}C NMR (101 MHz, $CDCl_3$): δ ppm 138.3 (NCN), 137.1 (benzyl C), 132.2 (phenyl C), 131.1 (q, $^2J_{CF}$ *= 32.3 Hz*), 130.7 (phenyl CH), 130.6 (phenyl CH), 129.2 (phenyl CH), 129.0 (benzyl CH), 126.0 (q, $^3J_{CF}$ = 3.7 Hz), 124.4 (NC=C), 123.7 (q, $^1J_{CF}$ = 274 Hz), 51.1 (s, 2C, CH_2).

^{19}F NMR (376 MHz, $CDCl_3$): δ ppm -62.9 (s).

ATR-IR (neat, cm^{-1}): 3122 (w), 2952 (m), 1563 (m), 1332 (s), 1066- 1162 (s), 700 (s).

Elemental analysis: Calculated: C 60.30 H 3.75 N 4.54 F 18.46 %; Found: C 59.95 H 3.51 N, 4.41 F 18.31 %.

HRMS (TOF, ESI+): calculated for $C_{31}H_{23}N_2F_6$ 537.1765, found 537.1763 (M^+)

Melting point: 276-278 °C.

(2) General procedure for imidazole-2-ylidene silver (I) acetate complexes

An imidazolium salt (**1b-c**) (0.500 mmol) and silver acetate (0.167 g, 1.00 mmol) were added to a flask flushed with nitrogen. Dichloromethane (20 mL) was distilled under nitrogen with calcium hydride and added to the flask. The mixture was stirred for 24 h at 40 °C in the absence of light. The mixture was filtered *in vacuo* to remove precipitated AgBr. The filtrate was concentrated to approx. 3 mL under reduced pressure. Diethyl ether (30 mL) was added, and the mixture was cooled to -18 °C overnight to allow the product to precipitate. The resulting white solid was filtered *in vacuo* and dried for 2 h to yield the pure product.

1,3-Di(*p*-fluoro) benzyl-4,5-diphenylimidazol-2-ylidene silver (I) acetate, 2a

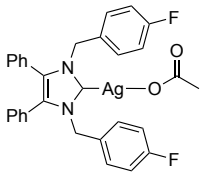

Chemical formula: $C_{31}H_{25}N_2O_2F_2Ag$
Exact mass: 602.0935

Imidazolium salt **1b** (0.259 g, 0.500 mmol) and silver acetate (0.167 g, 1.00 mmol) were treated according to the general procedure to produce a white, crystalline solid in a 65% yield (0.196 g, 0.645 mmol). A single crystal of **2a** was obtained from a saturated solution in DCM by slow infusion of pentane at -18 °C.

^{1}H NMR (400 MHz, $CDCl_3$): δ ppm 7.32 (t, *J* = 7.3 Hz, 2H, phenyl CH), 7.25 (t, *J* = 7.6 Hz, 4H, phenyl CH), 7.00 (d, *J* = 7.6 Hz, 4H, phenyl CH), 6.96-6.87 (m, 8H, benzyl CH), 5.31 (s, 4H, benzyl CH_2), 2.09 (s, 3H, acetate CH_3).

^{13}C NMR (101 MHz, $CDCl_3$): δ ppm 179.2 (C=O), 162.4 (d, $^1J_{CF}$ = 248 Hz), 132.6 (phenyl C), 131.8 (d, $^4J_{CF}$ = 3 Hz), 130.6 (phenyl CH), 129.4 (d, $^3J_{CF}$ = 7 Hz), 129.3 (phenyl CH), 128.7 (phenyl CH), 127.5 (NC=C), 115.6 (d, $^2J_{CF}$ = 22 Hz), 53.1 (benzyl CH_2), 22.8 (acetate CH_3). Carbene C signal not observed.

^{19}F NMR (376 MHz, $CDCl_3$): δ ppm -113.6 (m, CF).

ATR-IR (neat, cm^{-1}): 3062 (w), 2934 (w), 1574 (s), 1508 (s), 1443 (m), 1380 (s), 1329 (s), 1218 (s), 1158 (m), 1023 (w), 929 (w), 819 (s), 764 (m), 701 (s), 670 (m), 613 (m), 543 (m).

Elemental analysis: Calculated C 61.71, H 4.18, N 4.64, F 6.29 %; Found C 61.65, H 4.02, N 4.57, F 6.12 %.
HRMS (TOF, ESI+): Calculated for $C_{31}H_{25}N_2O_2F_2Ag^+$ 602.0935. Found 981.2534 ($[(NHC)_2Ag]^+$+2H$^+$).
Melting point:193-196 °C

1,3-Di(*p*-trifluoromethyl) benzyl-4,5-diphenylimidazol-2-ylidene silver (I) acetate, 2b

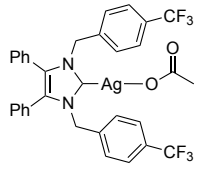

Chemical formula: $C_{33}H_{25}N_2O_2F_6Ag$
Exact mass: 702.0871

Imidazolium salt **1c** (0.309 g, 0.500 mmol) and silver acetate (0.167 g, 1.00 mmol) were treated according to the general procedure to produce the white, solid product in a 68% yield (0.238 g, 0.339 mmol).
^{1}H NMR (400 MHz, $CDCl_3$): δ ppm 7.49 (d, *J* = 7.9 Hz, 4H, benzyl CH), 7.33 (t, *J* = 7.4 Hz, 2H, phenyl CH), 7.26 (t, *J* = 7.4, 4H, phenyl CH), 7.10 (d, *J* = 8.0 Hz, 4H, benzyl CH), 7.00 (d, *J* = 7.6 Hz, 4H, phenyl CH), 5.42 (s, 4H, benzyl CH_2), 2.08 (s, 3H, acetate CH_3).
^{13}C NMR (101 MHz, $CDCl_3$): δ ppm 179.3 (C=O), 139.8 (benzyl C), 138.2 (phenyl C), 130.5 (phenyl CH), 130.4 (q, $^2J_{CF}$ = 32 Hz), 129.6 (phenyl CH), 128.8 (phenyl CH), 127.8 (benzyl CH), 127.2 (NC=C), 125.7 (q, $^3J_{CF}$ = 4 Hz), 123.8 (q, $^1J_{CF}$ = 274 Hz), 53.2 (benzyl CH_2), 22.7 (acetate CH_3). Carbene C signal not observed.
^{19}F NMR (376 MHz, $CDCl_3$): δ ppm -62.7 (s, CF_3).
ATR-IR (neat, cm^{-1}): 3403 (w, br), 3056 (w), 1594 (m), 1450 (w), 1380 (m), 1320 (s), 1156 (m), 1109 (s), 1065 (s), 1015 (m), 920 (w), 852 (m), 818 (m), 762 (m), 702 (s), 615 (m), 517 (w).
Elemental analysis: Calculated C 56.35, H 3.58, N 3.98, F 16.21 %; Found C 56.31, H 3.12, N 3.92, F 15.95 %.
HRMS (TOF, ESI+): Calculated for $C_{33}H_{25}N_2O_2F_6Ag^+$ 702.0871. Found 1181.2398 ($[(NHC)_2Ag]^+$+2H$^+$).
Melting point: 207-209 °C

(3) Synthesis of silver (I) *p*-trifluoromethyl benzoate

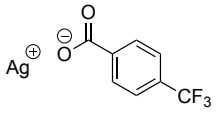

Chemical formula: $C_8H_4O_2F_3Ag$
Exact mass: 295.9215

Silver salt **3** was synthesised by stirring *p*-trifluoromethyl benzoic acid (1.14 g, 6.00 mmol) and silver oxide (0.962 g, 4.00 mmol) in acetonitrile (60 mL) for 24 h at room temperature. The product was filtered *in vacuo* then washed with hot acetonitrile (20 mL) followed by diethyl ether (20 mL) and dried for 4 h. The resulting product was a purple powder obtained in a 99% yield (1.76 g, 5.93 mmol).
^{1}H NMR (400 MHz, DMSO-d_6): δ ppm 8.12 (d, *J* = 7.8 Hz, 2H, benzoate CH), 7.73 (d, 2H, *J* = 7.9 Hz, benzoate CH).
^{13}C NMR (101 MHz, DMSO-d_6): δ ppm 168.7 (C=O), 141.1 (benzoate C), 130.0 (benzoate CH), 129.9 (q, $^2J_{CF}$ = 32 Hz), 124.6 (q, $^3J_{CF}$ = 4 Hz), 124.2 (q, $^1J_{CF}$ = 274 Hz).
^{19}F NMR (376 MHz, DMSO-d_6): δ ppm -61.6 (s, CF_3)
ATR-IR (neat, cm^{-1}): 3073.32 (w), 1509.28 (m), 1381.56 (m), 1312.96 (m), 1130.78 (s), 1099.05 (s), 1061.00 (s), 1013.40 (m), 868.15 (s), 783.81 (s), 708.44 (s), 500.28 (s).
Elemental analysis: Calculated C 32.35, H 1.36, F 19.19 %; Found C 31.96, H 1.41, F 18.83 %.
Melting point: 245-246 °C

(4) General procedure for imidazol-2-ylidene silver (*p*-trifluoromethyl) benzoates

An imidazolium (*p*-trifluoromethyl) benzoate salt **6a-b** (0.250 mmol) and silver (I) oxide (0.250 mmol, 0.058 g) were stirred in dry dichloromethane (25 mL) under nitrogen at room temperature for 3 d. The reaction mixture was filtered *in vacuo* through a grade 4 sinter funnel. Solvent was removed under reduced pressure. The solid was redissolved in chloroform and filtered *in vacuo* through a layer of celite. The reaction mixture was concentrated to 3 mL under reduced pressure. Pentane (40 mL) was added to precipitate the product. The mixture was filtered *in vacuo* and dried for 2 h.

1,3-Dibenzyl-4,5-diphenyl imidazol-2-ylidene silver (*p*-trifluoromethyl) benzoate, 4a:

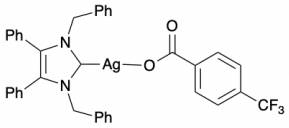

Chemical Formula: $C_{37}H_{28}N_2O_2F_3Ag$
Exact Mass: 696.1154

Compound **4a** was synthesised from imidazolium benzoate salt **6a** (0.250 mmol, 0.148 g) and silver oxide (0.250 mmol, 0.058 g) according to the general procedure to produce a light brown solid in a 53% yield (0.132 mmol, 0.092 g). A single crystal of **4a** was obtained from a saturated solution in DCM by slow infusion of pentane at -18 °C.

^{1}H NMR (400 MHz, $CDCl_3$): δ ppm 8.20 (d, *J* = 7.9 Hz, 2H, CH benzoate), 7.63 (d, *J* = 7.9 Hz, 2H, CH benzoate), 7.31-7.28 (m, 2H, carbene aromatic CH), 7.24-7.21 (m, 10 H, carbene aromatic CH), 7.02-6.99 (m, 8 H, carbene aromatic CH), 5.36 (s, 4H, CH_2).

^{13}C NMR (101 MHz, $CDCl_3$): δ ppm 172.3 (COO), 136.2 (aromatic C), 132.8 (aromatic C), 131.9 (q, $^2J_{CF}$ = 32 Hz, benzoate), 130.6 (carbene aromatic CH), 130.1 (benzoate aromatic CH), 129.2 (carbene aromatic CH), 128.7, 128.6, 128.1 (carbene aromatic CH), 127.7 (NC=C), 127.3 (carbene aromatic CH), 124.7 (q, $^3J_{CF}$ = 4 Hz, benzoate), 124.3 (q, $^1J_{CF}$ = 272 Hz, benzoate), 53.8 (CH_2). Carbene C signal not observed.

^{19}F NMR (376 MHz, $CDCl_3$): δ ppm -62.6 (s, CF_3)

ATR-IR: (neat, cm^{-1}) 3061 (w), 1611 (m), 1558 (m), 1448 (w), 1382 (m), 1317 (s), 1125 (m), 1062 (m), 1019 (m), 867 (w), 844 (w), 761 (m), 698 (s), 612 (m), 491 (m).

Elemental analysis: Calculated C 63.71, H 4.05, N 4.02, F 8.17 %; Found 62.54, H 3.79, N 3.85, F 8.52 %.

HRMS (ESI$^+$, TOF): Calculated for $C_{37}N_2O_2F_3Ag^+$ 696.1154. Found 907.2926 $[(NHC)_2Ag]^+$

Melting point: 140 °C (dec.)

1,3-Di(*p*-fluoro) benzyl-4,5-diphenyl imidazol-2-ylidene silver (*p*-trifluoromethyl) benzoate, 4b:

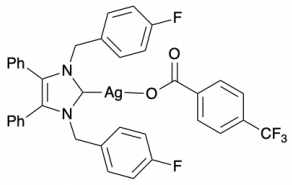

Chemical Formula: $C_{37}H_{26}N_2O_2F_5Ag$
Exact Mass: 732.0965

Compound **4b** was synthesised from imidazolium benzoate salt **6b** (0.250 mmol, 0.166 g) and silver oxide (0.250 mmol, 0.058 g) according to the general procedure. The product was a white solid obtained in an 58% yield (0.146 mmol, 0.107 g).

^{1}H NMR (400 MHz, $CDCl_3$): δ ppm 8.21 (d, *J* = 8.0 Hz, 2H, CH benzoate), 7.64 (d, *J* = 8.1 Hz, 2H, CH benzoate), 7.34-7.30 (m, 2H, carbene aromatic CH), 7.27 -7.23 (m, 4H, carbene aromatic CH), 7.01 – 6.94 (m, 8H, carbene aromatic CH), 6.90 (t, *J* = 8.6 Hz, 4H, carbene aromatic CH), 5.35 (s, 4H, CH_2).

^{13}C NMR (101 MHz, $CDCl_3$): δ ppm 172.5 (COO), 162.4 (d, $^1J_{CF}$ = 249 Hz, carbene), 139.1 (benzoate aromatic C), 132.8 (carbene aromatic C), 132.0 (q, $^2J_{CF}$ = 32 Hz, benzoate), 131.8 (carbene aromatic C), 130.6 (carbene aromatic CH), 130.1 (benzoate aromatic CH), 129.4 (carbene aromatic CH), 129.3 (d, $^3J_{CF}$ = 8 Hz, carbene), 128.7 (carbene aromatic CH), 127.5

(NC=C), 124.8 (q, $^3J_{CF}$ = 4 Hz, benzoate), 124.2 (q, $^1J_{CF}$ = 272 Hz, benzoate), 115.7 (d, $^2J_{CF}$ = 22 Hz, carbene), 53.2 (CH_2). Carbene C signal not observed.
^{19}F NMR (376 MHz, $CDCl_3$): δ ppm -62.6 (s, benzoate CF_3), -113.5 (m, carbene CF).
ATR-IR: (neat, cm^{-1}) 3059 (w), 2932 (w), 1599 (m), 1558 (m), 1509 (s), 1383 (m), 1319 (s), 1227 (m), 1158 (m), 1123 (m), 1076 (m), 1062 (m), 823 (m), 760 (m), 699 (s), 611 (m), 492 (m).
Elemental analysis: Calculated C 60.59, H 3.57, N 3.82, F 12.95 %; Found C 61.21, H 3.56, N 3.86, F 12.77 %.
HRMS (ESI$^+$, TOF): calculated for $C_{37}H_{26}N_2O_2F_5Ag^+$ 732.0965. Found 979.2557 $[(NHC)_2Ag]^+$
Melting point: 152-154 °C (dec.)

1,3-Di(*p*-trifluoromethyl) benzyl-4,5-diphenylimidazol-2-ylidene silver (*p*-trifluoromethyl) benzoate, 4c:

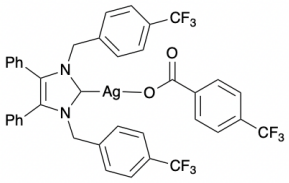

Chemical Formula: $C_{39}H_{26}N_2O_2F_9Ag$
Exact Mass: 832.0902

Compound **4c** was synthesised from imidazolium benzoate salt **6c** (0.250 mmol, 0.182 g) and silver oxide (0.250 mmol, 0.058 g) according to the general procedure. The product was a light brown solid obtained in a 59% yield.
^{1}H NMR (400 MHz, $CDCl_3$): δ ppm 8.18 (d, *J* = 8.0 Hz, 2H, benzoate CH), 7.60 (d, *J*= 8.0 Hz, 2 H, benzoate CH), 7.44 (d, *J* = 7.8 Hz, 4H, carbene CH), 7.30 (m, 2H, carbene CH), 7.22 (t, *J* = 7.5 Hz, 4H, carbene CH), 7.08 (d, *J* = 7.9 Hz, 4H, carbene CH), 6.95 (d, *J* = 7.5 Hz, 4H, carbene CH), 5.43 (s, 4H, benzyl CH_2).
^{13}C NMR (101 MHz, $CDCl_3$): δ ppm 172.0 (COO), 140.4 (benzoate C), 132.8 (carbene C), 131.6 (q, $^2J_{CF}$ = 32 Hz, carbene), 130.6 (carbene C) 130.4 (carbene CH), 129.9 (benzoate CH), 129.5 (carbene CH), 129.1 (q, $^2J_{CF}$ = 27 Hz, benzoate) 128.8 (carbene CH), 127.5 (carbene CH), 127.2 (NC=C), 125.7 (q, $^3J_{CF}$ = 4 Hz, carbene), 124.6 (q, $^3J_{CF}$ = 4 Hz, benzoate), 123.8 (q, $^1J_{CF}$ = 273 Hz, carbene), 121.6 (q, $^1J_{CF}$ = 275 Hz, benzoate), 53.0 (CH_2). Carbene C signal not observed.
^{19}F NMR (376 MHz, $CDCl_3$): δ ppm -62.5 (s, benzoate CF_3), -62.7 (s, carbene CF_3).
ATR-IR (neat, cm^{-1}): 3056 (w), 1608 (w), 1564 (w), 1372 (m), 1317 (s), 1125 (s), 1064 (s), 1015 (m), 869 (m), 821 (m), 700 (s), 610 (w), 491 (m).
Elemental analysis: Calculated C 56.20, H 3.14, N 3.36, F 20.51 %; Found C 55.57, H 3.11, N 3.26, F 19.53 %
HRMS (ESI$^+$, TOF): Calculated for $C_{39}H_{26}N_2O_2F_9Ag^+$ 823.0902. Found 1179.2417 $[(NHC)_2Ag]^+$
Melting point: 161-162 °C (dec.)

(5) Synthesis of potassium (*p*-trifluoromethyl) benzoate

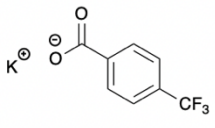

Chemical Formula: $C_8H_4O_2F_3K$
Exact Mass: 227.9800

Potassium carbonate (1.00 mmol, 0.138 g) and (4-trifluoromethyl) benzoic acid (2 mmol, 0.380 g) were stirred in methanol (30 mL) at room temperature for 24 h. The solvent was removed under reduced pressure. The resulting solid was dried *in vacuo* for 1 h to yield a white solid in a 94% yield (1.88 mmol, 0.431 g).
^{1}H NMR (400 MHz, DMSO-d_6): δ ppm 8.05 (d, *J* = 7.7 Hz, 2H), 7.62 (d, *J* = 7.9 Hz, 2H).
^{13}C NMR (101 MHz, DMSO-d_6): δ ppm 167.4 (COO), 144.2 (aromatic C), 129.4 (aromatic CH), 128.9 (q, $^2J_{CF}$ = 31 Hz), 124.6 (q, $^1J_{CF}$ = 273 Hz), 124.0 (q, $^3J_{CF}$ = 4 Hz).
^{19}F NMR (376 MHz, DMSO-d_6): δ ppm -61.3 (s, CF_3).
ATR-IR: (neat, cm^{-1}) 3063 (w), 1599 (m), 1548 (s), 1393 (m), 1322 (m), 1138 (s), 1067 (s), 1013 (m), 874 (m), 835 (m), 798 (s), 770 (m), 711 (s), 556 (w), 476 (m).
Elemental analysis: Calculated C 42.10, H 1.77, F 24.97 %; Found C 42.85, H 1.53, F 24.49 %.
Melting point: >300 °C

(6) General procedure for imidazolium (*p*-trifluoromethyl) benzoate salts:

An imidazolium salt, **1a-c** (1.00 mmol), and potassium (4-trifluoromethyl) benzoate, **5** (1 mmol, 0.228 g), were stirred in a 10:1 mixture of acetonitrile and methanol (40 mL) at room temperature for 3 d. Methanol was removed under reduced pressure and the resulting mixture was filtered *in vacuo* to remove any precipitates. The filtrate was concentrated and dried under reduced pressure to yield the product.

1,3-Dibenzyl-4,5-diphenyl imidazolium (*p*-trifluoromethyl) benzoate, 6a:

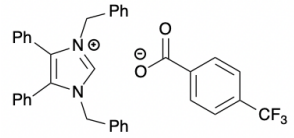

Chemical Formula: $C_{37}H_{29}N_2O_2F_3$
Exact Mass: 590.2181

Compound **6a** was synthesised from 1,3-dibenzyl-4,5-diphenyl imidazolium bromide **1a** (0.500 mmol, 0.241 g) and potassium (*p*-trifluoromethyl) benzoate **5** (0.500 mmol, 0.115 g) according to the general procedure to yield a white solid in a 97% yield (0.484 mmol, 0.286 g).

^{1}H NMR (400 MHz, DMSO-d_6): δ ppm 10.03 (s, 1H, NCHN), 8.04 (d, *J* = 7.9 Hz, 2H, CH benzoate), 7.63 (d, *J* = 8.0 Hz, 2H, CH benzoate), 7.41 (m, 2H), 7.35 (t, *J* = 7.4 Hz, 4H), 7.32 – 7.28 (m, 10H), 7.09 (m, 4H), 5.46 (s, 4H, CH_2).

^{13}C NMR (101 MHz, DMSO-d_6): δ ppm 167.2 (COO), 144.1 (benzoate aromatic C), 137.0 (NCN), 134.0 (imid. aromatic C), 131.7 (imid. aromatic C), 130.7 (imid. aromatic CH), 130.0 (imid. aromatic CH), 129.4 (benzoate CH), 128.9 (q, $^2J_{CF}$ = 32 Hz, benzoate aromatic C), 128.7 (imid. aromatic CH), 128.7 (imid. aromatic CH), 128.4 (imid. aromatic C), 127.8 (imid. aromatic CH), 124.9 (NC=C), 124.5 (q, $^1J_{CF}$ = 273 Hz, benzoate CF_3), 124.1 (q, $^3J_{CF}$ = 3 Hz, benzoate CH), 50.4 (CH_2).

^{19}F NMR (376 MHz, DMSO-d_6): δ ppm -61.3 (s, CF_3).

ATR-IR: (neat, cm^{-1}) 3366 (w, br), 3057 (w), 1605 (m), 1549 (m), 1455 (m), 1373 (m), 1320 (s), 1152 (m), 1118 (s), 1061 (s), 1015 (m), 972 (w), 839 (m), 788 (m), 729 (s), 606 (m), 478 (m).

Elemental analysis: Calculated C 75.24, H 4.95, N 4.74, F 9.65 %; Found C 64.84, H 4.39, N 4.05, F 7.99 %.

HRMS (ESI$^+$, TOF): Calculated for $C_{29}H_{25}N_2$ 401.2020. Found 401.2011 (M^+).

Melting point: 156-160 °C

1,3-Di(4-fluoro) benzyl-4,5-diphenyl imidazolium (*p*-trifluoromethyl) benzoate, 6b:

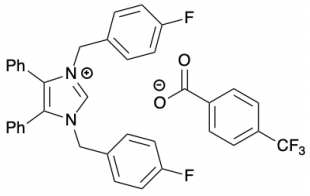

Chemical Formula: $C_{37}H_{27}N_2O_2F_5$
Exact Mass: 626.1993

Compound **6b** was synthesised from 1,3-di(*p*-fluoro) benzyl-4,5-diphenyl imidazolium bromide **1b** (0.500 mmol, 0.259 g) and potassium (*p*-trifluoromethyl) benzoate **5** (0.500 mmol, 0.115 g) according to the general procedure to yield an off-white solid in a 96% yield (0.478 mmol, 0.300 g).

^{1}H NMR (400 MHz, DMSO-d_6): δ ppm 10.03 (s, 1H, NCHN), 8.05 (d, *J* = 7.7 Hz, 2H, CH benzoate), 7.64 (d, *J* = 8.0 Hz, 2H, CH benzoate), 7.46 – 7.41 (m, 2H), 7.38 (t, *J* = 7.4 Hz, 4H), 7.33 – 7.29 (m, 4H), 7.20 – 7.11 (m, 8H), 5.47 (s, 4H, CH_2 benzyl).

^{13}C NMR (101 MHz, DMSO-d_6): δ ppm 167.2 (COO), 162.0 (d, $^1J_{CF}$ = 245 Hz, imid.), 144.5 (benzoate aromatic C), 137.1 (NCN), 131.7 (imid. aromatic C), 130.8 (imid. aromatic CH), 130.4 (d, $^3J_{CF}$ = 8 Hz, imid.), 130.2 (d, $^4J_{CF}$ = 3 Hz, imid.), 130.1 (imid. aromatic CH), 129.5 (CH benzoate), 128.8 (q, $^2J_{CF}$ = 31 Hz, benzoate), 128.8 (imid. aromatic CH), 125.0 (NC=C), 124.6 (q, $^1J_{CF}$ = 274 Hz, benzoate), 124.1 (q, $^3J_{CF}$ = 4 Hz, benzoate), 115.6 (d, $^2J_{CF}$ = 22 Hz, imid.), 49.8 (CH_2).

^{19}F NMR (376 MHz, DMSO-d_6): δ ppm -61.2 (s, CF_3), -113.9 (m, CF).

ATR-IR: (neat, cm^{-1}) 3356 (w), 3064 (w), 2954 (w), 1602 (m), 1559 (m), 1511 (s), 1450, (m), 1375 (m), 1320 (s), 1222 (m), 1160 (m), 1123 (s), 1062 (m), 1022 (m), 819 (m), 753 (m), 695 (s), 614 (m).
Elemental analysis: Calculated C 70.92, H 4.34, N 4.47, F 15.16 %; Found C 62.43, H 3.86, N 3.87, F 12.89 %.
HRMS (ESI^+, TOF): Calculated for $C_{29}H_{23}N_2F_2$ 437.1829. Found 437.1825 (M^+).
Melting point: 179-184°C

4,5-Diphenyl-1,3-di(*p*-trifluoromethyl) benzyl imidazolium (*p*-trifluoromethyl) benzoate, 6c:

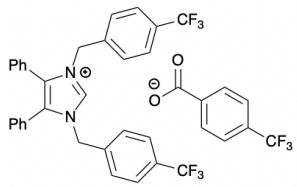

Chemical Formula: $C_{39}H_{27}N_2O_2F_9$
Exact Mass: 726.1929

Compound **6c** was synthesised from 1,3-di(*p*-trifluoromethyl) benzyl-4,5-diphenyl imidazolium bromide **1c** (0.500 mmol, 0.309 g) and potassium (*p*-trifluoromethyl) benzoate **5** (0.500 mmol, 0.115 g) according to the general procedure to yield a white solid in an 94% yield (0.468 mmol, 0.340 g).
^{1}H NMR (400 MHz, DMSO-d_6): δ ppm 10.20 (s, 1H, NCHN), 8.04 (d, J = 7.5 Hz, 2H, CH benzoate), 7.67 (d, J = 8.1 Hz, 4H), 7.62 (d, J = 8.0 Hz, 2H, CH benzoate), 7.44 – 7.29 (m, 14H), 5.63 (s, 4H, CH_2, benzyl).
^{13}C NMR (101 MHZ, DMSO-d_6): δ ppm 167.2 (COO), 144.4 (benzoate aromatic C), 138.8 (aromatic C), 137.8 (NCN), 131.8 (imid. aromatic C), 130.8 (imid. aromatic CH), 130.2 (imid. aromatic CH), 129.5 (benzoate CH), 128.8 (q, $^2J_{CF}$ = 32 Hz, imid.), 128.8 (imid. aromatic CH), 128.7 (imid. aromatic CH), 125.2 (q, $^3J_{CF}$ = 4 Hz, imid.), 124.9 (NC=C), 124.6 (q, $^1J_{CF}$ = 274 Hz, benzoate), 124.1 (q, $^3J_{CF}$ = 4 Hz, benzoate), 124.0 (q, $^1J_{CF}$ = 274 Hz, imid.), 50.0 (CH_2), (C)-CF_3 signal for benzoate not observed.
^{19}F NMR (376 MHz, DMSO-d_6): δ ppm -61.3 (s, 3F, CF_3 benzoate), -61.7 (s, 6F, CF_3 imid.).
ATR-IR: (neat, cm^{-1}) 3367 (w), 3219 (w), 3059 (w), 2955 (w), 1555 (m), 1417 (w), 1324 (s), 1162 (m), 1112 (s), 1065 (s), 1015 (m), 818 (m), 790 (m), 696 (m), 582 (w), 481 (w).
Elemental analysis: Calculated C 64.46, H 3.75, N 3.86, F 23.5313 %; Found C 57.62, H 3.19, N 3.38, F 19.67 %.
HRMS (ESI^+, TOF): Calculated for $C_{31}H_{23}N_2F_6$ 537.1765. Found 537.1761 (M^+).
Melting point: 204-209 °C

(7) General procedure for imidazolium hexafluorophosphate salts

A substituted imidazolium bromide, **1a-c**, (1.00 mmol) and potassium hexafluorophosphate (1.50 mmol, 0.276 g) were stirred in a 4:1 mixture of methanol and water (25 mL) at room temperature for 4 hours. The mixture was then poured into deionised water (100 mL). A white precipitate was observed. The mixture was filtered *in vacuo*, washed with deionised water (20 mL) and dried for 2 h to give the products as white solids.

1,3-Dibenzyl-4,5-diphenyl imidazolium hexafluorophosphate, 7a:

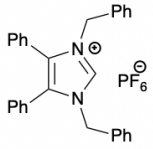

Chemical Formula: $C_{29}H_{25}N_2F_6P$
Exact Mass: 546.1660

Compound **7a** was synthesised from 1,3-dibenzyl-4,5-diphenyl imidazolium bromide, **1a**, (0.481 g, 1.00 mmol) and potassium hexafluorophosphate (0.276 g, 1.50 mmol) according to the general procedure. The product was a white solid (0.501g, 0.917 mmol) obtained in a 92% yield.

^{1}H NMR (400 MHz, $CDCl_3$): δ ppm 8.70 (s, 1H, NCHN), 7.38 (t, *J* = 7.4 Hz, 2H), 7.31 (t, *J* = 7.4 Hz, 2H) 7.26-7.25 (m, 6H), 7.19-7.16 (m, 4H), 7.04-7.02 (m, 4H), 5.24, (s, 4H, CH_2).

^{13}C NMR (101 MHz, $CDCl_3$): δ ppm 135.3 (s, NCN), 132.9 (phenyl C), 132.6 (benzyl C), 130.9 (phenyl CH), 130.4 (phenyl CH), 129.2 (benzyl CH), 129.1 (benzyl CH), 129.0 (phenyl CH), 128.4 (benzyl CH), 124.7 (s, NC=C), 51.8 (CH_2).

^{19}F NMR: (376 MHz, $CDCl_3$) δ ppm -72.5 (d, *J* = 711 Hz, PF_6).

ATR-IR (neat, cm^{-1}): 3258 (w), 1554 (m), 1451 (m), 1349 (w), 1189 (m), 822 (s), 757 (m), 701 (s), 555 (s), 481 (m).

Elemental analysis: Calculated: C 63.74, H 4.61, N 5.13, F 20.86 %; Found: C 63.60, H 4.44, N 5.08, F 21.08 %.

HRMS (ESI$^+$, TOF): Calculated for $C_{29}H_{25}N_2$ 401.2020. Found 401.2013 (M^+).

Melting point: 133-134 °C.

1,3-Di(*p*-fluoro) benzyl-4,5-diphenyl imidazolium hexafluorophosphate, 7b:

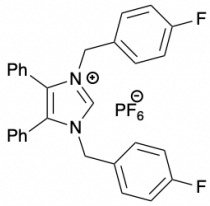

Chemical Formula: $C_{29}H_{23}N_2F_8P$
Exact Mass: 582.1471

Compound **7b** was synthesised from 1,3-di(*p*-fluoro) benzyl-4,5-diphenyl imidazolium bromide, **1b**, (0.517 g, 1.00 mmol) and potassium hexafluorophosphate (0.276 g, 1.50 mmol) according to the general procedure. The product was a fine white solid (0.422 g, 0.724 mmol) retrieved in an 85% yield.

^{1}H NMR (400 MHz, $CDCl_3$): δ ppm 8.91 (s, 1H, NCHN), 7.40-7.36 (m, 2H), 7.31 (t, 4H, *J* = 7.4 Hz), 7.16-7.13 (m, 4H), 7.00-6.97 (m, 4H), 6.91-6.86 (m, 4H), 5.25 (s, 4H, CH_2).

^{13}C NMR (101 MHz, $CDCl_3$): δ ppm 162.9 (d, $^1J_{CF}$ = 249 Hz), 135.5 (s, NCN), 132.8 (phenyl C), 130.8 (phenyl CH), 130.5 (d, $^3J_{CF}$ = 9 Hz), 130.5 (phenyl CH), 129.1 (phenyl CH), 128.5 (d, $^4J_{CF}$ = 3 Hz), 124.7 (NC=C), 116.1 (d, $^2J_{CF}$ = 22 Hz), 51.2 (s, CH_2).

^{19}F NMR (376 MHz, $CDCl_3$): δ ppm -72.0 (d, *J* = 713 Hz, PF_6), -112.0 (m, CF).

ATR-IR (neat, cm^{-1}): 3157 (w), 3081 (w), 1606 (w), 1511 (m), 1349 (w), 1225 (m), 1159 (m), 1019 (w), 831 (s), 698 (m), 556 (s), 494 (m).

Elemental analysis: Calculated: C 59.79, H 3.98, N 4.81, F 26.09 %; Found: C 59.62, H 3.87, N 4.74, F 25.84 %.

HRMS (ESI$^+$, TOF): Calculated for $C_{29}H_{23}N_2F_2$ 437.1829. Found 437.1824 (M^+).

Melting point: 63-65 °C

4,5-Diphenyl-1,3-di(*p*-trifluoromethyl) benzyl imidazolium hexafluorophosphate, 7c:

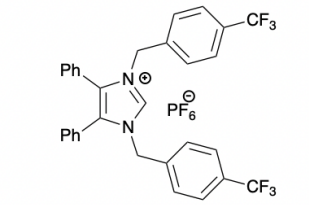

Chemical Formula: $C_{31}H_{23}N_2F_{12}P$
Exact Mass: 682.1407

Compound **7c** was synthesised from 4,5-diphenyl-1,3-di(*p*-trifluoromethyl) benzyl imidazolium bromide (0.617 g, 1.00 mmol), **1c**, and potassium hexafluorophosphate (0.276 g, 1.50 mmol) according to the general procedure. The product was a white solid (0.593 g, 0.869 mmol) obtained in an 91% yield.

^{1}H NMR (400 MHz, $CDCl_3$): δ ppm 9.21 (s, 1H, NCHN), 7.43 (d, *J* = 7.9 Hz 4H), 7.37 (t, *J* = 7.5 Hz, 2H), 7.27 (t, *J* = 7.9 Hz, 4H), 7.09 (dd, *J* = 6.8, 1.6 Hz, 8H), 5.37 (s, 4H, CH_2).

^{13}C NMR (101 MHz, $CDCl_3$): δ ppm 136.5 (benzyl C), 136.3 (s, NCN), 132.9 (phenyl C), 131.1 (q, $^2J_{CF}$ = 33 Hz), 130.7 (phenyl CH), 130.6 (phenyl CH), 129.1 (phenyl CH), 128.6 (benzyl CH), 126.0 (q, $^3J_{CF}$ = 4 Hz), 124.4 (NC=C), 123.6 (q, $^1J_{CF}$ =274 Hz) 51.3 (s, CH_2).

^{19}F NMR (376 MHz, $CDCl_3$): δ ppm -63.0 (s, CF_3), -71.6 (d, *J* = 711 Hz, PF_6).

ATR-IR (neat, cm^{-1}): 3166 (w), 1561 (w), 1324 (s), 1115 (m), 1020 (m), 835 (s), 697 (m), 557 (s), 514 (w).

Elemental analysis: calculated C 54.56, H 3.39, N 4.11, F 33.41 %; Found C 54.41, H 3.17, N 4.03, F 33.71 %.

HRMS (ESI$^+$, TOF): Calculated for $C_{31}H_{23}N_2F_6$ 537.1765. Found 537.1761 (M^+).

Melting point: 194 °C.

(8) General procedure for imidazolium tetrafluoroborate salts

A substituted imidazolium bromide, **1a-c**, (1.00 mmol) and sodium tetrafluoroborate (0.169 g, 1.50 mmol) were stirred in a 4:1 mixture of methanol and water (25 mL) at room temperature for 4 hours. The mixture was then poured into deionised water (100 mL). A white precipitate was observed. The mixture was filtered *in vacuo*, washed with deionised water (20 mL) and dried for 2 h to give a white solid.

1,3-Dibenzyl-4,5-diphenyl imidazolium tetrafluoroborate, 8a:

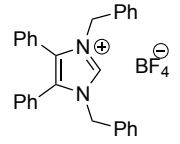

Chemical formula: $C_{29}H_{25}N_2F_4B$
Exact mass: 488.2047

Compound **8a** was synthesised from 1,3-dibenzyl-4,5-diphenyl imidazolium bromide, **1a**, (0.962 g, 2.00 mmol) and sodium tetrafluoroborate (0.338 g, 3.00 mmol) according to the general procedure to yield a white solid in an 87% yield (0.852 g, 0.872 mmol).

^{1}H NMR (400 MHz, $CDCl_3$): δ ppm 9.18 (s, 1H), 7.41-7-37 (m, 2H), 7.33-7.29 (m, 4H), 7.27 – 7.22 (m, 6H), 7.18 – 7.14 (m, 4H), 7.06 – 7.01 (m, 4H), 5.31 (s, 4H, CH_2).

^{13}C NMR (101 MHz, $CDCl_3$): δ ppm 136.1 (NCN), 133.1 (aromatic C), 132.6 (aromatic C), 130.9 (aromatic CH), 130.4 (aromatic CH), 129.1 (aromatic CH), 128.9 (aromatic CH), 128.9 (aromatic CH), 128.4 (aromatic CH), 124.8 (NC=C), 51.7 (CH_2).

^{19}F NMR (376 MHz, $CDCl_3$): δ ppm -151.7 (s, $^{10}BF_4$), -151.70 (m, $^{11}BF_4$).

ATR-IR (neat, cm^{-1}): 3164 (w), 3066 (w), 1522 (m), 1451 (m), 1350 (w), 1185 (m), 1034 (s, br), 782 (m), 740 (s), 513 (m), 463 (m).

Elemental analysis: Calculated C 71.03, H 5.55, N 5.71 %; Found C 71.29, H 5.08, N 5.74 %.

HRMS (ESI$^+$, TOF): Calculated for $C_{29}H_{25}N_2$ 401.2020. Found 401.2012 (M^+).

Melting point: 143-144 °C.

1,3-Di(*p*-fluoro) benzyl-4,5-diphenyl imidazolium tetrafluoroborate, 8b:

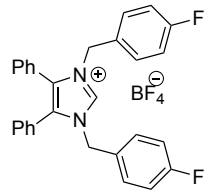

Chemical formula: $C_{29}H_{23}N_2F_6B$
Exact mass: 524.1858

Compound **8b** was synthesised from 1,3-di(*p*-fluoro) benzyl-4,5-diphenyl imidazolium bromide, **1b**, (1.036 g, 2.00 mmol) and sodium tetrafluoroborate (0.338 g, 3.00 mmol) according to the general procedure to produce a white solid product in a yield of 81 % (0.852 g, 0.812 mmol).

^{1}H NMR (400 MHz, $CDCl_3$): δ ppm 9.36 (s, 1H, NCHN), 7.41 – 7.35 (m, 2H), 7.32-7.28 (m, 4H), 7.16 – 7.12 (m, 4H), 7.03 – 6.97 (m, 4H), 6.90 – 6.83 (m, 4H), 5.32 (s, 4H, CH_2).

^{13}C NMR (101 MHz, $CDCl_3$): δ ppm 162.8 (d, $^1J_{CF}$ = 249 Hz,), 136.4 (s, NCN), 132.4 (aromatic C), 130.8 (aromatic CH), 130.5 (d, $^3J_{CF}$ = 8 Hz), 130.4 (aromatic CH), 129.0 (aromatic CH), 128.9 (d, $^4J_{CF}$ = 3 Hz), 124.8 (NC=C), 116.0 (d, $^2J_{CF}$ = 22 Hz), 51.0 (CH_2).

^{19}F NMR (376 MHz, $CDCl_3$): δ ppm -112.3 (m, CF), -150.9 (s, $^{10}BF_4$), -150.9 (m, $^{11}BF_4$).

ATR-IR (neat, cm^{-1}): 3159 (w), 3088 (w), 1632 (w), 1608 (m), 1561 (m), 1420 (w), 1356 (w), 1224 (m), 1160 (m), 1050 (s), 1011 (s), 863 (s), 817 (m), 763 (s), 593 (m), 475 (m), 424 (m).

Elemental analysis: Calculated C 66.43, H 4.42, N 5.34 %; Found C 66.41, H 4.34, N 5.30 %.

HRMS (ESI$^+$, TOF): Calculated for $C_{29}H_{23}N_2F_2$ 437.1829. Found 437.1821 (M^+).

Melting point: 164-165 °C.

4,5-Diphenyl-1,3-di(4-trifluoromethyl) benzyl imidazolium tetrafluoroborate, 8c:

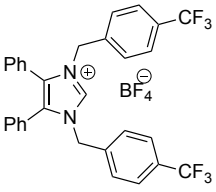

Chemical formula: $C_{31}H_{23}N_2F_{10}B$
Exact mass: 624.1795

Compound **8c** was synthesised from 4,5-diphenyl-1,3-di(trifluoromethyl)benzyl imidazolium bromide, **1c**, (0.617 g, 1.00 mmol) and sodium tetrafluoroborate (0.169 g, 1.50 mmol) according to the general procedure to produce a white solid product in a yield of 84% (0.526 g, 0.842 mmol).

^{1}H NMR (400 MHz, $CDCl_3$): δ ppm 9.88 (s, 1H, NCHN), 7.44 (d, *J* = 7.7 Hz, 4H), 7.39 (t, *J* = 7.5 Hz, 2H), 7.31 – 7.27 (m, 4H), 7.17 – 7.07 (m, 8H), 5.47 (s, 4H, CH_2).

^{13}C NMR (101 MHz, $CDCl_3$): δ ppm 137.3 (NCN), 136.9 (aromatic C), 132.6 (aromatic C), 131.0 (q, $^2J_{CF}$ = 33 Hz), 130.7 (aromatic CH), 130.6 (aromatic CH), 129.1 (aromatic CH), 128.8 (aromatic CH), 125.9 (q, $^3J_{CF}$ = 4 Hz), 124.5 (NC=C), 123.6 (q, $^1J_{CF}$ = 274 Hz), 51.2 (CH_2).

^{19}F NMR (376 MHz, $CDCl_3$): δ ppm -63.0 (s, CF_3), -150.5 (s, br, $^{10}BF_4$), -150.6 (m, $^{11}BF_4$).

ATR-IR (neat, cm^{-1}): 3155 (w), 3085 (w), 1560 (m), 1419 (m), 1323 (s), 1161 (m), 1116 (s), 1065 (s), 1015 (s), 817 (m), 699 (m), 592 (m), 516 (m).

Elemental analysis: Calculated C 59.64, H 3.71, N 4.49 %; Found C 59.44, H 3.44, N 4.41 %

HRMS (ESI$^+$, TOF): Calculated for $C_{31}H_{23}N_2F_6$ 537.1765. Found 537.1760 (M^+).

Melting point: 226-227 °C

(9) General procedure for synthesis of *bis*-Imidazol-2-ylidene silver hexafluorophosphate complexes

The *bis*-imidazol-2-ylidene silver hexafluorophosphate complexes were synthesised from the respective imidazolium hexafluorophosphate salt (**7a-c**) (0.500 mmol) and silver oxide (0.500 mmol, 0.116 g) in acetonitrile (25 mL). The product was filtered *in vacuo* over a celite bed to remove excess silver oxide. The solvent volume was reduced to approximately 3 mL under reduced pressure followed by the addition of isopropyl alcohol (30 mL). The solution

was cooled to -18 ° C for 24 h. The resulting white precipitate was filtered *in vacuo* and washed with cold isopropyl alcohol (15 mL) to yield the pure product.

***Bis*-(1,3-dibenzyl-4,5-diphenyl imidazol-2-ylidene) silver (I) hexafluorophosphate, 9a:**

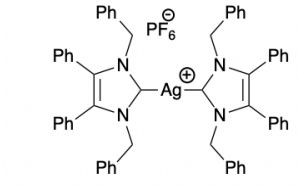

Chemical Formula: $C_{58}H_{48}N_4F_6PAg$
Exact Mass: 1052.2571

Complex **9a** was synthesised by stirring hexafluorophosphate salt **7a** (0.273 g, 0.500 mmol) and silver oxide (0.116 g, 0.500 mmol) in acetonitrile (25 mL) at 40 °C for 24 h. The mixture was purified according to the general procedure to achieve a white solid (0.203 g, 0.193 mmol) in a 77% yield. A single crystal of **9a** was obtained from a saturated solution in DCM by slow infusion of pentane at -18 °C.

^{1}H NMR (400 MHz, DMSO-*d*$_6$): δ ppm 7.37-7.28 ppm (m, 12 H), 7.24 - 7.16 (m, 20H), 6.93 - 6.86 (m, 8H), 5.25 (s, 8H, CH_2 benzyl).

^{13}C NMR (126 MHz, DMSO-*d*$_6$): δ ppm 180.9 (d, *J* = 188 Hz, C-Ag), 136.7 (benzyl C), 132.3 (phenyl C), 130.6 (phenyl CH), 129.2 (phenyl CH), 128.6 (benzyl CH), 127.7 (benzyl CH), 127.3 (NC=C), 126.7 (benzyl CH), 52.4 (CH_2).

^{19}F NMR (376 MHz, DMSO-*d*$_6$): δ ppm -70.7 (d, *J* = 711 Hz, PF_6).

ATR-IR (neat, cm^{-1}): 3062 (w), 1604 (w), 1466 (w), 1352 (w), 1024 (w), 833 (s), 698 (m), 555 (m).

Elemental analysis: Calculated C 66.10, H 4.59, N 5.32, F 10.82 %; Found C 65.54, H 4.47, N 5.20, F 11.47 %.

HRMS (TOF, ESI+): calculated for $C_{58}H_{48}N_4Ag^+$ 907.2930, found 907.2932 (M^+)

Melting point: 194-197 °C (dec.)

***Bis*-(1,3-di(4-fluoro) benzyl-4,5-diphenyl imidazol-2-ylidene) silver (I) hexafluorophosphate, 9b:**

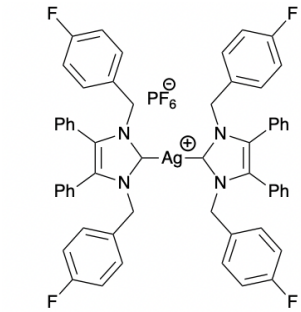

Chemical Formula: $C_{58}H_{44}N_4F_{10}PAg$
Exact Mass: 1124.2195

Complex **9b** was synthesised by stirring hexafluorophosphate salt **7b** (0.291 g, 0.500 mmol) and silver oxide (0.116 g, 0.500 mmol) in acetonitrile (25 mL) at 40 °C for 3d. The mixture was purified according to the general procedure to obtain a white solid (0.276 g, 0.245 mmol) in a 91% yield.

^{1}H NMR (400 MHz, DMSO-*d*$_6$): δ ppm 7.36 – 7.27 (m, 12H), 7.17 – 7.15 (m, 8H), 6.99 (t, *J* = 8.8 Hz, 8H), 6.92-6.88 (m, 8H), 5.25 (s, 8H, CH_2).

^{13}C NMR (126 MHz, DMSO-*d*$_6$): δ ppm 180.9 (dd, *J* = 198, 13 Hz, C-Ag) 161.5 (d, $^1J_{CF}$= 244 Hz), 132.9 (d, $^4J_{CF}$ = 3 Hz), 132.3 (phenyl C), 130.6 (phenyl CH), 129.4 (phenyl CH), 128.7 (d, $^3J_{CF}$ = 8 Hz), 128.6 (phenyl CH), 127.2 (NC=C), 115.4 (d, $^2J_{CF}$ = 22 Hz), 51.7 (CH_2).

^{19}F NMR (376 MHz, DMSO-*d*$_6$): δ ppm -70.7 (d, *J* = 711 Hz, PF_6), -115.0 (m, CF).

ATR-IR (neat, cm^{-1}): 3065 (w), 1605 (w), 1509 (m), 1342 (w), 1224 (m), 1159 (m), 1023 (w), 834 (s), 764 (m), 697 (m), 556 (m), 498 (m).

Elemental analysis: Calculated: C 61.88, H 3.94, N 4.98, F 16.88 %; Found C 61.51, H 3.82, N 5.18, F 16.97 %.

HRMS (TOF, ESI+): calculated for $C_{58}H_{44}N_4F_4Ag^+$ 979.2553, found 979.2550 (M^+)

Melting Point: 185 °C (dec.)

***Bis*-(1,3-di(4-trifluoromethyl) benzyl-4,5-diphenylimidazol-2-ylidene) silver (I) hexafluorophosphate, 9c:**

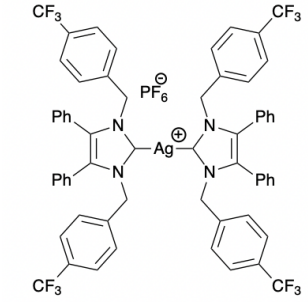

Chemical Formula: $C_{62}H_{44}N_4F_{18}PAg$
Exact Mass: 1324.2067

Complex **9c** was synthesised by stirring hexafluorophosphate salt **7c** (0.327 g, 0.500 mmol) and silver oxide (0.116 g, 0.500 mmol) in acetonitrile (25 mL) at 40 °C for 4d. The mixture was purified according to the general procedure to yield the product (0.267 g, 0.202 mmol) in an 81% yield. A single crystal of **9c** was obtained from a saturated solution in DCM by slow infusion of pentane at -18 °C.

^{1}H NMR (400 MHz, DMSO-d_6): δ ppm 7.49 (d, J = 8.1 Hz, 4H), 7.34 – 7.27 (m, 6H), 7.15 (d, 7.6 Hz, 4H), 7.10 (d, J = 7.9 Hz, 4H), 5.40 (s, 4H, CH_2).

^{13}C NMR (126 MHz, DMSO-d_6): δ ppm 181.3 (dd, J = 197, 16 Hz, C-Ag), 141.2 (benzyl C), 132.4 (phenyl C), 130.4 (phenyl CH), 129.3 (phenyl CH), 128.5 (phenyl CH), 128.2 (q, $^2J_{CF}$ = 32 Hz) 127.3 (benzyl CH), 126.9 (NC=C), 125.3 (q, $^3J_{CF}$ = 4 Hz), 123.8 (q, $^1J_{CF}$ =272 Hz, CF_3), 51.5 (CH_2).

^{19}F NMR (376 MHz, DMSO-d_6): δ ppm -61.8 (s, CF_3), -70.7 (d, J = 711 Hz, PF_6).

ATR-IR (neat, cm^{-1}): 3162 (w), 3064 (w), 1561 (w), 1421 (w), 1323 (s), 1161 (m), 1113 (m), 1066 (m), 1018 (m), 831 (s), 698 (m), 556 (s).

Elemental analysis: Calculated C 56.16, H 3.35, N 4.23, F 25.79 %; Found: C 56.06, H 3.16, N 4.06, F 25.97 %.

HRMS: Calculated for $C_{62}H_{44}N_4F_{12}Ag^+$ 1179.2425, found 1179.2419 (M^+)

Melting point: 171-173 °C (dec.)

(10) General procedure for synthesis of *bis*-imidazole-2-ylidene silver (I) tetrafluoroborate complexes

The *bis*-imidazol-2-ylidene silver tetrafluoroborate complexes were synthesised from the respective imidazolium tetrafluoroborate salt (**8a-c**) (0.500 mmol) and silver oxide (0.500 mmol, 0.116 g) in acetonitrile (25 mL). The product was filtered *in vacuo* over a celite bed to remove excess silver oxide. The solvent volume was reduced to approximately 3 mL under reduced pressure followed by the addition of isopropyl alcohol (30 mL). The solution was allowed to crystallise at 4° C for 24 h. The resulting white crystals were filtered *in vacuo* and washed with cold isopropyl alcohol (15 mL) to yield the pure product.

***Bis*-(1,3-dibenzyl-4,5-diphenyl imidazol-2-ylidene) silver (I) tetrafluoroborate, 10a:**

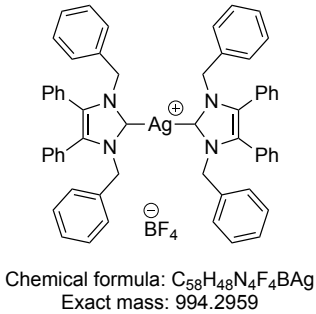

Chemical formula: $C_{58}H_{48}N_4F_4BAg$
Exact mass: 994.2959

Imidazolium tetrafluoroborate salt **8a** (0.488 g, 1.00 mmol) and silver oxide (0.230 g, 1.00 mmol) were stirred in acetonitrile (25 mL) at 40 °C for 24 h in the absence of light. The reaction mixture was then purified according to the general procedure to yield the white solid product in a 79% yield (0.396 g, 0.397 mmol).

^{1}H NMR (500 MHZ, DMSO-d_6): δ ppm 7.35-7.32 (m, 4 H), 7.30-7.37 (m, 8H), 7.19-7.16 (m, 20 H), 6.89-6.88 (m, 8 H), 5.24 (s, 8 H, CH_2).

^{13}C NMR (126 MHz, DMSO-d_6): δ ppm 136.6 (benzyl C) 132.2 (phenyl C), 130.5 (phenyl CH), 129.2 (phenyl CH), 128.5 (phenyl CH), 128.5 (benzyl CH), 127.7 (benzyl CH), 127.2 (NC=C), 126.6 (benzyl CH), 52.3 (CH_2). Carbene C signal not observed.

^{19}F NMR (470 MHz, DMSO-d_6): δ ppm -148.8 (s, $^{10}BF_4$), -148.9 (m, $^{11}BF_4$).

ATR-IR (neat, cm^{-1}): 3027 (w), 1497 (w), 1448 (m), 1349 (w), 1048 (s), 761 (m), 732 (s), 694 (s), 595 (w), 513 (w).
Elemental analysis: Calculated C 69.96, H 4.86, N 5.63 %; Found C 69.31, H 4.60, N 5.56 %.
HRMS (ESI^+, TOF): Calculated for $C_{58}H_{48}N_4Ag^+$ 907.2930. Found 907.2923 (M^+).
Melting point: 108 °C (dec.)

***Bis*-(1,3-di(4-fluoro) benzyl-4,5-diphenyl imidazole-2-ylidene) silver (I) tetrafluoroborate, 10b:**

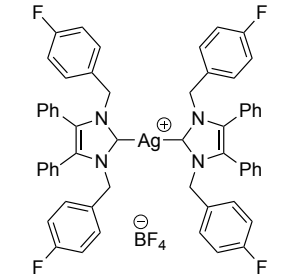

Chemical formula: $C_{58}H_{44}N_4F_8BAg$
Exact mass: 1066.2582

Imidazolium tetrafluoroborate salt **8b** (0.262 g, 0.500 mmol) and silver oxide (0.116 g, 0.500 mmol) were stirred in acetonitrile (25 mL) at 40 °C for 3 d in the absence of light. The reaction mixture was purified according to the general procedure to yield a white solid product in an 94 % yield (0.251 g, 0.235 mmol). A single crystal of **10b** was obtained from a saturated solution in DCM by slow infusion of pentane at -18 °C.
^{1}H NMR (500 MHZ, DMSO-d_6): δ ppm 7.36 – 7.28 (m, 12H), 7.18 – 7.16 (m, 8H), 7.01 (t, J = 8.8 Hz, 8H), 6.91 (dd, J = 8.5, 5.4 Hz, 8H), 5.27 (s, 8H, CH_2).
^{13}C NMR (126 MHz, DMSO-d_6): δ ppm 161.4 (d, $^1J_{CF}$ = 244 Hz), 132.8 (d, $^4J_{CF}$ = 3 Hz), 132.2 (phenyl C), 130.5 (phenyl CH), 129.2 (phenyl CH), 128.9 (d, $^3J_{CF}$ = 8 Hz), 128.5 (phenyl CH), 127.1 (NC=C), 115.3 (d, $^2J_{CF}$ = 21 Hz), 51.7 (CH_2). Carbene C signal not observed.
^{19}F NMR (470 MHz, DMSO-d_6): δ ppm -115.0 (m, CF), -148.8 (s,$^{10}BF_4$), -148.9 (m, $^{11}BF_4$).
ATR-IR (neat, cm^{-1}): 3054 (w), 1604 (w), 1508 (s), 1420 (m), 1342 (w), 1220 (s), 1162 (m), 1048 (s), 919 (w), 818 (s), 778 (m), 701 (s), 612 (m), 557 (m), 505 (m), 430 (m).
Elemental analysis: Calculated C 65.25, H 4.15, N 5.25 %; Found C 64.51, H 4.00, N 5.12 %.
HRMS (ESI^+, TOF): $C_{58}H_{44}N_4F_4Ag^+$ 979.2553. Found 979.2547 (M^+).
Melting point: 110-112 °C (dec.)

***Bis*-(1,3-di(4-trifluoromethyl) benzyl-4,5-diphenylimidazol-2-ylidene) silver (I) tetrafluoroborate, 10c:**

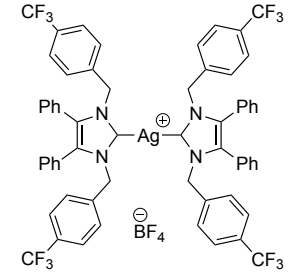

Chemical formula: $C_{63}H_{44}N_4F_{16}BAg$
Exact mass: 1278.2454

Imidazolium tetrafluoroborate salt **8c** (0.624 g, 1.00 mmol) and silver oxide (0.230 g, 1.00 mmol) were stirred in acetonitrile (25 mL) at 40 °C for 4 d in the absence of light. The reaction mixture was purified according to the general procedure to yield a white solid product in a 80 % yield (0.507 g, 0.400 mmol).
^{1}H NMR (400 MHZ, DMSO-d_6): δ ppm 7.50 (d, J = 8.0 Hz, 8H), 7.35 – 7.26 (m, 12H), 7.15 (dd, J = 8.1, 1.5 Hz, 8H), 7.10 (d, J = 8.1 Hz, 8H), 5.40 (s, 8H, CH_2).
^{13}C NMR (101 MHZ, DMSO-d_6): δ ppm 141.2 (benzyl C), 132.4 (phenyl C), 130.4 (phenyl CH), 129.3 (phenyl CH), 128.5 (phenyl CH), 128.1 (q, $^2J_{CF}$ = 32 Hz), 127.3 (benzyl CH), 126.9 (NC=C), 125.3 (q, $^3J_{CF}$ = 4 Hz), 123.8 (q, $^1J_{CF}$ = 271 Hz), 51.9 (CH_2). Carbene C signal not observed.
^{19}F NMR (376 MHZ, DMSO-d_6): δ ppm -61.8 (s, CF_3), -148.8 (s, $^{10}BF_4$), -148.9 (m, $^{11}BF_4$).
ATR-IR: (neat, cm^{-1}) 3553 (w, br), 3057 (w), 1621 (w), 1325 (s), 1163 (m), 1110 (s), 1066 (s), 818 (m), 760 (m), 698 (m), 591 (w), 524 (w).
Elemental analysis: Calculated C 58.74, H 3.50, N 4.42 %; Found C 58.42, H 3.31, N 4.34 %.
HRMS (ESI^+, TOF): Calculated for $C_{62}H_{44}N_4F_{12}Ag^+$ 1179.2425. Found 1179.2419 (M^+).

Melting point: 130-133 °C (dec.)

(11) Preparation of gluconate ion exchange resin

Amberlite IRA-402 Cl- type resin (5.00 g, 12.35 mmol Cl-) was loaded into a column and washed with deionised water (20 mL). Sodium gluconate (16.15 g, 74.10 mmol) was dissolved in deionised water (250 mL) and passed through the column at a flow rate of 0.5 mL min^{-1}. The resin was then washed with deionised water (20 mL) followed by methanol (20 mL). The resin was dried *in vacuo* for 1 h.
Elemental analysis: Initial Cl 8.77%; Found Cl 1.14%.
Resin loading: 2.15 mmol gluconate g^{-1}

(12) General procedure for *bis*-imidazol-2-ylidene silver (I) gluconate complexes

Gluconate resin (**11**) (1.00 g, 2.15 mmol gluconate) was loaded onto a column and washed with 2:1 mixture of acetonitrile and deionised water (7 mL). A *bis*-imidazole-2-ylidene silver (I) tetrafluoroborate complex (**10a-c**) (0.20 mmol) was dissolved in a 2:1 mixture of acetonitrile and deionised water (15 mL) passed through the column at a flow rate of 0.113 mL min^{-1} (residence time 15 min). The column was then washed with 7 mL of the solvent mixture. All eluent was collected into a pre-weighed round bottom flask. The product mixture was heated to 45 under reduced pressure on a rotary evaporator to remove acetonitrile. The remaining aqueous mixture was filtered *in vacuo* to isolate the white solid product.

***Bis*-(1,3-dibenzyl-4,5-diphenylimidazol-2-ylidene) silver (I) gluconate, 12a:**

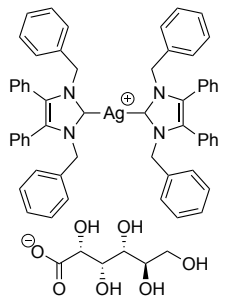

Chemical formula: $C_{64}H_{59}N_4O_7Ag$
Exact mass: 1102.3435

The corresponding tetrafluoroborate complex (0.199 g, 0.200 mmol), **10a**, was dissolved in a 2:1 mixture of acetonitrile and deionised water (15 mL) and treated according to the general procedure to achieve the desired white, solid product in a 66% yield (0.147 g, 0.133 mmol).
^{1}H NMR (400 MHz, DMSO-d_6): δ ppm 7.35-7.27 (m, 12 H), 7.19-7.16 (m, 20 H), 6.88 (d, J = 5.4 Hz, 8 H, phenyl CH), 5.24 (s, 8 H, benzyl CH_2), 4.61 (s, 1 H, gluconate OH), 4.50 (s, 1 H, gluconate OH), 3.75 (dd, J = 4.8, 1.6 Hz, 1 H, gluconate CH), 3.59-3.55 (m, 2 H, gluconate CH), 3.52-3.48 (m, 2 H, gluconate CH). Some gluconate CH signals not observed due to masking by H_2O peak.
^{13}C NMR (101 MHz, DMSO-d_6): δ ppm 175.0 (C=O), 136.6 (phenyl C), 132.2 (benzyl C), 130.5 (phenyl CH), 129.2 (phenyl CH), 128.5 (phenyl CH), 128.5 (benzyl CH), 127.6 (benzyl CH), 127.2 (NC=C), 126.6 (benzyl CH), 72.3 (gluconate C2), 71.9 (gluconate C4), 71.6 (gluconate C5), 63.7 (gluconate C6), 52.3 (benzyl CH_2). Carbene C signal not observed.
ATR-IR (neat, cm^{-1}): 3354 (m, br), 3058 (w), 3029 (w), 1603 (m), 1445 (m), 1328 (s), 1161 (m), 1112 (m), 1069 (m), 1020 (m), 924 (w), 868 (w), 764 (m), 696 (s), 613 (m), 517 (m).
Elemental analysis: Calculated for $C_{64}H_{59}N_4O_7Ag$ x H_2O: C 68.51, H 5.48, N 4.99 %; Found C 68.29, H 5.20, N 5.02 %.
HRMS (ESI$^+$, TOF): Calculated for $C_{58}H_{48}N_4Ag^+$ 907.2927. Found 907.2921 (M^+).
Melting point: 64-65 °C

***Bis*-(1,3-di(*p*-fluoro) benzyl-4,5-diphenylimidazol-2-ylidene) silver (I) gluconate, 12b:**

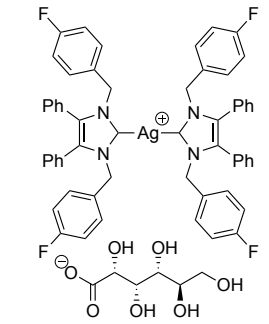

Chemical formula: $C_{64}H_{55}N_4O_7F_4Ag$
Exact mass: 1174.3058

The corresponding tetrafluoroborate complex, **10b** (0.214 g, 0.200 mmol) was dissolved in a 2:1 mixture of acetonitrile and deionised water and treated according to the general procedure. The product was a white powder isolated in an 81% yield (0.153 g, 0.161 mmol).

^{1}H NMR (400 MHz, DMSO-d_6): δ ppm 7.35-7.27 (m, 12 H, phenyl CH), 7.16 (dd, J = 8.2, 1.6 Hz, phenyl CH), 6.99 (t, J = 8.4 Hz, 8 H, benzyl CH), 6.91 (dd, J = 8.7, 5.4 Hz, 8 H, benzyl CH), 5.27 (s, 8H, benzyl CH_2), 4.62 (s, 1H, gluconate OH), 4.50 (s, 1H, gluconate OH), 3.74 (dd, J = 5.2, 2.1 Hz, 1 H, gluconate CH), 3.57 (dd, J = 11.0, 3.3 Hz, gluconate CH_2), 3.55 (d, J = 5.5 Hz, 1H, gluconate CH), 3.52-3.47 (m, 1H, gluconate CH), 3.42 (dd, J= 8.2, 2.3 Hz, 1H, gluconate CH). Signal not observed for gluconate CH_2 due to masking by H_2O peak.

^{13}C NMR (101 MHz, DMSO-d_6): δ ppm 175.0 (C=O), 161.4 (d, $^1J_{CF}$ = 244 Hz), 132.8 (d, $^4J_{CF}$ = 3 Hz), 132.2 (phenyl C), 130.5 (phenyl CH), 129.2 (phenyl CH), 128.6 (d, $^3J_{CF}$ = 9 Hz), 128.5 (phenyl CH), 127.2 (NC=C), 115.3 (d, $^2J_{CF}$ = 3 Hz), 72.3 (gluconate C2), 71.9 (gluconate C4), 71.6 (gluconate C5), 71.0 (gluconate C3), 63.7 (gluconate C6), 51.7 (benzyl CH_2). Carbene C signal not observed.

^{19}F NMR (376 MHz, DMSO-d_6): δ ppm -115.0 (m, CF).

ATR-IR (neat, cm^{-1}): 3358 (m, br), 3056 (w), 2924 (w), 1603 (m), 1509 (s), 1445 (m), 1350 (m), 1222 (s), 1158 (m), 1095 (m), 1022 (m), 924 (w), 817 (s), 764 (m), 698 (s), 612 (m), 491 (m), 422 (w).

Elemental analysis: Calculated for $C_{64}H_{55}N_4F_{12}O_7Ag$ x H_2O: C 64.38, H 4.81, N 4.69, F 6.36 %; Found C 63.34, H 4.43, N 4.62, F 5.63 %.

HRMS (ESI$^+$, TOF): $C_{58}H_{44}N_4F_4Ag^+$ 979.2553. Found 979.2545 (M^+).

Melting point: 85-87 °C

***Bis*-(1,3-di(*p*-trifluoromethyl) benzyl-4,5-diphenylimidazol-2-ylidene) silver (I) gluconate, 12c:**

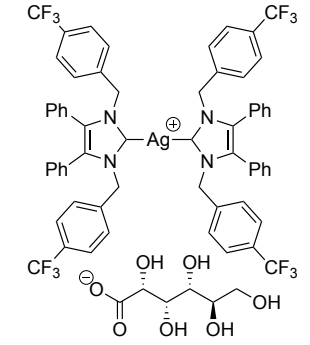

Chemical formula: $C_{64}H_{55}N_4O_7F_4Ag$
Exact mass: 1374.2930

The corresponding tetrafluoroborate complex, **10c** (0.254 g, 0.200 mmol), was dissolved in a 2:1 mixture of acetonitrile and deionised water and treated according to the general procedure. Following the removal of acetonitrile, the product mixture formed a gel which was dried at 60°C for 48 h, to give the product as a white solid in a 97% yield (0.267 g, 0.194 mmol). A single crystal of 1**2c** was obtained from a saturated solution in DCM by slow infusion of pentane at rt.

^{1}H NMR (400 MHz, DMSO-d_6): δ ppm 7.48 (d, J = 8 Hz, benzyl CH), 7.32-7.25 (m, 12H, phenyl CH), 7.15 (d, J = 6.9 Hz, 8H, phenyl CH), 7.10 (d, J = 8.1 Hz, 8H, benzyl CH), 5.41 (s, 8H, benzyl CH_2), 4.77 (s, br, 1H, gluconate OH), 4.61 (s, br, 1H, gluconate OH), 4.49 (s, br, 2H, gluconate OH), 4.25 (s. br, 1H, gluconate OH), 3.77 (s, 1H, gluconate CH), 3.58 (d, J = 5.3 Hz, 2H, CH gluconate), 3.51 (s, br, 1H, gluconate CH), 3.45 (s, br, 1H, gluconate CH). Some gluconate signals were not observed due to masking by the H_2O peak.

^{13}C NMR (101 MHz, DMSO-d_6): δ ppm 175.1 (C=O), 141.2 (benzyl C), 132.3 (phenyl C), 130.4 (phenyl CH), 129.3 (phenyl CH), 128.5 (phenyl CH), 128.1 (q, $^2J_{CF}$ = 32 Hz), 127.3 (benzyl CH), 126.9 (NC=C), 125.3 (q, $^3J_{CF}$ = 4 Hz), 123.8 (q, $^1J_{CF}$ = 273 Hz), 72.4 (gluconate C2), 72.0 (gluconate

C4), 71.6 (gluconate C5), 71.0 (gluconate C3), 63.7 (gluconate C6), 51.9 (benzyl CH_2). Carbene C signal not observed.
^{19}F NMR (376 MHz, DMSO-d_6): δ ppm -61.8 (CF_3).
ATR-IR (neat, cm^{-1}): 3312 (w, br), 3056 (w), 2925 (w), 1619 (m), 1406 (w), 1323 (s), 1160 (m), 1109 (s), 1067 (s), 1018 (s), 942 (w), 818 (m), 768 (m), 698 (s), 613 (m), 519 (m).
Elemental Analysis: Calculated for $C_{68}H_{55}N_4F_{12}O_7Ag$ x H_2O C 58.59, H 4.12, N 4.02, F 16.35 %; Found C 55.54, H 3.72, N 3.64, F 15.21 %.
HRMS (ESI$^+$, TOF): Calculated for $C_{62}H_{44}N_4F_{12}Ag^+$ 1179.2425. Found 1179.2415 (M^+).
Melting point: 155 °C (dec.)

(13) General procedure for *bis*-imidazol-2-ylidene silver (I) dichloroargentate complexes

A *bis*-imidazol-2-ylidene silver (I) tetrafluoroborate complex (**10a-c**) (0.200 mmol) was dissolved in a 2:1 mixture of methanol and acetonitrile. The mixture was passed through a column with amberlite IRA-402 Cl^- type resin (1.00 g, 2.47 mmol Cl^-) at a flow rate of 0.137 mL min^{-1} (residence time 15 min). The eluent was collected, and the solvent was removed under reduced pressure. The resulting yellow solid was redissolved in ethanol. The product was crystallised by slow evaporation of ethanol at room temperature. The crystals were filtered *in vacuo* and washed with cold ethanol to give the product.

***Bis*-(1,3-dibenzyl-4,5-diphenylimidazol-2-ylidene) silver (I) dichloroargentate, 13a:**

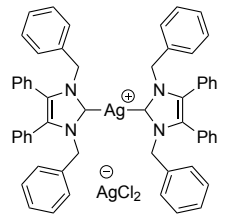

Chemical formula: $C_{58}H_{48}N_4Cl_2Ag_2$
Exact mass: 1084.1358

The corresponding tetrafluoroborate complex, **10a**, (0.199 g, 0.200 mmol) was treated according to the general procedure to give the clear, crystalline product in a 63% yield (0.069 g, 0.063 mmol). A single crystal of **13a** was obtained by slow evaporation of ethanol at 4°C.
^1H NMR (400 MHz, DMSO-d_6): δ ppm 7.35-7.31 (m, 4H), 7.28 (t, J = 7.2 Hz, 8H), 7.26-7.24 (m, 12H), 7.20-7.16 (m, 8H), 6.97-6.95 (m, 8H), 5.34 (s, 8H, benzyl CH_2).
^{13}C NMR (101 MHz, DMSO-d_6): δ ppm 136.7 (benzyl C), 132.2 (phenyl C), 130.6 (phenyl CH), 129.1 (phenyl CH), 128.5 (phenyl CH), 128.5 (benzyl CH), 127.7 (benzyl CH), 127.4 (NC=C), 126.7 (benzyl CH), 52.5 (benzyl CH_2). Carbene C signal not observed.
ATR-IR (neat, cm^{-1}): 3060 (w), 3030 (w), 2923 (w), 1603 (w), 1575 (m), 1495 (m), 1344 (m), 1206 (w), 1180 (w), 1155 (w), 1077 (w), 1020 (m), 868 (m), 768 (m), 693 (s), 615 (m), 571 (m), 512 (m).
Elemental analysis: Calculated C 64.05, H 4.45, N 5.15 %; Found C 65.51, H 4.28, N 5.24 %.
HRMS (ESI$^+$, TOF): Calculated for $C_{58}H_{48}N_4Ag^+$ 907.2927. Found 907.2920 (M^+).
Melting point: 223-225 °C

***Bis*-(1,3-di(*p*-fluoro) benzyl-4,5-diphenylimidazol-2-ylidene) silver (I) dichloroargentate, 13b:**

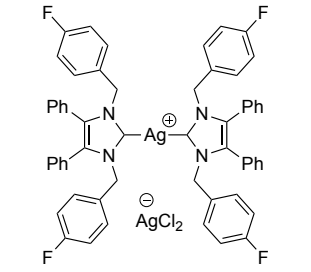

Chemical formula: $C_{58}H_{44}N_4F_4Cl_2Ag_2$
Exact mass: 1156.0981

The corresponding tetrafluoroborate complex, **10b**, (0.214 g, 0.200 mmol) was treated according to the general procedure to yield the clear, crystalline product in a 36% yield (0.042 g, 0.073 mmol).

^{1}H NMR (400 MHz, DMSO-d_6): δ ppm 7.34-7.27 (m, 12H, phenyl CH), 7.19-7.17 (m, 8H, phenyl CH), 7.07 (t, J = 8.8 Hz, 8H, benzyl CH), 6.98 (dd, J = 8.5, 5.7 Hz, 8H, benzyl CH), 5.34 (s, 8H, benzyl CH_2).

^{13}C NMR (101 MHz, DMSO-d_6): δ ppm 161.4 (d, $^1J_{CF}$ = 245 Hz), 132.8 (d, $^4J_{CF}$ = 3 Hz), 132.1 (phenyl C), 130.5 (phenyl CH), 129.2 (phenyl CH), 128.8 (d, $^3J_{CF}$ = 9 Hz), 128.5 (phenyl CH), 127.3 (NC=C), 115.3 (d, $^2J_{CF}$ = 21 Hz), 51.8 (benzyl CH_2). Carbene C signal not observed.

^{19}F NMR (376 MHz, DMSO-d_6): δ ppm -115.1 (m, CF).

ATR-IR (neat, cm^{-1}): 3068 (w), 1604 (m), 1508 (s), 1445 (m), 1390 (m), 1335 (m), 1222 (s), 1156 (m), 1072 (w), 1024 (m), 929 (w), 814 (s), 764 (s), 670 (s), 610 (m), 492 (m).

Elemental analysis: Calculated C 60.07, H 3.82, N 4.83, F 6.55 %; Found C 60.42, H 3.80, N 4.79, F 6.26 %.

HRMS (ESI$^+$, TOF): $C_{58}H_{44}N_4F_4Ag^+$ 979.2553. Found 979.2546 (M^+).

Melting point: 231-232 °C

***Bis*-(1,3-di(*p*-trifluoromethyl) benzyl-4,5-diphenylimidazol-2-ylidene) silver (I) dichloroargentate, 13c:**

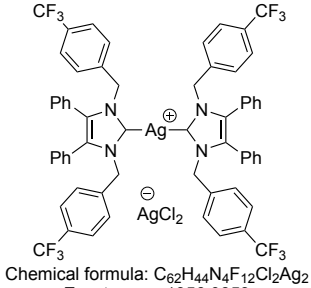

Chemical formula: $C_{62}H_{44}N_4F_{12}Cl_2Ag_2$
Exact mass: 1356.0853

The corresponding tetrafluoroborate complex, **10c**, (0.254 g, 0.200 mmol) was treated according to the general procedure to achieve the clear crystalline product in a 27% yield (0.037 g, 0.055 mmol).

^{1}H NMR (400 MHz, DMSO-d_6): δ ppm 7.61 (d, J = 8.0 Hz, 8H, benzyl CH), 7.34-7.25 (m, 12H, phenyl CH), 7.19-7.17 (m, 16H, phenyl & benzyl CH), 5.48 (s, 8H, CH_2 benzyl).

^{13}C NMR (101 MHz, DMSO-d_6): δ ppm 141.4 (benzyl C), 132.3 (phenyl C), 130.5 (phenyl CH), 129.3 (phenyl CH), 128.5 (phenyl CH), 128.1 (q, $^2J_{CF}$ = 32 Hz), 127.3 (benzyl CH), 127.1 (NC=C), 125.4 (q, $^3J_{CF}$ = 4 Hz), 124.0 (q, $^1J_{CF}$ = 274 Hz), 52.0 (benzyl CH_2). Carbene C signal not observed.

^{19}F NMR (376 MHz, DMSO-d_6): δ ppm -61.6 (s, CF_3).

ATR-IR (neat, cm^{-1}): 3045 (w), 2956 (w), 2919 (w), 1619 (w), 1502 (w), 1447 (m), 1321 (s), 1190 (s), 1127 (s), 1065 (s), 1016 (m), 941 (w), 929 (w), 878 (w), 815 (m), 755 (m), 700 (s), 624 (m), 518 (w), 459 (w).

Elemental analysis: Calculated C 54.77, H 3.26, N 4.12, F 16.77 %; Found C 54.96, H 3.19, N 4.07, F 16.39

HRMS (ESI$^+$, TOF): Calculated for $C_{62}H_{44}N_4F_{12}Ag^+$ 1179.2425. Found 1179.2420 (M^+).

Melting point:263-265 °C

(14) Preparation of acetate ion exchange resin

A 500 mL aqueous solution of sodium acetate (25.0 g, 0.305 mol) was passed through a column packed Amberlite IRA-402 Cl- type resin (11.5 g, 35.7 mmol Cl-) at a flow rate of 0.50

mL min^{-1} (residence time 21.2 min). The resin was then washed with deionised water followed by methanol and dried *in vacuo* for 1 h.
Elemental analysis: Initial Cl 10.94 %; Found Cl 0.6 %.
Resin loading: 2.93 mmol acetate g^{-1}

(15) Synthesis of *bis*-(1,3-dibenzyl-4,5-diphenylimidazol-2-ylidene) silver (I) acetate

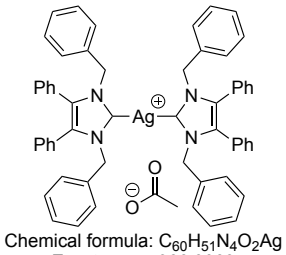

Chemical formula: $C_{60}H_{51}N_4O_2Ag$
Exact mass: 966.3063

Acetate resin, **14**, (1.00 g, 3.00 mmol acetate) was added to a column and washed with a 2:1 mixture of methanol and acetonitrile. *Bis*-(1,3-dibenzyl-4,5-diphenylimidazol-2-ylidene) silver (I) tetrafluoroborate, **10a**, (0.149 g, 0.150 mmol) was dissolved in a 2:1 mixture of methanol and acetonitrile (15 mL) and passed through the column at a flow rate of 0.14 mL min^{-1} (residence time 15 min). The column was then washed with the solvent mixture (7 mL). The eluent was collected and concentrated under reduced pressure to approximately 3 mL. Diethyl ether (30 mL) was added, and the precipitate was filtered *in vacuo* and dried for 2 h to give the white product in a 90 % yield (0.131 g, 0.135 mmol). A single crystal of **15** was grown from a saturated solution in diethyl ether at -18°C.
^{1}H NMR (400 MHz, DMSO-d_6): δ ppm 7.33 (t, *J* = 7.3 Hz, 4H), 7.30-7.27 (m, 8H), 7.19-7.15 (m, 20H), 6.88 (dd, *J* = 7.3, 2.2 Hz, 8H), 5.24 (s, 8H, benzyl CH_2), 1.54 (s, 3H, acetate CH_3).
^{13}C NMR (101 MHZ, DMSO-d_6): δ ppm 172.8 (C=O), 136.7 (benzyl C), 132.2 (phenyl C), 130.5 (phenyl CH), 129.2 (phenyl CH), 128.5 (phenyl CH), 128.5 (benzyl CH), 127.6 (benzyl CH), 127.4 (NC=C), 126.6 (benzyl CH), 52.3 (benzyl CH_2), 25.9 (acetate CH_3). Carbene C signal not observed.
ATR-IR (neat, cm^{-1}): 3383 (w, br), 3061 (w), 3031 (w), 2990 (w), 1562 (m), 1495 (m), 1447 (m), 1378 (m), 1355 (m), 1181 (w), 1077 (w), 1020 (m), 916 (w), 868 (m), 771 (m), 694 (s), 614 (m), 512 (w).
Elemental analysis: Calculated for $C_{60}H_{51}N_4O_2Ag$ x H_2O: C 73.09, H 5.42, N 5.68 %; Found C 72.81, H 5.44, N 5.68 %.
HRMS (ESI$^+$, TOF): Calculated for $C_{58}H_{48}N_4Ag^+$ 907.2930. Found 907.2920 (M^+).
Melting point: 119-122 °C

3.3 Biological Testing

Biological testing was carried out using the Kirby-Bauer disk diffusion method.[4] Complexes were tested against gram-negative *Escherichia coli* (ATC25922) and gram-positive methicillin resistant *Staphylococcus aureus* (ATC43300). All equipment and growth media which were not already sterile were sterilised by autoclave.

Agar plates were prepared by dissolving commercially available powdered Luria-Bertani broth with agar (17.5 g) in deionised water (500 mL). After autoclaving, the broth was poured into plastic petri dishes, filling 2/3 of the depth, and allowed to cool and harden for 45 min. Bacteria were streaked onto an agar plate using a loop stick and incubated overnight at 37°C to allow the growth of bacterial colonies. A single colony of bacteria was taken from the plate with a loop stick and placed in 2 mL of sterile lysogeny broth (N-Z amine (5.00 g), NaCl (2.50 g), yeast extract (2.50 g), and deionised water (50 mL)). The broth containing the bacteria was incubated for 24 h at 37°C while shaking. After 24 h, the growth of bacteria in the broth was confirmed by turbidity of the solution. 50 µL of a bacterial solution was pipetted onto a clean agar plate and spread evenly with a plastic L-shaped spreader. The plate was divided into quadrants and a 5.5 mm diameter circle of Whatman filter paper was placed in the centre of each quadrant.

Solutions of each novel complex as well as standards were made at a concentration of 1 mg mL^{-1} in DMSO. Each solution was pipetted onto a filter paper disk (on the agar plate) at a volume of 5 µL and 10 µL. Novel complexes were tested in triplicate at each loading volume and standards **SBC3** and tetracycline were tested once at each volume. A control of DMSO was also tested once at each volume. After solutions of the complexes were added, the plates were incubated at 37°C for 24 h. The zone of inhibition was measured as the diameter of a circle centred on the filter paper disk which showed no bacterial growth. Zone of inhibition was recorded to the nearest millimetre.

3.4 Crystallography Data

3.4.1 Crystal Structure and Refinement Data

Complex	**2a**	**9a**
Empirical formula	C_{31} H_{25} N_2 O_2 F_2 Ag	C_{58} H_{48} N_4 F_6 P Ag
Formula weight	603.40	1053.84
Temperature	100(2) K	100(2) K
Wavelength	0.71073 Å	0.71073 Å
Crystal system	Monoclinic	Monoclinic
Space group	$P2_1/n$ (#14)	$P2_1/c$ (#15)
Unit cell dimensions	a = 14.6108(2) Å α= 90°.	a = 16.9755(2) Å α= 90°.
	b = 11.1105(2) Å β= 91.383(2)°.	b = 18.9862(3) Å β= 92.7538(10)°.
	c = 16.3201(2) Å γ = 90°.	c = 15.2935(2) Å γ = 90°.
Volume	2648.52(7) $Å^3$	4923.41(12) $Å^3$
Z	4	4
Density (calculated)	1.513 Mg/m^3	1.422 Mg/m^3
Absorption coefficient	0.806 mm^{-1}	0.508 mm^{-1}
F(000)	1224	2160
Crystal size	0.320 x 0.230 x 0.189 mm^3	0.310 x 0.170 x 0.110 mm^3
θ range for data collection	3.098 to 30.046°.	2.770 to 32.978°.
Index ranges	–19<=h<=20, –15<=k<=15, –21<=l<=22	–24<=h<=24, –28<=k<=27, –23<=l<=21
Reflections collected	32662	158468
Independent reflections	7743 [R(int) = 0.0306]	17720 [R(int) = 0.0444]
Completeness to θ = 25.242°	99.8 %	99.8 %
Absorption correction	Gaussian	Gaussian
Max. and min. transmission	0.896 and 0.855	1.000 and 0.716
Refinement method	Full–matrix least–squares on F^2	Full–matrix least–squares on F^2
Data / restraints / parameters	7743 / 0 / 344	17720 / 0 / 631
Goodness–of–fit on F^2	1.051	1.073
Final R indices [I>2sigma(I)]	R1 = 0.0262, wR2 = 0.0556	R1 = 0.0325, wR2 = 0.0785
R indices (all data)	R1 = 0.0345, wR2 = 0.0603	R1 = 0.0441, wR2 = 0.0871
Extinction coefficient	n/a	n/a
Largest diff. peak and hole	0.446 and –0.340 $e.Å^{-3}$	0.928 and –0.879 $e.Å^{-3}$

Complex	**9c**	**10b**
Empirical formula	C_{62} H_{44} N_4 F_{18} P Ag	C_{58} H_{44} B N_4 F_8 Ag
Formula weight	1325.85	1067.65
Temperature	100(2) K	100(2) K
Wavelength	1.54184 Å	1.54184 Å
Crystal system	Orthorhombic	Monoclinic
Space group	$Pna2_1$ (#33)	$P2_1/n$ (#14)
Unit cell dimensions	a = 31.8772(4) Å α= 90°.	a = 13.55810(6) Å α= 90°.
	b = 17.1336(2) Å β= 90°.	b = 15.46517(7) Å β= 102.4673(4)°.
	c = 10.4178(1) Å γ = 90°.	c = 23.8808(1) Å γ = 90°.
Volume	5689.90(11) $Å^3$	4889.21(4) $Å^3$
Z	4	4
Density (calculated)	1.548 Mg/m^3	1.450 Mg/m^3
Absorption coefficient	4.031 mm^{-1}	3.940 mm^{-1}
F(000)	2672	2176
Crystal size	0.262 x 0.045 x 0.032 mm^3	0.250 x 0.200 x 0.110 mm^3
θ range for data collection	3.788 to 76.845°.	3.429 to 76.842°.
Index ranges	–38<=h<=40, –21<=k<=21, –11<=l<=13	–17<=h<=16, –19<=k<=19, –30<=l<=30
Reflections collected	34292	99246
Independent reflections	9623 [R(int) = 0.0604]	10288 [R(int) = 0.0314]
Completeness to θ = 67.684°	99.9 %	100.0 %
Absorption correction	Gaussian	Gaussian
Max. and min. transmission	0.961 and 0.631	1.000 and 0.399
Refinement method	Full–matrix least–squares on F^2	Full–matrix least–squares on F^2
Data / restraints / parameters	9623 / 1 / 775	10288 / 0 / 663
Goodness–of–fit on F^2	1.046	1.035
Final R indices [I>2sigma(I)]	R1 = 0.0385, wR2 = 0.0879	R1 = 0.0233, wR2 = 0.0587
R indices (all data)	R1 = 0.0472, wR2 = 0.0953	R1 = 0.0258, wR2 = 0.0608
Extinction coefficient	n/a	0.000239(18)
Largest diff. peak and hole	0.689 and –0.957 e.$Å^{-3}$	0.439 and –0.424 e.$Å^{-3}$

Complex	**13a**	**15**
Empirical formula	C_{116} H_{96} N_8 Cl_4 Ag_4	C_{60} H_{53} N_4 O_3 Ag
Formula weight	2175.28	985.93
Temperature	100(2) K	100(2) K
Wavelength	1.54184 Å	1.54184 Å
Crystal system	Triclinic	Triclinic
Space group	P–1 (#2)	P–1 (#2)
Unit cell dimensions	a = 18.98722(6) Å α= 108.7062(2)°.	a = 15.0939(2) Å α= 71.166(2)°.
	b = 22.41275(7) Å β= 91.0516(2)°.	b = 15.3718(3) Å β= 80.754(1)°.
	c = 23.93923(6) Å γ = 98.3266(2)°.	c = 22.3865(4) Å γ = 76.134(2)°.
Volume	9524.76(5) $Å^3$	4753.11(16) $Å^3$
Z	8	4
Density (calculated)	1.517 Mg/m^3	1.378 Mg/m^3
Absorption coefficient	7.964 mm^{-1}	3.807 mm^{-1}
F(000)	4416	2048
Crystal size	0.160 x 0.100 x 0.090 mm^3	0.170 x 0.080 x 0.030 mm^3
θ range for data collection	3.404 to 76.854°.	3.523 to 78.596°.
Index ranges	–23<=h<=23, –25<=k<=28, –30<=l<=30	–19<=h<=19, –19<=k<=19, –28<=l<=28
Reflections collected	261491	22266
Independent reflections	39770 [R(int) = 0.0363]	22266 [R(int) = 0.0554]
Completeness to θ = 67.684°	100.0 %	99.9 %
Absorption correction	Gaussian	Analytical
Max. and min. transmission	0.979 and 0.728	0.914 and 0.640
Refinement method	Full–matrix least–squares on F^2	Full–matrix least–squares on F^2
Data / restraints / parameters	39770 / 0 / 2377	22266 / 0 / 1228
Goodness–of–fit on F^2	1.030	1.048
Final R indices [I>2sigma(I)]	R1 = 0.0222, wR2 = 0.0522	R1 = 0.0455, wR2 = 0.1174
R indices (all data)	R1 = 0.0268, wR2 =0.0546	R1 = 0.0542, wR2 =0.1247
Extinction coefficient	n/a	n/a
Largest diff. peak and hole	0.993 and –1.196 e.$Å^{-3}$	2.680 and –1.095 e.$Å^{-3}$

The crystal structures for complexes **4a** and **12c** do not have completes sets of accompanying data as the structures were significantly disordered and not of publishable quality. However, the images of each presented in sections **2.3.1** and **2.5.1**, respectively, are indicative of the molecular structure of each complex. Available data are in the table below:

Complex	**4a**	**12c**
Empirical formula	Unknown	C_{64} H_{55} Ag Cl F_{12} N_4 O_7
Formula weight	n/a	1363.45
Temperature	100(2) K	100(2) K
Wavelength	1.54184 Å	1.54184 Å
Crystal system	Triclinic	Monoclinic
Space group	P–1 (#2)	P 2_1 (#4)
Unit cell dimensions	a = 10.82540(10) Å α= 106.7210(10) °.	a = 9.2734(2) Å α= 90°.
	b = 11.4883(2) Å β= 95.4040(10)°.	b = 16.9675(2) Å β= 106.589(2)°.
	c = 16.6595(2) Å γ = 93.7815(9)°.	c = 21.2040(3) Å γ = 90°.
Volume	1966.01 $Å^3$	6645.54 $Å^3$
Z	2	4

3.4.2 Selected Bond Lengths and Angles

(**2a**) 1,3-Di(*p*-fluoro) benzyl-4,5-diphenylimidazol-2-ylidene silver (I) acetate

Bond Lengths (Å)		Bond Angles (°)	
Ag–C(1)	2.0616(15)	C(1)–Ag–O(1)	174.38(5)
Ag–O(1)	2.1157(12)	N(2)–C(1)–Ag	127.39(11)
C(1)–N(2)	1.3565(19)	N(1)–C(1)–Ag	128.19(11)
C(1)–N(1)	1.3586(19)	N(2)–C(1)–N(1)	104.30(13)
N(1)–C(2)	1.3911(19)	C(1)–N(1)–C(2)	111.64(12)
C(3)–N(2)	1.3966(19)	C(2)–C(3)–N(2)	106.28(13)
C(2)–C(3)	1.362(2)	C(1)–N(2)–C(3)	111.46(12)
N(1)–C(4)	1.4743(18)	C(30)–O(1)–Ag	108.14(10)
N(2)–C(23)	1.4649(19)	O(2)–C(30)–O(1)	123.98(15)
C(8)–F(1)	1.3651(19)	O(2)–C(30)–C(31)	120.33(15)
C(27)–F(2)	1.3590(19)	O(1)–C(30)–C(31)	115.68(14)
O(1)–C(30)	1.281(2)		
C(30)–O(2)	1.2404(19)		

(**9a**) *Bis*-(1,3-dibenzyl-4,5-diphenyl imidazol-2-ylidene) silver (I) hexafluorophosphate

Bond Lengths (Å)		Bond Angles (°)	
Ag–C(8)	2.0832(13)	C(8)–Ag–C(37)	175.86(5)
Ag–C(37)	2.0834(13)	C(8)–N(1)–C(9)	111.40(11)
N(1)–C(8)	1.3549(16)	N(2)–C(8)–N(1)	104.83(11)
N(1)–C(9)	1.3996(16)	N(2)–C(8)–Ag	124.69(9)
C(7)–N(1)	1.4625(17)	N(1)–C(8)–Ag	130.47(10)
C(8)–N(2)	1.3485(17)	C(16)–C(9)–N(1)	105.65(11)
N(2)–C(23)	1.4704(17)	C(9)–C(16)–N(2)	106.55(11)
C(9)–C(16)	1.3688(18)	C(8)–N(2)–C(16)	111.55(11)
C(16)–N(2)	1.3896(16)	C(37)–N(3)–C(38)	111.57(11)
N(3)–C(37)	1.3524(17)	N(3)–C(37)–N(4)	104.77(11)
N(3)–C(38)	1.3925(16)	N(3)–C(37)–Ag	124.53(9)
C(37)–N(4)	1.3526(16)	N(4)–C(37)–Ag	130.69(10)
C(38)–C(45)	1.3673(18)	C(45)–C(38)–N(3)	106.17(11)
C(45)–N(4)	1.3968(16)	C(38)–C(45)–N(4)	106.11(11)
C(36)–N(3)	1.4716(16)	C(37)–N(4)–C(45)	111.38(11)
N(4)–C(52)	1.4633(17)	F(6)–P–F(1)	89.98(6)
P–F(1)	1.6001(10)	F(5)–P–F(3)	179.34(7)
P–F(3)	1.6010(10)	F(3)–P–F(2)	90.40(6)
P–F(2)	1.6073(10)		

(**9c**) *Bis*-(1,3-di(4-trifluoromethyl) benzyl-4,5-diphenylimidazol-2-ylidene) silver (I) hexafluorophosphate

Bond Lengths (Å)		Bond Angles (°)	
Ag–C(1)	2.093(4)	C(1)–Ag–C(32)	175.71(17)
Ag–C(32)	2.095(5)	N(1)–C(1)–N(2)	105.5(4)
C(1)–N(1)	1.341(6)	N(1)–C(1)–Ag	126.0(3)
C(1)–N(2)	1.345(6)	N(2)–C(1)–Ag	128.4(3)
N(1)–C(2)	1.395(5)	C(1)–N(1)–C(2)	111.4(4)
C(2)–C(3)	1.361(7)	F(1)–C(11)–F(2)	105.4(6)
C(3)–N(2)	1.403(5)	F(3)–C(11)–C(8)	111.8(6)
N(1)–C(4)	1.458(6)	C(3)–C(2)–N(1)	106.1(4)
N(2)–C(24)	1.462(6)	C(2)–C(3)–N(2)	106.2(4)
C(28)–C(31)	1.498(7)	C(1)–N(2)–C(3)	110.8(4)
C(31)–F(6)	1.336(7)	N(3)–C(32)–N(4)	105.4(4)
C(32)–N(3)	1.341(6)	N(3)–C(32)–Ag	131.8(3)

C(32)–N(4)	1.351(6)	N(4)–C(32)–Ag	122.8(3)
N(3)–C(33)	1.412(6)	C(32)–N(3)–C(33)	111.2(4)
C(33)–C(34)	1.362(7)	C(34)–C(33)–N(3)	105.7(4)
C(34)–N(4)	1.396(6)	C(33)–C(34)–N(4)	106.5(4)
N(3)–C(35)	1.454(6)	F(17)–P–F(18)	90.24(19)
N(4)–C(55)	1.460(6)	F(16)–P–F(18)	179.2(2)
C(62)–F(10)	1.285(10)		
P–F(13)	1.596(3)		

(**10b**) *Bis*-(1,3-di(4-fluoro) benzyl-4,5-diphenyl imidazole-2-ylidene) silver (I) tetrafluoroborate

Bond Lengths (Å)		Bond Angles (°)	
Ag(1)–C(30)	2.0881(14)	C(30)–Ag(1)–C(1)	177.15(6)
Ag(1)–C(1)	2.0883(15)	N(2)–C(1)–N(1)	104.53(12)
C(1)–N(2)	1.3518(19)	N(2)–C(1)–Ag(1)	131.43(11)
C(1)–N(1)	1.3565(19)	N(1)–C(1)–Ag(1)	124.01(10)
N(1)–C(9)	1.3922(18)	C(1)–N(1)–C(9)	111.43(12)
N(1)–C(2)	1.4632(18)	C(16)–C(9)–N(1)	106.38(12)
C(9)–C(16)	1.361(2)	C(9)–C(16)–N(2)	106.13(12)
C(16)–N(2)	1.3964(18)	C(1)–N(2)–C(16)	111.53(12)
N(2)–C(23)	1.4782(18)	C(1)–N(2)–C(23)	123.12(12)
C(27)–F(2)	1.362(2)	N(4)–C(30)–N(3)	104.43(12)
C(30)–N(4)	1.3499(19)	N(4)–C(30)–Ag(1)	129.77(10)
C(30)–N(3)	1.3571(19)	N(3)–C(30)–Ag(1)	125.41(10)
N(3)–C(38)	1.3956(18)	C(30)–N(3)–C(38)	111.52(12)
N(3)–C(31)	1.4640(18)	C(30)–N(3)–C(31)	121.52(12)
C(38)–C(45)	1.362(2)	C(38)–C(45)–N(4)	106.43(12)
C(45)–N(4)	1.3919(18)	C(45)–C(38)–N(3)	105.94(12)
N(4)–C(52)	1.4706(18)	F(7A)–B(1)–F(5)	F(7A)–B(1)–F(5)
C(56)–F(4)	1.3686(17)		
B(1)–F(5)	1.373(2)		

(**13a**) *Bis*-(1,3-dibenzyl-4,5-diphenylimidazol-2-ylidene) silver (I) dichloroargentate

Bond Lengths (Å)		Bond Angles (°)	
Ag(1)–C(8)	2.0794(16)	C(8)–Ag(1)–C(37)	171.49(7)
Ag(1)–C(37)	2.0840(17)	C(8)–N(1)–C(9)	110.99(14)
N(1)–C(8)	1.354(2)	N(2)–C(8)–N(1)	105.16(14)
N(1)–C(9)	1.396(2)	N(2)–C(8)–Ag(1)	125.57(12)
C(8)–N(2)	1.351(2)	C(16)–C(9)–N(1)	106.32(14)
C(9)–C(16)	1.364(2)	C(9)–C(16)–N(2)	106.35(14)
C(16)–N(2)	1.394(2)	C(8)–N(2)–C(16)	111.18(13)
N(2)–C(23)	1.473(2)	C(37)–N(3)–C(38)	111.20(13)
C(36)–N(3)	1.479(2)	N(4)–C(37)–N(3)	104.98(14)
N(3)–C(37)	1.352(2)	N(4)–C(37)–Ag(1)	125.26(12)
N(3)–C(38)	1.400(2)	N(3)–C(38)–C(39)	125.01(14)
C(37)–N(4)	1.348(2)	C(38)–C(45)–N(4)	106.59(14)
C(38)–C(45)	1.363(2)	C(37)–N(4)–C(45)	111.35(14)
C(45)–N(4)	1.390(2)	C(37)–N(4)–C(52)	124.29(14)
N(4)–C(52)	1.466(2)	C(66)–Ag(2)–C(95)	171.34(7)
Ag(2)–C(66)	2.0794(16)	C(66)–N(5)–C(67)	110.80(14)
Ag(2)–C(95)	2.0821(17)	N(6)–C(66)–N(5)	105.30(14)
N(5)–C(66)	1.353(2)	N(6)–C(66)–Ag(2)	126.17(12)
N(5)–C(67)	1.402(2)	C(74)–C(67)–N(5)	106.22(14)
C(66)–N(6)	1.347(2)	C(66)–N(6)–C(74)	111.33(14)
C(67)–C(74)	1.363(2)	C(66)–N(6)–C(81)	123.11(14)
C(74)–N(6)	1.394(2)	C(95)–N(7)–C(96)	111.32(14)
N(6)–C(81)	1.473(2)	C(96)–N(7)–C(94)	124.16(14)
N(7)–C(95)	1.350(2)	N(7)–C(95)–N(8)	105.07(14)
N(7)–C(96)	1.389(2)	N(7)–C(95)–Ag(2)	124.93(12)
C(95)–N(8)	1.352(2)	C(95)–N(8)–C(103)	110.95(14)
C(96)–C(103)	1.363(2)	Cl(2)–Ag(3)–Cl(1)	166.340(19)
C(103)–N(8)	1.396(2)	Ag(3)–Cl(1)–Ag(4)	86.628(13)
N(8)–C(110)	1.475(2)	Cl(4)–Ag(4)–Cl(3)	165.004(18)
Ag(3)–Cl(1)	2.3947(4)	Cl(3)–Ag(4)–Cl(1)	92.855(13)
Ag(3)–Cl(3)	2.8581(5)		
Cl(1)–Ag(4)	2.8772(4)		
Ag(4)–Cl(3)	2.3894(4)		

(**15**) Synthesis of *bis*-(1,3-dibenzyl-4,5-diphenylimidazol-2-ylidene) silver (I) acetate

Bond Lengths (Å)		Bond Angles (°)	
Ag(1)–C(8)	2.079(3)	C(8)–Ag(1)–C(37)	176.52(12)
Ag(1)–C(37)	2.089(3)	C(8)–N(1)–C(9)	111.5(2)
N(1)–C(8)	1.344(4)	C(9)–N(1)–C(7)	124.9(3)
N(1)–C(9)	1.388(4)	N(1)–C(8)–N(2)	105.0(3)
C(8)–N(2)	1.358(4)	N(1)–C(8)–Ag(1)	126.1(2)
C(9)–C(16)	1.362(4)	C(16)–C(9)–N(1)	106.5(3)
C(16)–N(2)	1.397(4)	C(9)–C(16)–N(2)	106.1(3)
C(7)–N(1)	1.473(4)	C(8)–N(2)–C(16)	110.9(2)
N(2)–C(23)	1.461(4)	C(37)–N(3)–C(38)	111.3(3)
C(36)–N(3)	1.467(4)	N(4)–C(37)–N(3)	105.0(3)
N(3)–C(37)	1.352(4)	N(4)–C(37)–Ag(1)	127.5(2)
N(3)–C(38)	1.390(4)	C(45)–C(38)–N(3)	106.7(3)
C(37)–N(4)	1.351(4)	C(38)–C(45)–N(4)	105.8(3)
C(38)–C(45)	1.364(4)	C(37)–N(4)–C(45)	111.3(2)
C(45)–N(4)	1.401(4)	O(1)–C(117)–O(2)	126.1(3)
N(4)–C(52)	1.471(4)	O(1)–C(117)–C(118)	117.2(3)
O(1)–C(117)	1.239(4)	O(2)–C(117)–C(118)	116.6(3)
O(2)–C(117)	1.260(4)		
C(117)–C(118)	1.522(5)		

3.5 References

[1] R.C. Clark, J.S. Reid, The Analytical Calculation of Absorption in Multifaceted Crystals, *Acta Crystallograph. Sect. A* 51 (1995) 887-897.

[2] G.M. Sheldrick, Crystal Structure Refinement with SHELXL, *Acta Crystallograph. Sect. C - Struct. Chem.* 71 (2015) 3-8.

[3] S. Patil, A. Deally, B. Gleeson, H. Mueller-Bunz, F. Paradisi, M. Tacke, Novel benzyl-substituted N-heterocyclic carbene-silver acetate complexes: synthesis, cytotoxicity and antibacterial studies, *Metallomics* 3(1) (2011) 74-88.

[4] A.W. Bauer, W.M.M. Kirby, J.C. Sherris, M. Turck, Antibiotic Susceptibility Testing by a Standardized Single Disk Method, *Am. J. Clin. Pathol.* 45(4) (1966) 493-496.

Appendix 1: Spectral Data

(**1b**): 1,3-Di(4-fluoro)benzyl-4,5-diphenyl imidazolium bromide ^{1}H NMR (400 MHz, $CDCl_3$)

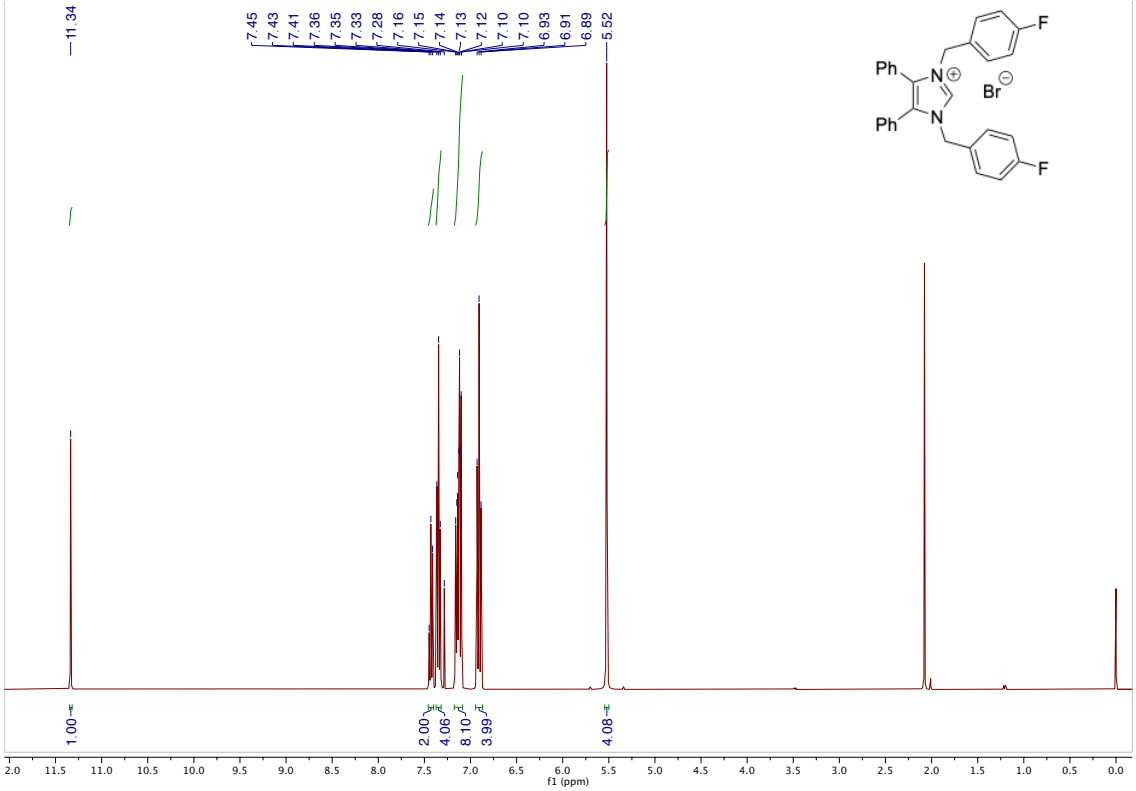

(**1b**): 1,3-Di(4-fluoro)benzyl-4,5-diphenyl imidazolium bromide ^{13}C NMR (101 MHz, $CDCl_3$)

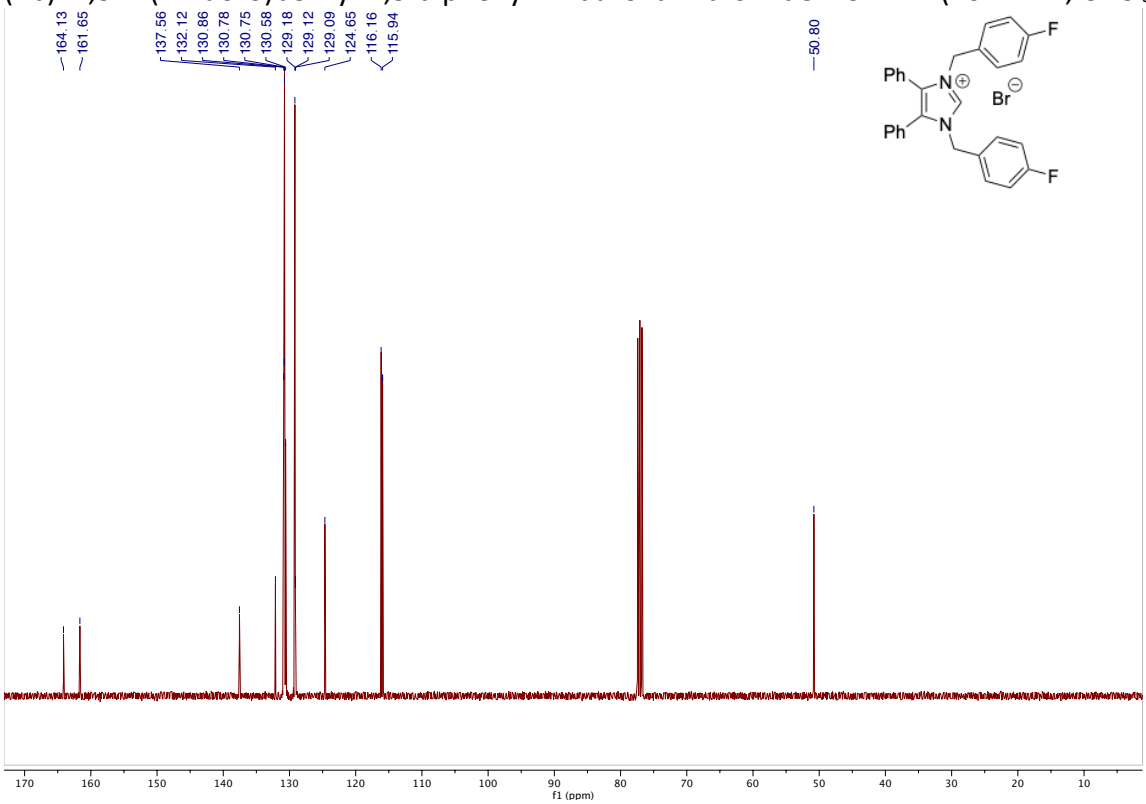

(**1b**): 1,3-Di(4-fluoro)benzyl-4,5-diphenyl imidazolium bromide ^{19}F NMR (376 MHz, $CDCl_3$)

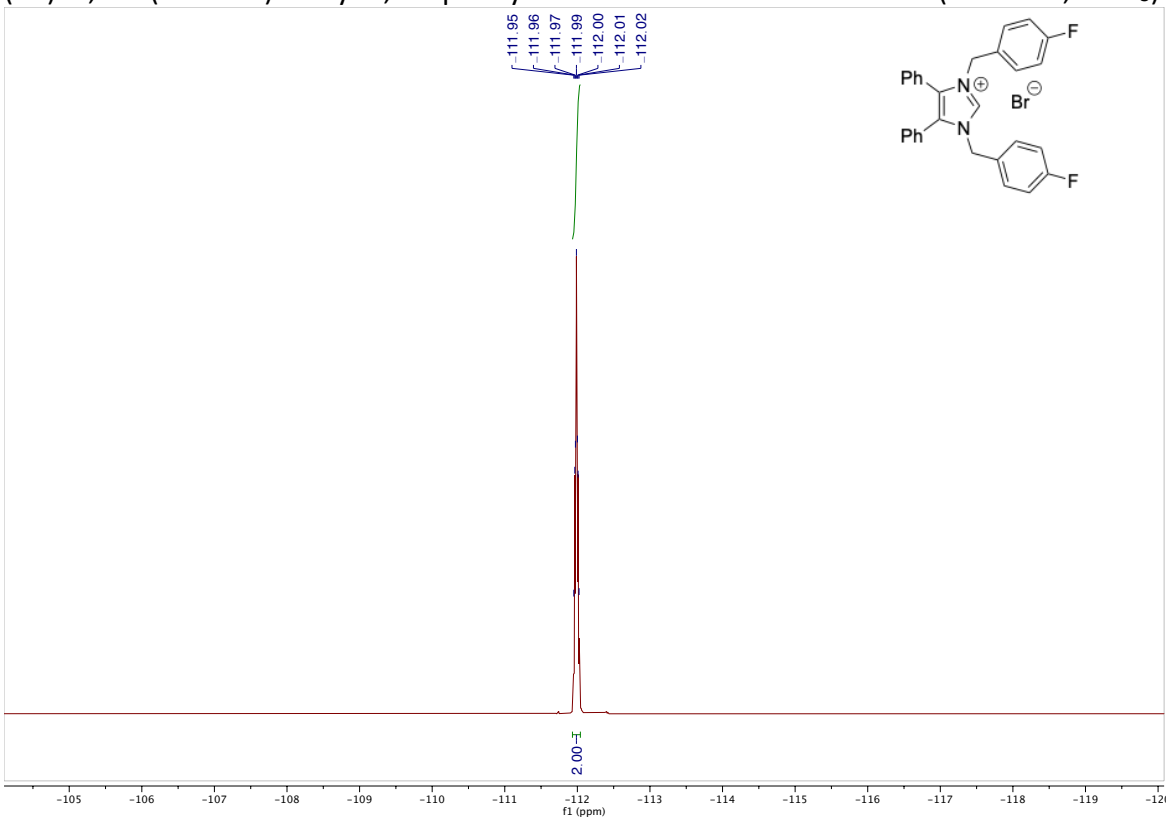

(**1c**)4,5-diphenyl-1,3-di(*p*-trifluoromethyl) benzyl imidazolium bromide ^{1}H NMR (400 MHz, $CDCl_3$)

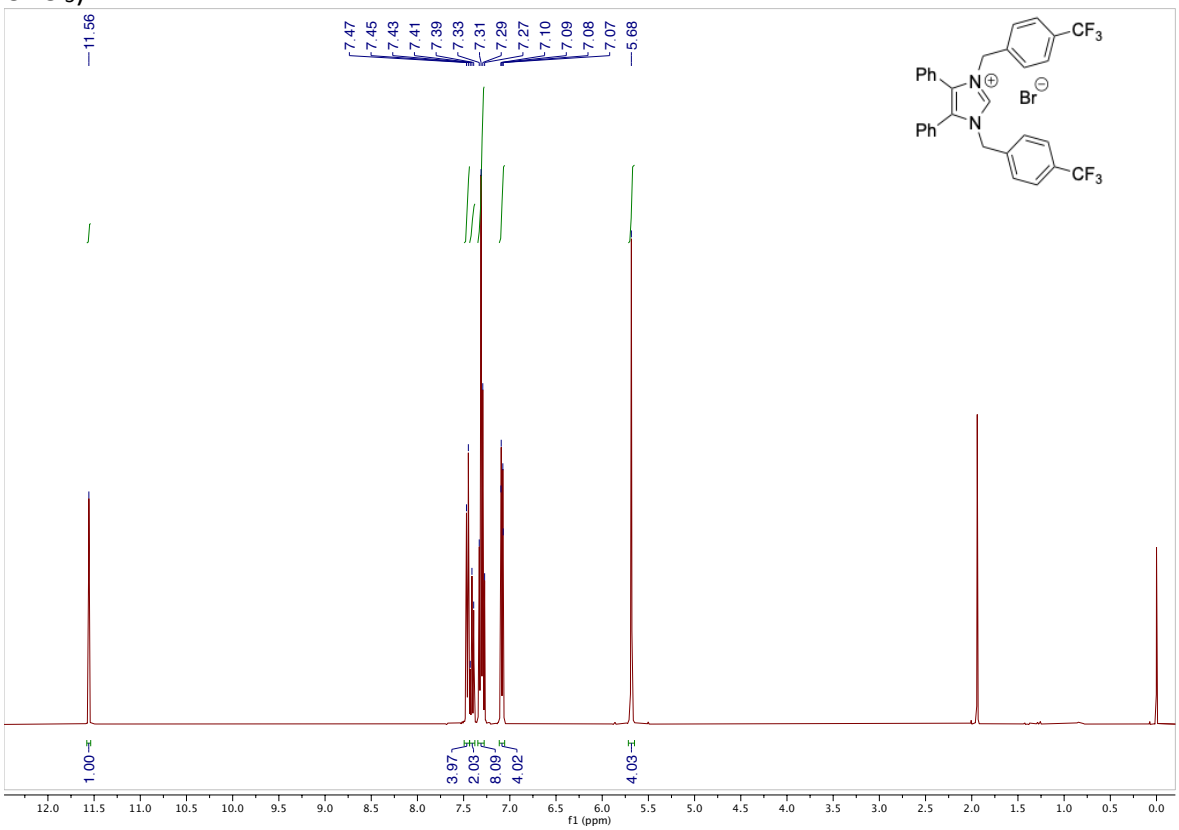

(**1c**) 4,5-diphenyl-1,3-di(*p*-trifluoromethyl) benzyl imidazolium bromide ^{13}C NMR (101 MHz, $CDCl_3$)

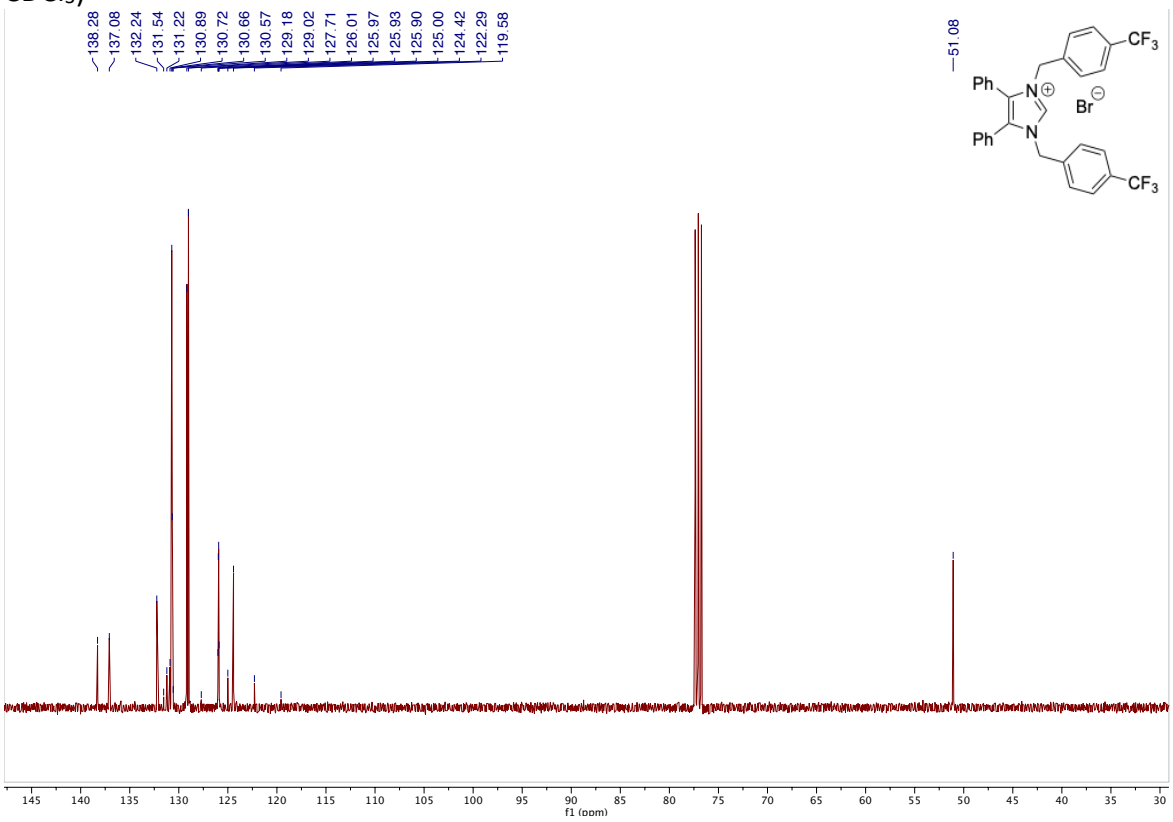

(**1c**) 4,5-diphenyl-1,3-di(*p*-trifluoromethyl) benzyl imidazolium bromide ^{19}F NMR (376 MHz, $CDCl_3$)

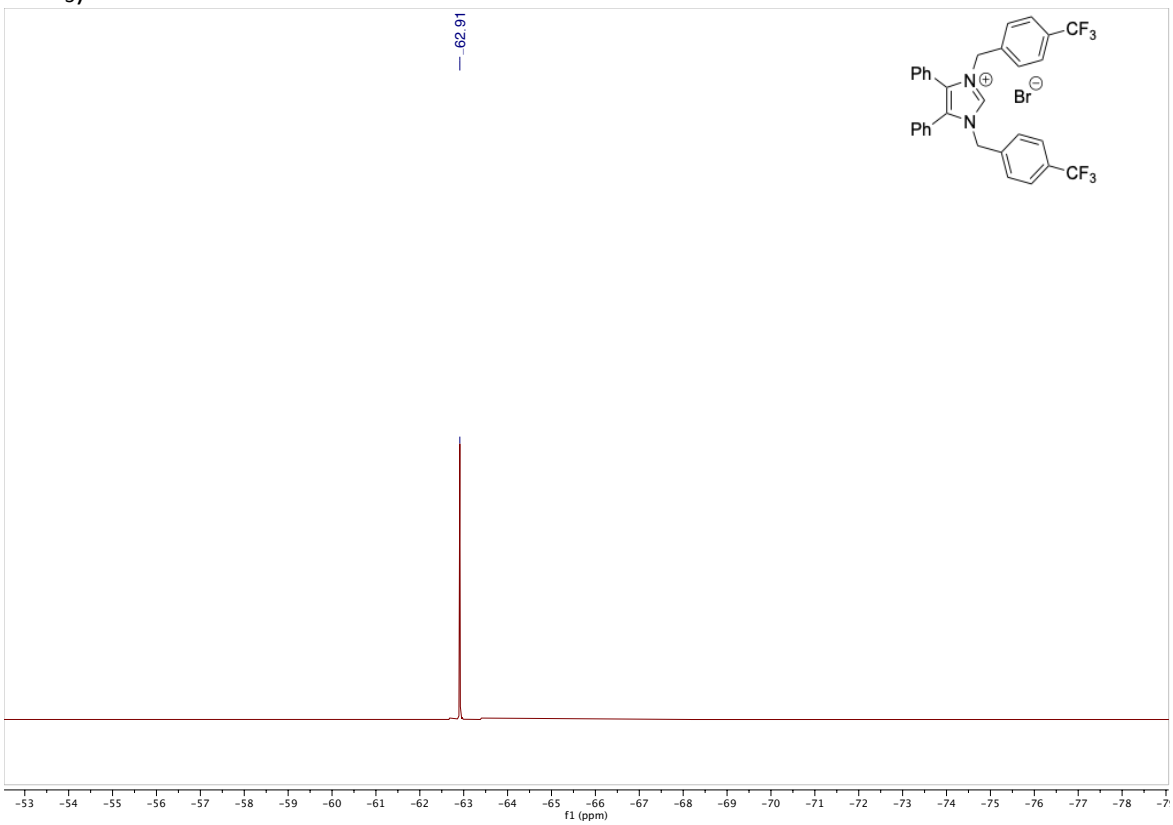

(**2a**) 1,3-Di(*p*-fluoro) benzyl-4,5-diphenylimidazol-2-ylidene silver (I) acetate ^{1}H NMR (400 MHz, $CDCl_3$)

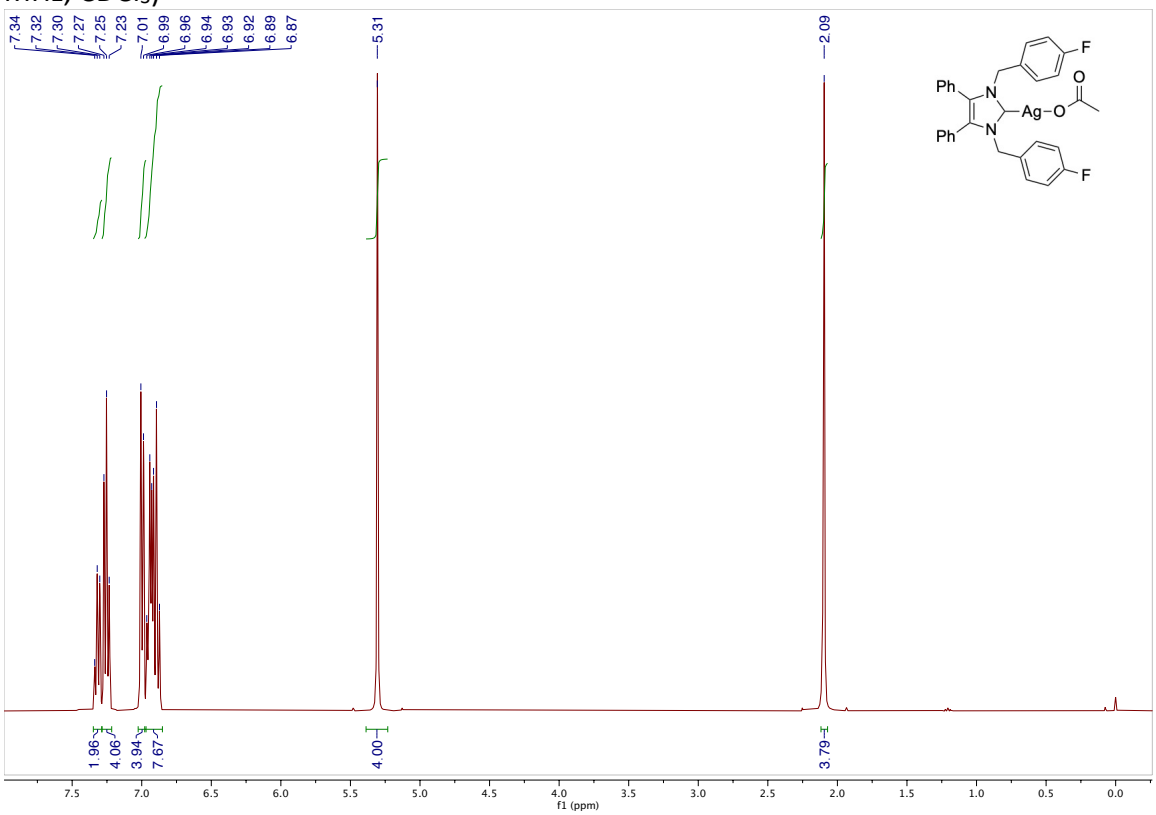

(**2a**) 1,3-Di(*p*-fluoro) benzyl-4,5-diphenylimidazol-2-ylidene silver (I) acetate ^{13}C NMR (101 MHZ, $CDCl_3$)

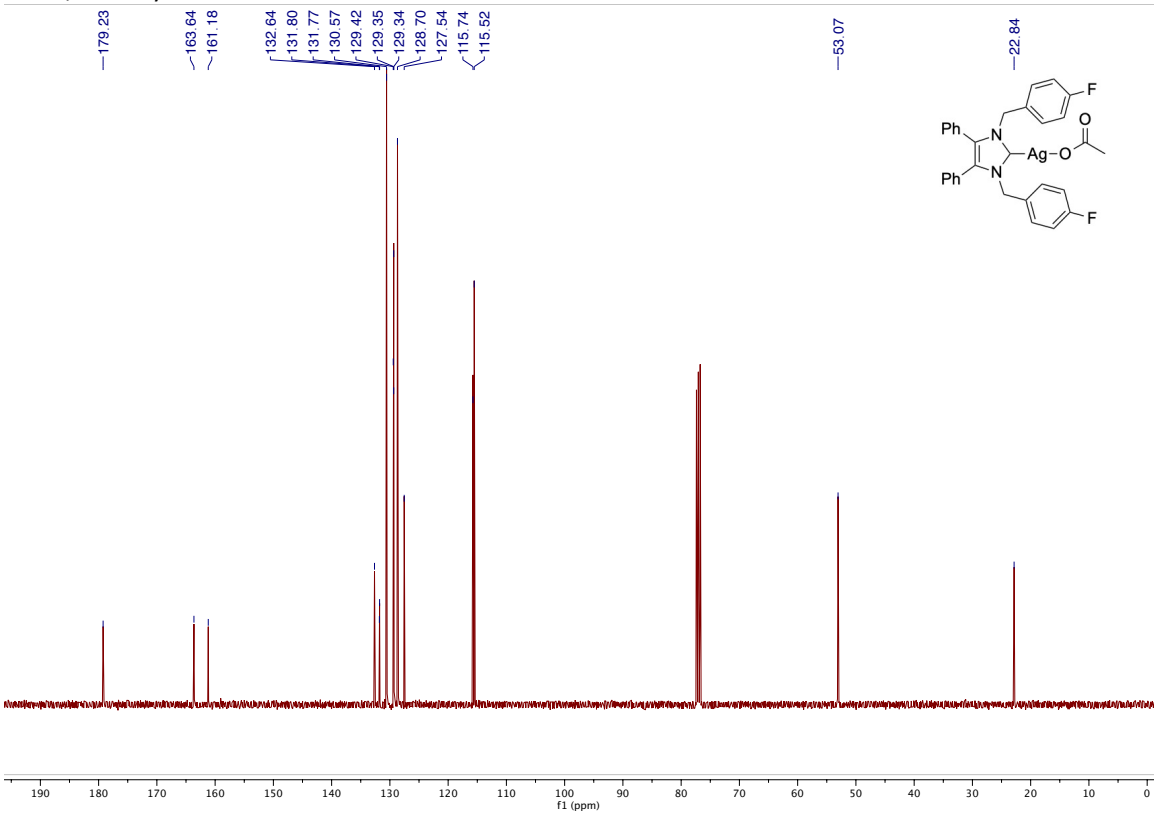

(**2a**) 1,3-Di(*p*-fluoro) benzyl-4,5-diphenylimidazol-2-ylidene silver (I) acetate ^{19}F NMR (376 MHZ, $CDCl_3$)

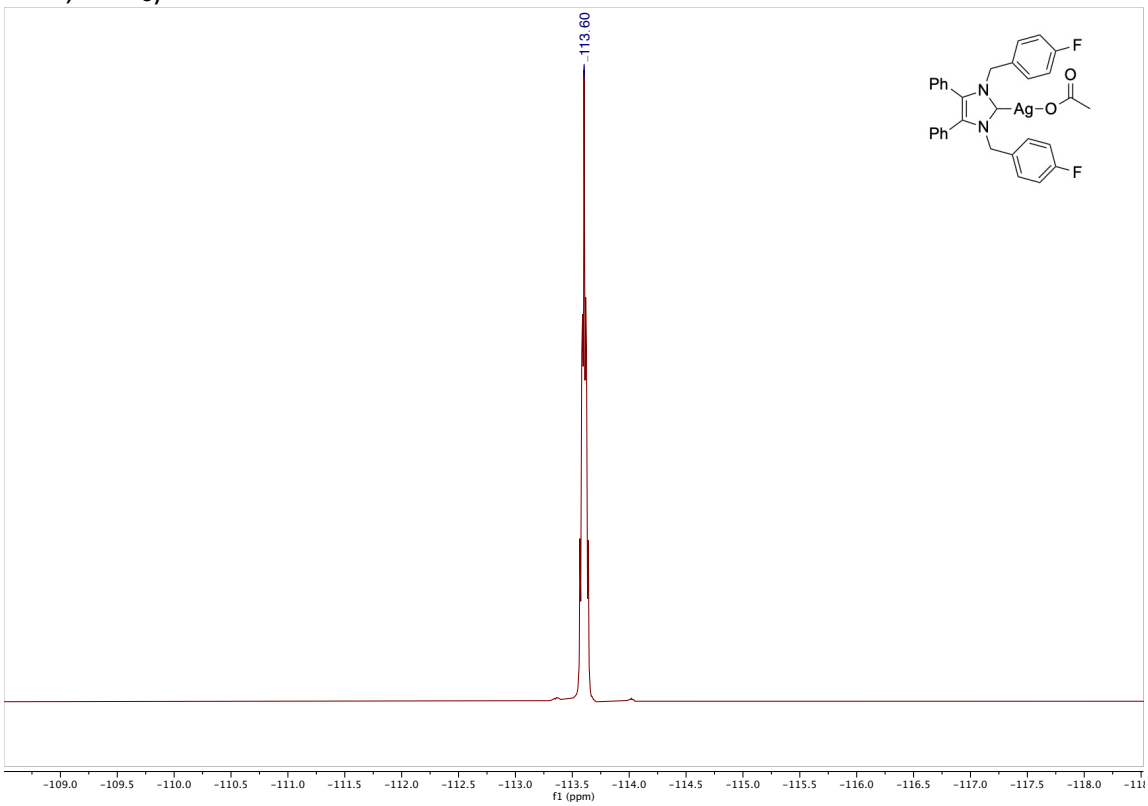

(**2b**) 1,3-Di(*p*-trifluoromethyl) benzyl-4,5-diphenylimidazol-2-ylidene silver (I) acetate ^{1}H NMR (400 MHz, $CDCl_3$)

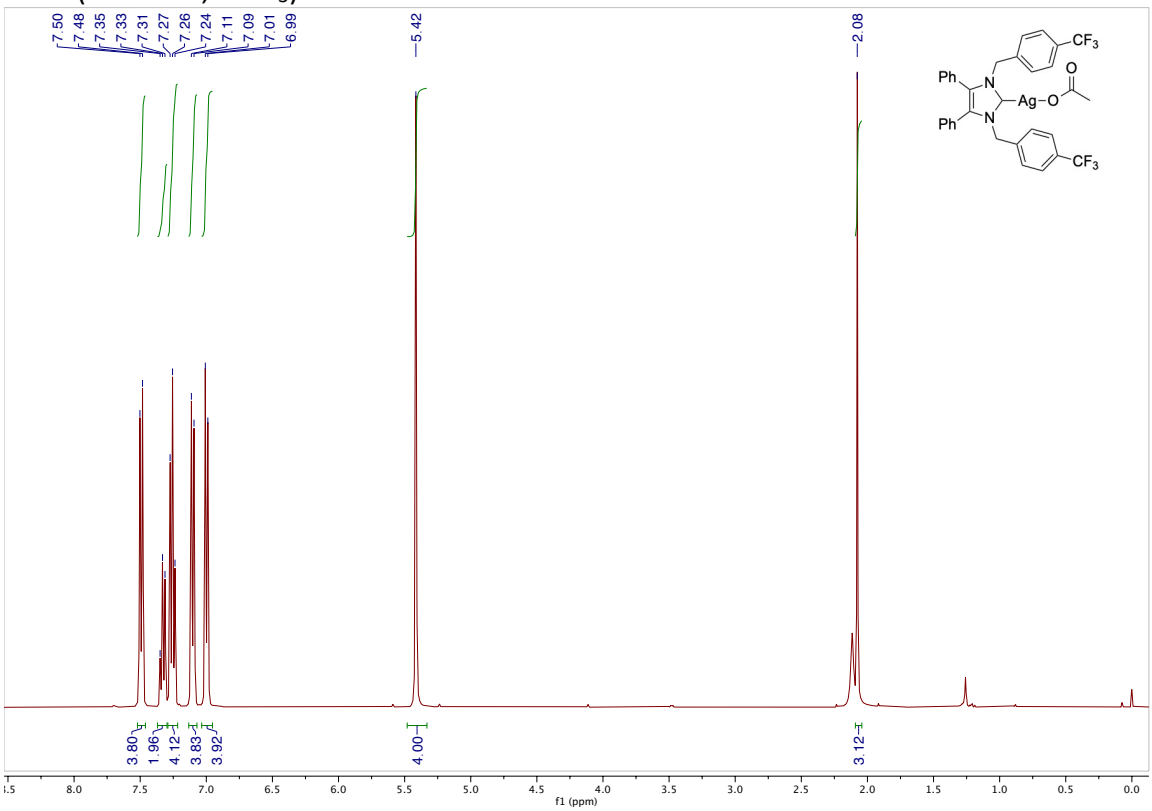

(**2b**) 1,3-Di(*p*-trifluoromethyl) benzyl-4,5-diphenylimidazol-2-ylidene silver (I) acetate ^{13}C NMR (101 MHz, $CDCl_3$)

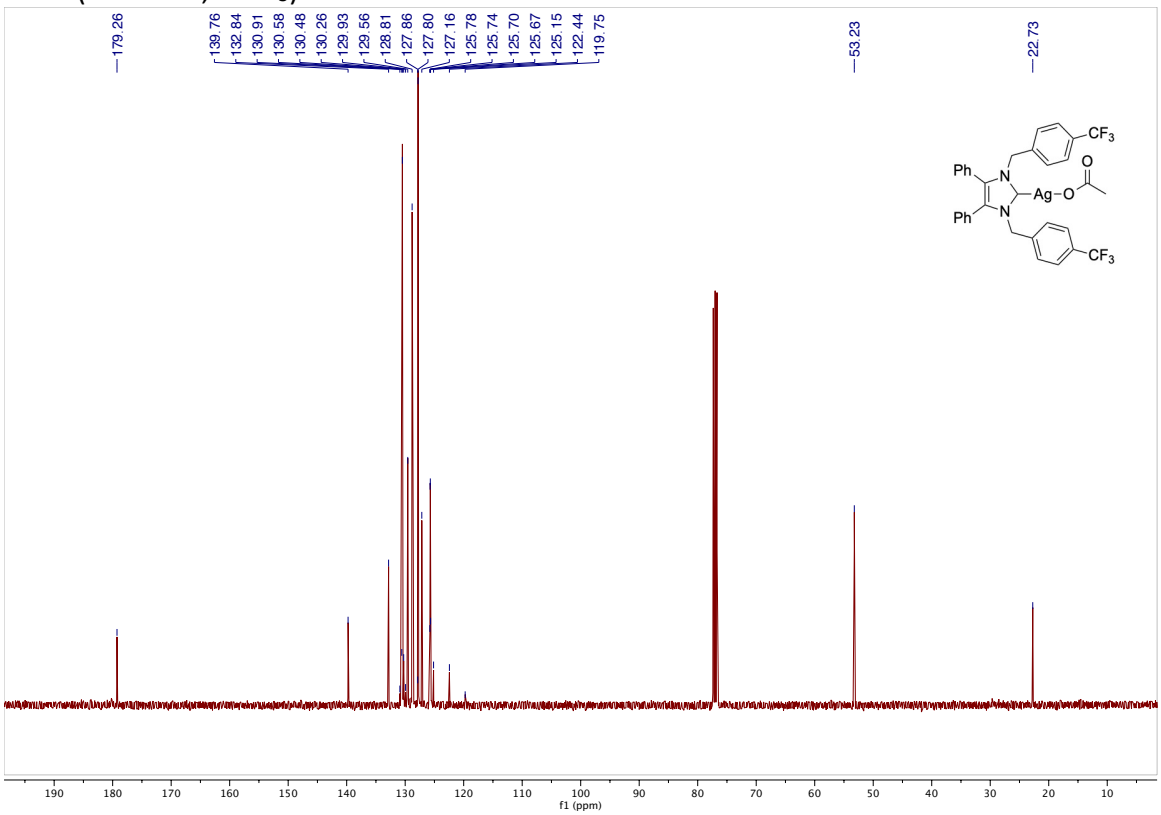

(**2b**) 1,3-Di(*p*-trifluoromethyl) benzyl-4,5-diphenylimidazol-2-ylidene silver (I) acetate ^{19}F NMR (376 MHz, $CDCl_3$)

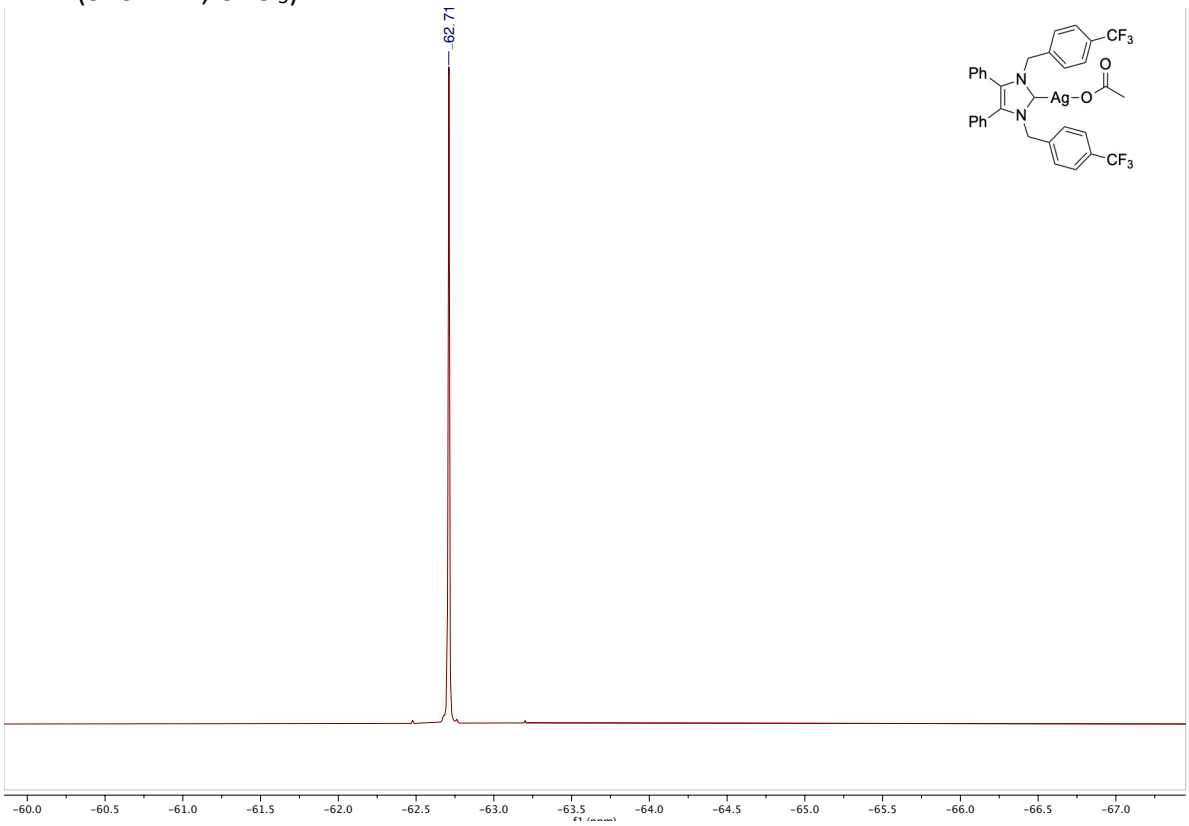

(**3**) Silver (I) *p*-trifluoromethyl benzoate ^{1}H NMR (400 MHz, DMSO-d_6)

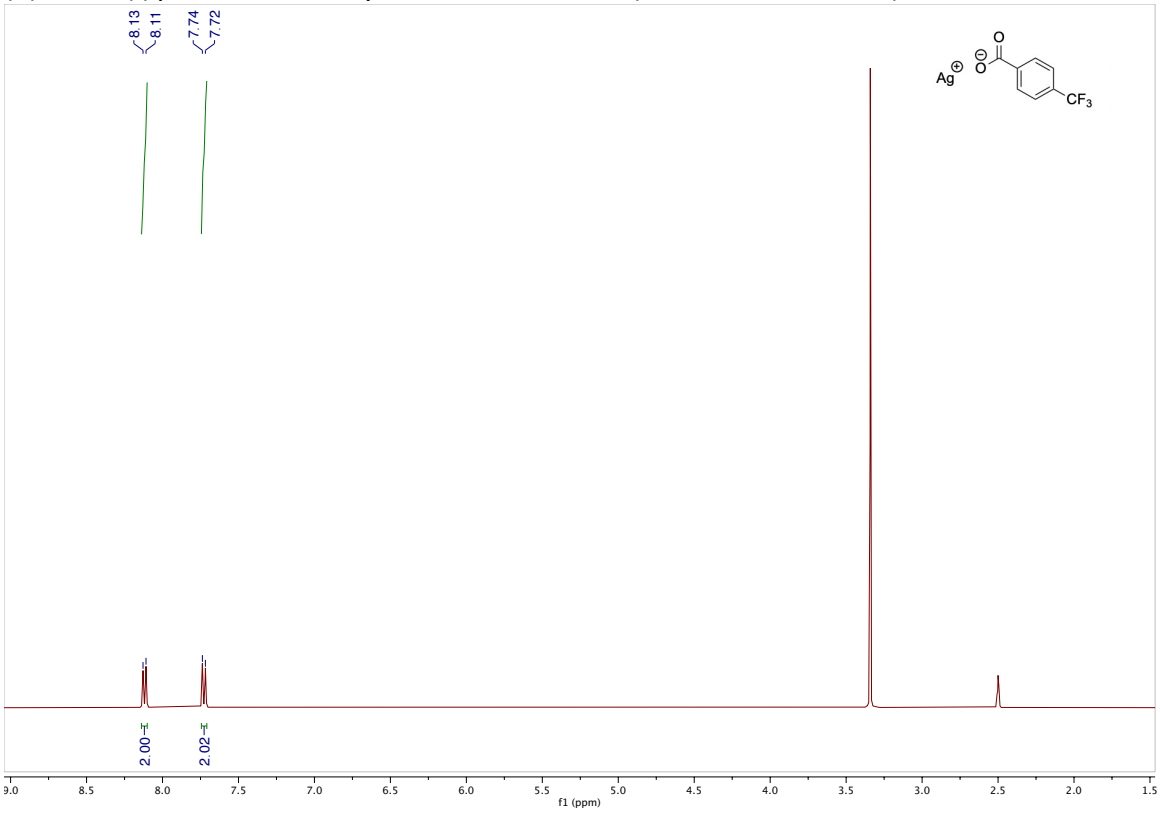

(**3**) Silver (I) *p*-trifluoromethyl benzoate ^{13}C NMR (101 MHz, DMSO-d_6)

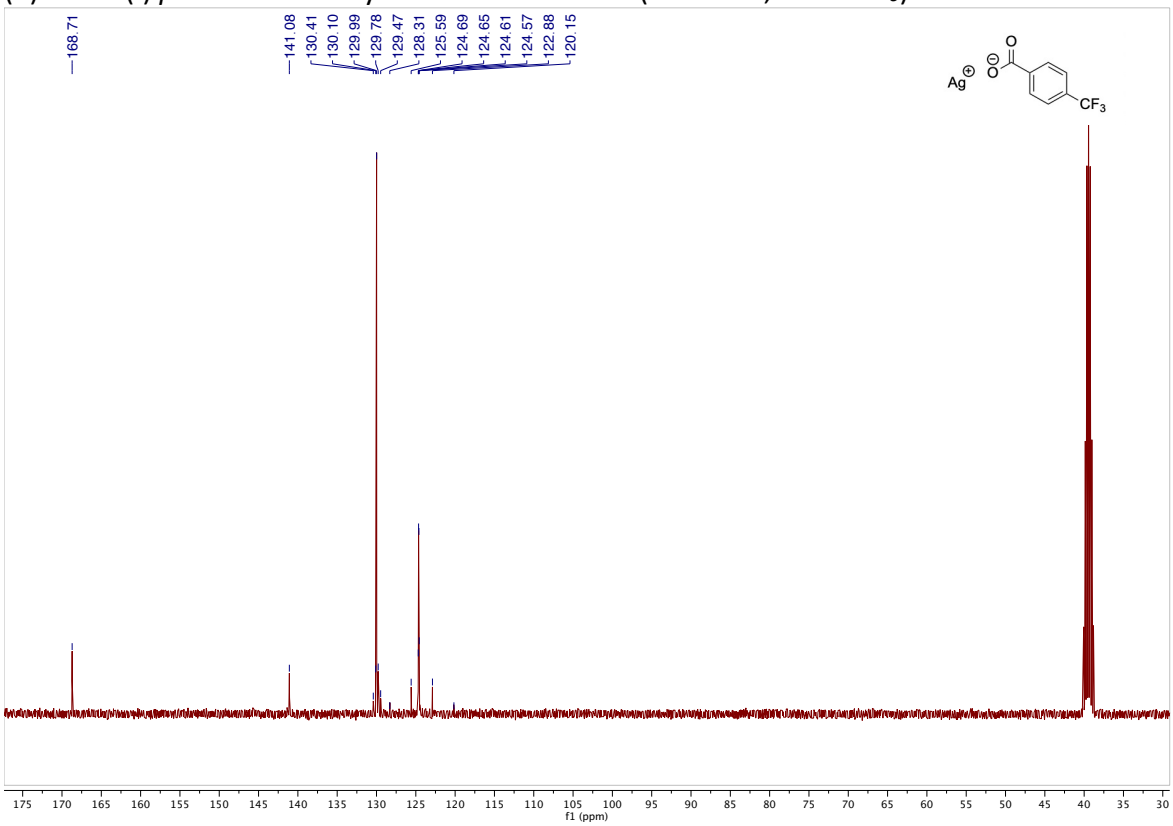

(**3**) Silver (I) *p*-trifluoromethyl benzoate ^{19}F NMR (376 MHz, DMSO-d_6)

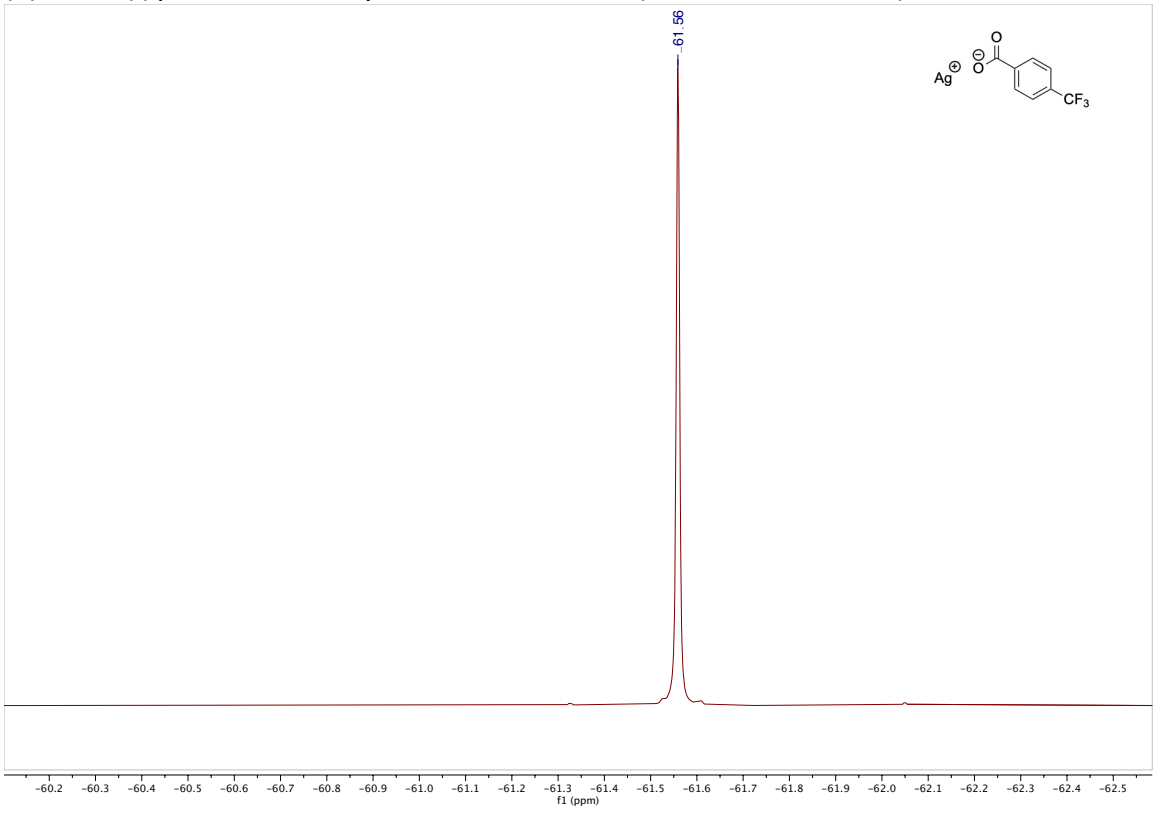

(**4a**) 1,3-Dibenzyl-4,5-diphenyl imidazol-2-ylidene silver (4-trifluoromethyl) benzoate ^{1}H NMR (400 MHz, $CDCl_3$)

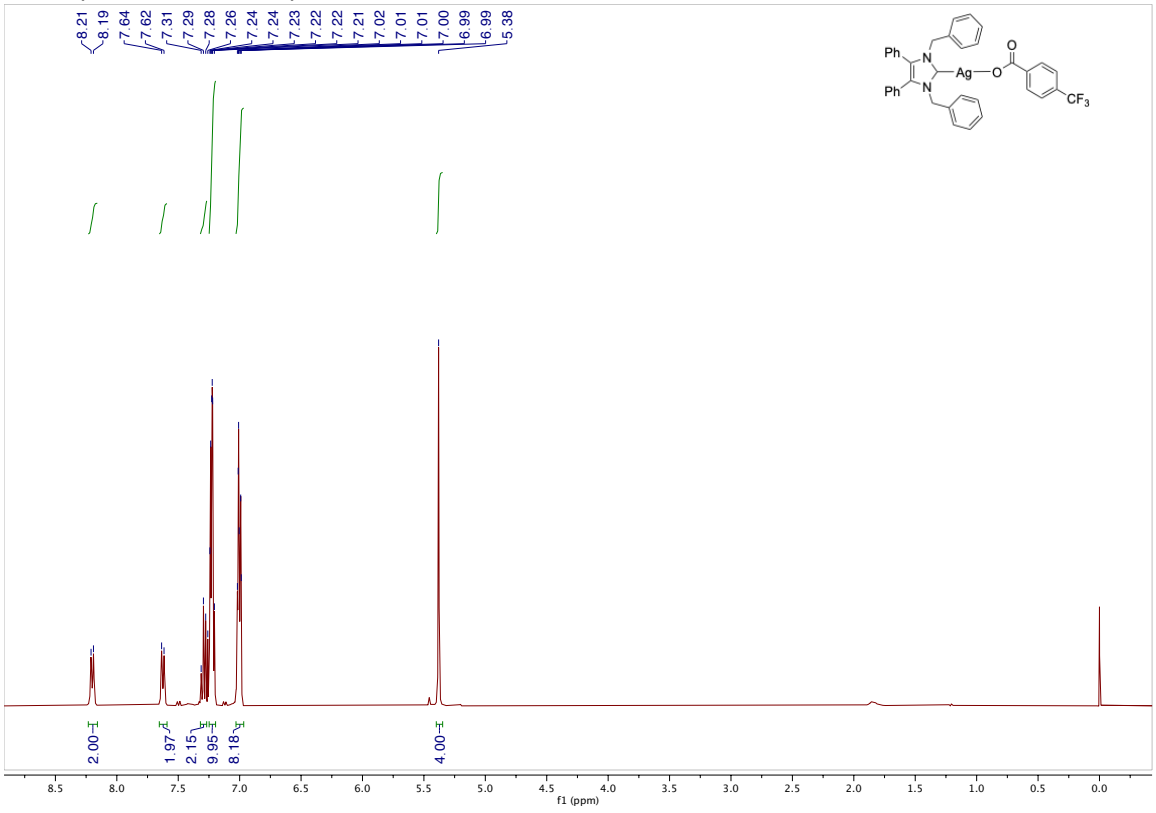

(**4a**) 1,3-Dibenzyl-4,5-diphenyl imidazol-2-ylidene silver (4-trifluoromethyl) benzoate ^{13}C NMR (101 MHz, $CDCl_3$)

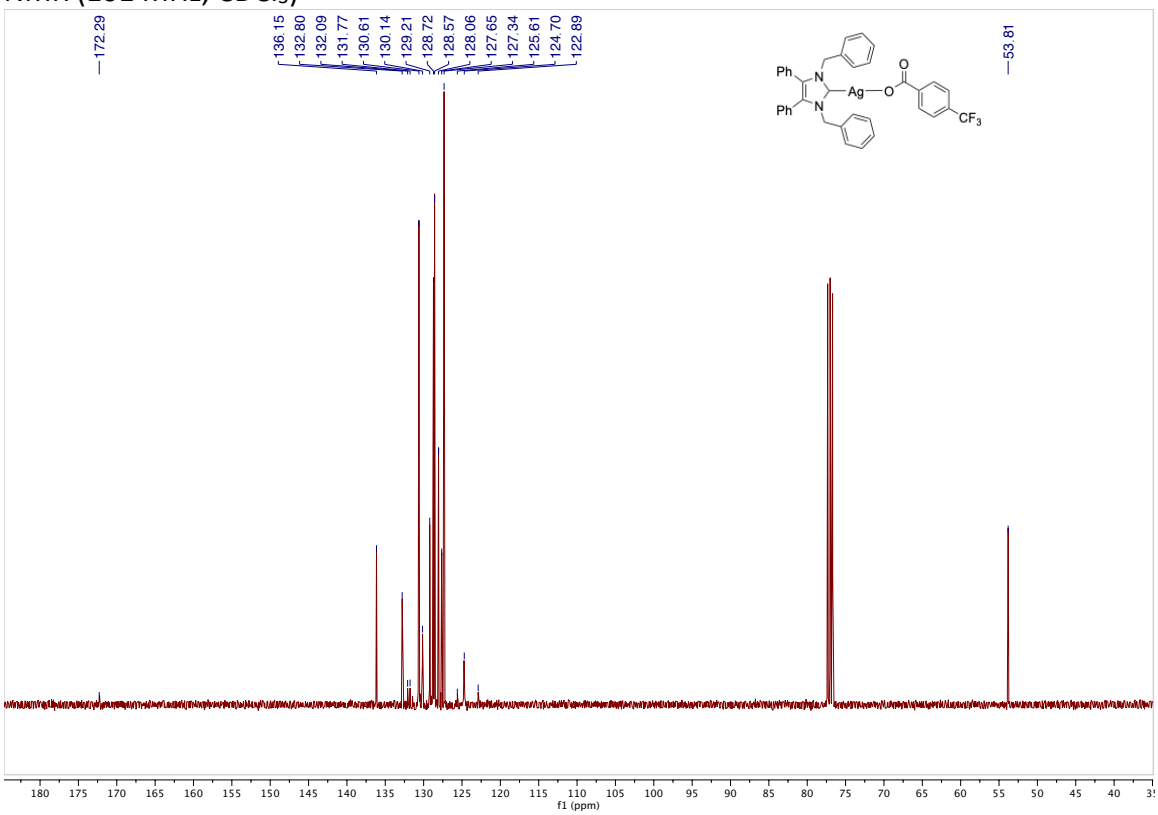

(**4a**) 1,3-Dibenzyl-4,5-diphenyl imidazol-2-ylidene silver (4-trifluoromethyl) benzoate ^{19}F NMR (376 MHz, $CDCl_3$)

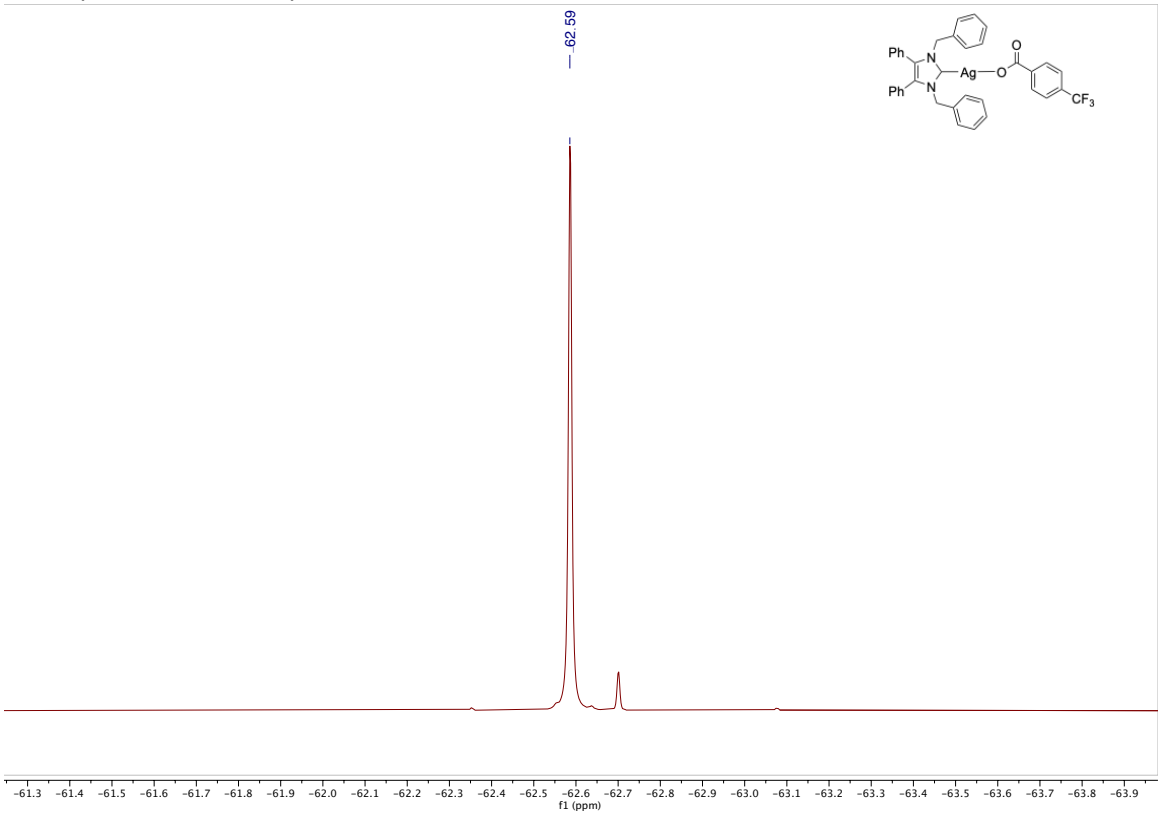

(**4b**) 1,3-Di(4-fluoro) benzyl-4,5-diphenyl imidazol-2-ylidene silver (4-trifluoromethyl) benzoate ^{1}H NMR (400 MHz, $CDCl_3$)

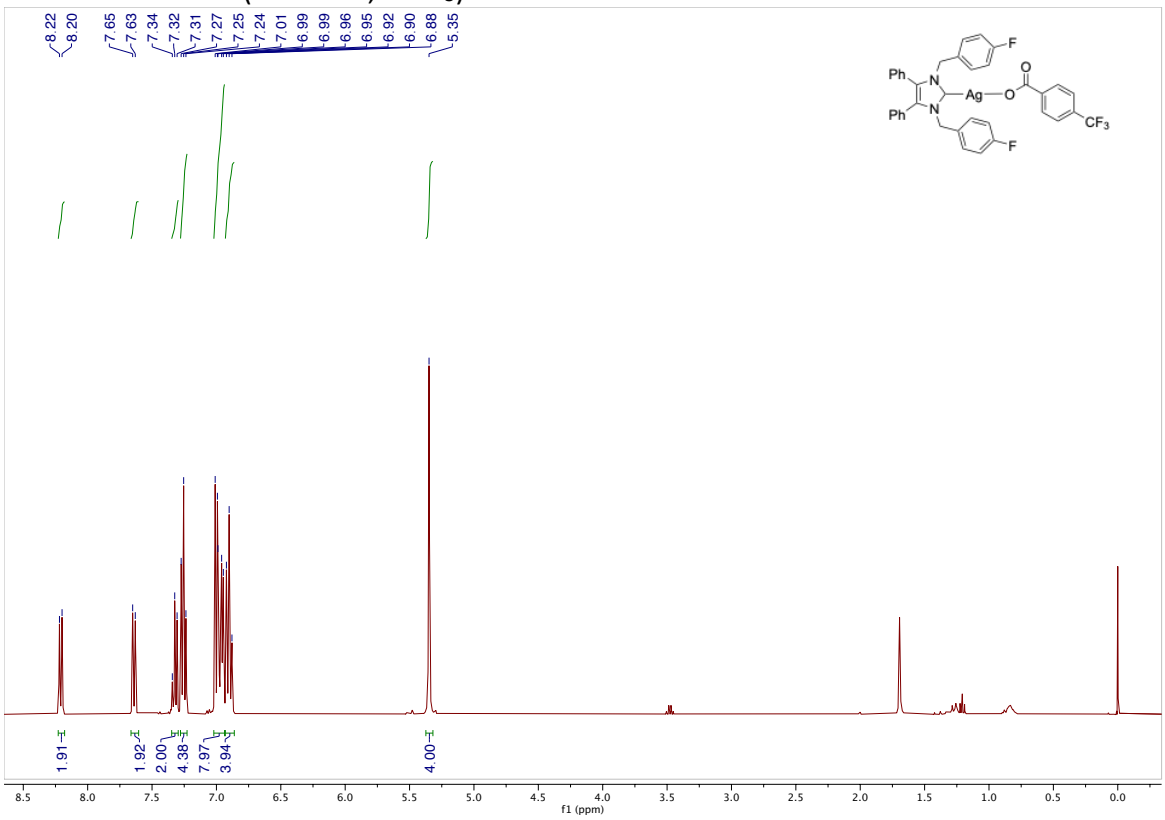

(**4b**) 1,3-Di(4-fluoro) benzyl-4,5-diphenyl imidazol-2-ylidene silver (4-trifluoromethyl) benzoate ^{13}C NMR (101 MHz, $CDCl_3$)

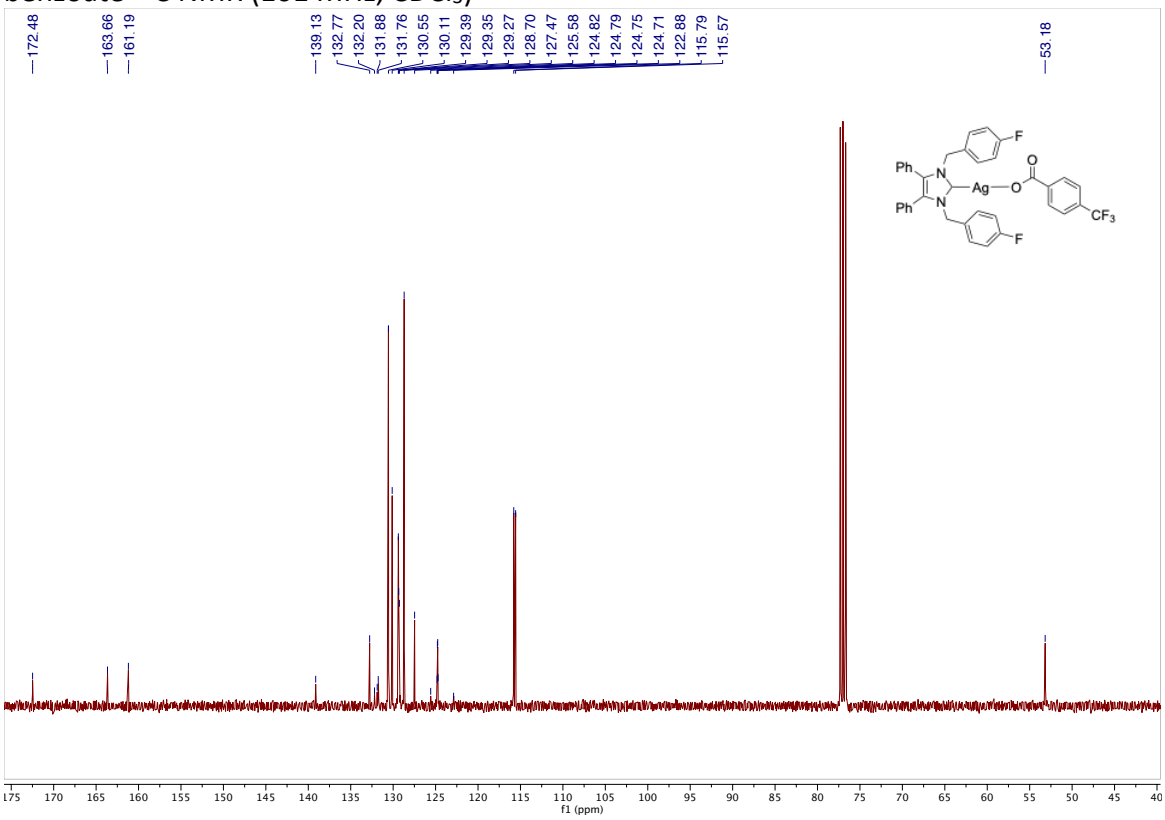

(**4b**) 1,3-Di(4-fluoro) benzyl-4,5-diphenyl imidazol-2-ylidene silver (4-trifluoromethyl) benzoate ^{19}F NMR (376 MHz, $CDCl_3$)

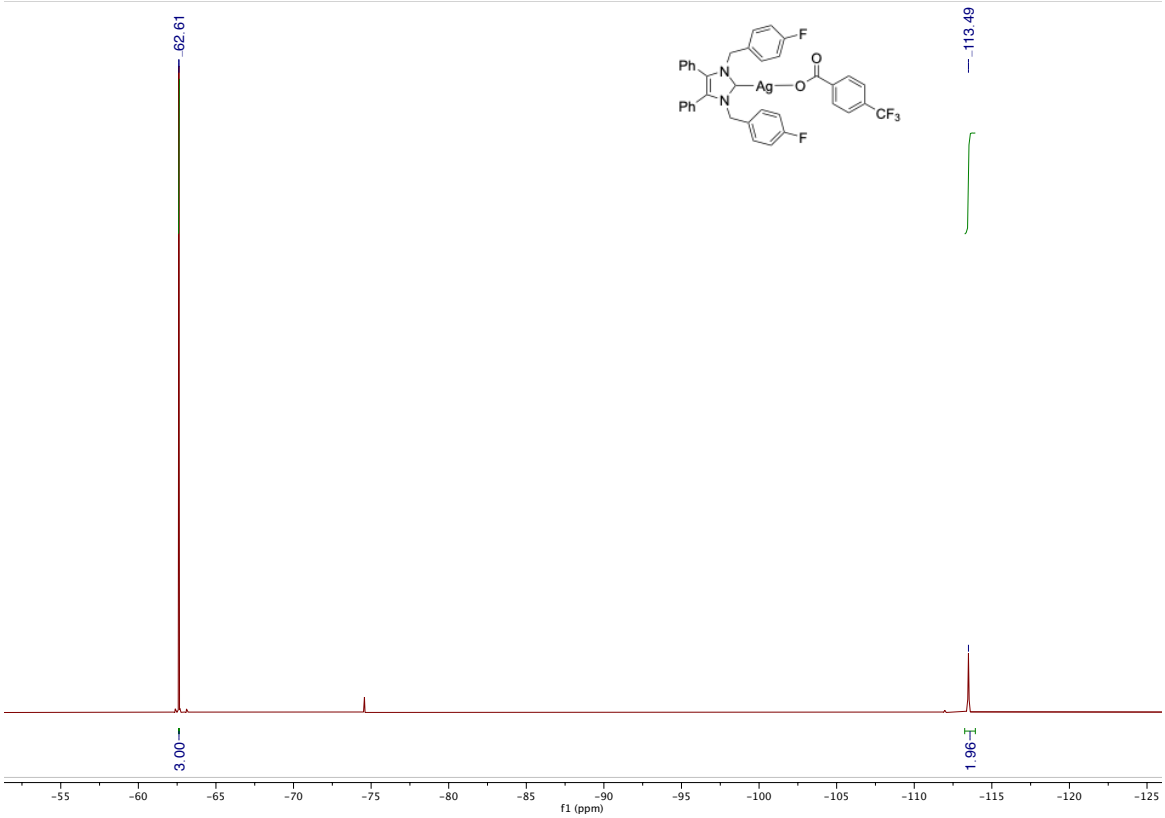

(**4c**) 1,3-Di(4-trifluoromethyl) benzyl-4,5-diphenylimidazol-2-ylidene silver (4-trifluoromethyl) benzoate ^{1}H NMR (400 MHz, $CDCl_3$)

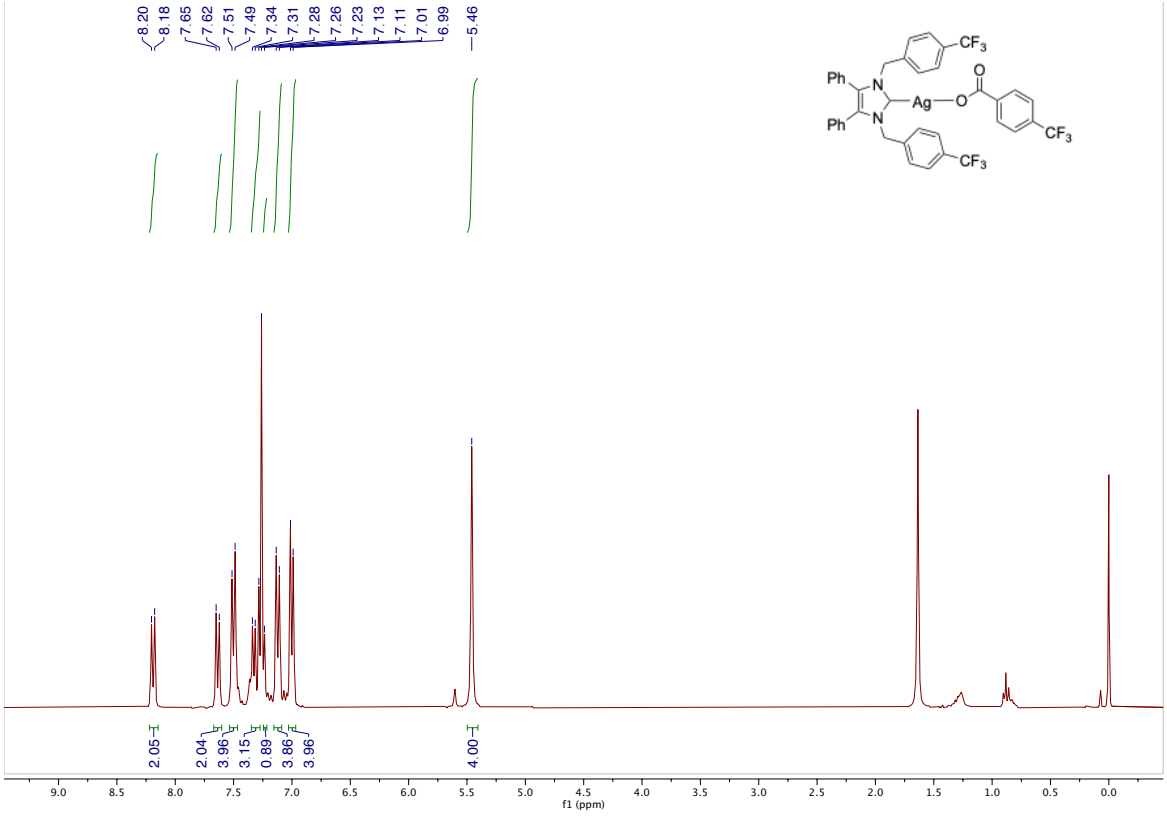

(**4c**) 1,3-Di(4-trifluoromethyl) benzyl-4,5-diphenylimidazol-2-ylidene silver (4-trifluoromethyl) benzoate ^{13}C NMR (101 MHz, $CDCl_3$)

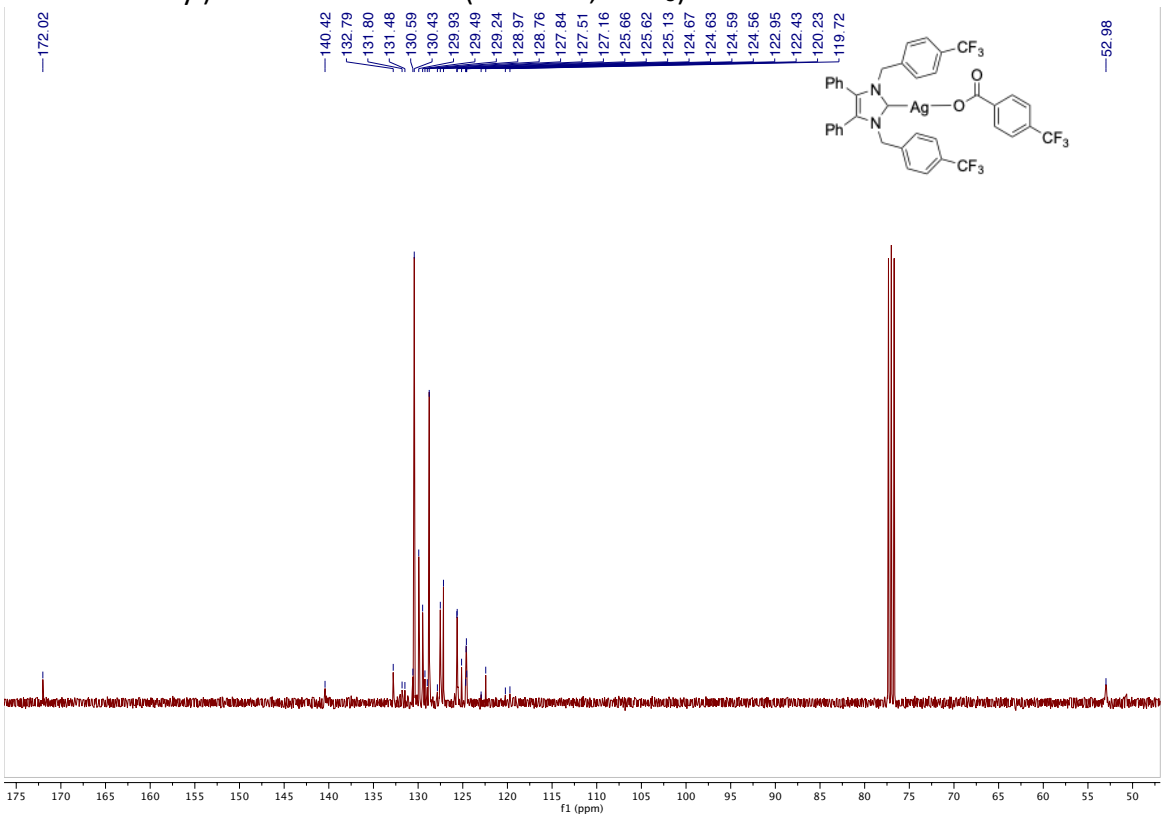

(**4c**) 1,3-Di(4-trifluoromethyl) benzyl-4,5-diphenylimidazol-2-ylidene silver (4-trifluoromethyl) benzoate ^{19}F NMR (376 MHz, $CDCl_3$)

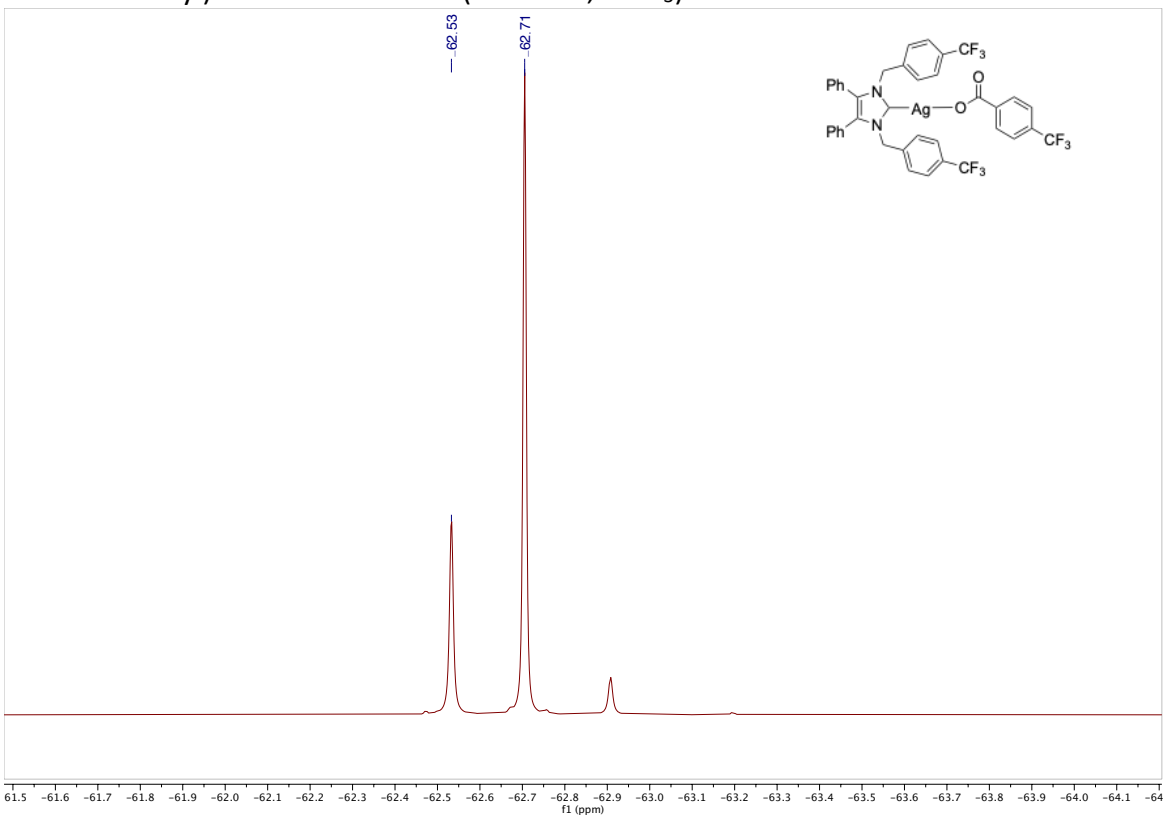

(**5**) Potassium *p*-trifluoromethylbenzoate ^{1}H NMR (400 MHz, DMSO-d_6)

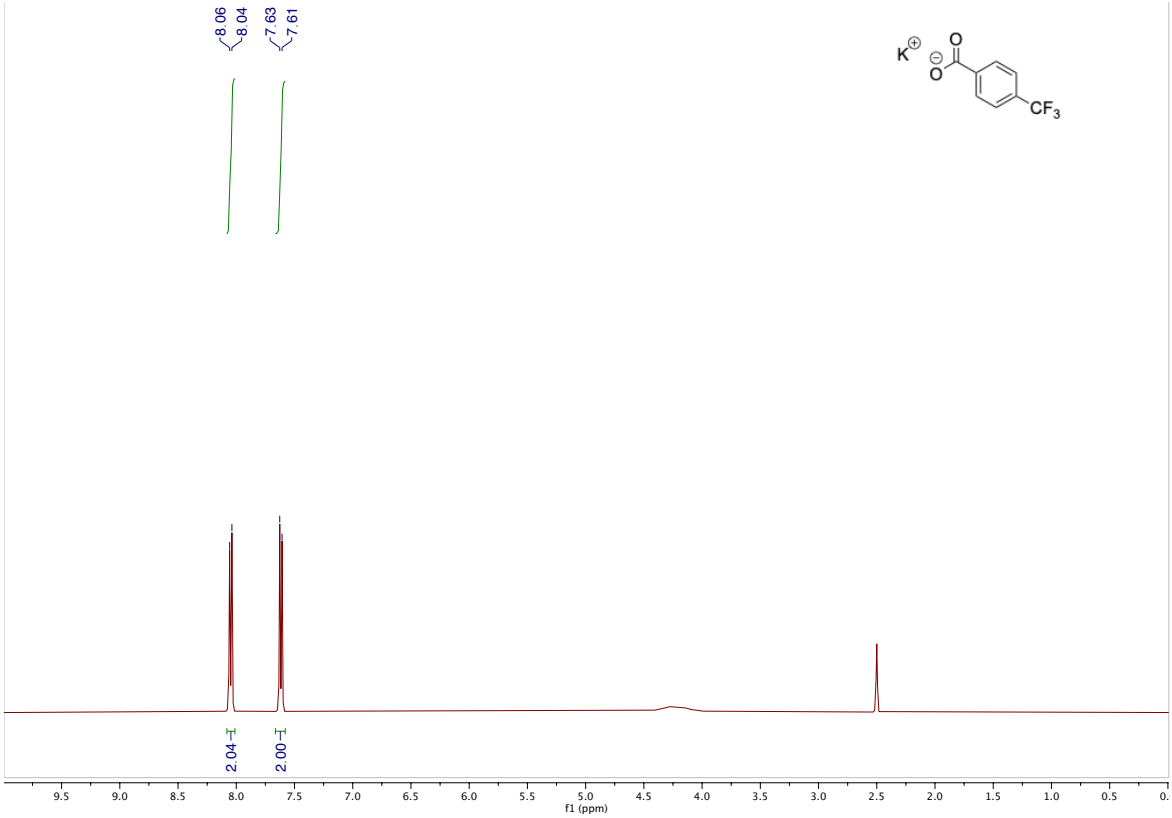

(**5**) Potassium *p*-trifluoromethylbenzoate ^{13}C NMR (101 MHz, DMSO-d_6)

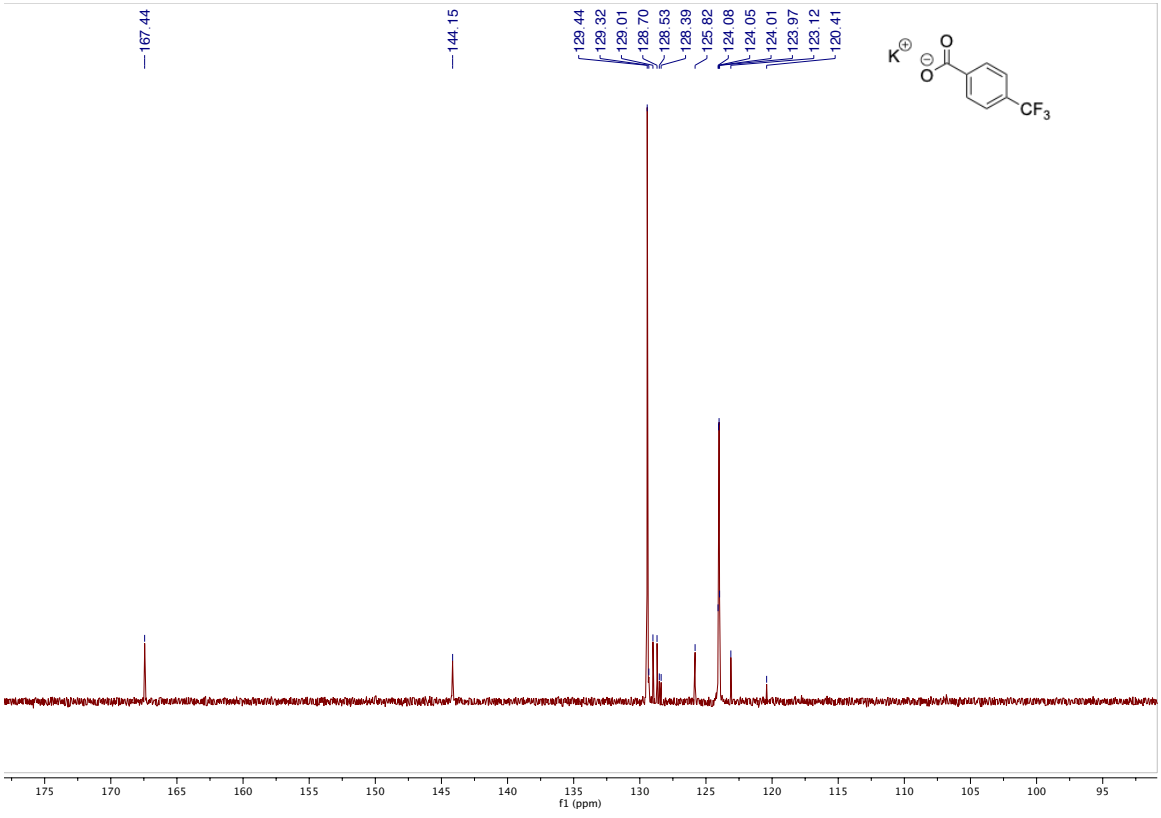

(**5**) Potassium *p*-trifluoromethylbenzoate ^{19}F NMR (376 MHz, DMSO-d_6)

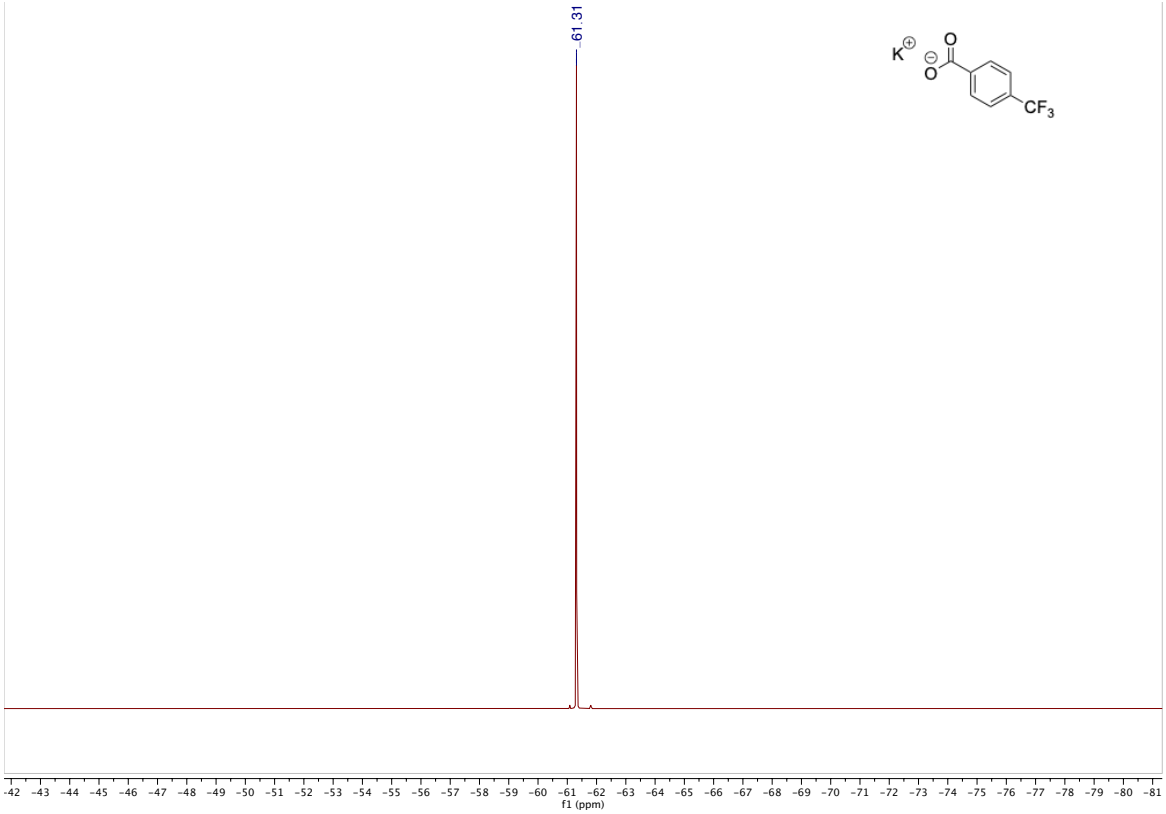

(**6a**) 1,3-Dibenzyl-4,5-diphenyl imidazolium (*p*-trifluoromethyl) benzoate ^{1}H NMR (400 MHz, DMSO-d_6)

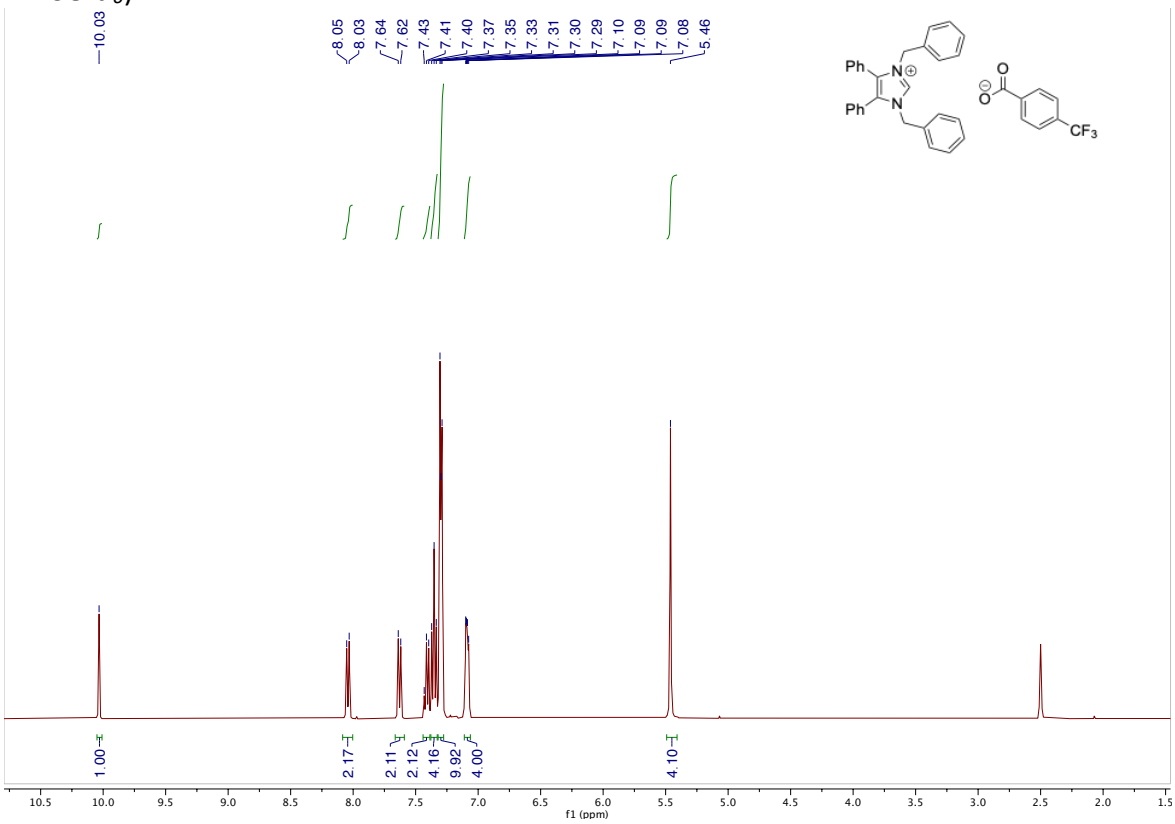

(**6a**) 1,3-Dibenzyl-4,5-diphenyl imidazolium (*p*-trifluoromethyl) benzoate ^{13}C NMR (101 MHz, DMSO-d_6)

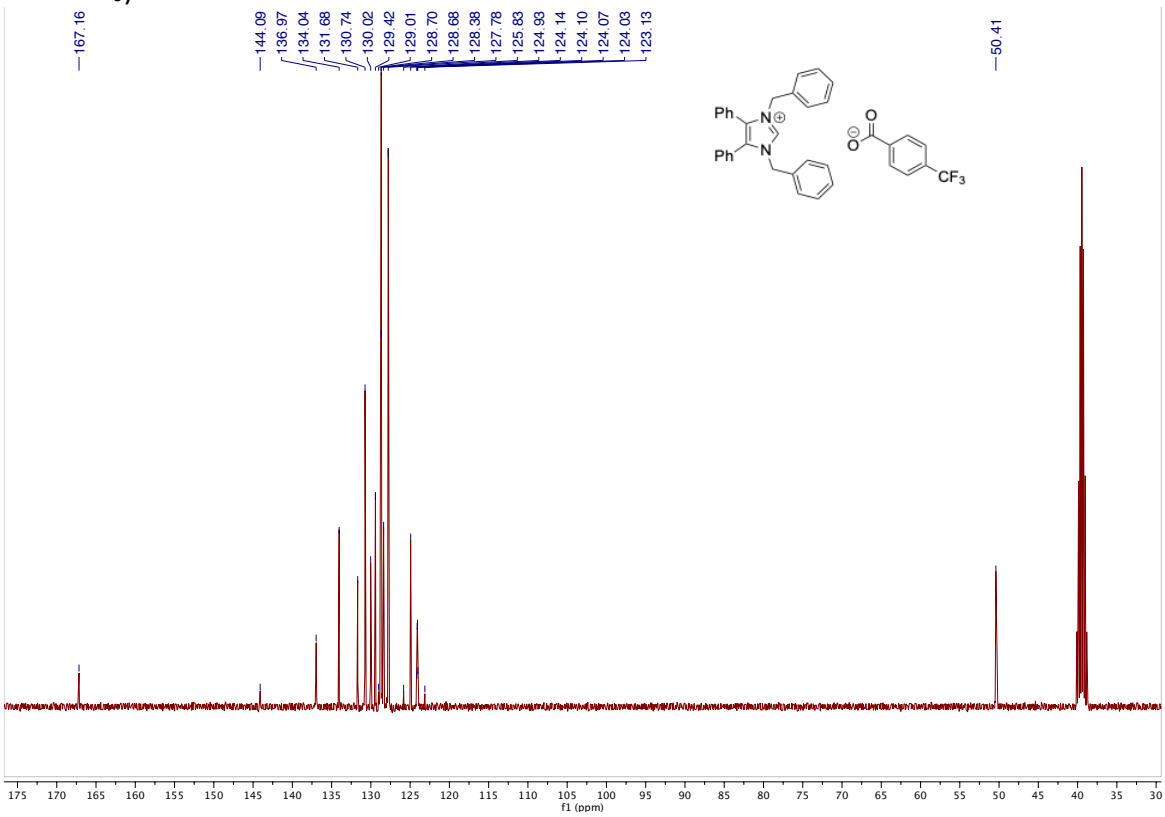

(**6a**) 1,3-Dibenzyl-4,5-diphenyl imidazolium (*p*-trifluoromethyl) benzoate ^{19}F NMR (376 MHz, DMSO-d_6)

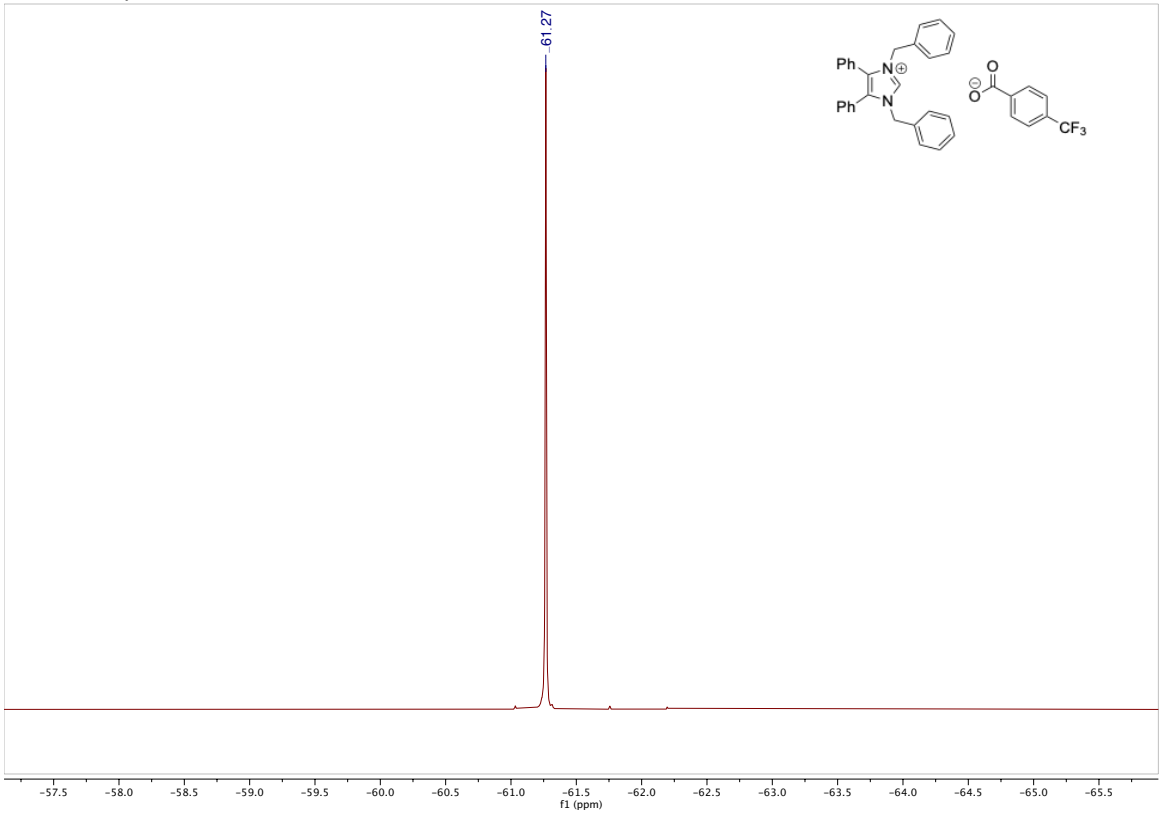

(**6b**) 1,3-Di(4-fluoro) benzyl-4,5-diphenyl imidazolium (*p*-trifluoromethyl) benzoate ^{1}H NMR (400 MHz, DMSO-d_6)

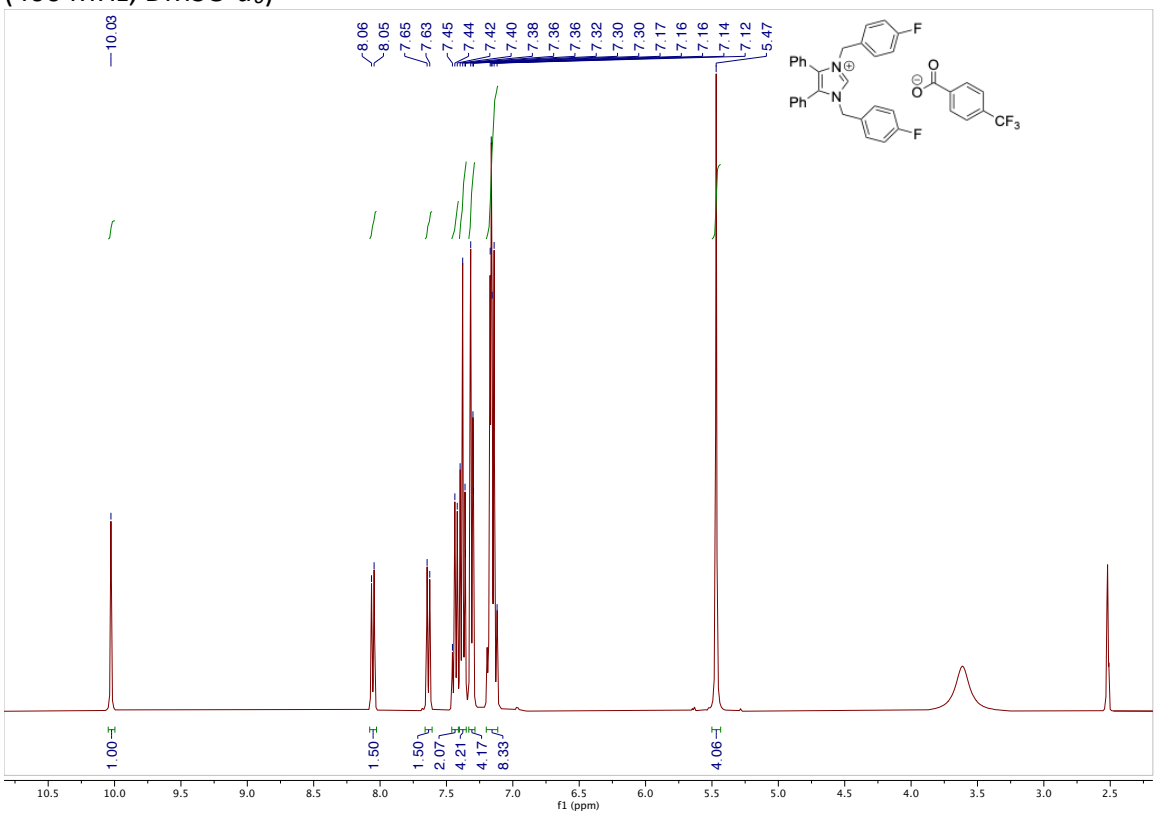

(**6b**) 1,3-Di(4-fluoro) benzyl-4,5-diphenyl imidazolium (*p*-trifluoromethyl) benzoate ^{13}C NMR (101 MHz, DMSO-d_6)

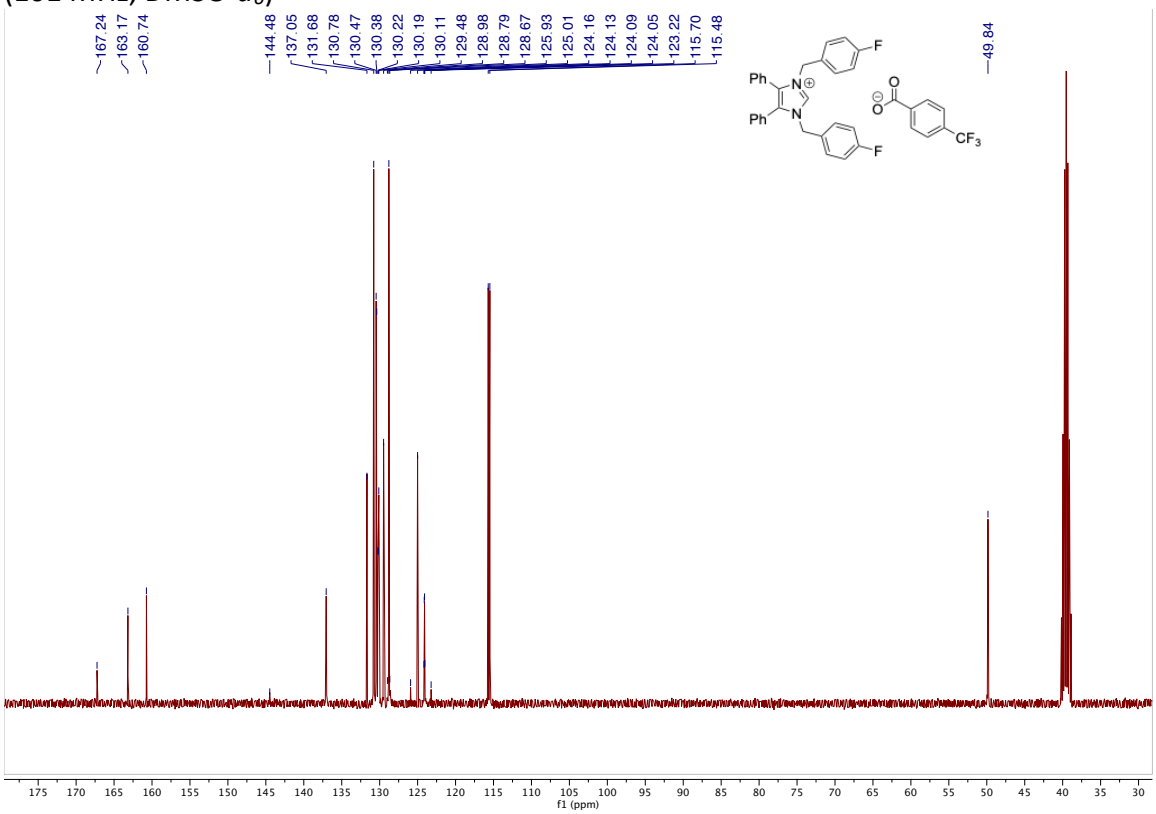

(**6b**) 1,3-Di(4-fluoro) benzyl-4,5-diphenyl imidazolium (*p*-trifluoromethyl) benzoate ^{19}F NMR (376 MHz, DMSO-d_6)

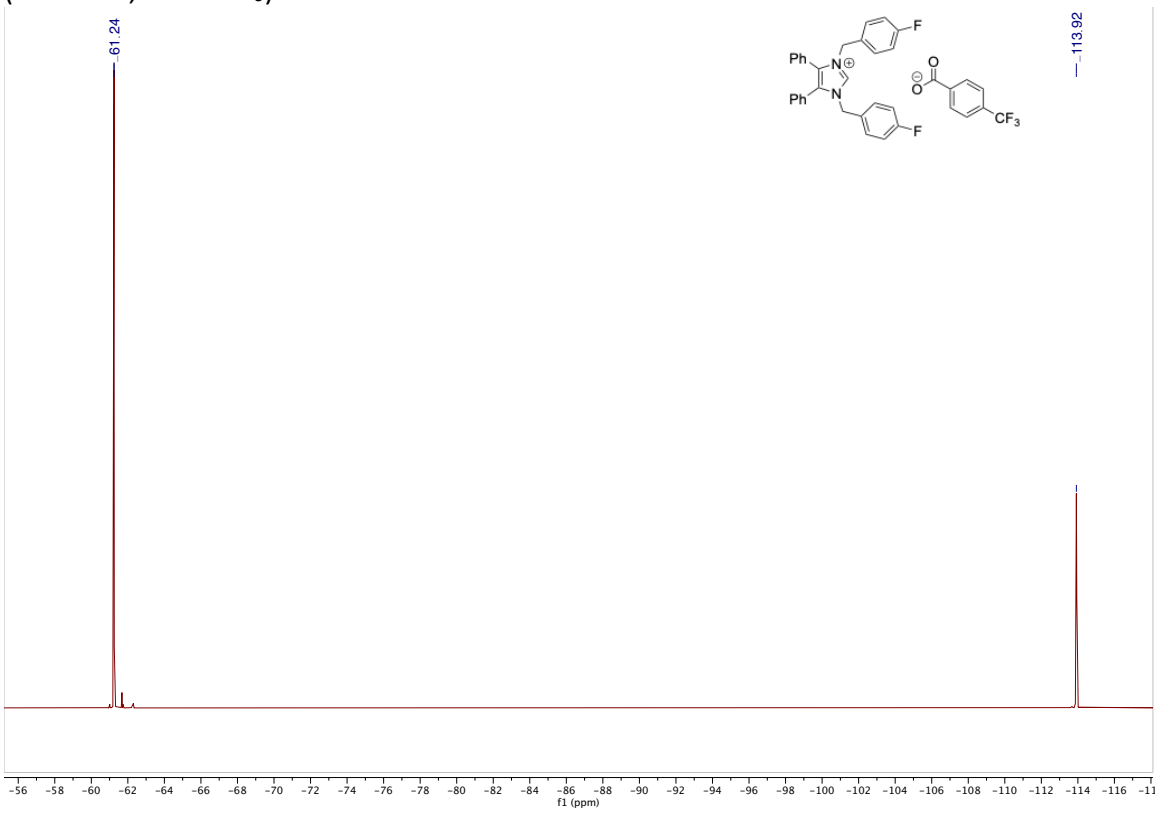

(**6c**) 4,5-Diphenyl-1,3-di(*p*-trifluoromethyl) benzyl imidazolium (*p*-trifluoromethyl) benzoate ^{1}H NMR (400 MHz, DMSO-d_6)

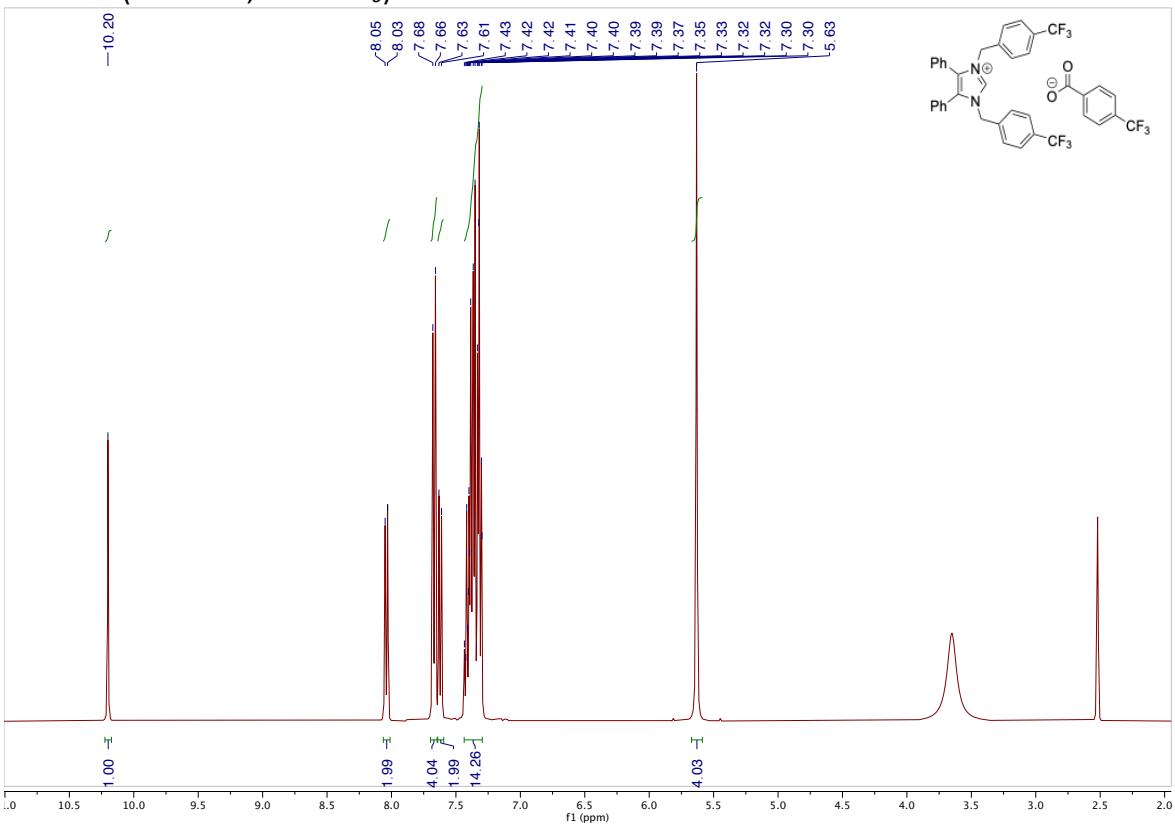

(**6c**) 4,5-Diphenyl-1,3-di(*p*-trifluoromethyl) benzyl imidazolium (*p*-trifluoromethyl) benzoate ^{13}C NMR (101 MHz, DMSO-d_6)

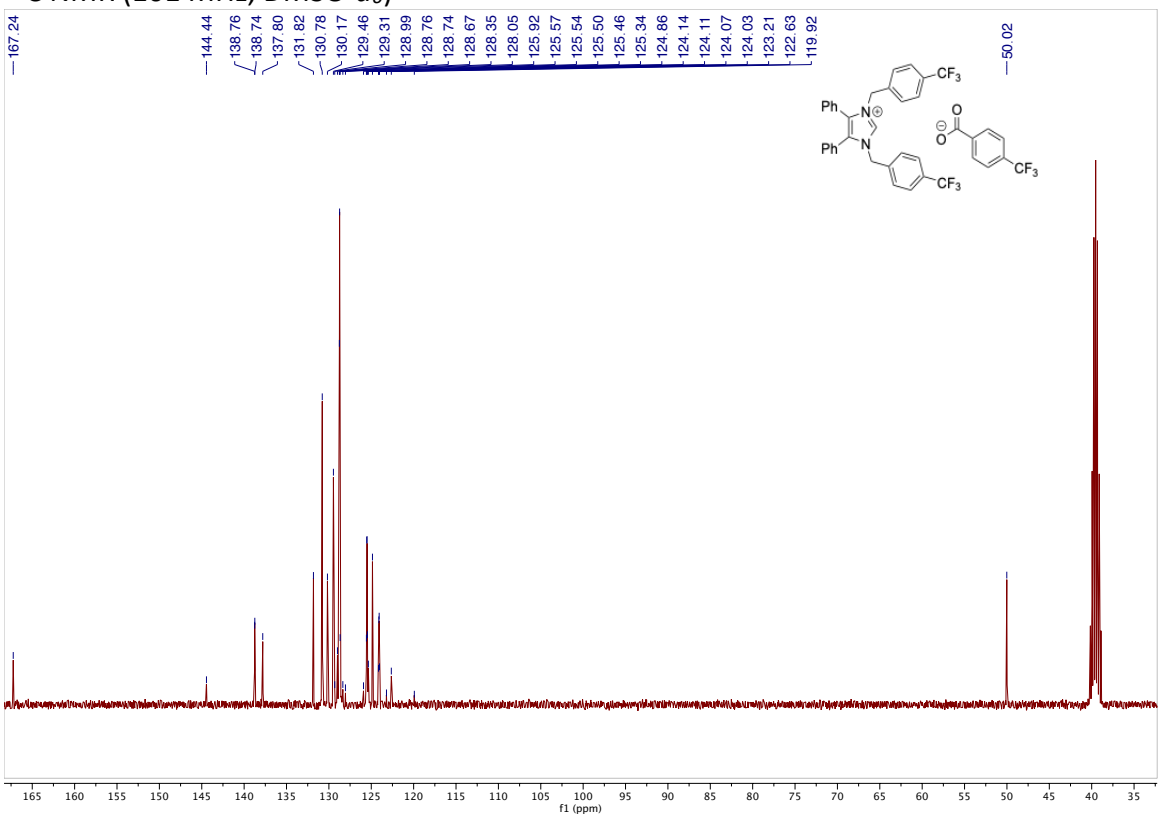

(**6c**) 4,5-Diphenyl-1,3-di(*p*-trifluoromethyl) benzyl imidazolium (*p*-trifluoromethyl) benzoate ^{19}F NMR (376 MHz, DMSO-d_6)

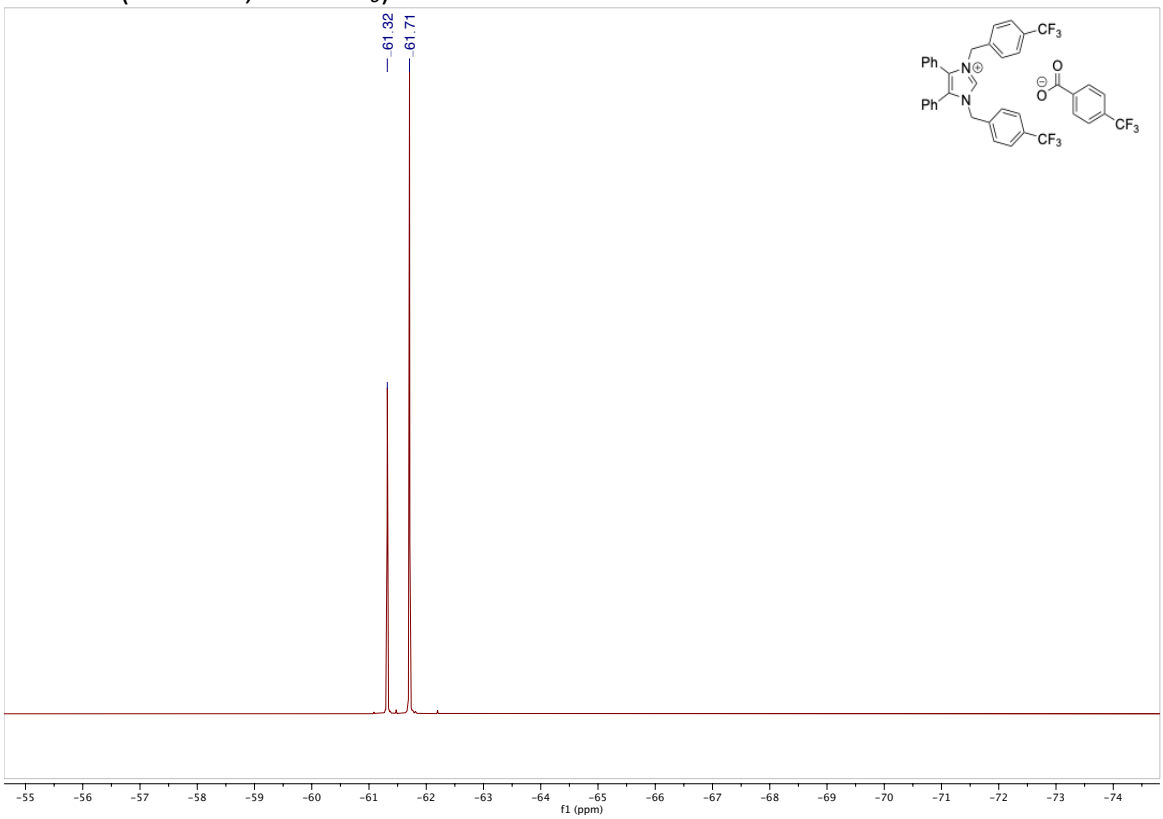

(**7a**) 1,3-Dibenzyl-4,5-diphenyl imidazolium hexafluorophosphate ^{1}H NMR (400 MHz, $CDCl_3$)

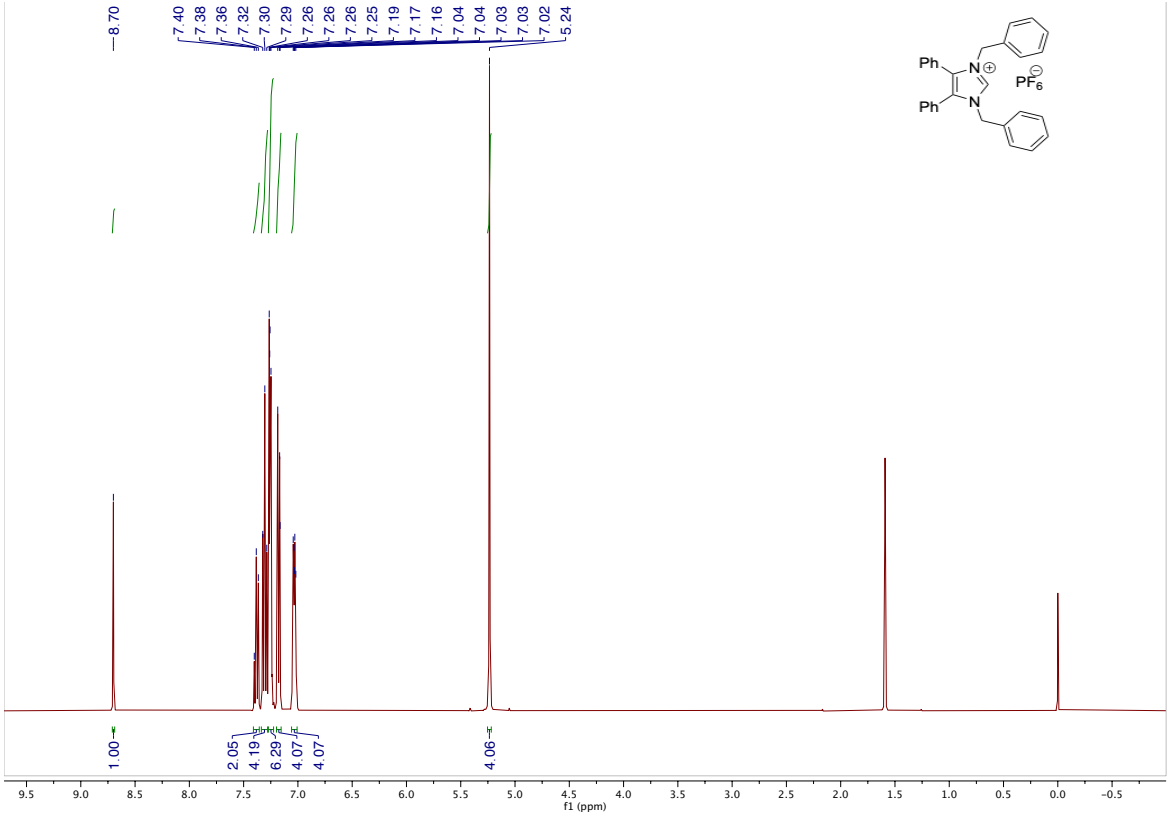

(**7a**) 1,3-Dibenzyl-4,5-diphenyl imidazolium hexafluorophosphate ^{13}C NMR (101 MHz, $CDCl_3$)

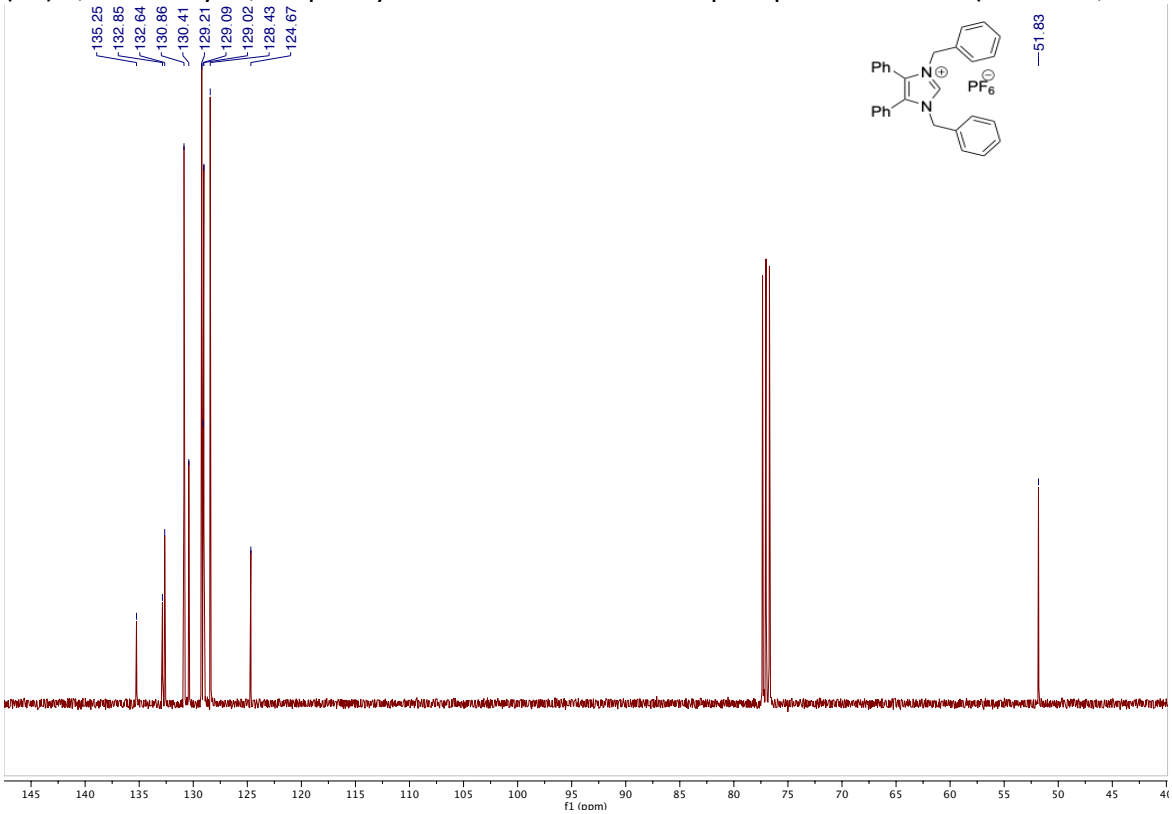

(**7a**) 1,3-Dibenzyl-4,5-diphenyl imidazolium hexafluorophosphate ^{19}F NMR: (376 MHz, $CDCl_3$)

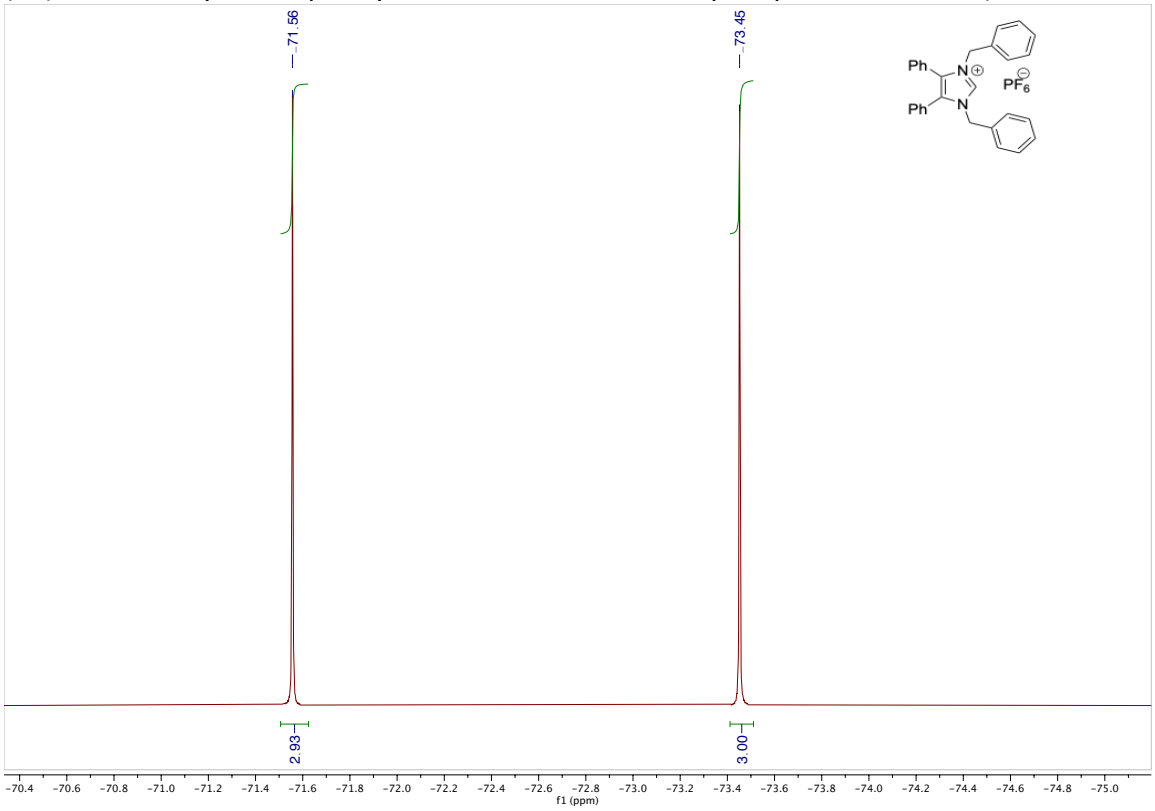

(**7b**) 1,3-Di(*p*-fluoro) benzyl-4,5-diphenyl imidazolium hexafluorophosphate ^{1}H NMR (101 MHz, $CDCl_3$)

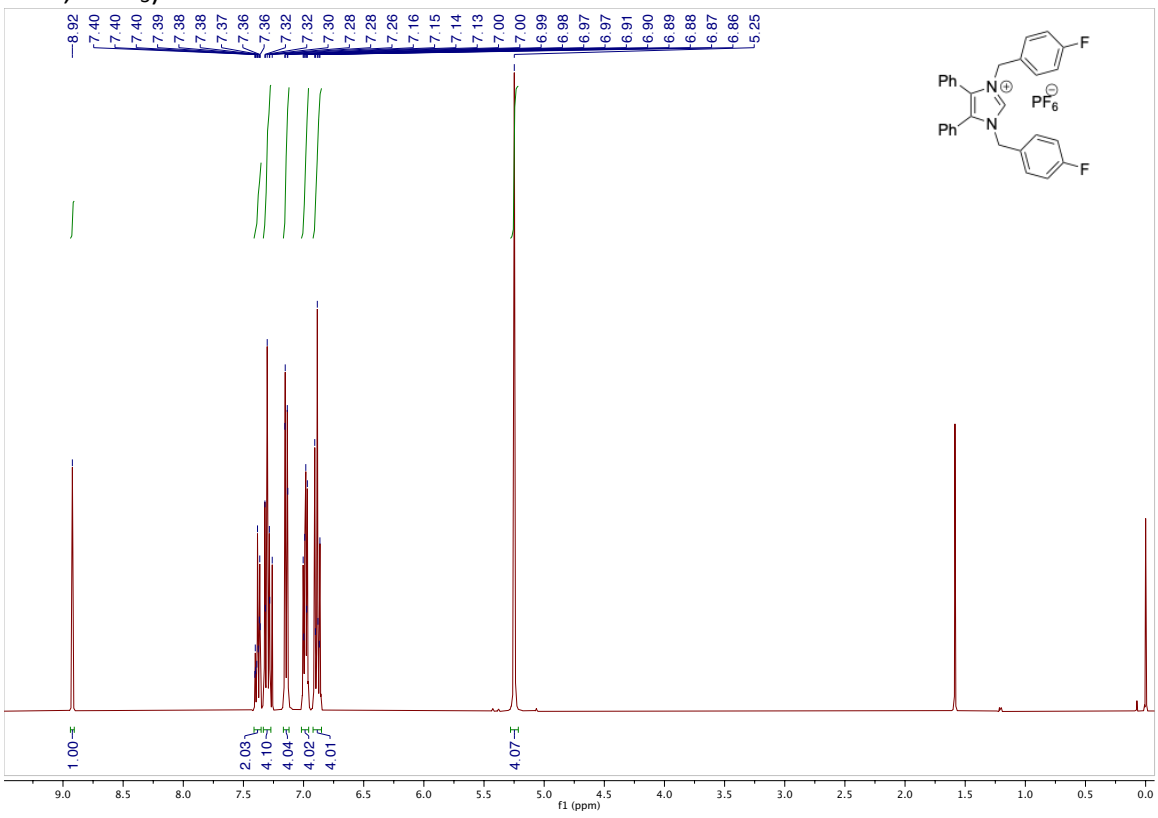

(**7b**) 1,3-Di(*p*-fluoro) benzyl-4,5-diphenyl imidazolium hexafluorophosphate ^{13}C NMR (101 MHz, $CDCl_3$)

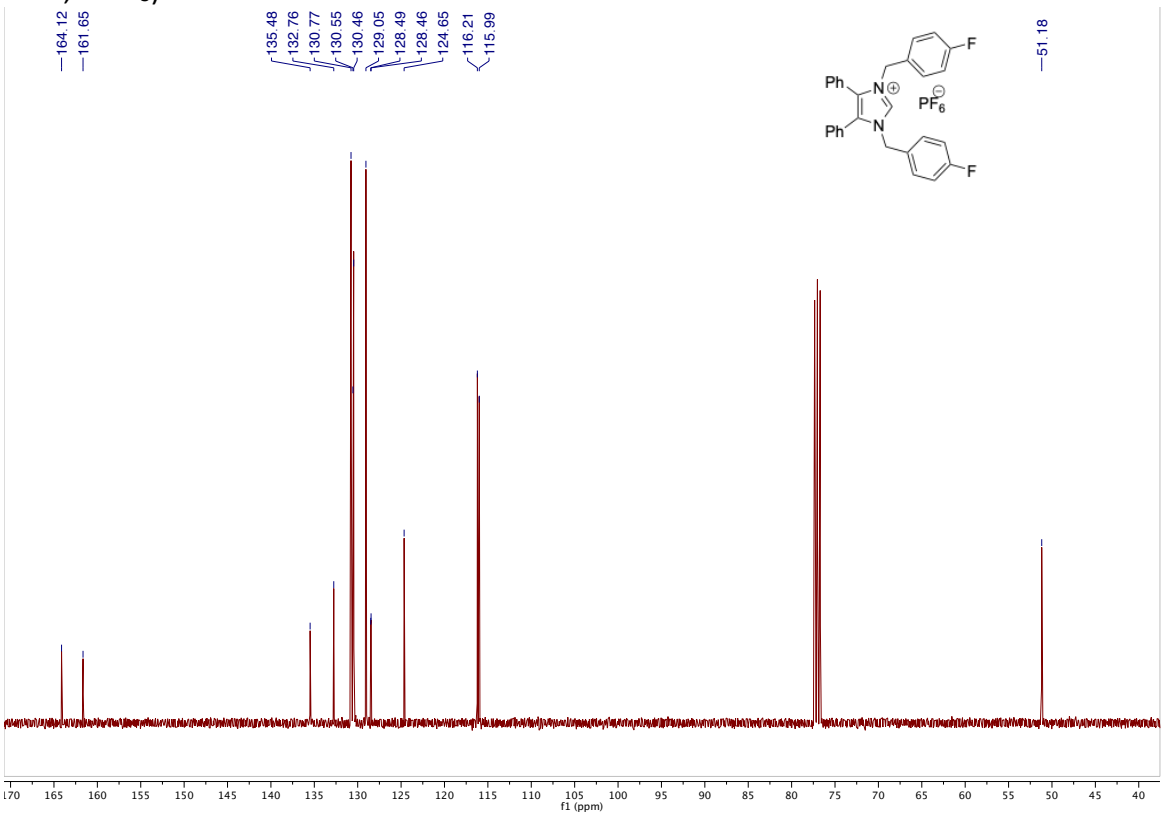

(**7b**) 1,3-Di(*p*-fluoro) benzyl-4,5-diphenyl imidazolium hexafluorophosphate ^{19}F NMR (376 MHz, $CDCl_3$)

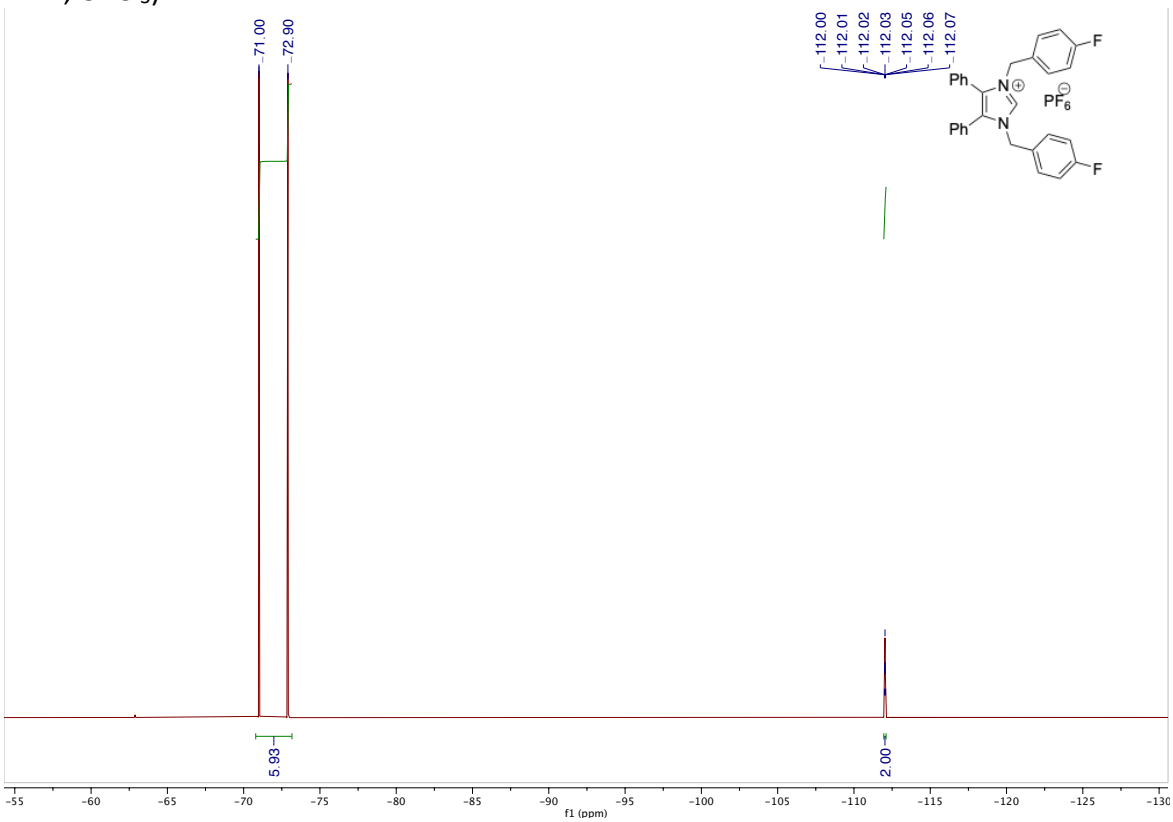

(**7c**) 1,3-Di(*p*-trifluoromethyl) benzyl-4,5-diphenyl imidazolium hexafluorophosphate ^{1}H NMR (400 MHz, $CDCl_3$)

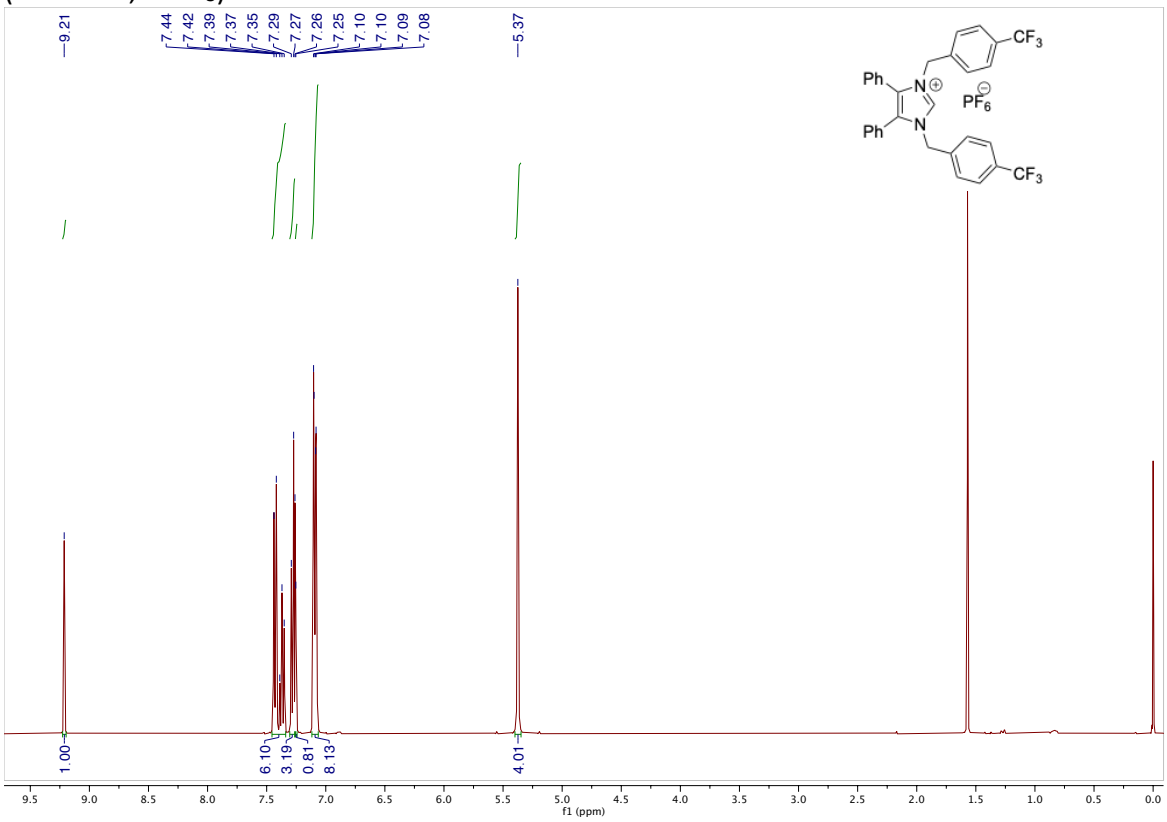

(**7c**) 1,3-Di(*p*-trifluoromethyl) benzyl-4,5-diphenyl imidazolium hexafluorophosphate ^{13}C NMR (101 MHz, $CDCl_3$)

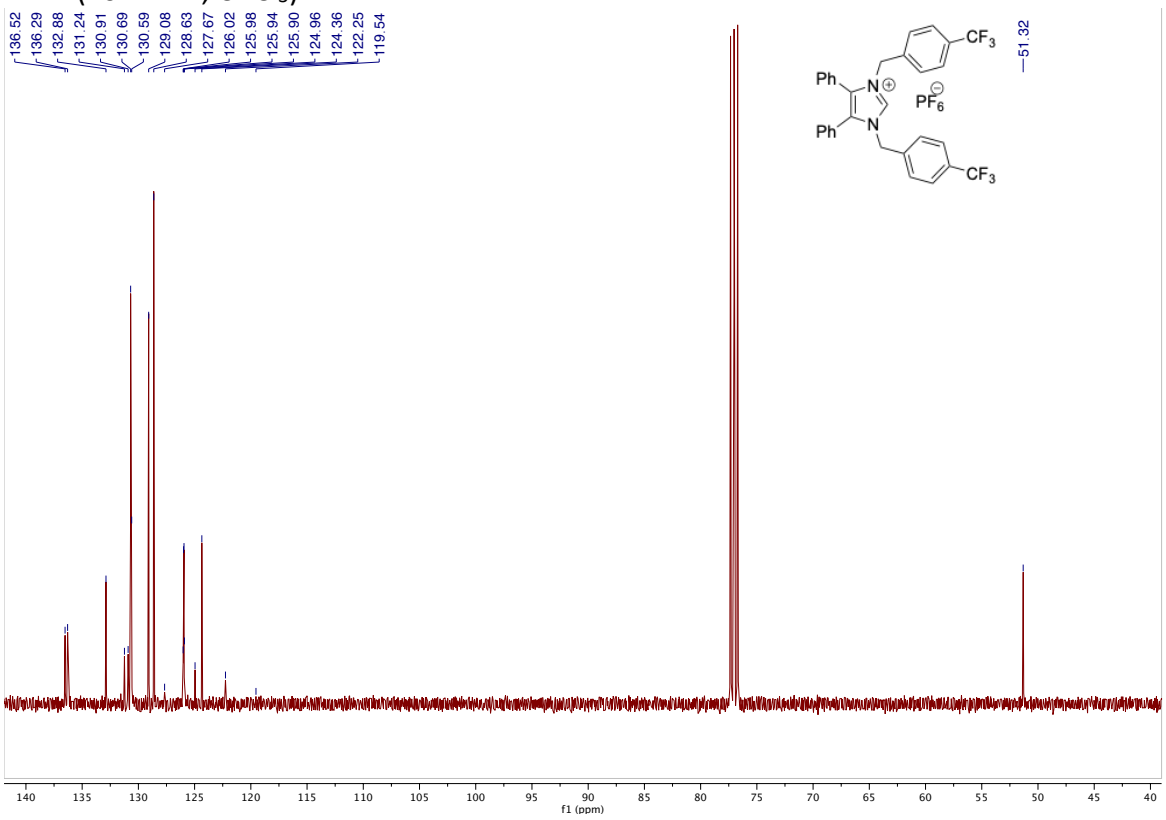

(**7c**) 1,3-Di(*p*-trifluoromethyl) benzyl-4,5-diphenyl imidazolium hexafluorophosphate ^{19}F NMR (376 MHz, $CDCl_3$)

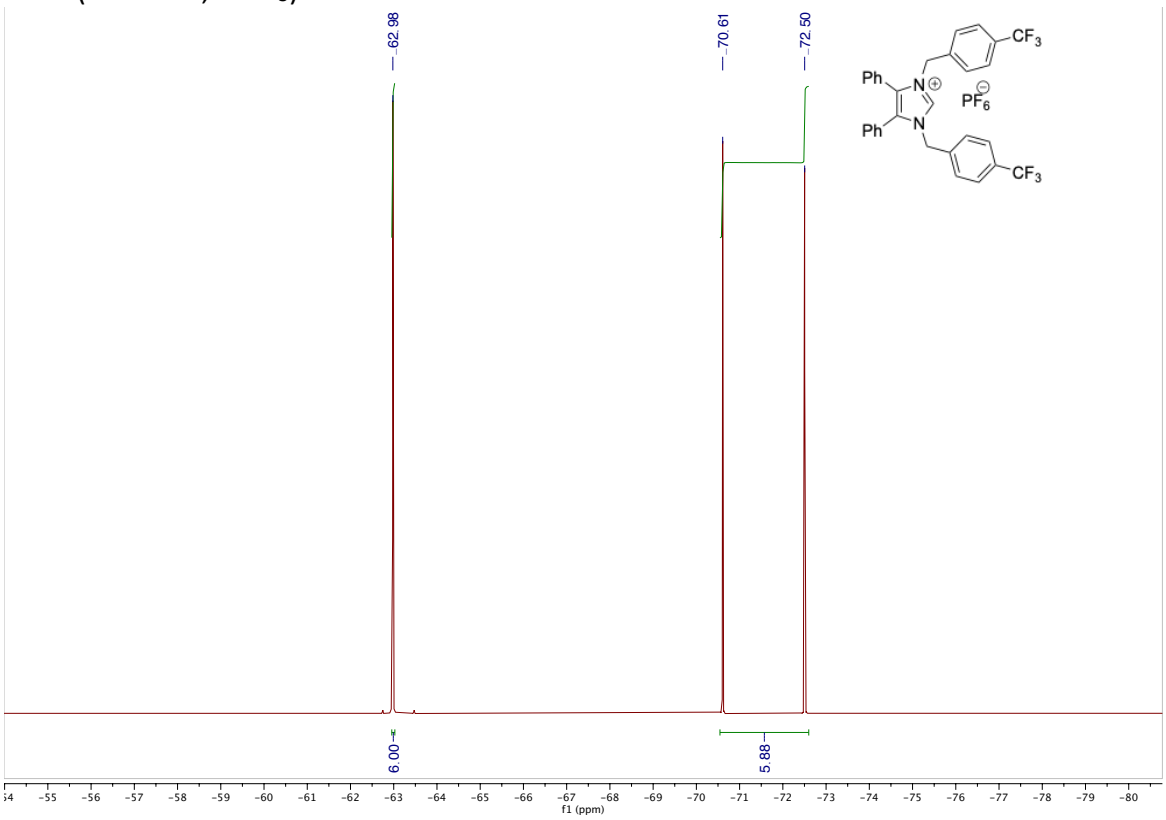

(**8a**) 1,3-Dibenzyl-4,5-diphenyl imidazolium tetrafluoroborate ^1H NMR (400 MHz, $CDCl_3$)

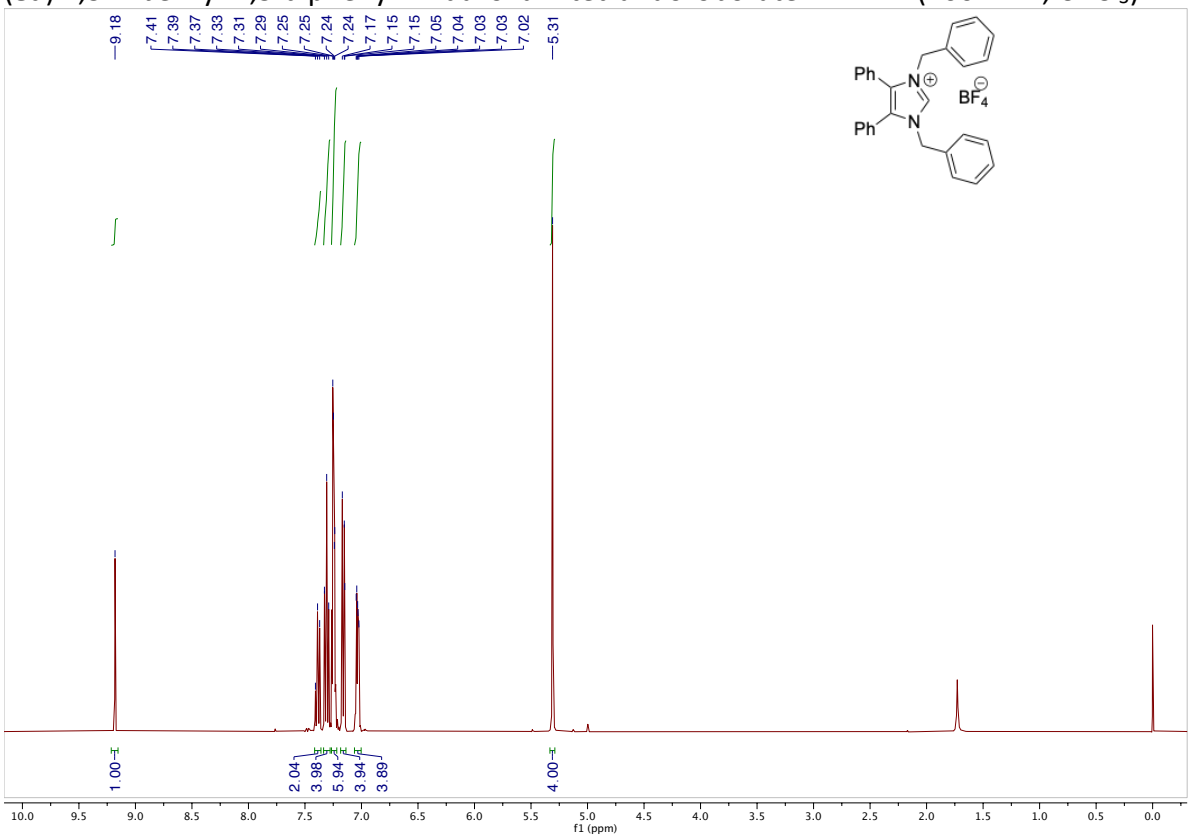

(**8a**) 1,3-Dibenzyl-4,5-diphenyl imidazolium tetrafluoroborate ^{13}C NMR (101 MHz, $CDCl_3$)

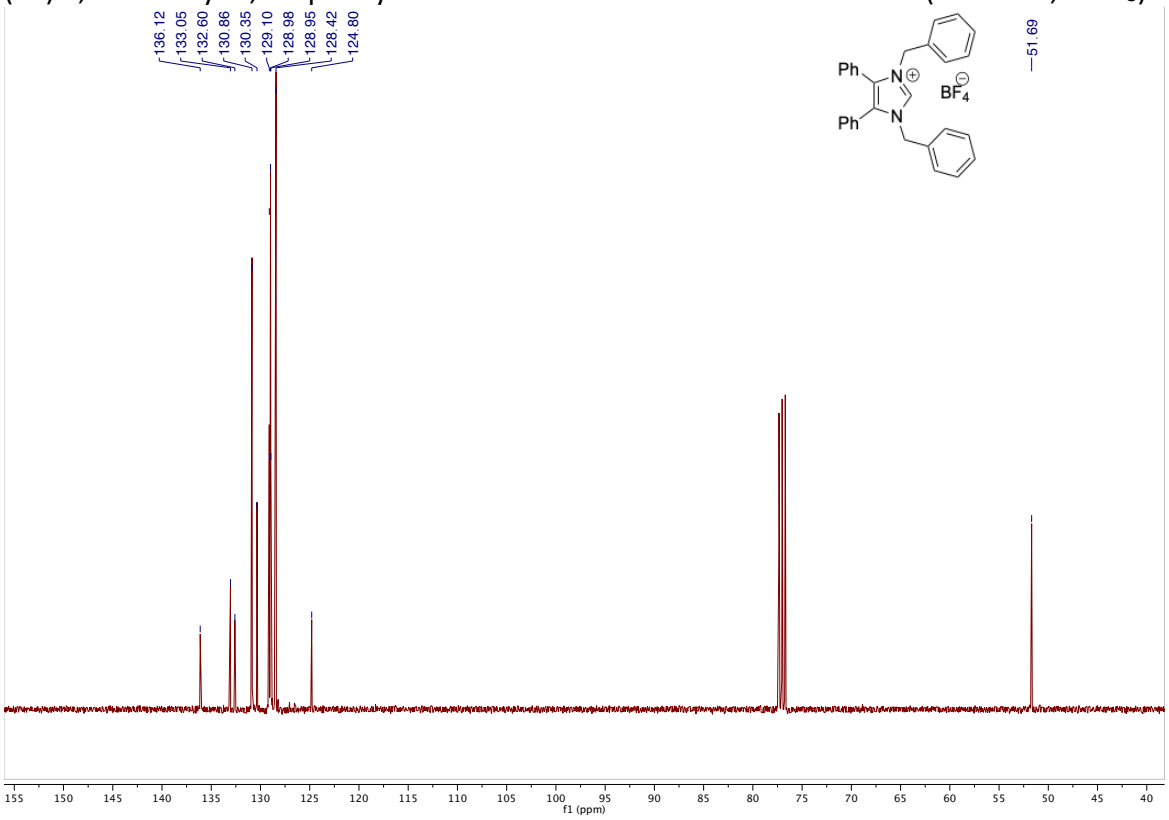

(**8a**) 1,3-Dibenzyl-4,5-diphenyl imidazolium tetrafluoroborate ^{19}F NMR (376 MHz, $CDCl_3$)

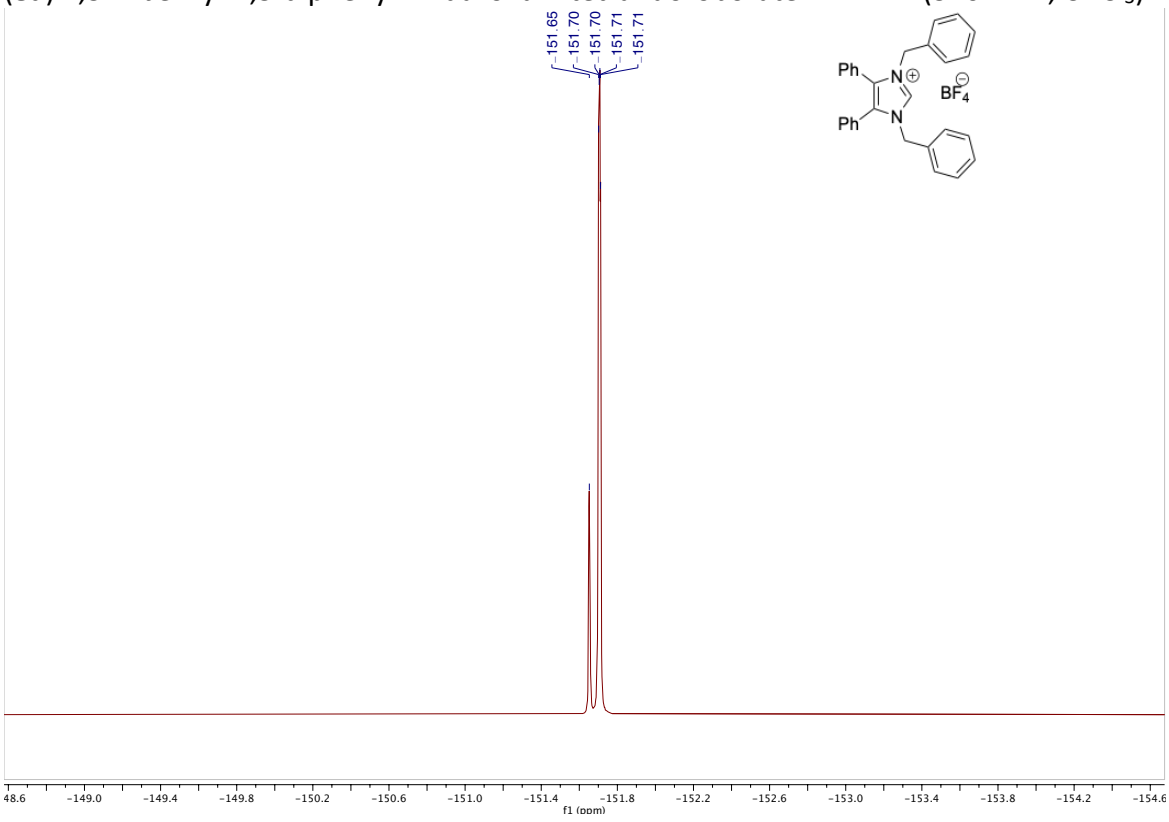

(**8b**) 1,3-Di(*p*-fluoro) benzyl-4,5-diphenyl imidazolium tetrafluoroborate ^{1}H NMR (400 MHz, $CDCl_3$)

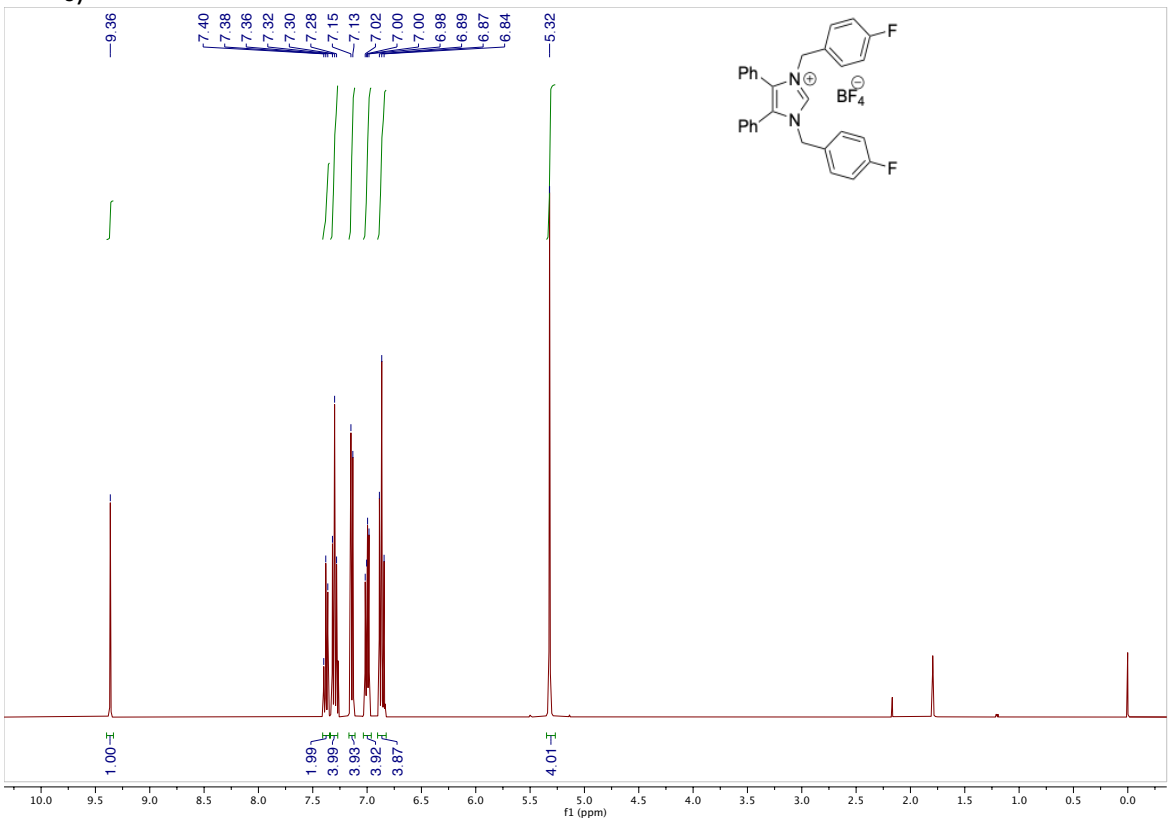

(**8b**) 1,3-Di(*p*-fluoro) benzyl-4,5-diphenyl imidazolium tetrafluoroborate ^{13}C NMR (101 MHz, $CDCl_3$)

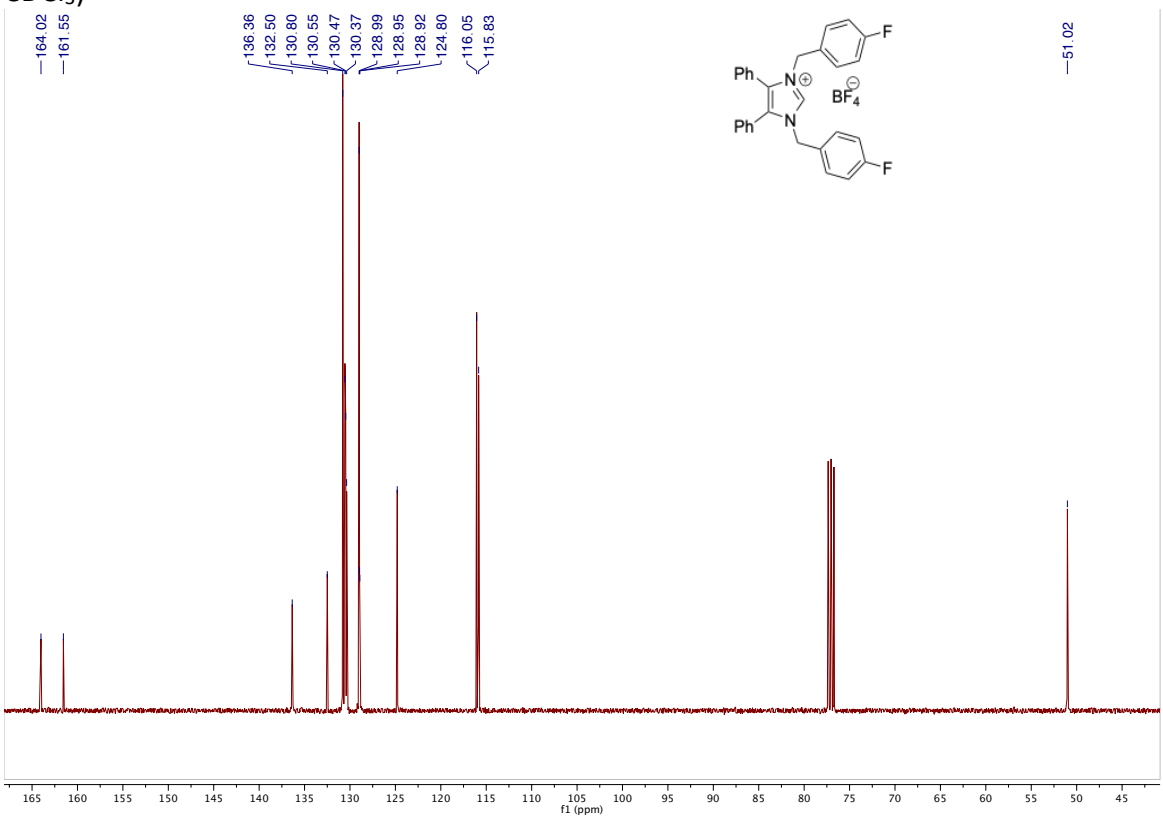

(**8b**) 1,3-Di(*p*-fluoro) benzyl-4,5-diphenyl imidazolium tetrafluoroborate ^{19}F NMR (376 MHz, $CDCl_3$)

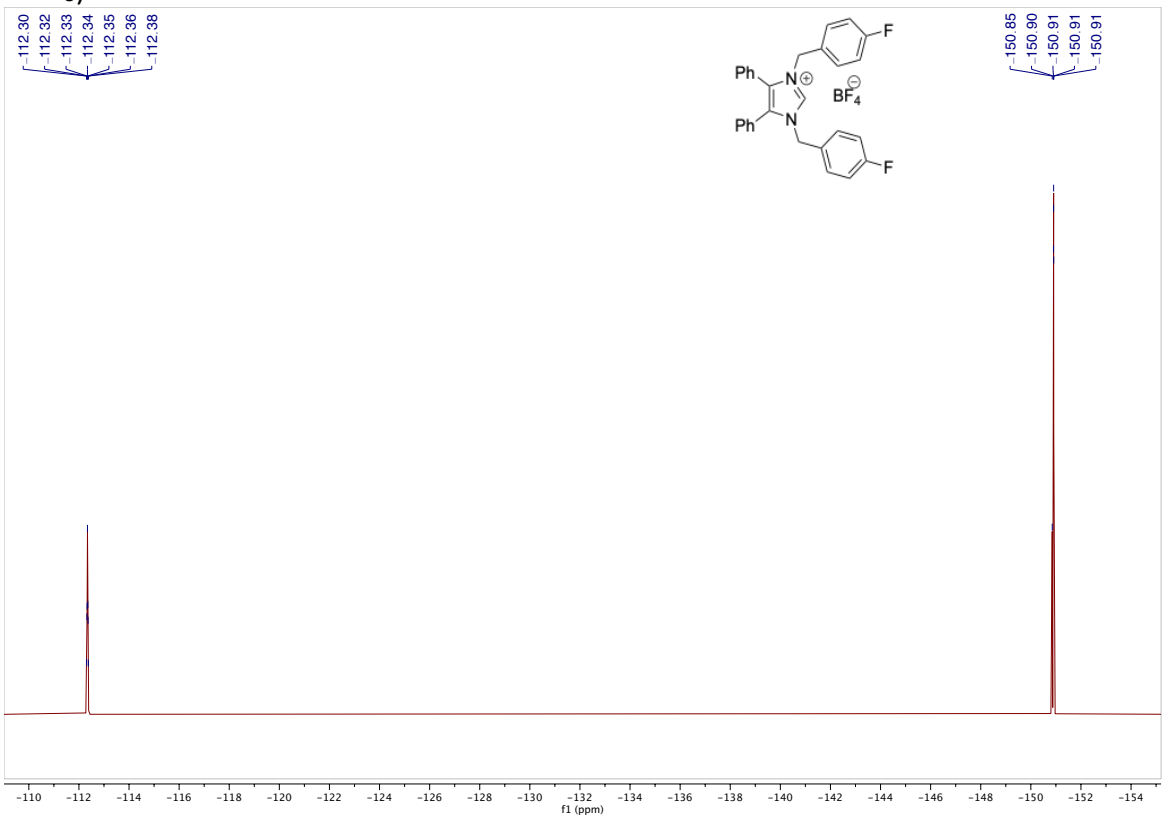

(**8c**) 1,3-Di(*p*-trifluoromethyl) benzyl-4,5-diphenyl imidazolium tetrafluoroborate ^{1}H NMR (400 MHz, $CDCl_3$)

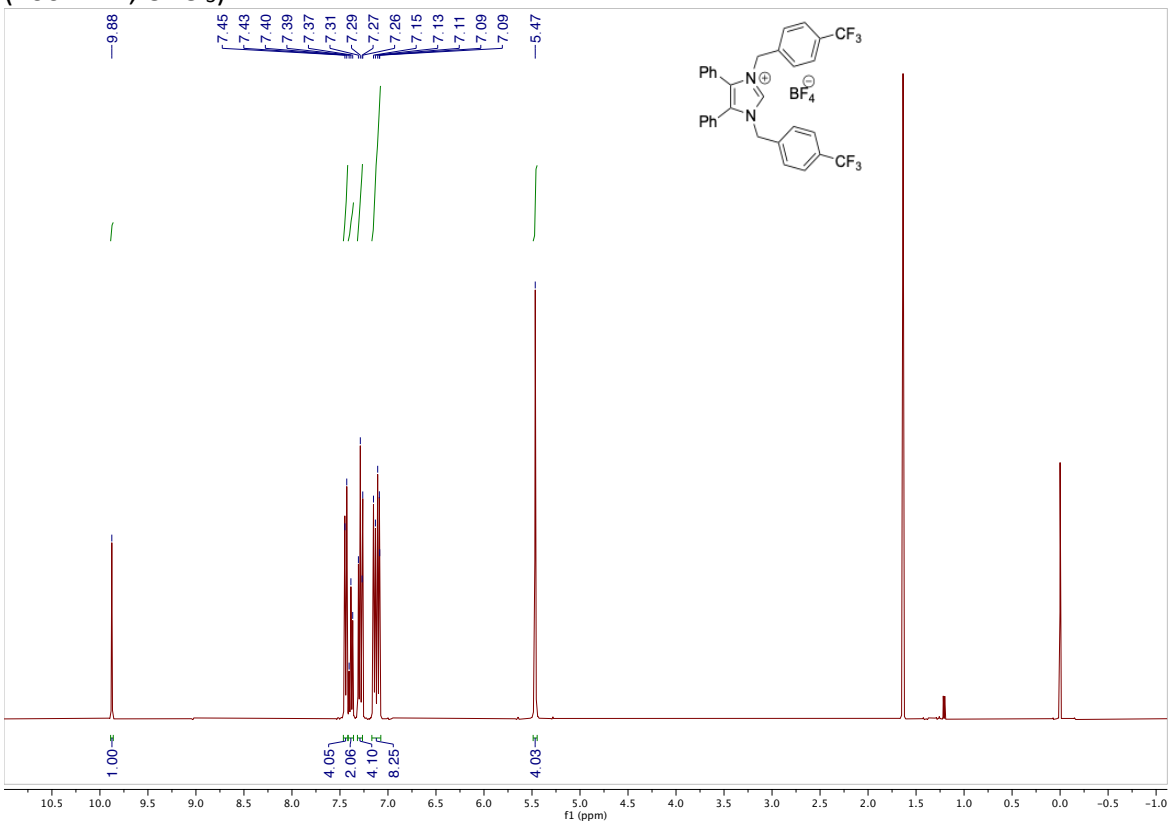

(**8c**) 1,3-Di(*p*-trifluoromethyl) benzyl-4,5-diphenyl imidazolium tetrafluoroborate ^{13}C NMR (101 MHz, $CDCl_3$)

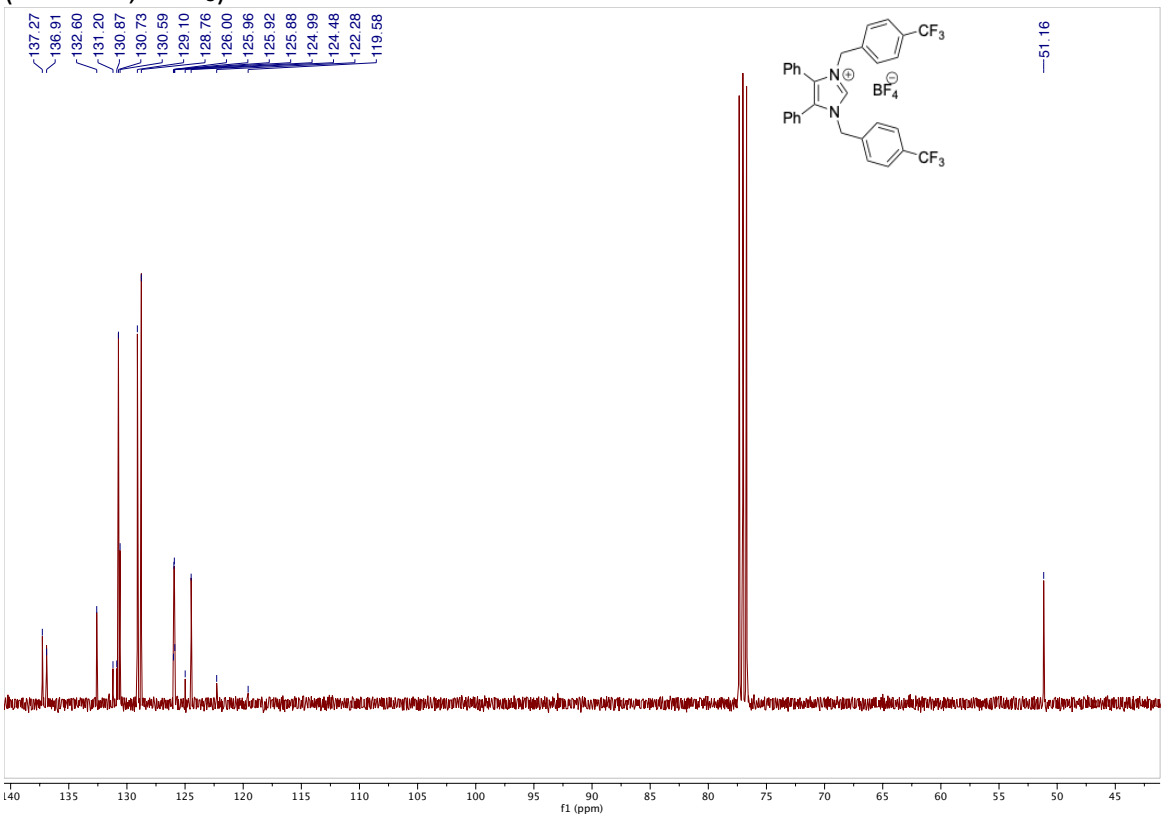

(**8c**) 1,3-Di(*p*-trifluoromethyl) benzyl-4,5-diphenyl imidazolium tetrafluoroborate ^{19}F NMR (376 MHz, $CDCl_3$)

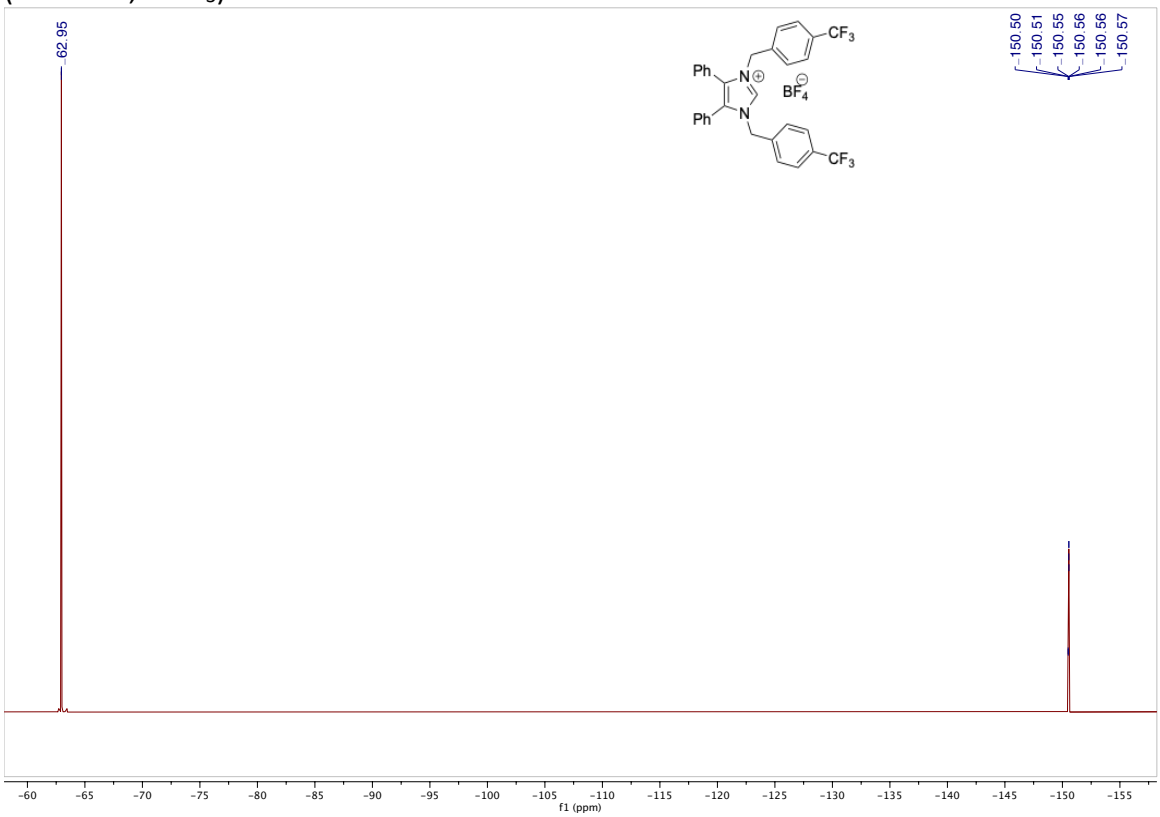

(**9a**) *Bis*-(1,3-dibenzyl-4,5-diphenyl imidazol-2-ylidene) silver (I) hexafluorophosphate ^{1}H NMR (400 MHz, DMSO-d_6)

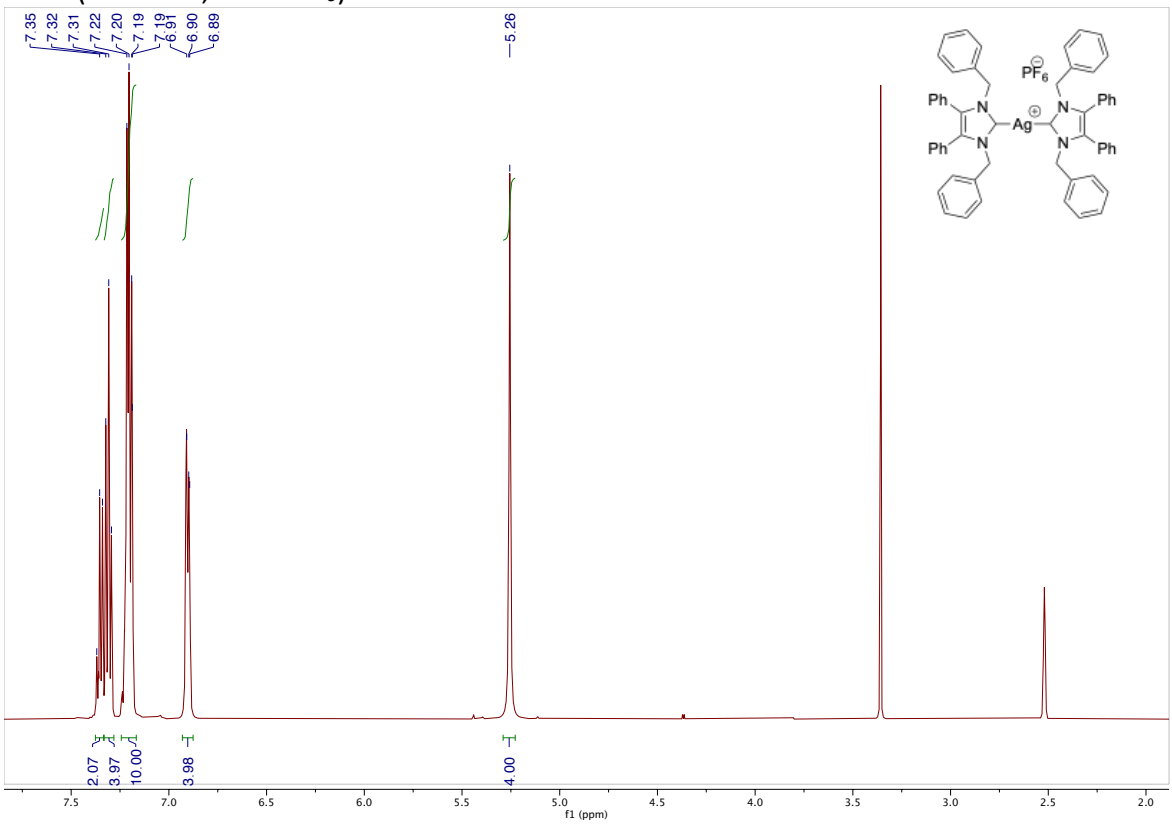

(**9a**) *Bis*-(1,3-dibenzyl-4,5-diphenyl imidazol-2-ylidene) silver (I) hexafluorophosphate ^{13}C NMR (126 MHz, DMSO-d_6)

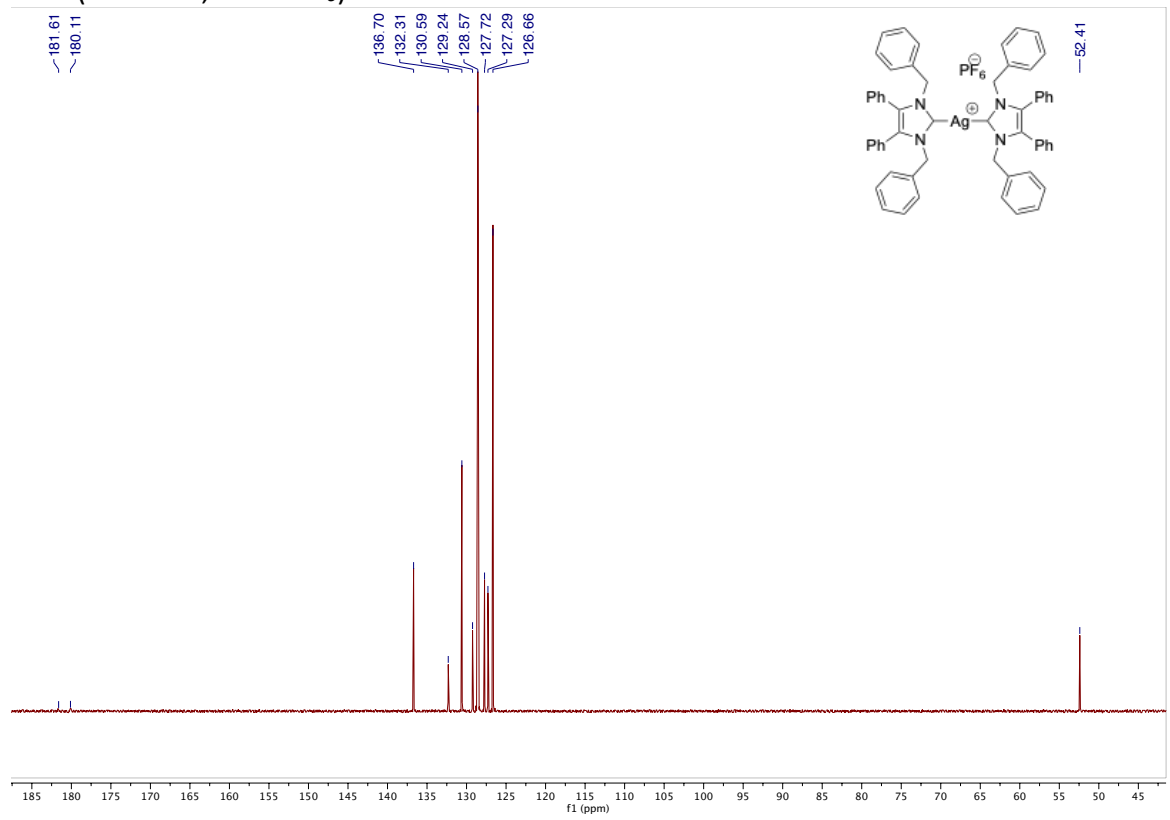

(**9a**) *Bis*-(1,3-dibenzyl-4,5-diphenyl imidazol-2-ylidene) silver (I) hexafluorophosphate ^{19}F NMR (376 MHz, DMSO-d_6)

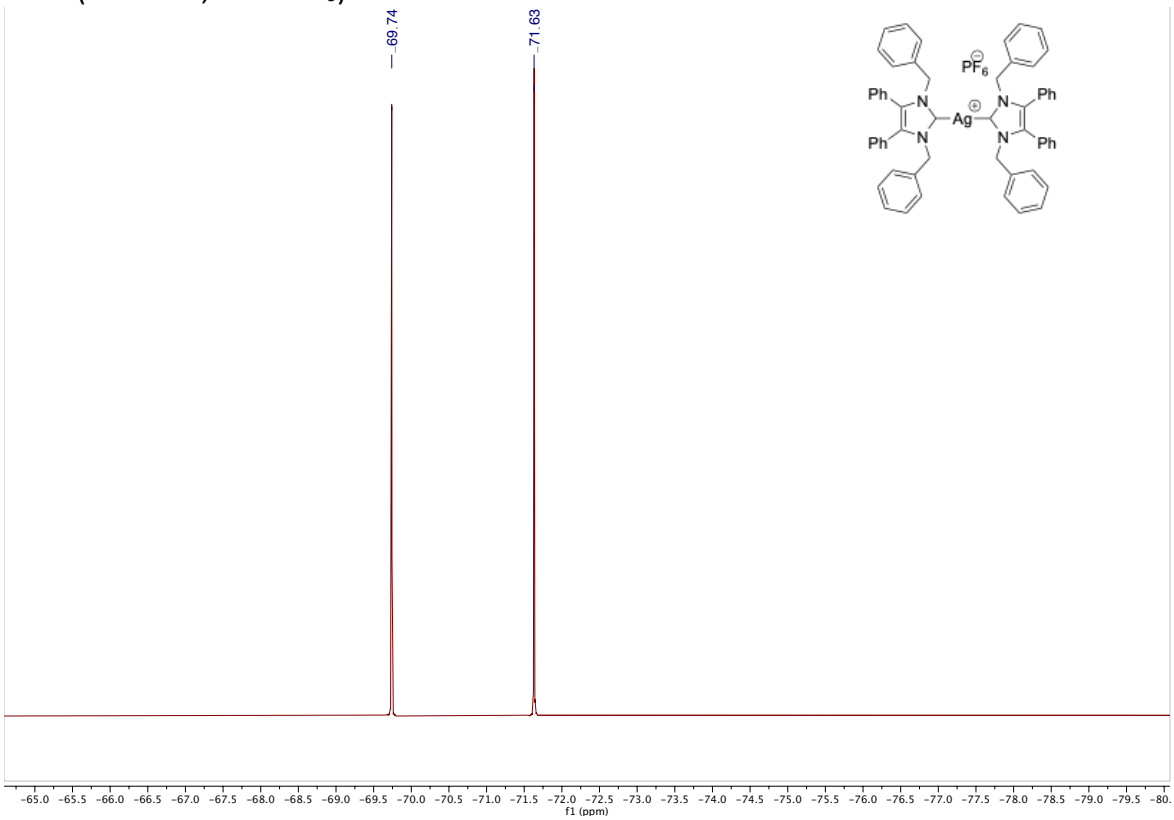

(**9b**) *Bis*-(1,3-di(*p*-fluoro) benzyl-4,5-diphenyl imidazol-2-ylidene) silver (I) hexafluorophosphate ^{1}H NMR (400 MHz, DMSO-d_6)

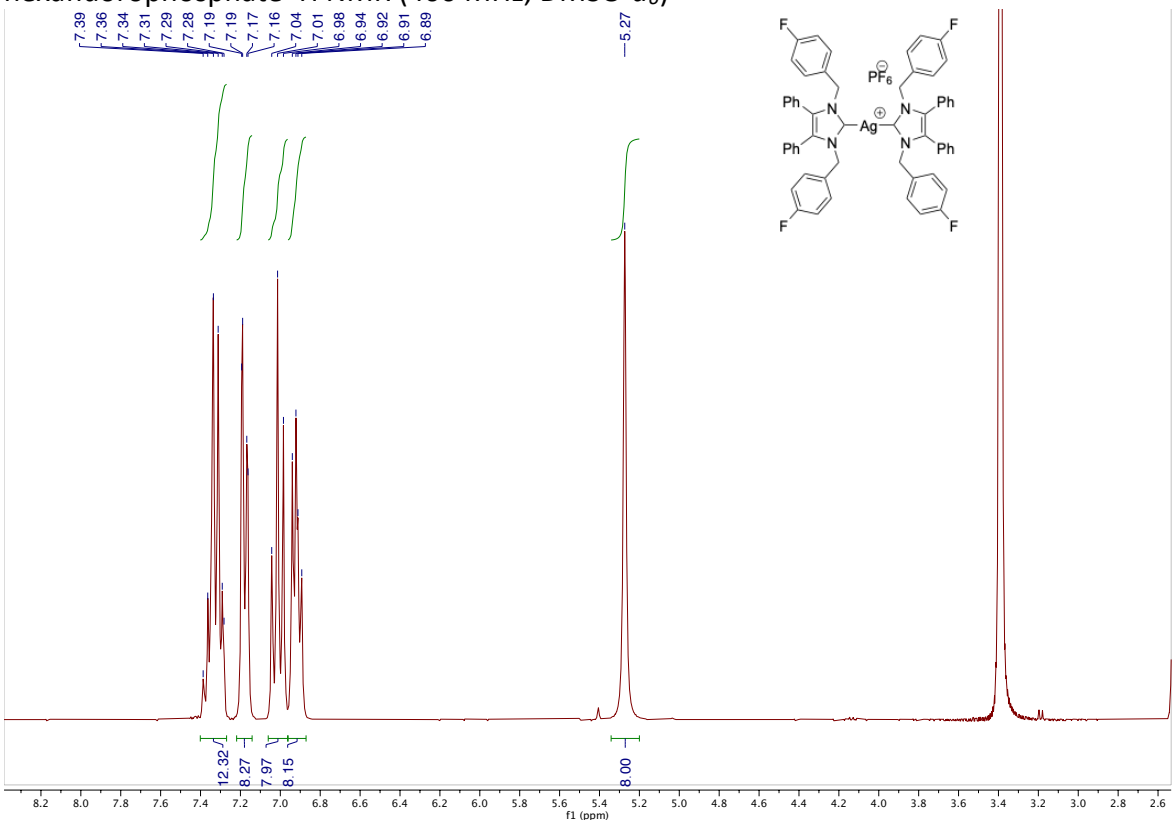

(**9b**) *Bis*-(1,3-di(*p*-fluoro)benzyl-4,5-diphenyl imidazol-2-ylidene) silver (I) hexafluorophosphate ^{13}C NMR (126 MHz, DMSO-d_6)

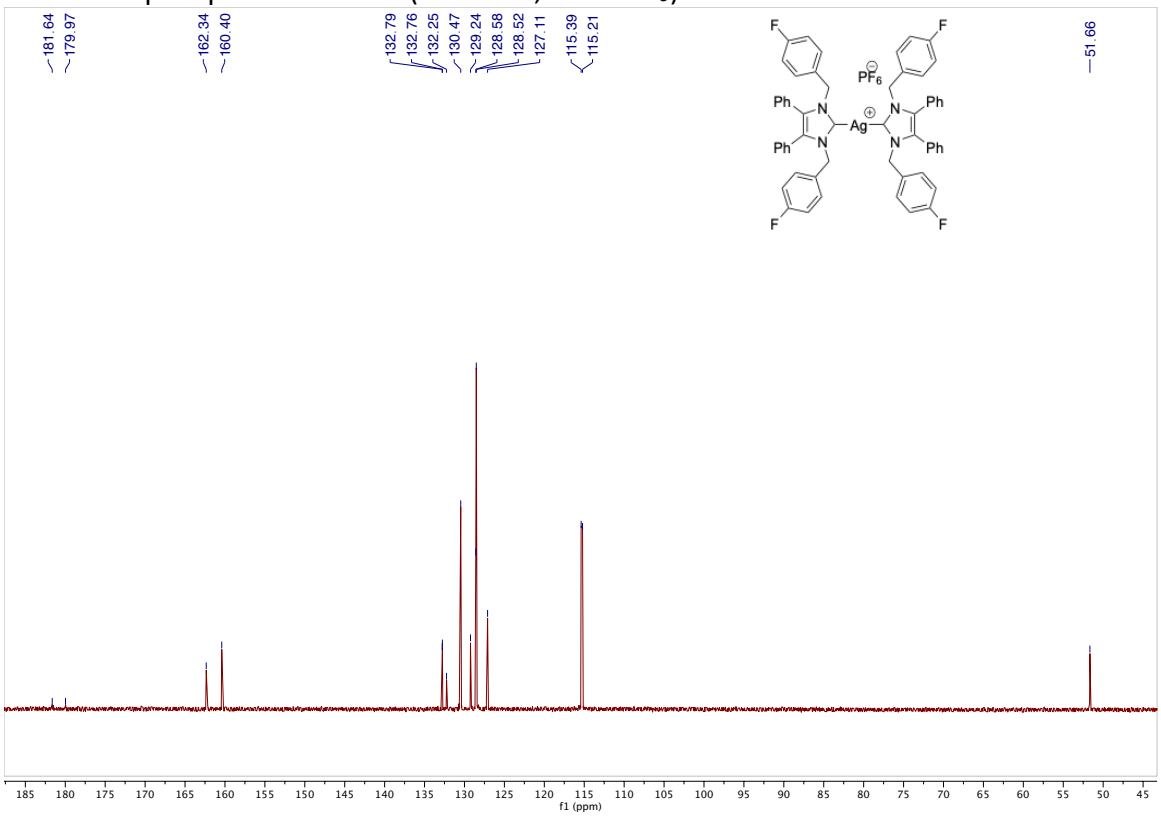

(**9b**) *Bis*-(1,3-di(*p*-fluoro)benzyl-4,5-diphenyl imidazol-2-ylidene) silver (I) hexafluorophosphate ^{19}F NMR (376 MHz, DMSO-d_6)

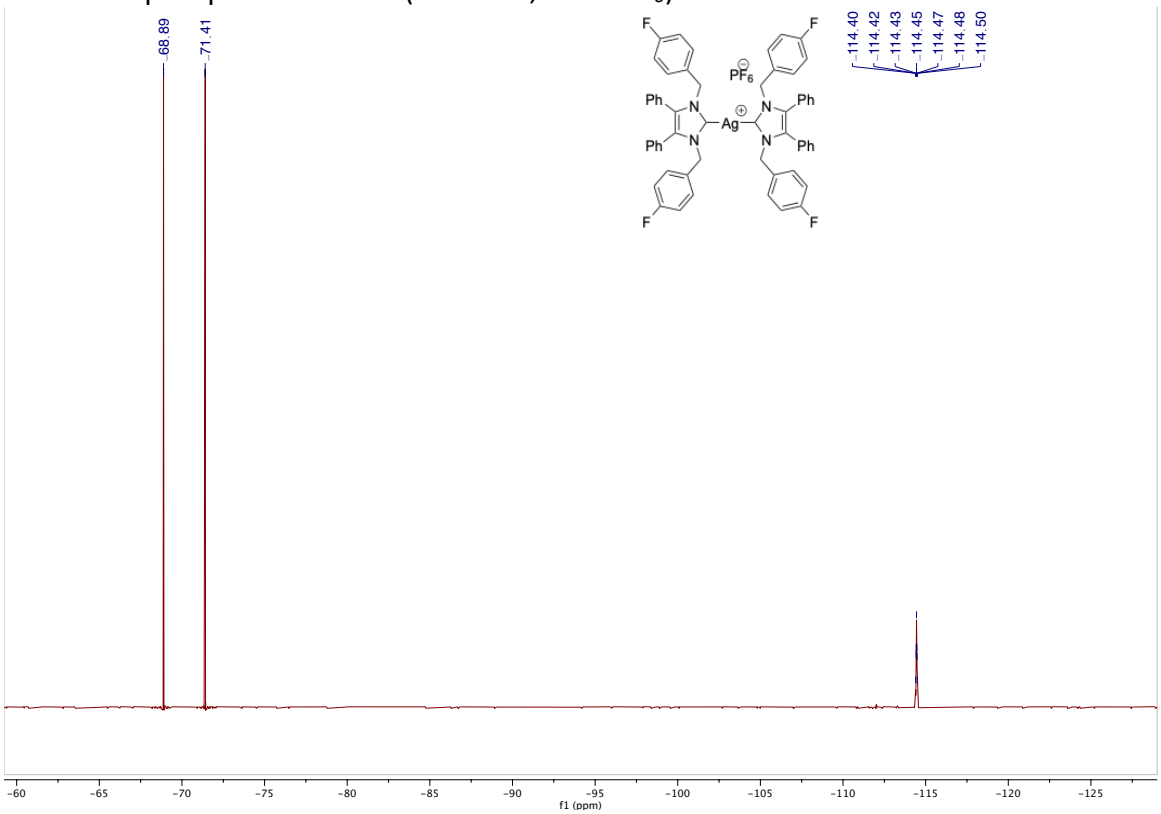

(**9c**) *Bis*-(1,3-di(*p*-trifluoromethyl)benzyl-4,5-diphenyl imidazol-2-ylidene) silver (I) hexafluorophosphate ^{1}H NMR (400 MHz, DMSO-d_6)

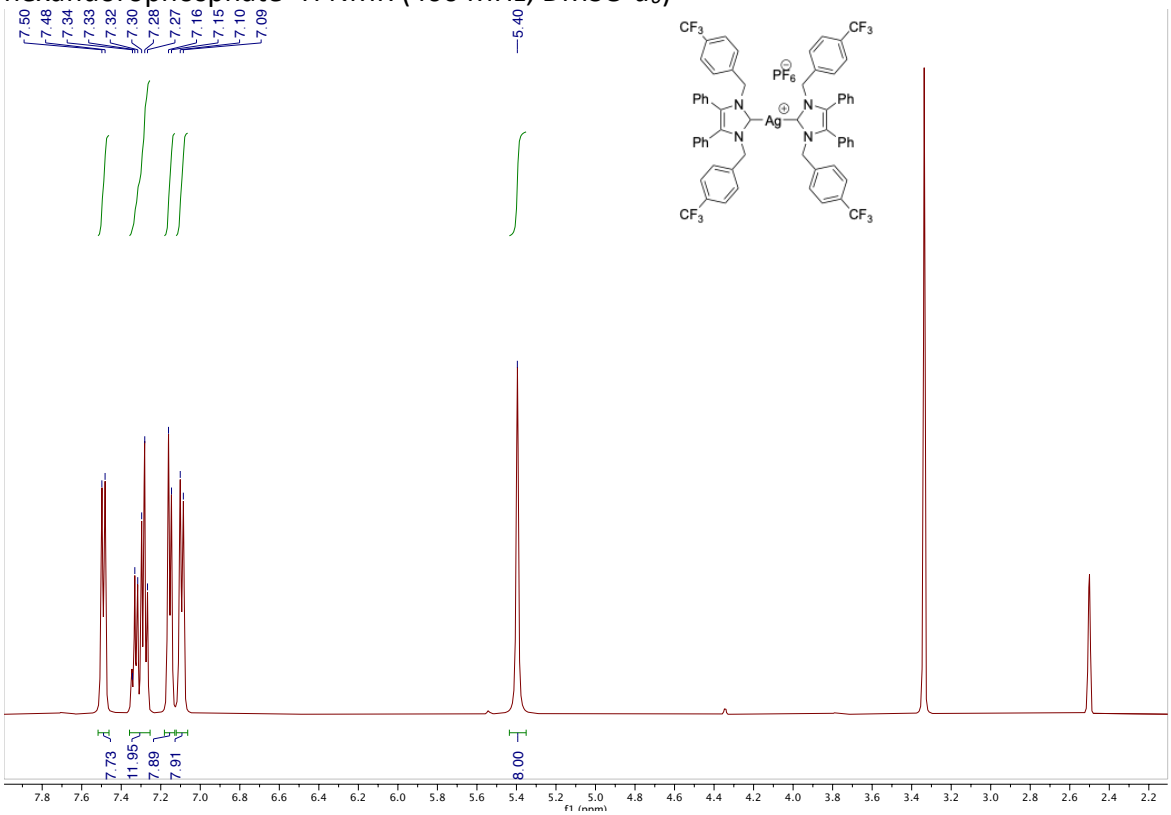

(**9c**) *Bis*-(1,3-di(*p*-trifluoromethyl) benzyl-4,5-diphenyl imidazol-2-ylidene) silver (I) hexafluorophosphate ^{13}C NMR (126 MHz, DMSO-d_6)

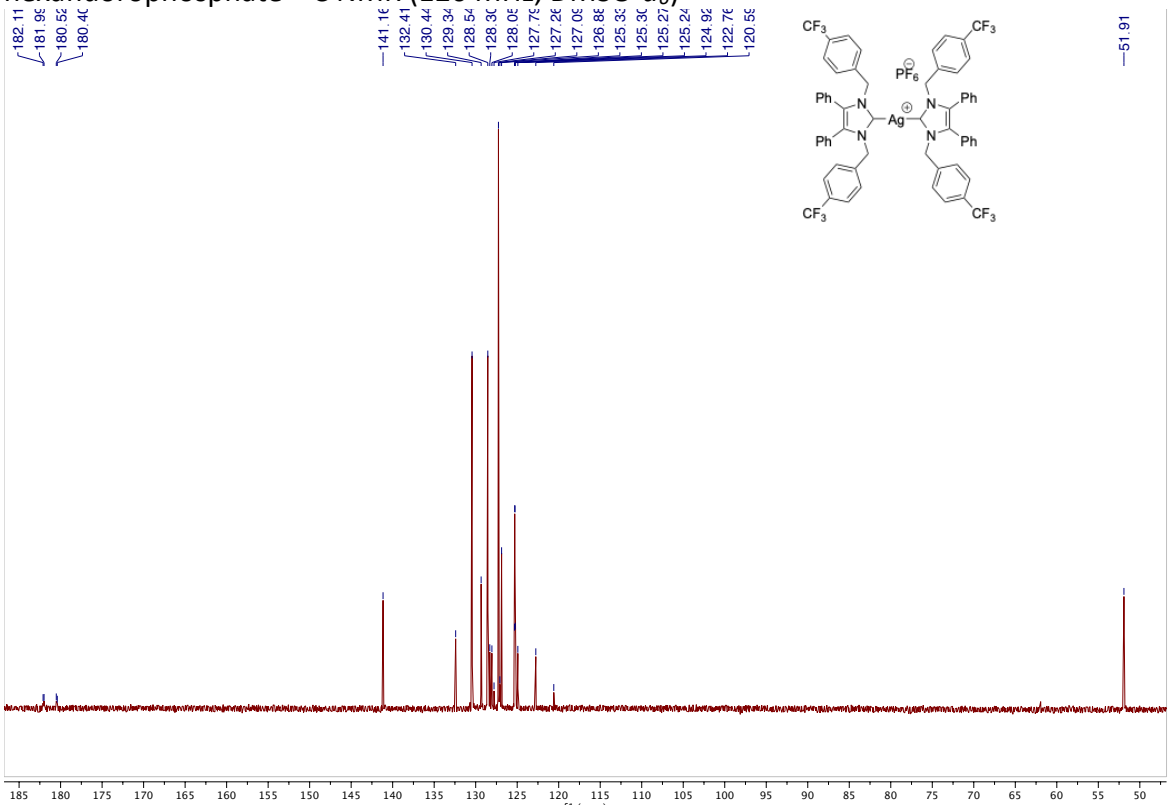

(**9c**) *Bis*-(1,3-di(*p*-trifluoromethyl) benzyl-4,5-diphenyl imidazol-2-ylidene) silver (I) hexafluorophosphate ^{19}F NMR (376 MHZ, DMSO-d_6)

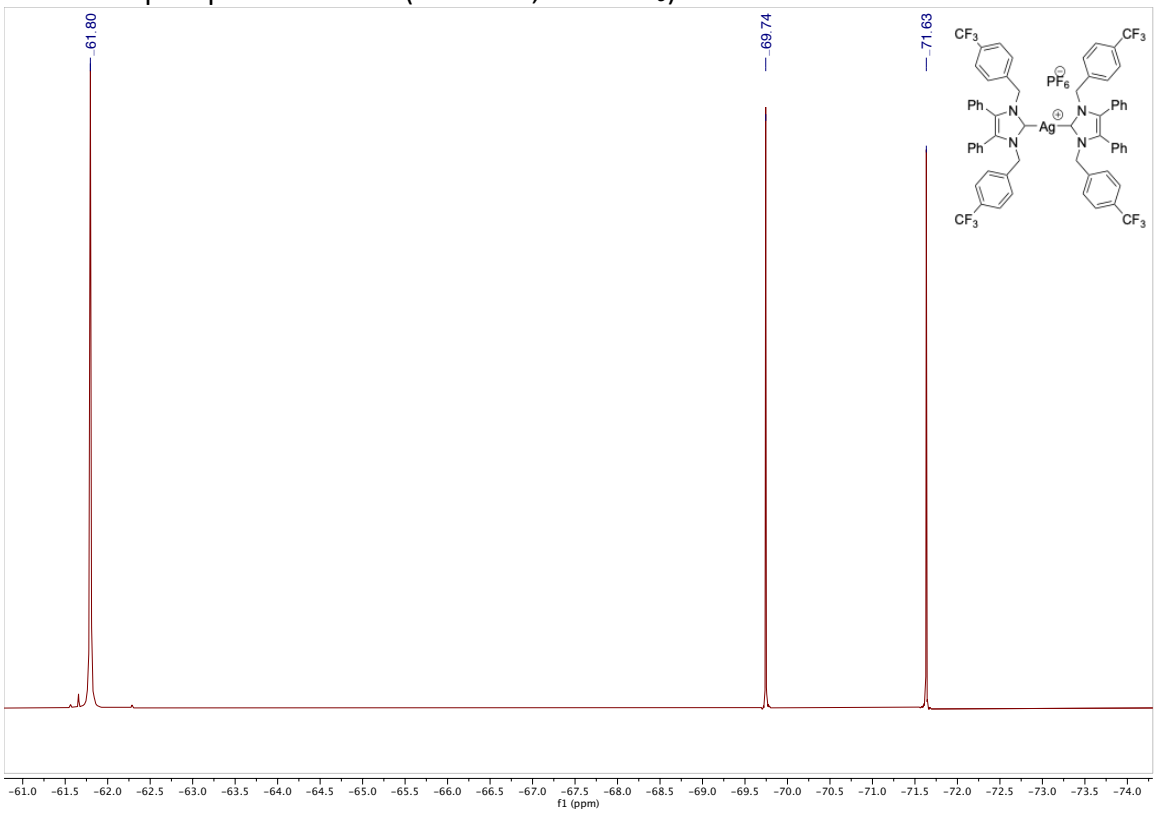

(**10a**) *Bis*-(1,3-dibenzyl-4,5-diphenyl imidazol-2-ylidene) silver (I) tetrafluoroborate ^{1}H NMR (500 MHZ, DMSO-d_6)

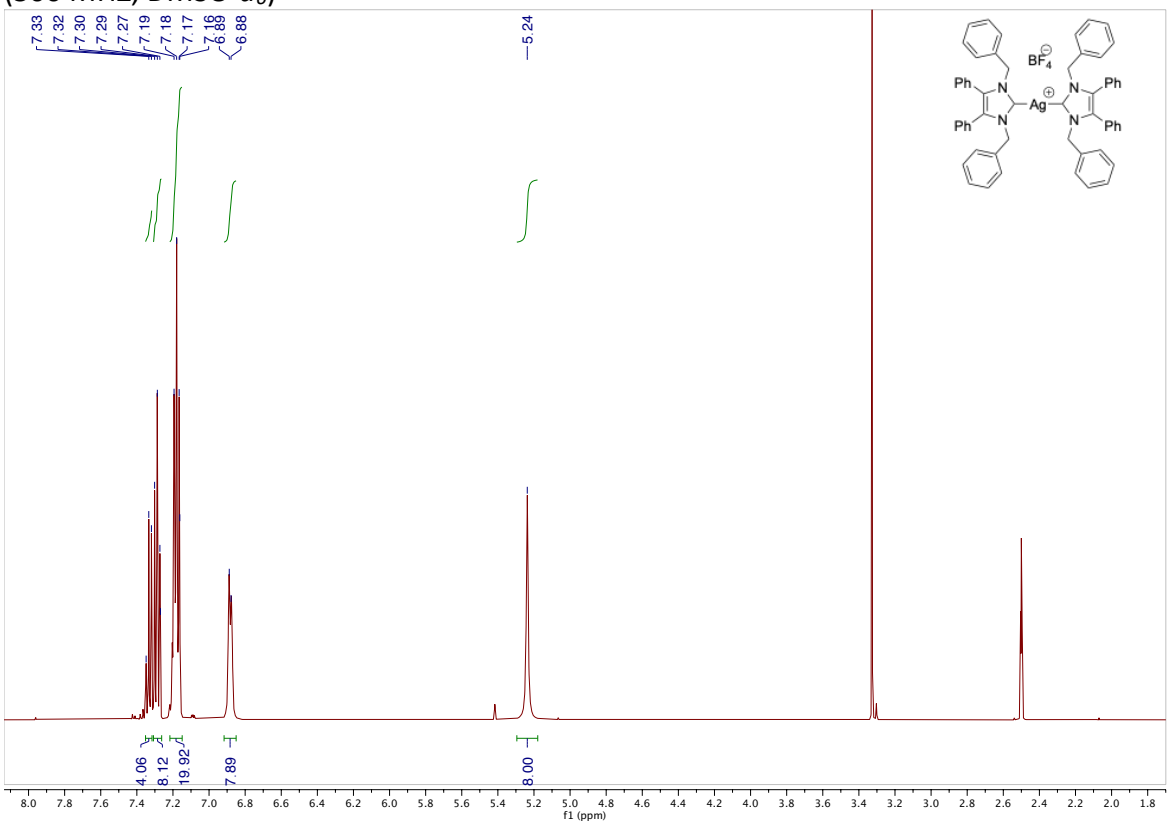

(**10a**) *Bis*-(1,3-dibenzyl-4,5-diphenyl imidazol-2-ylidene) silver (I) tetrafluoroborate ^{13}C NMR (126 MHz, DMSO-d_6)

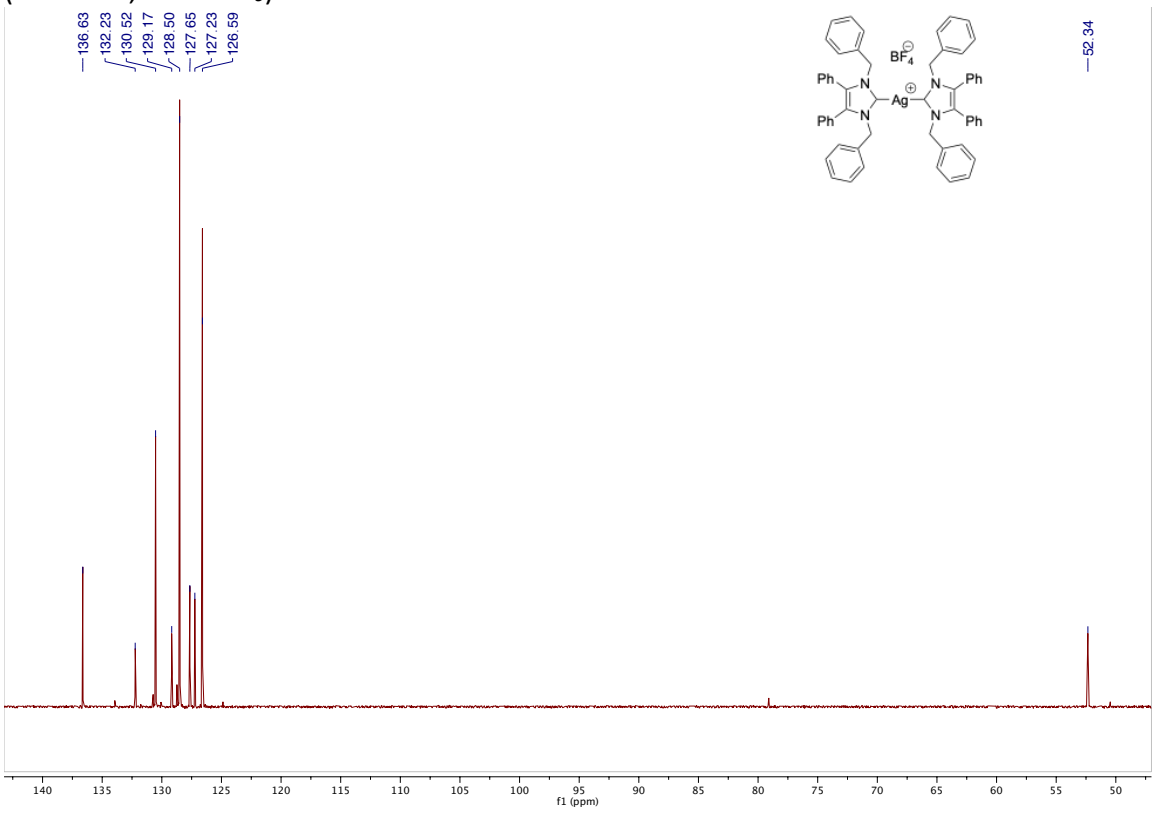

(**10a**) *Bis*-(1,3-dibenzyl-4,5-diphenyl imidazol-2-ylidene) silver (I) tetrafluoroborate ^{19}F NMR (470 MHz, DMSO-d_6)

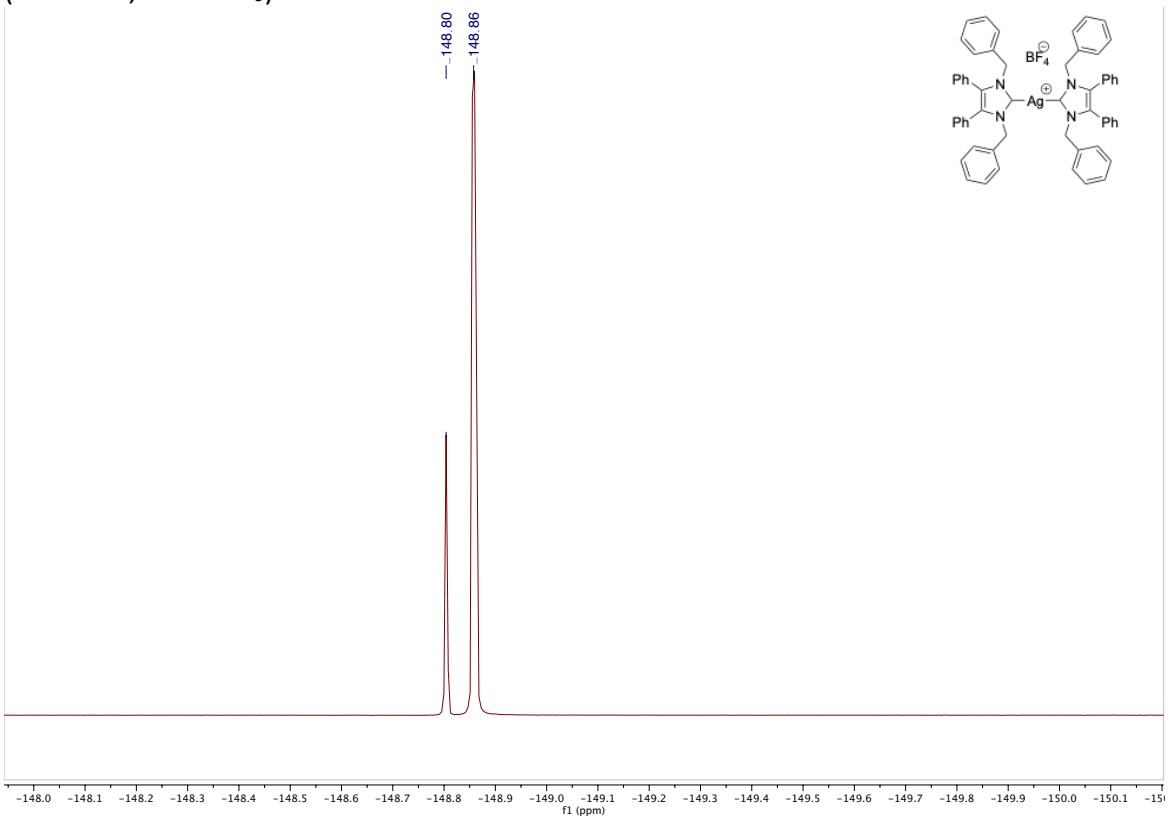

(**10b**) *Bis*-(1,3-di(*p*-fluoro) benzyl-4,5-diphenyl imidazol-2-ylidene) silver (I) tetrafluoroborate
^{1}H NMR (500 MHz, DMSO-d_6)

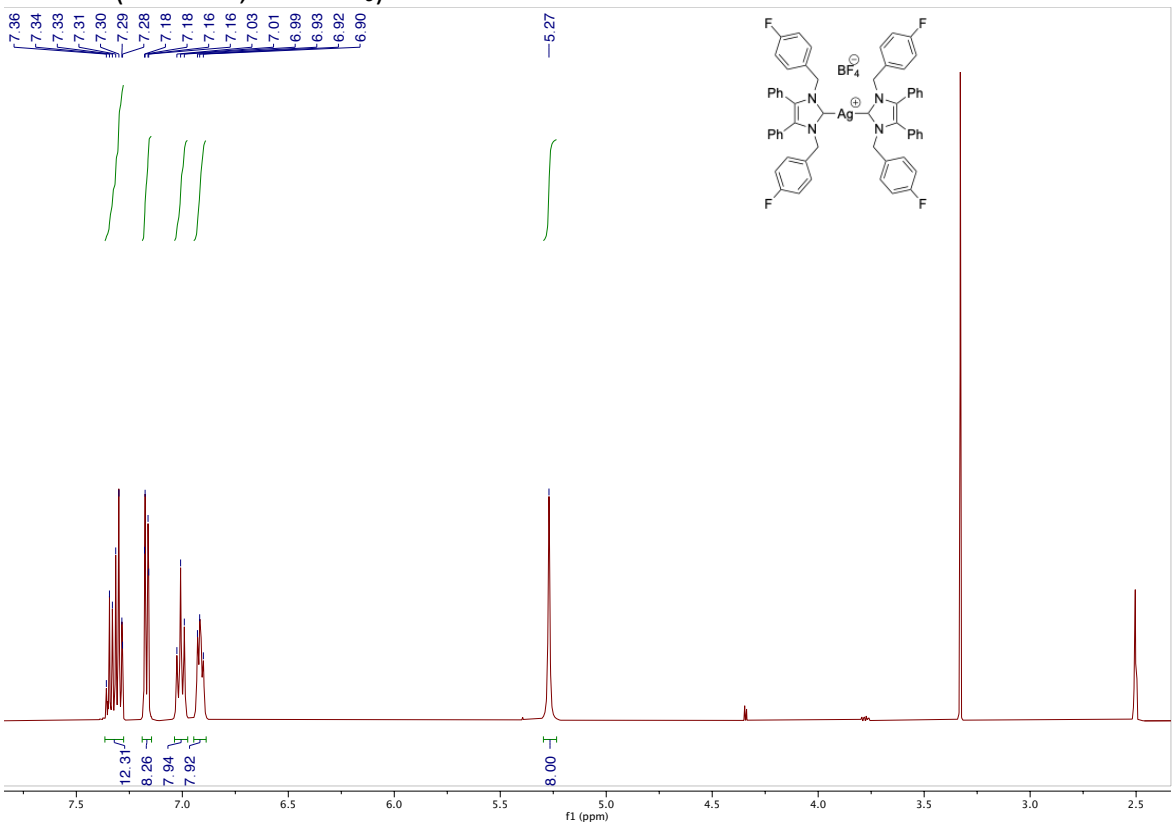

(**10b**) *Bis*-(1,3-di(*p*-fluoro) benzyl-4,5-diphenyl imidazol-2-ylidene) silver (I) tetrafluoroborate
^{13}C NMR (126 MHz, DMSO-d_6)

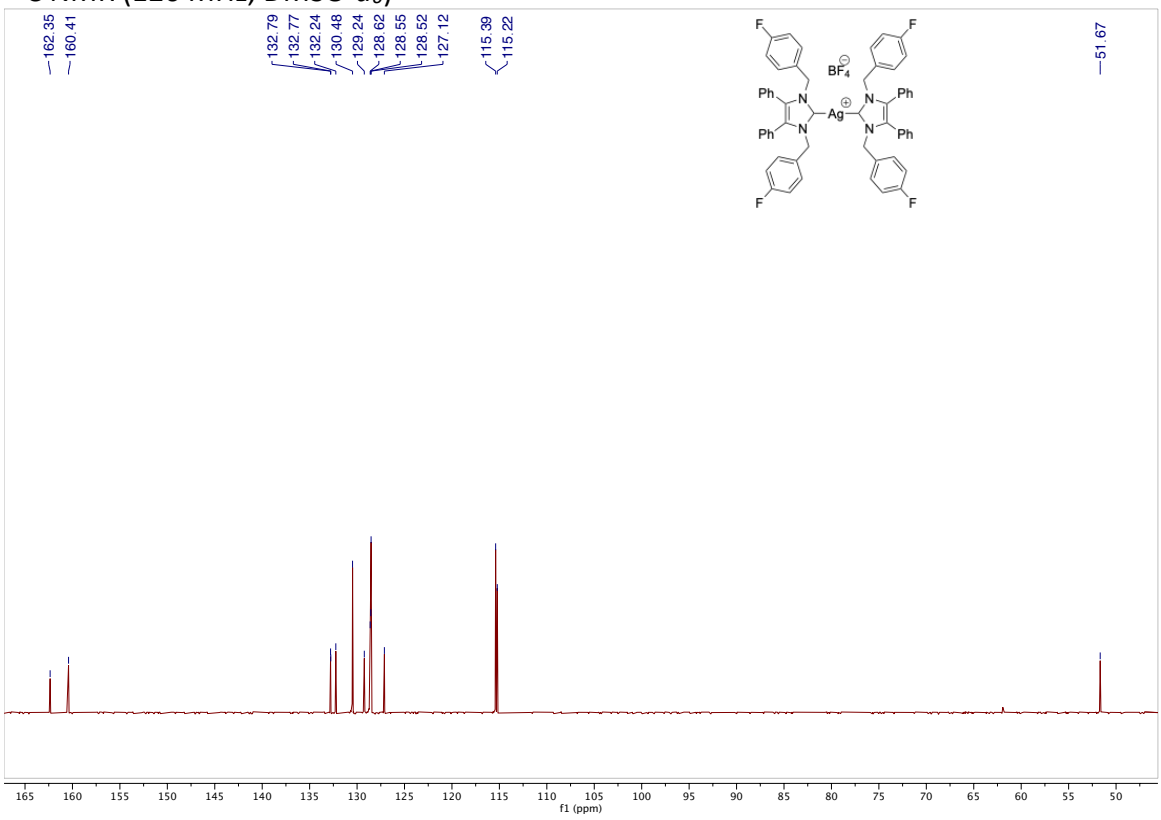

(**10b**) *Bis*-(1,3-di(*p*-fluoro) benzyl-4,5-diphenyl imidazol-2-ylidene) silver (I) tetrafluoroborate ^{19}F NMR (470 MHz, DMSO-d_6)

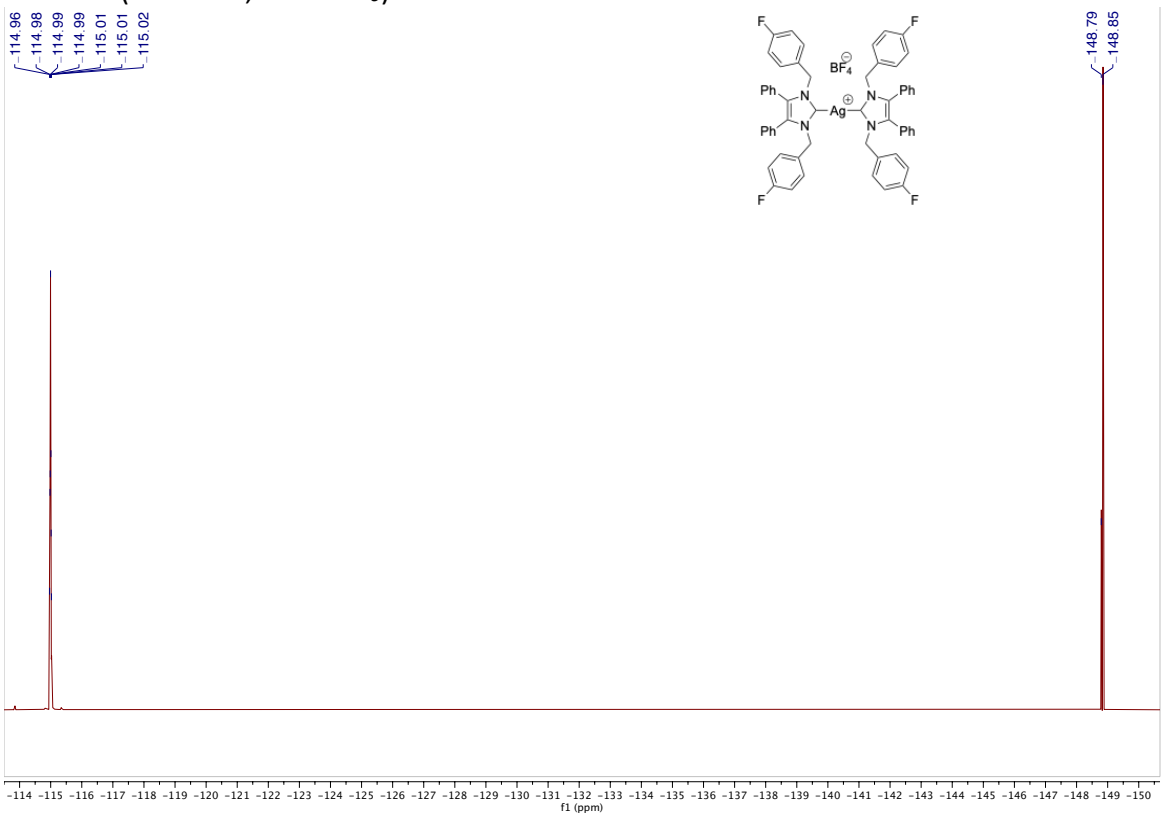

(**10c**) *Bis*-(1,3-di(*p*-trifluoromethyl) benzyl-4,5-diphenyl imidazol-2-ylidene) silver (I) tetrafluoroborate ^{1}H NMR (400 MHz, DMSO-d_6)

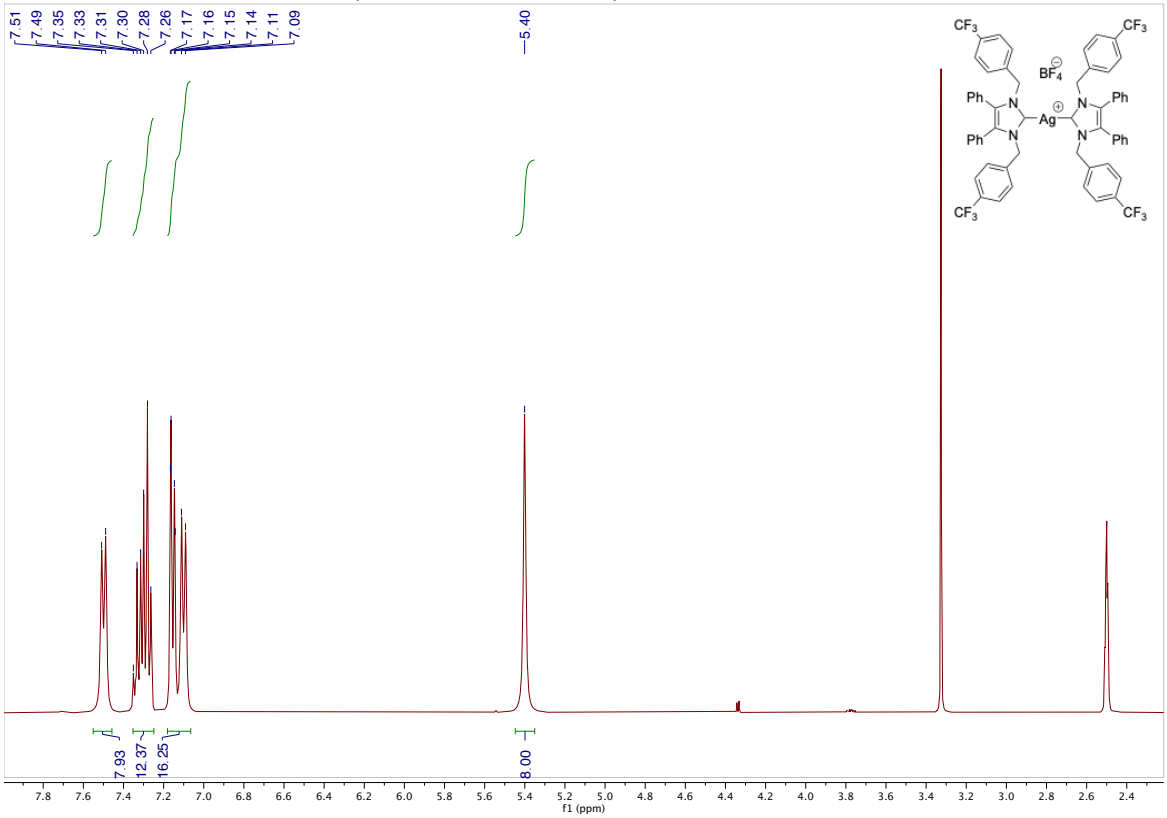

(**10c**) *Bis*-(1,3-di(*p*-trifluoromethyl) benzyl-4,5-diphenyl imidazol-2-ylidene) silver (I) tetrafluoroborate ^{13}C NMR (101 MHz, DMSO-d_6)

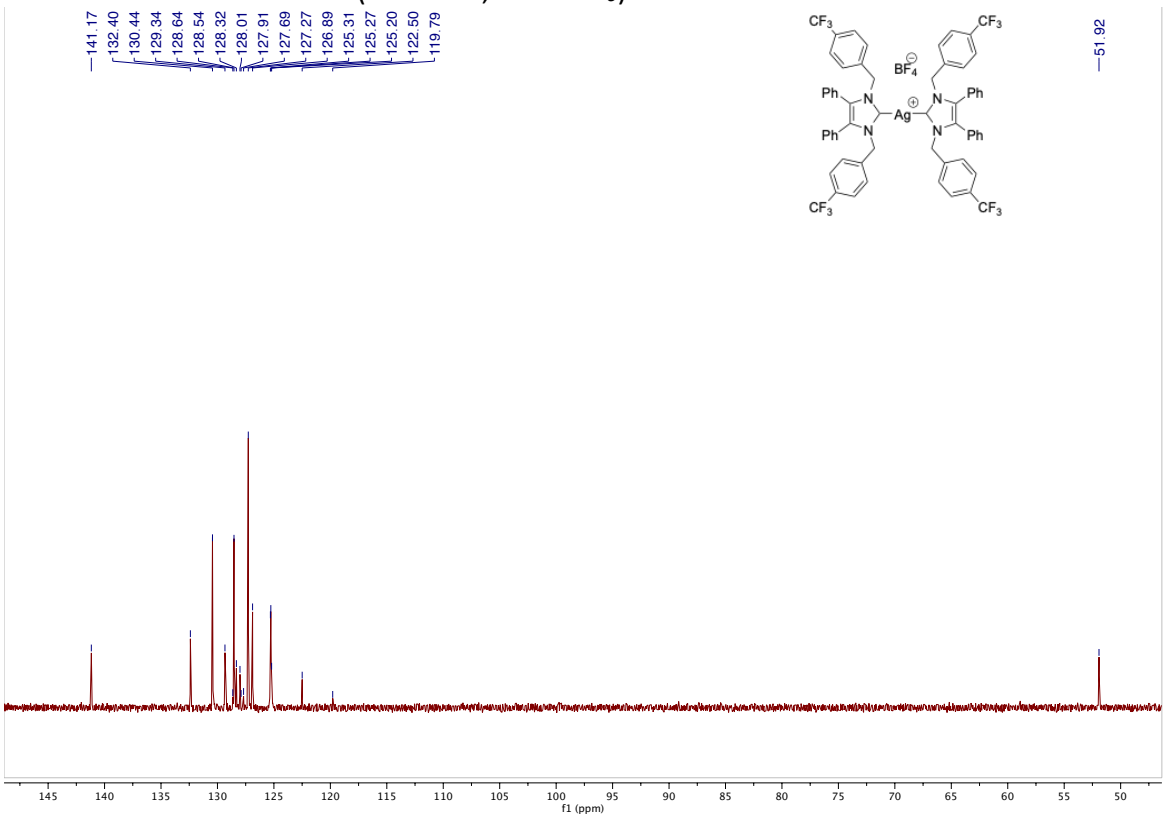

(**10c**) *Bis*-(1,3-di(*p*-trifluoromethyl) benzyl-4,5-diphenyl imidazol-2-ylidene) silver (I) tetrafluoroborate ^{19}F NMR (376 MHz, DMSO-d_6)

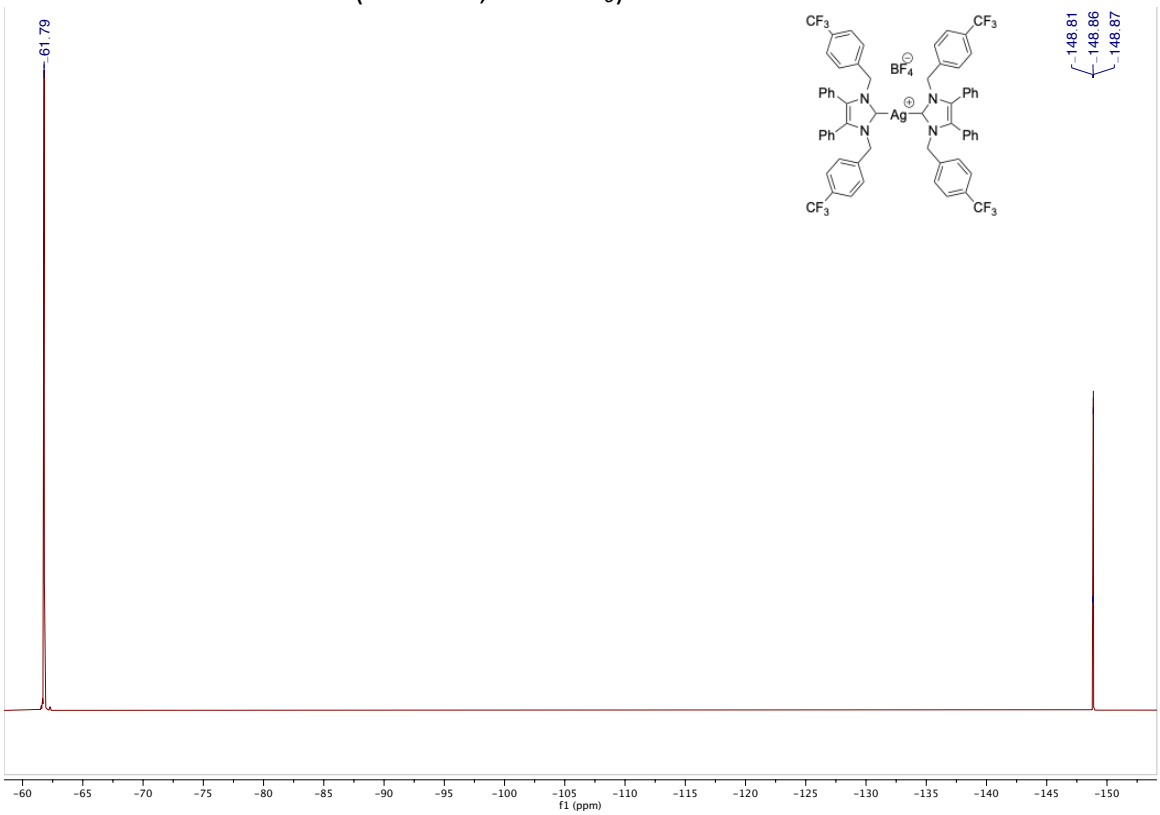

(**12a**) *Bis*-(1,3-dibenzyl-4,5-diphenyl imidazol-2-ylidene) silver (I) gluconate ^{1}H NMR (400 MHz, DMSO-d_6)

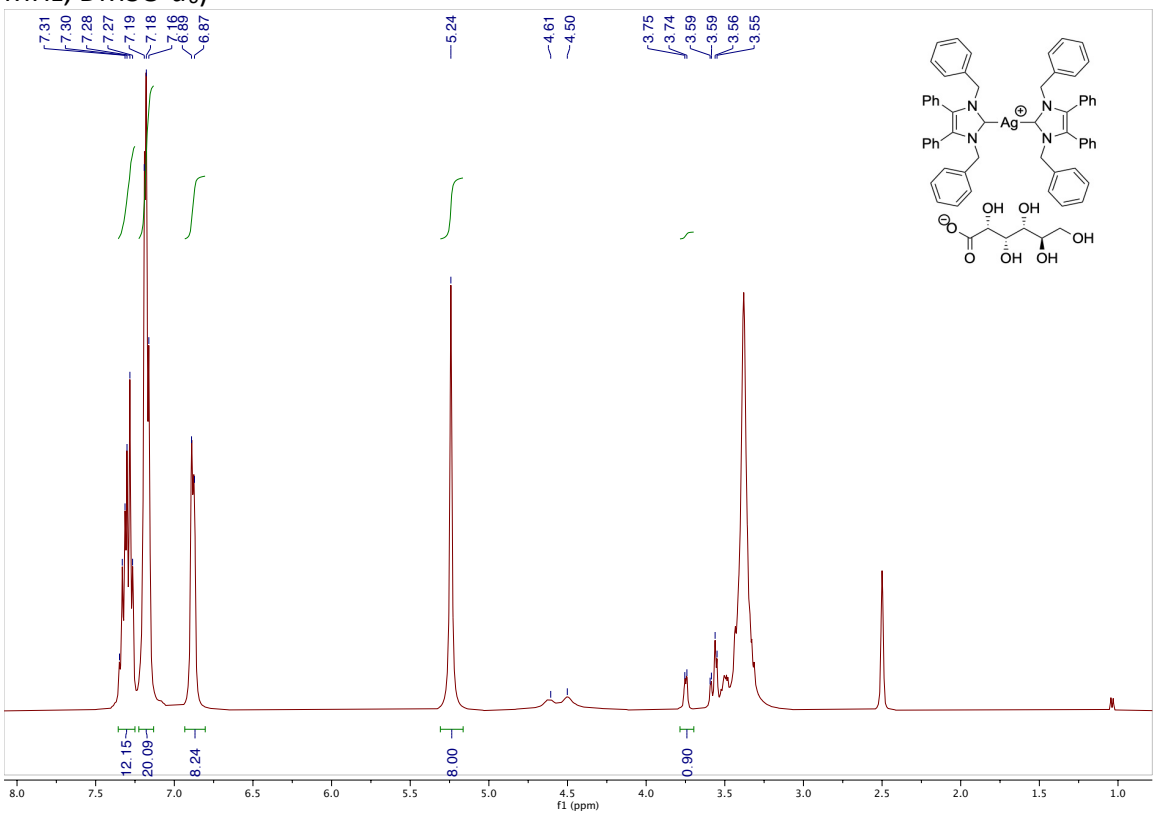

(**12a**) *Bis*-(1,3-dibenzyl-4,5-diphenyl imidazol-2-ylidene) silver (I) gluconate ^{13}C NMR (101 MHz, DMSO-d_6)

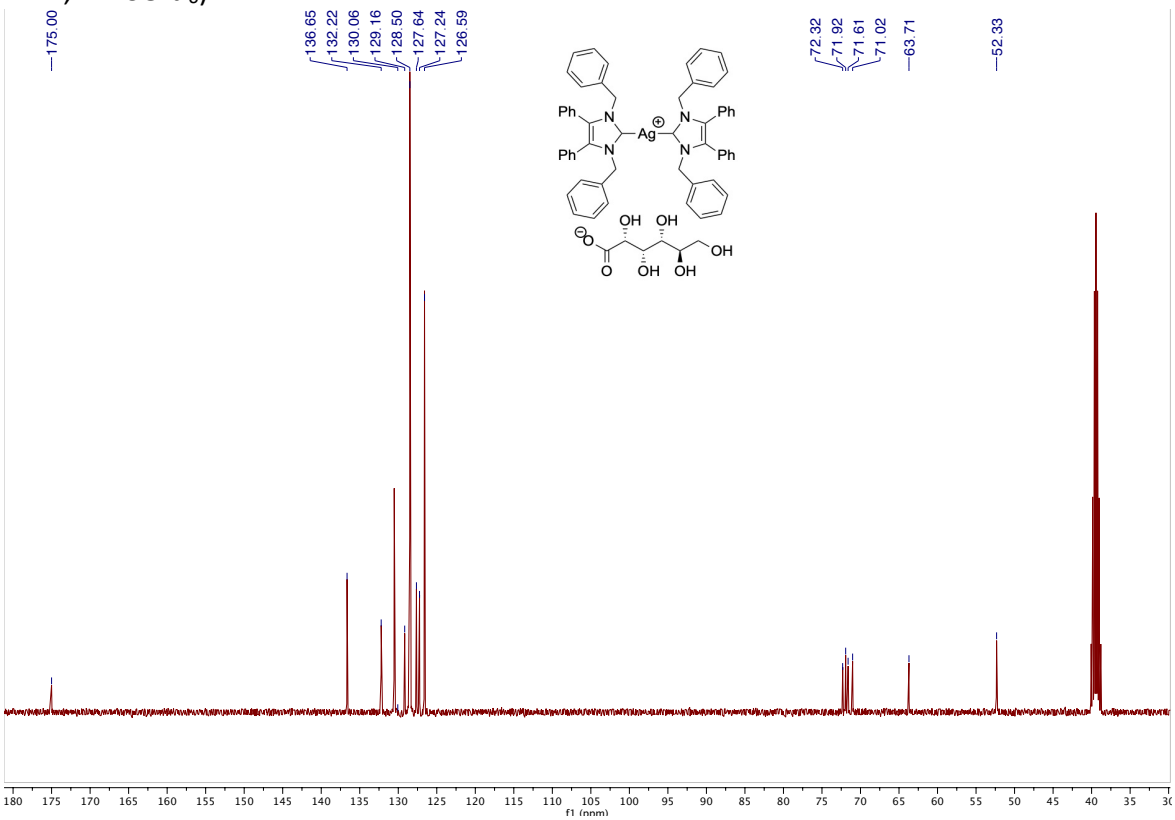

(**12b**) *Bis*-(1,3-di(*p*-fluoro) benzyl-4,5-diphenyl imidazol-2-ylidene) silver (I) gluconate ^{1}H NMR (400 MHz, DMSO-d_6)

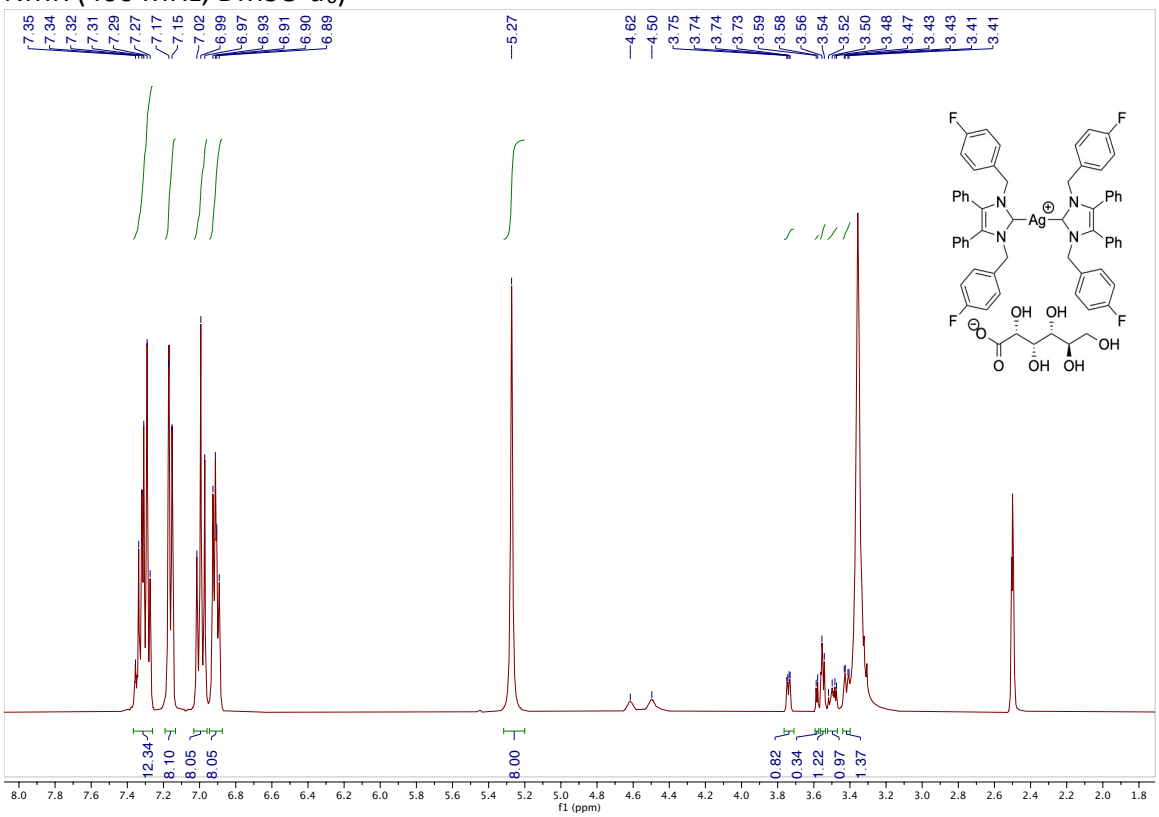

(**12b**) *Bis*-(1,3-di(*p*-fluoro) benzyl-4,5-diphenyl imidazol-2-ylidene) silver (I) gluconate ^{13}C NMR (101 MHz, DMSO-d_6)

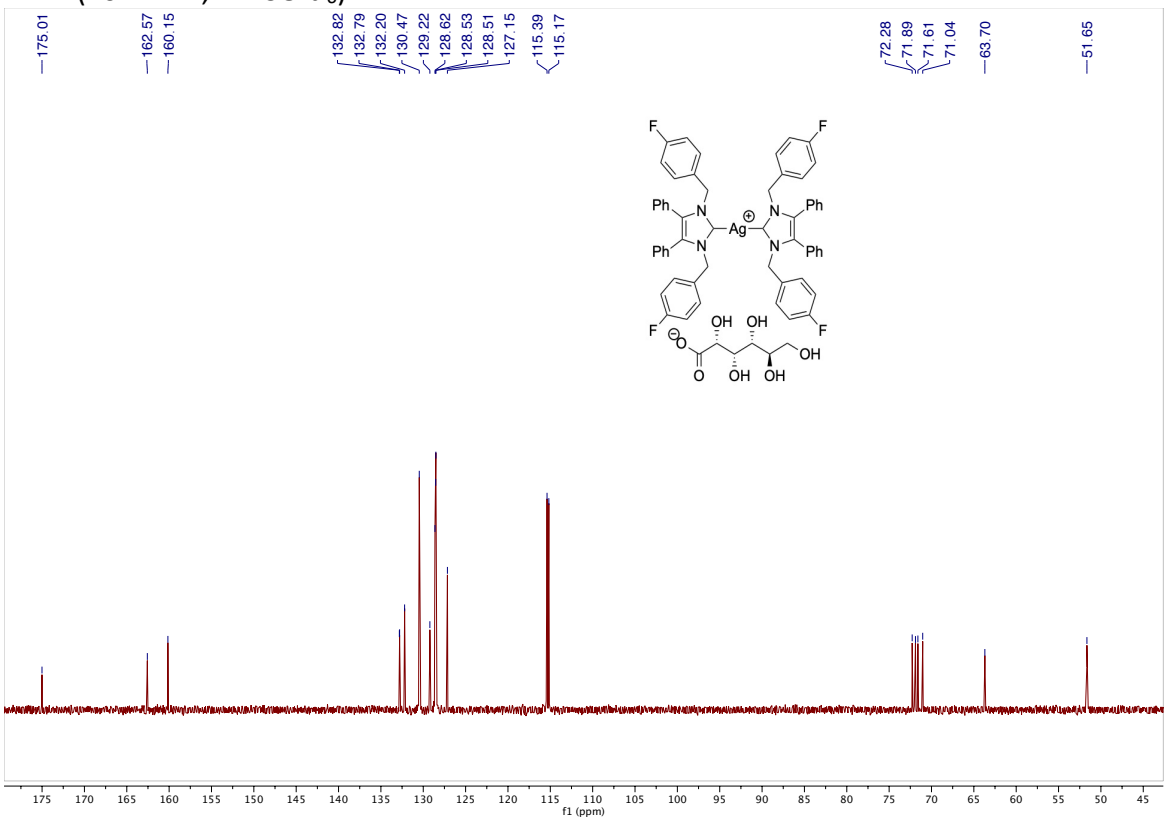

(**12b**) *Bis*-(1,3-di(*p*-fluoro) benzyl-4,5-diphenyl imidazol-2-ylidene) silver (I) gluconate ^{19}F NMR (376 MHz, DMSO-d_6)

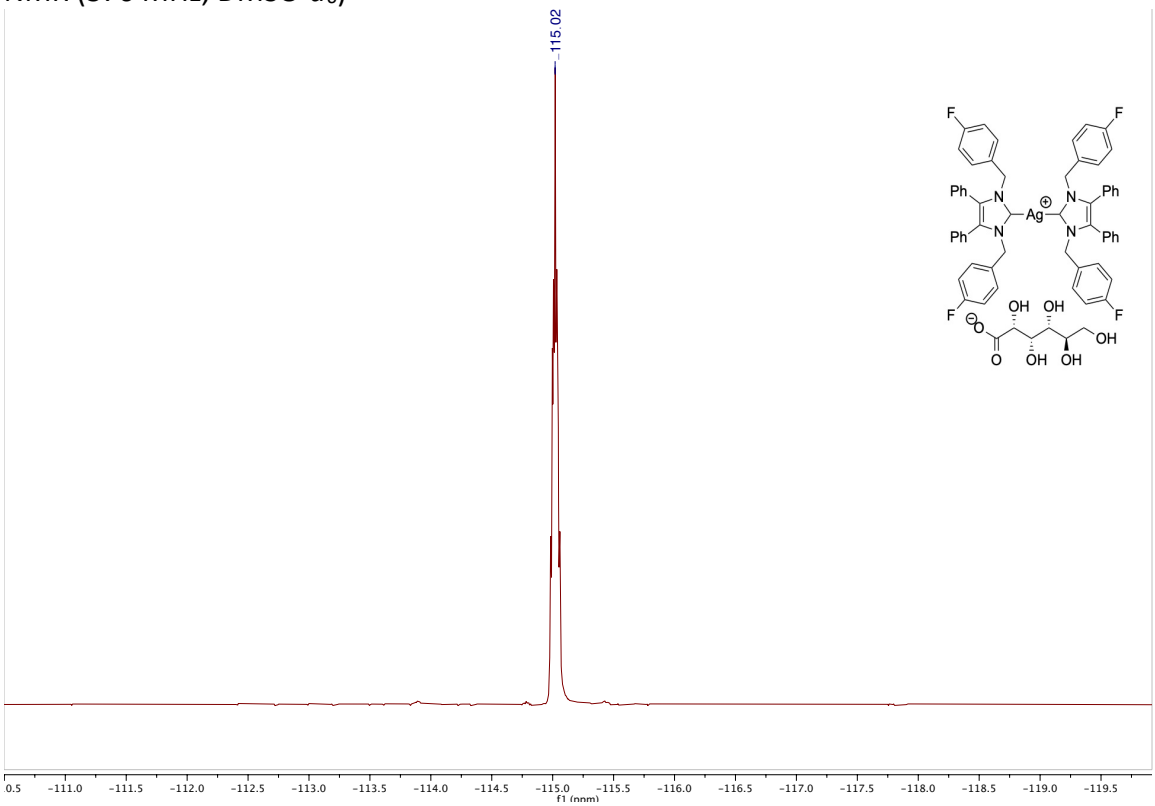

(**12c**) *Bis*-(1,3-di(*p*-trifluoromethyl) benzyl-4,5-diphenyl imidazol-2-ylidene) silver (I) gluconate ^{1}H NMR (400 MHz, DMSO-d_6)

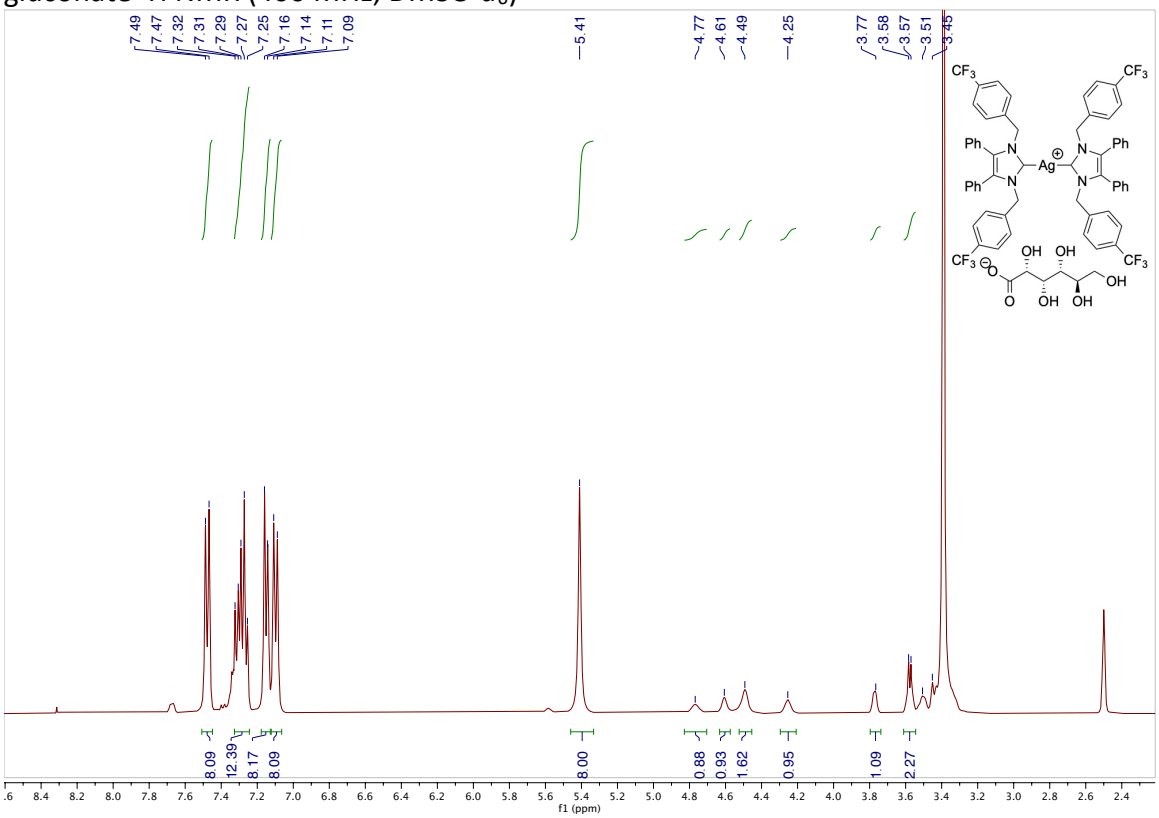

(**12c**) *Bis*-(1,3-di(*p*-trifluoromethyl) benzyl-4,5-diphenyl imidazol-2-ylidene) silver (I) gluconate ^{13}C NMR (101 MHz, DMSO-d_6)

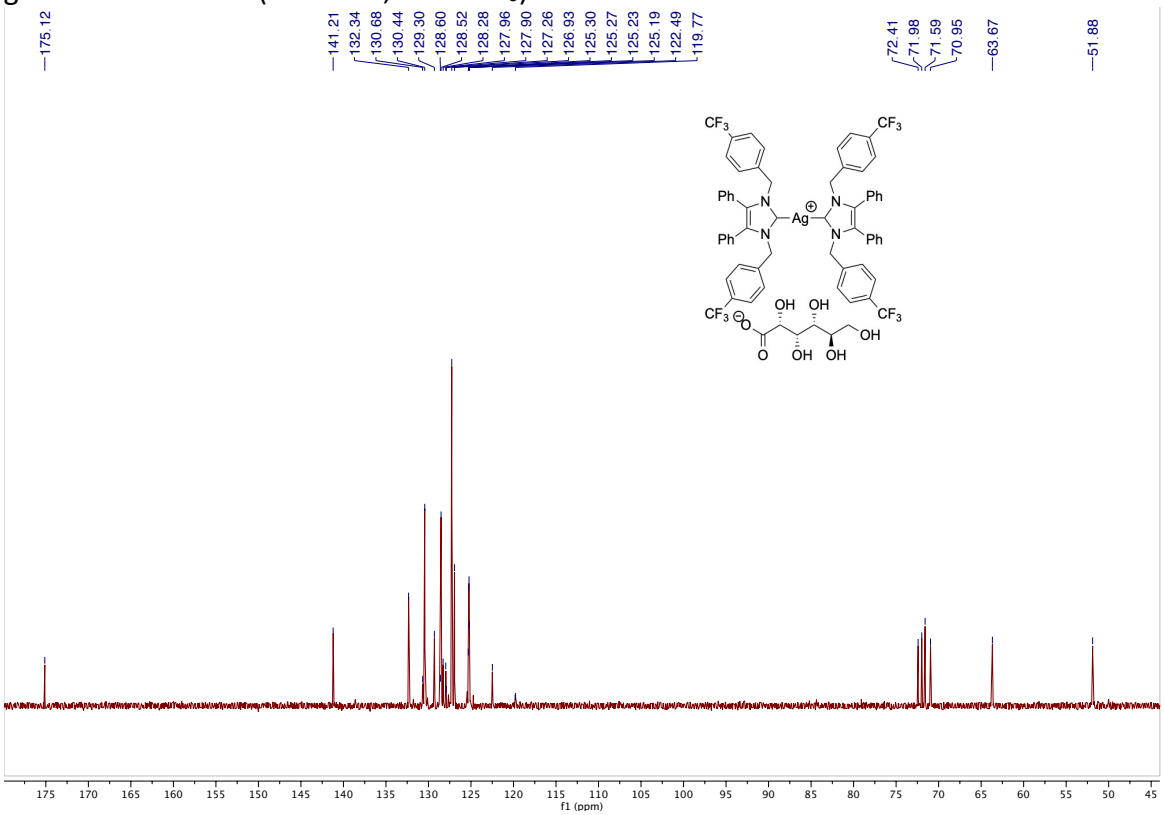

(**12c**) *Bis*-(1,3-di(*p*-trifluoromethyl) benzyl-4,5-diphenyl imidazol-2-ylidene) silver (I) gluconate ^{19}F NMR (376 MHz, DMSO-d_6)

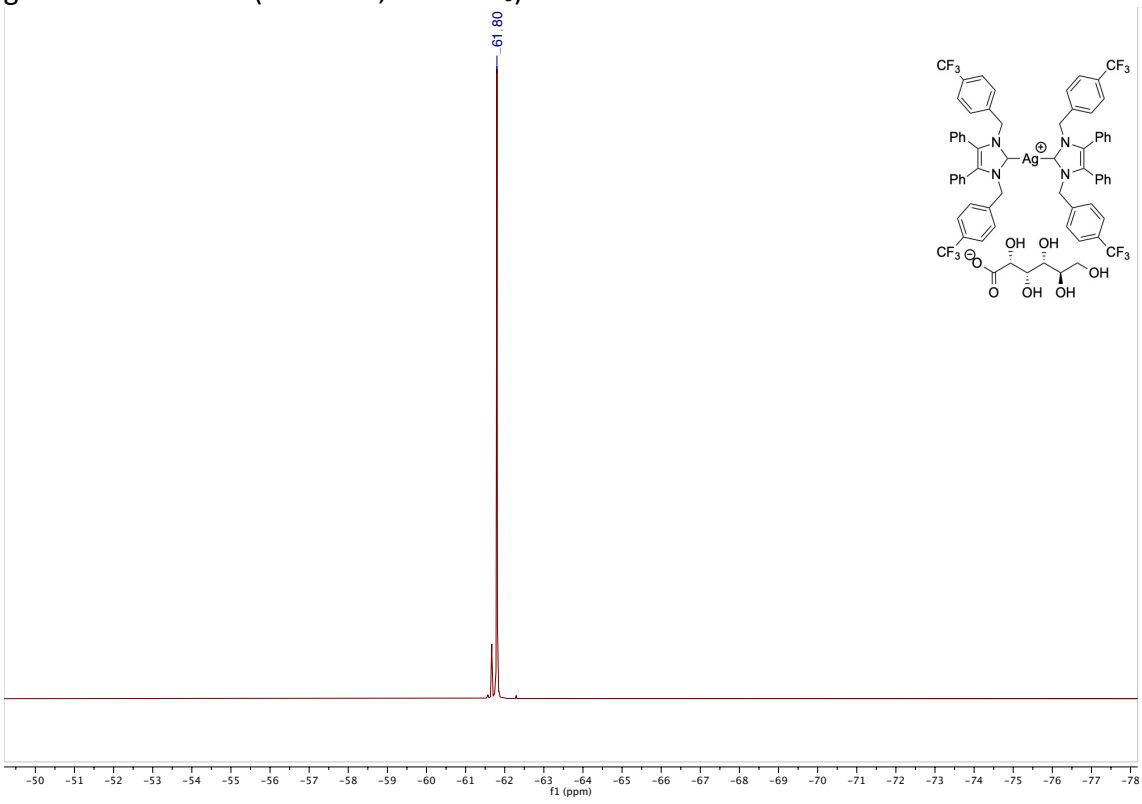

(**13a**) *Bis*-(1,3-dibenzyl-4,5-diphenyl imidazol-2-ylidene) silver (I) dichloroargentate ^{1}H NMR (400 MHz, DMSO-d_6)

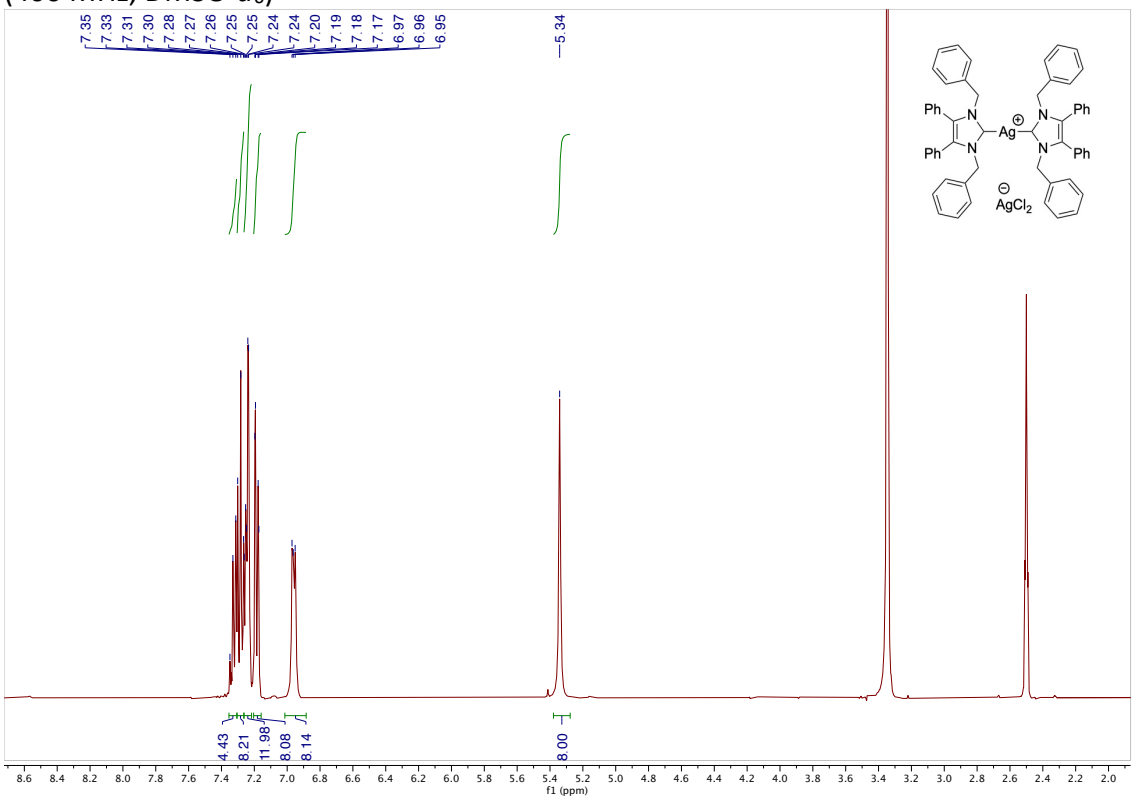

(**13a**) *Bis*-(1,3-dibenzyl-4,5-diphenyl imidazol-2-ylidene) silver (I) dichloroargentate ^{13}C NMR (101 MHz, DMSO-d_6)

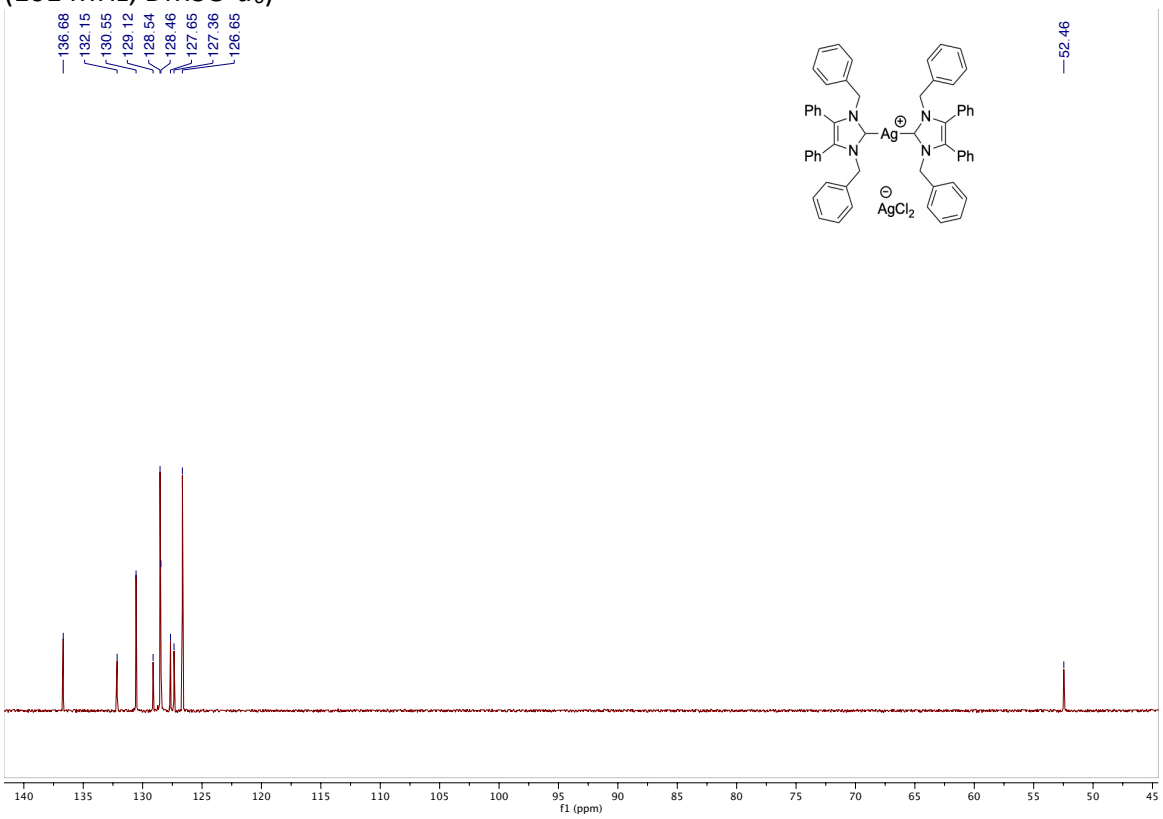

(**13b**) *Bis*-(1,3-di(*p*-fluoro) benzyl-4,5-diphenyl imidazol-2-ylidene) silver (I) dichloroargentate ^{1}H NMR (400 MHz, DMSO-d_6)

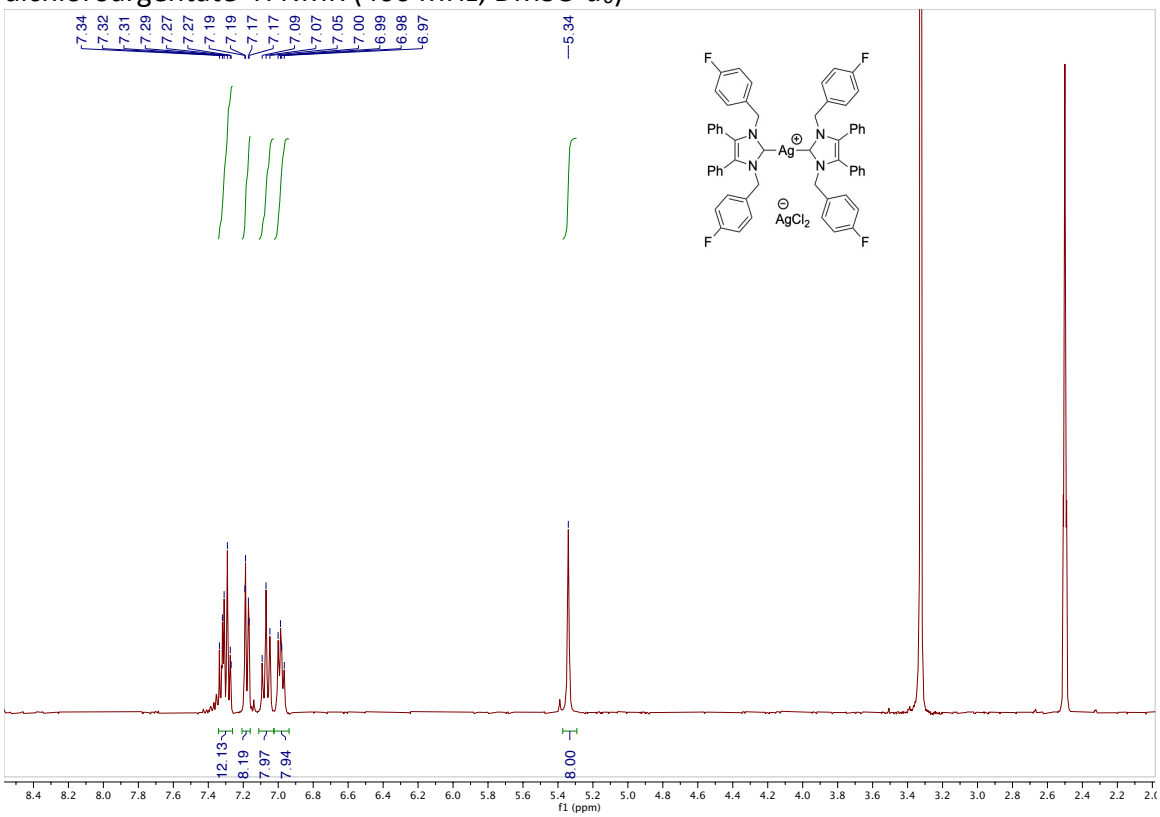

(**13b**) *Bis*-(1,3-di(*p*-fluoro) benzyl-4,5-diphenyl imidazol-2-ylidene) silver (I) dichloroargentate ^{13}C NMR (101 MHz, DMSO-d_6)

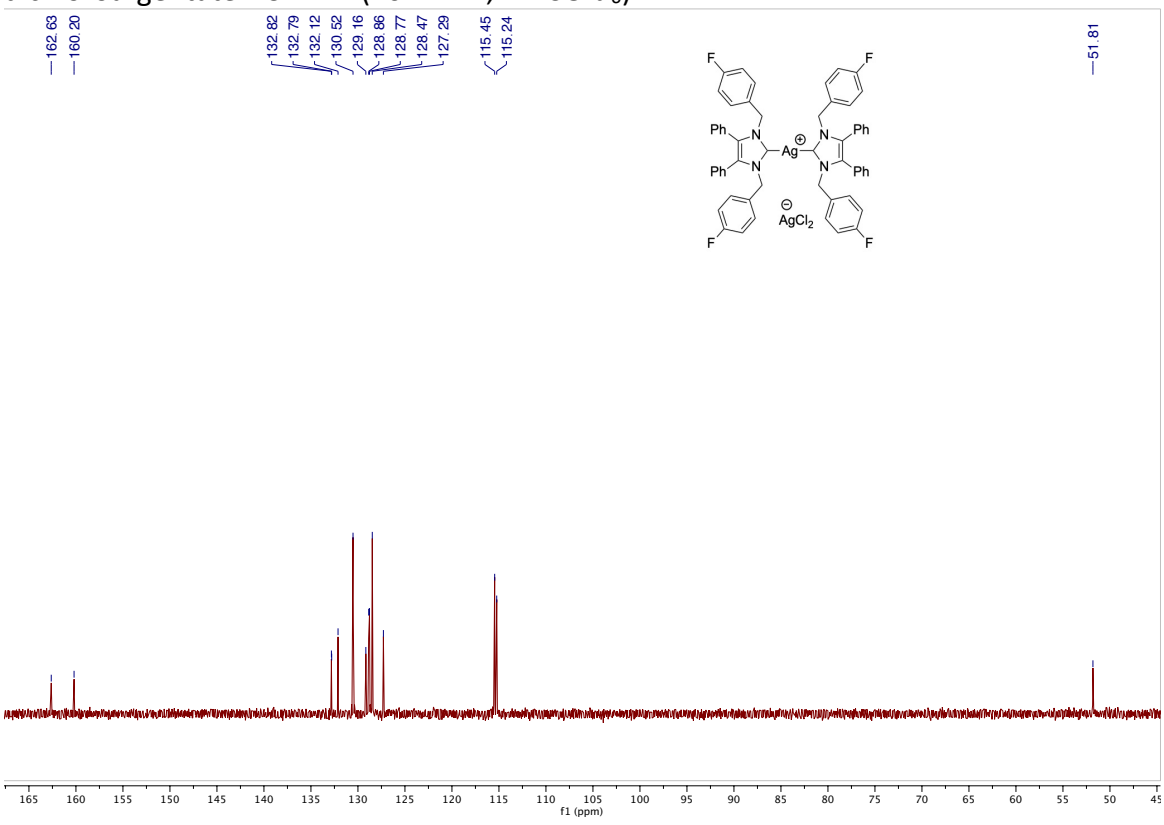

(**13b**) *Bis*-(1,3-di(*p*-fluoro) benzyl-4,5-diphenyl imidazol-2-ylidene) silver (I) dichloroargentate ^{19}F NMR (376 MHz, DMSO-d_6)

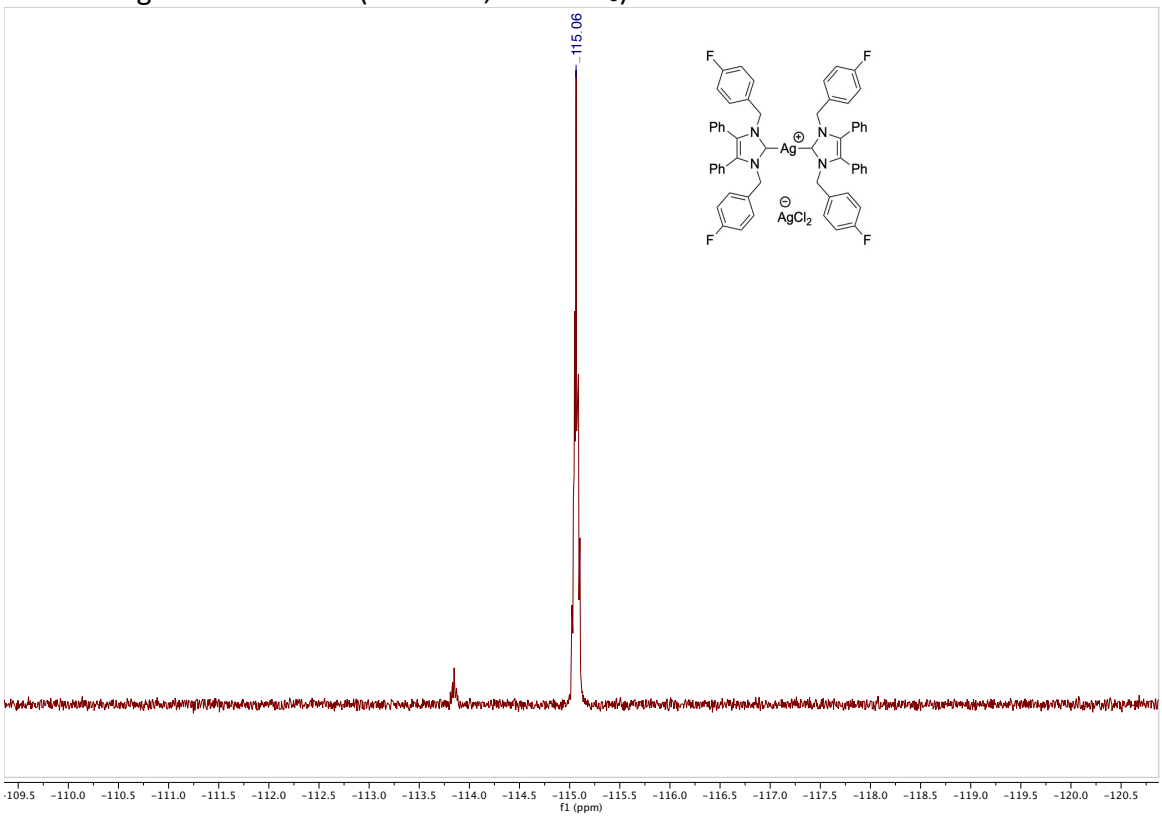

(**13c**) *Bis*-(1,3-di(*p*-trifluoromethyl) benzyl-4,5-diphenyl imidazol-2-ylidene) silver (I) dichloroargentate ^{1}H NMR (400 MHz, DMSO-d_6)

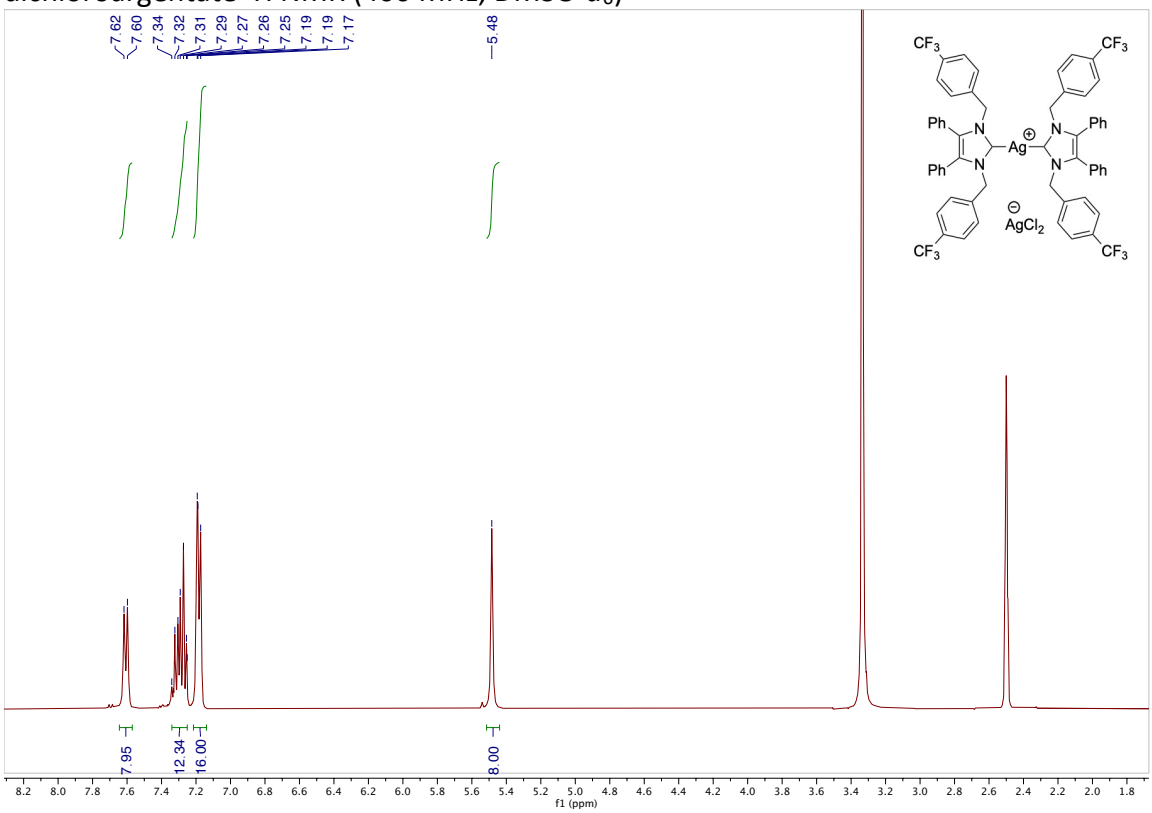

(**13c**) *Bis*-(1,3-di(*p*-trifluoromethyl) benzyl-4,5-diphenyl imidazol-2-ylidene) silver (I) dichloroargentate ^{13}C NMR (101 MHz, DMSO-d_6)

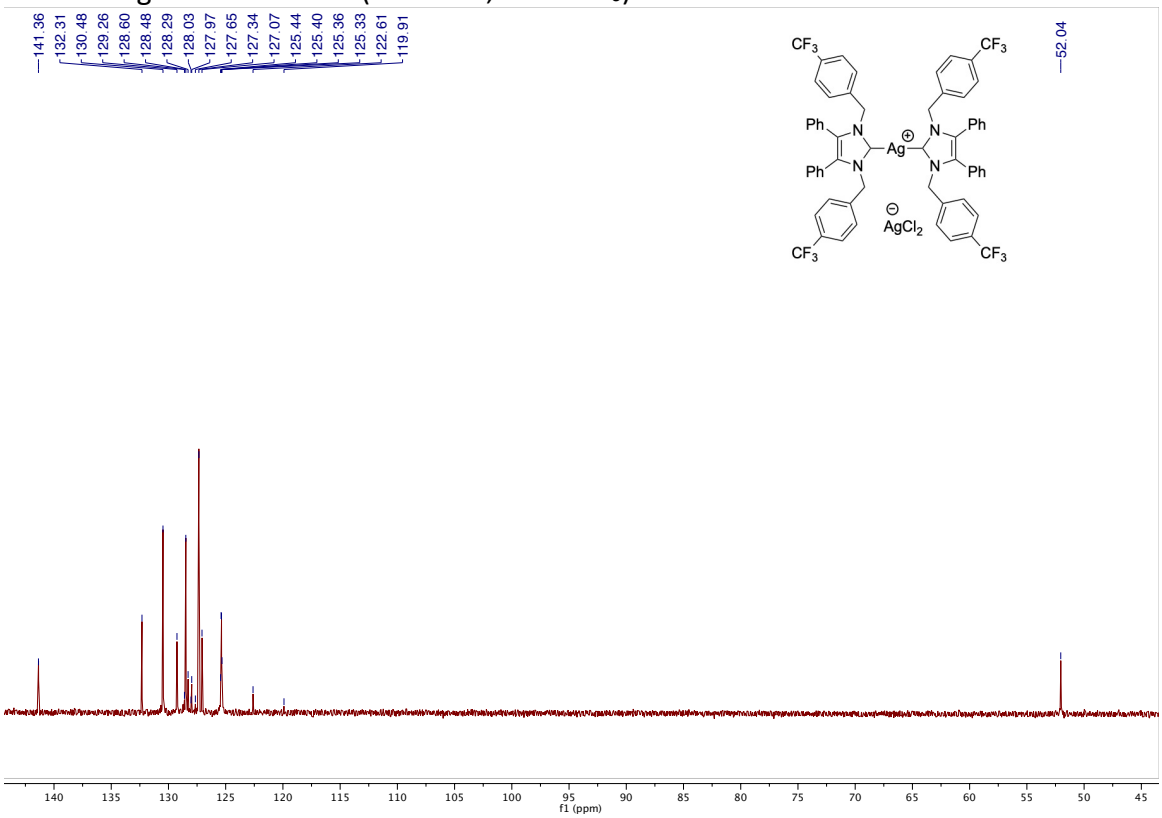

(**13c**) *Bis*-(1,3-di(*p*-trifluoromethyl) benzyl-4,5-diphenyl imidazol-2-ylidene) silver (I) dichloroargentate ^{19}F NMR (376 MHz, DMSO-d_6)

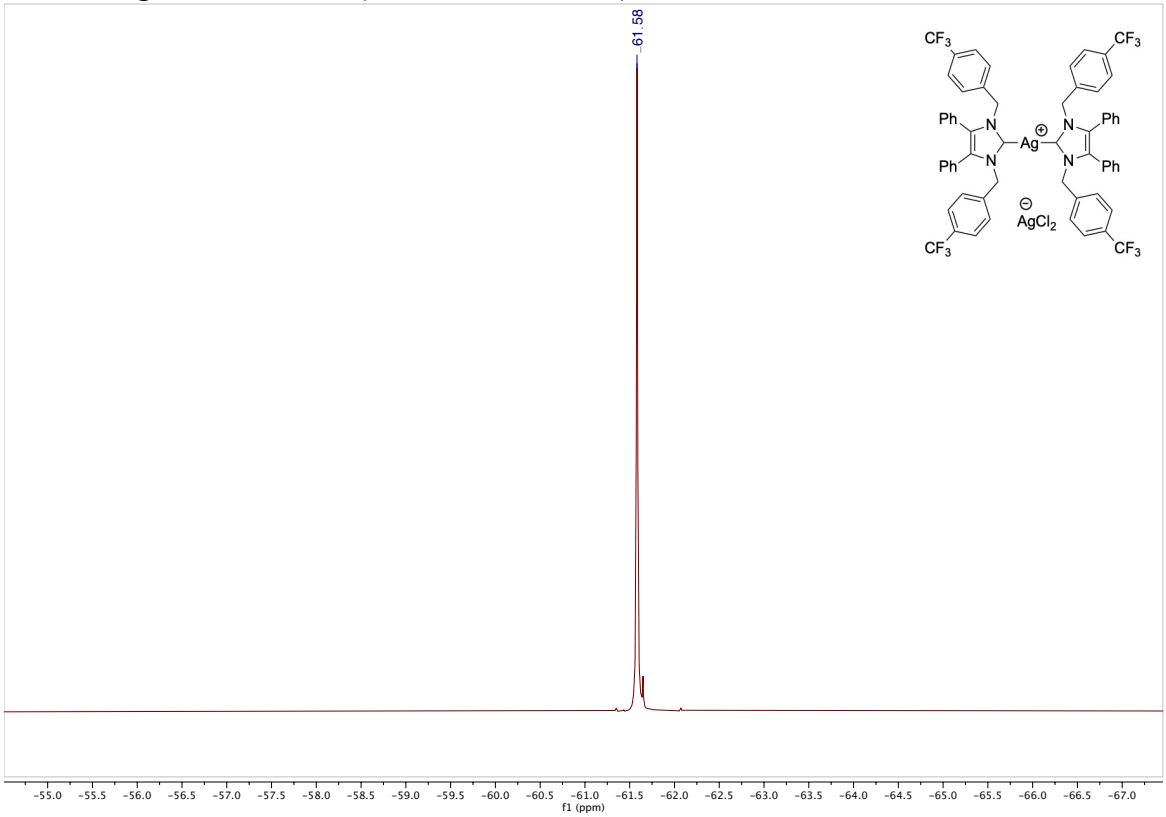

(**15**) *Bis*-(1,3-dibenzyl-4,5-diphenyl imidazol-2-ylidene) silver (I) acetate ^{1}H NMR (400 MHz, DMSO-d_6)

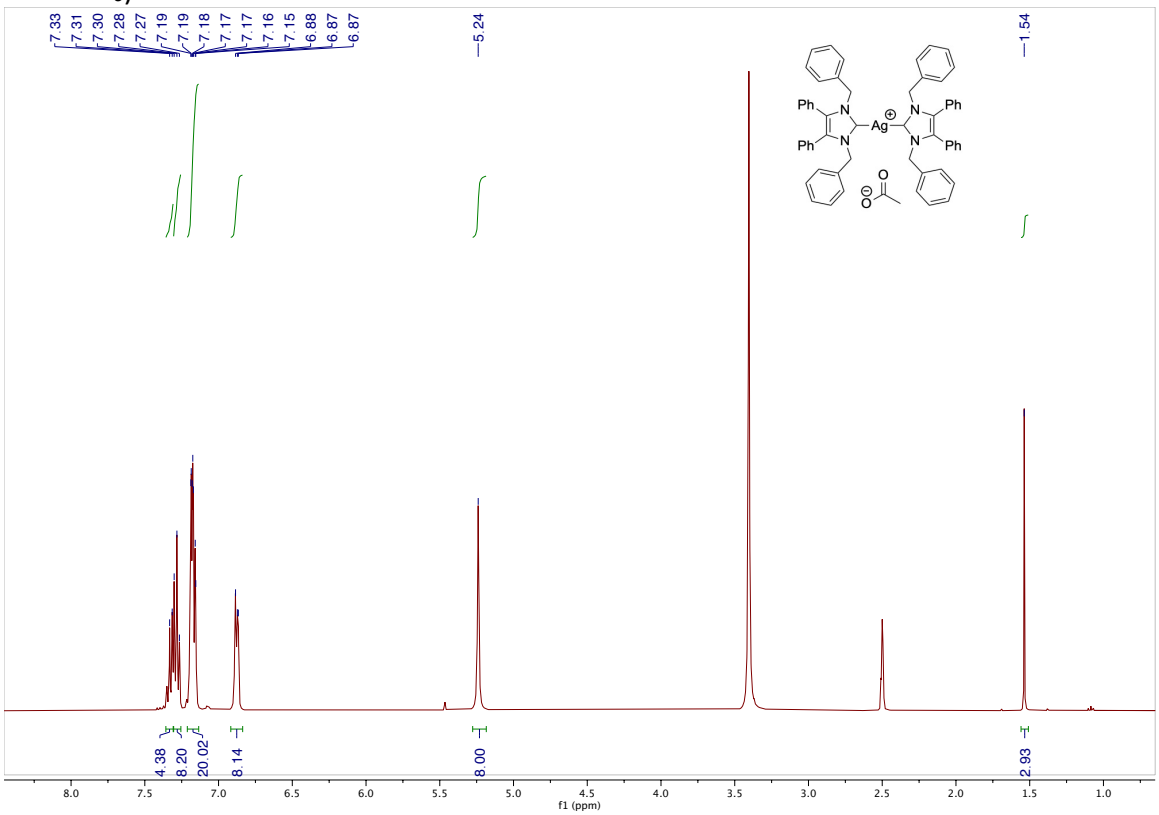

(**15**) *Bis*-(1,3-dibenzyl-4,5-diphenyl imidazol-2-ylidene) silver (I) acetate ^{13}C NMR (101 MHz, DMSO-d_6)